

**MOLECULAR PRODUCTS, THERMAL EMISSIONS, AND RADICAL KINETICS
FROM THE THERMAL DEGRADATION OF *Croton megalocarpus* BIODIESEL
AND BINARY TRANSPORT FUELS**

MOSONIK BORNES CHELANGAT

**A Thesis Submitted to the Graduate School in Partial Fulfilment of the Requirements
for the Degree of Doctor of Philosophy in Chemistry of Egerton University**

EGERTON UNIVERSITY

JUNE 2020

DECLARATION AND RECOMMENDATION

Declaration

This thesis is my original work and has not been submitted for any academic award in any institution.

Signature..... Date

Mosonik Bornes Chelangat

SD11/14662/15

Recommendation

This thesis has been submitted to the Graduate School for examination with our approval as University supervisors.

Signature Date.....

Dr. Joshua K. Kibet, PhD

Department of Chemistry, Egerton University

Signature Date.....

Prof. Mwaniki S. Ngari, PhD

Department of Chemistry, Egerton University

COPYRIGHT

©2020, Bornes C. Mosonik

All Rights Reserved. No part of this thesis may be reproduced, scanned, photocopied, stored in a retrievable system or transmitted in any form without the permission of Egerton University on behalf of the author.

DEDICATION

It is with sincere regards that I dedicate this work to my loving family, husband (Mathew Rotich) and children, Brenda, Lynn, Olive and Trevor.

ACKNOWLEDGEMENTS

I give thanks to God for giving me the strength to successfully complete this study. My sincere gratitude to my supervisors Dr. J. K. Kibet and Prof. M. S. Ngari of Egerton University for giving me the opportunity to do this research and ensuring that everything was done right during my entire period as a student. Their unparalleled efforts, patience and guidance throughout the research and thesis writing will not go unnoticed. May the Almighty God bless my supervisors and their families as they endeavour to serve humanity. I am truly honoured to have been their student.

My family and friends are greatly acknowledged for their prayers, financial and moral support throughout this research, and specifically my Husband Mathew Rotich who went out of his way to ensure our children were well taken care of when I was away. I thank the Department of Chemistry and Department of Animal Health of Egerton University for providing the necessary support and facilities towards the success of this study. Mr. Mutumba the chief technician Animal Health Department is greatly thanked for training me on how to use the Muffle furnace. Additionally, I am sincerely grateful to Mrs. Thiloshini Naidoo and Mr. Vishal Bharuth both of the University of KwaZulu-Natal, College of Agriculture, Engineering and Science for according me the opportunity to use FTIR and SEM for my sample analysis. My regards go to the University of KwaZulu-Natal (UKZN), the National Research Foundation (NRF), UKZN nanotechnology platform for funding part of this research and allowing me to use their facilities with unparalleled assistance of Prof. Vincent Nyamori. The University of Illinois, School of Chemical Science at Urbana Champaign (USA) is truly appreciated for according me the opportunity to conduct EPR analysis of the thermal char reported in this study. Applied Research Associates (ARA), Inc., Albuquerque, New Mexico, is honestly appreciated for providing me with Multpath Particle Deposition (MPPD) model ver. 3.04 software used in the respiratory simulation of deposition and clearance of particulates from combustion of transport fuels.

Special thanks to Nathan Kipsang from Kabarak University for helping in collection and drying of *Croton megalocarpus* seeds. My research assistant Josephate Bosire and my laboratory workmate Audriy Chebet are appreciated for standing with me throughout my entire period as a student at Egerton University.

ABSTRACT

There is an urgent interest initiated to develop clean energy resources with the aim of reducing exposure to environmental pollutants and explore model fuels that can hasten the achievement of clean energy combustion. In order to optimize the pyrolysis of binary transport fuels, diesel blends of ratios 1:1, 3:2 and 2:3 were each pyrolyzed at a contact time of 5 seconds in a quartz reactor at 1 atmosphere pressure, at a model temperature of 500 °C. The surface morphology of the particulate emission was imaged using a field emission gun scanning electron microscope (FEG SEM) while free radical characteristics such as radical intensities and radical kinetics was investigated using an X-band electron paramagnetic resonance spectrometer (EPR). Surface bound functional groups on thermal char were studied using Fourier Transform infra-red spectrometer (FTIR). Optimized molecular structures were performed using the quantum level of theory incorporated in Gaussian '16 and CHEMISIAN computational codes. The charcoal content for pure fossil diesel was compared with the binary diesel residue. Gas-phase molecular components were determined using Gas chromatography (GC) coupled to a mass selective detector (MSD). Elemental composition of thermal char was determined using Smart Elemental Analyzer. It was noted that at a ratio of 2:3 (Biodiesel: Fossil diesel), harmful molecular products reduced significantly, 76 – 99%. Elemental analysis data indicated that the carbon content from commercial diesel was very high ($\approx 70.61\%$) as compared to approximately 53% for biodiesel-fossil diesel mixture in the same ratio 2:3. Interestingly, the free radical content was reduced by nearly 50% in favour of the biodiesel/fossil diesel mixture. Electron paramagnetic resonance (EPR) results gave a g-value of 2.0024 and a narrow ΔH_{p-p} of 3.65 G. The radical concentration for the first EPR experiment was 9.12×10^{19} spins/g and 4.19×10^{17} spins/cm. The decay rate constant for the radicals was low ($1.86 \times 10^{-8} \text{ s}^{-1}$) while the half-life was ≈ 431 days. Fourier transform infrared (FTIR) results showed the presence of aromatic hydrocarbons, methyl and methylene groups on the surface of biochar while scanning electron microscopy (SEM) images indicated the existence a polymeric structure believed to be highly carbonaceous. The low g-values and low decay rate constant suggest that the free radicals in the biochar are carbon-based and stabilized by a strong π - π conjugated system. This study reports that a binary biodiesel – fossil diesel ratio of 2:3 is a future promising transport fuel because of reduced molecular emissions and decreased free radicals in particulate emissions.

TABLE OF CONTENTS

DECLARATION AND RECOMMENDATION	ii
COPYRIGHT	iii
DEDICATION.....	iv
ACKNOWLEDGEMENTS	v
ABSTRACT.....	vi
TABLE OF CONTENTS	vii
LIST OF TABLES	xi
LIST OF SCHEMES	xii
LIST OF FIGURES	xiii
LIST OF ABBREVIATIONS ANDACRONYMS	xv
INTRODUCTION.....	1
1.1 Background information.....	1
1.2 Statement of the problem.....	4
1.3 Objectives	4
1.3.1 General objective	4
1.3.2 Specific objectives	4
1.4 Hypotheses.....	5
1.5 Justification.....	5
References.....	7
CHAPTER TWO	10
LITERATURE REVIEW	10
2.1 The <i>Croton megalocarpus</i> seed oil.....	10
2.2. Transesterification of bio-oil	11
2.3 Biodiesel fuel.....	12
2.4 Types of biofuels	13
2.5 Pyrolysis	14
2.5.1 Pyrolysis of binary mixture of <i>Croton megalocarpus</i> biodiesel and fossil diesel.....	15
2.5.2 Solid particulate matter	15
2.5.3 Biochars	16
2.5.4 Elemental composition of biochars.....	17
2.6 Kinetic modeling and computational chemistry	18
2.6.1 Radical kinetics.....	18
2.6.2 Pyrolysis model.....	19
2.7 Reactor design for the thermal degradation of biomass fuels.....	19

2.8 Computational chemistry	20
2.8.1 The density functional theory (DFT)	20
2.8.2 Chemission software	22
2.8.3 Multipath particle deposition model (MPPD).....	22
2.9 The theory of electron paramagnetic resonance spectroscopy (EPR).....	24
References	26
CHAPTER THREE	42
ENVIRONMENTALLY PERSISTENT FREE RADICALS AND PARTICULATE EMISSIONS FROM THE THERMAL DEGRADATION OF <i>Croton megalocarpus</i> BIODIESEL.....	42
3.1 Introduction	42
3.2 Materials and methods	45
3.2.1 Sample collection and preparation	45
3.2.2 Bio-oil extraction	45
3.2.3 Extraction of biodiesel	46
3.2.4 Gas chromatography mass spectrometry (GC-MS) characterization of <i>Croton megalocarpus</i> biodiesel.....	46
3.2.5 The combustion reactor system.....	47
3.2.6 Electron paramagnetic resonance (EPR) spectroscopy	48
3.2.7 FTIR and scanning electron microscopy characterization of thermal emissions	48
3.3 Results and discussion	49
3.3.1 Molecular components of <i>Croton megalocarpus</i> biodiesel	49
3.3.2 Mechanistic description for the formation of thermal char from model biodiesel compound.....	50
3.3.3 Electron paramagnetic resonance (EPR) analysis.....	52
3.3.4 The kinetics of free radicals in <i>Croton megalocarpus</i> particulates.....	54
3.3.5 Fourier transform infrared spectroscopy features of <i>Croton megalocarpus</i> bio-oil particulate.....	55
3.3.6 Scanning electron microscopy (SEM) and Energy Dispersive X-ray Analysis (EDX)	57
References	60
CHAPTER FOUR.....	65
FREE RADICALS AND ULTRAFINE PARTICULATE EMISSIONS FROM THE CO-PYROLYSIS OF <i>Croton megalocarpus</i> BIODIESEL AND FOSSIL DIESEL	65
4.1 Introduction	66
4.2 Materials and Methods	69
4.2.1 Materials	69
4.2.2 Co-pyrolysis of <i>Croton megalocarpus</i> biodiesel and petroleum diesel	69

4.2.3 Electron paramagnetic resonance spectroscopy.....	70
4.2.4 Scanning electron microscopy (SEM) analysis.....	70
4.2.5 Fourier transform infrared (FTIR) spectroscopy.....	70
4.3 Results and discussions.....	71
4.3.1 Scanning electron microscopy	71
4.3.2 Electron paramagnetic resonance spectroscopy.....	72
4.3.3 FTIR spectrum of the thermal char	73
4.3.4 The health and environmental concerns.....	74
References.....	78
CHAPTER FIVE	82
SIMULATING THE HEALTH IMPACT OF PARTICULATE EMISSIONS FROM TRANSPORT FUELS USING MULTIPATH PARTICLE DEPOSITION MODEL (MPPD)	82
5.1 Introduction	82
5.2 Materials and Methods	84
5.2.1 The pyrolysis reactor system.....	84
5.2.2 Scanning electron microscopy analysis and particulate distribution using image J.....	85
5.2.3 Respiratory tract deposition model	85
5.3 Results and discussion	86
5.3.1 Respiratory tract deposition model for co-pyrolysis of <i>C. megalocarpus</i> biodiesel blend ...	86
References.....	91
CHAPTER SIX	95
OPTIMIZATION OF BINARY MIXTURES OF BIODIESEL AND FOSSIL DIESEL FOR CLEAN ENERGY COMBUSTION	95
6.1 Introduction	95
6.2 Materials and methods.....	99
6.2.1 Co-pyrolysis of <i>C. megalocarpus</i> biodiesel and petroleum diesel.....	99
6.2.2 GC-MS identification of molecular products.....	100
6.2.3 Electron paramagnetic resonance spectroscopy.....	100
6.3 Results and discussion	101
6.3.1 Mechanistic description for the formation of reaction products	104
6.3.2 The fate of elements during biomass pyrolysis.....	106
6.3.3 Inorganic salts present in biomass materials.....	108
6.3.4 Elemental composition of char and electron paramagnetic spectra	109

References	114
CHAPTER SEVEN	121
MOLECULAR MODELLING OF SELECTED COMBUSTION BY-PRODUCTS FROM THE THERMAL DEGRADATION OF <i>Croton megalocarpus</i> BIODIESEL BLEND	121
7.1 Introduction	121
7.2 Materials and Methods	123
7.2.1 Density functional theory (DFT) calculations.....	123
7.3 Results and discussion	123
7.3.1 Molecular geometries of major molecular emissions	123
7.3.2 Mechanistic degradation of 5-(3-phenylpropanoyl) dihydro-2(3H)-furanone.....	125
7.3.3 Frontier molecular orbitals and electron density maps	127
7.3.4 Electron density contour maps	130
References	132
GENERAL DISCUSSION, CONCLUSIONS AND RECOMMENDATIONS	134
8.1 General discussion	134
8.1.1 Rationale of the study	134
8.1.2 Findings of the study.....	135
8.2 Conclusions	139
8.3 Recommendations.....	140
APPENDICES	141
Appendix I: Characterization of croton char	141
Appendix II: Electron density maps and molecular orbitals.....	146
Appendix III: Copyrights.....	155
Appendix IV: Abstracts of published papers	160
Appendix V: NACOSTI Permit.....	163

LIST OF TABLES

Table 3.1: Major molecular components of <i>C. megalocarpus</i> biodiesel characterized using gas chromatography-mass spectrometer	49
Table 4.1: The electron paramagnetic resonance parameters for the thermal char formed from the co-pyrolysis of the binary mixture of biodiesel and conventional diesel.	73
Table 6.1: Yield of molecular products from the pyrolysis of various diesel blends	102
Table 6.2: Molecular structures of the compounds identified using gas chromatography-mass spectrometer	104
Table 7.1: HOMO-LUMO band gap energies for the selected volatile organic compounds	128

LIST OF SCHEMES

Scheme 3.1: Proposed mechanistic pathways for the formation of carbon-centred free radicals from (E)-methyl dodec-9-enoate model compound.	51
Scheme 4.1: Mechanistic channels showing the generation of toxic species from the pyrolysis of binary diesel (Δ indicates pyrolysis) and their predictive effects on the biological and the environmental systems.	76
Scheme 6.1: Proposed mechanistic pathway for the formation of tetradecane.....	105
Scheme 7.1: Proposed mechanistic pathways for the thermal degradation of 5(3phenylpropanoyl)dihydro-2-(3H)-furanone.....	126

LIST OF FIGURES

Figure 1.1: The <i>C. megalocarpus</i> plant (a) and croton seeds (b) (photos taken by the author).	2
Figure 2.1: Batch transesterification chemical reaction.....	11
Figure 2.2: The kinetic model scheme for the co-pyrolysis of diesel blend (fossil diesel and bio-diesel)	20
Figure 2.3: The fate of inhaled particles through different regions of the respiratory system based on mechanisms of transport and deposition.....	23
Figure 2.4: Energy levels for an electron spin ($m_s = \pm 1/2$) in an applied magnetic field, B_z .	25
Figure 3.1: Reactor assembly and gas-phase trapping apparatus	49
Figure 3.2: The Gas chromatogram showing the major components of <i>C. megalocarpus</i> biodiesel	52
Figure 3.3: The <i>C. megalocarpus</i> char particulate electron paramagnetic resonance overlay spectra - radical intensity as a function of magnetic field.	54
Figure 3.4: A model of free radicals immobilized on the surface of croton char particulate and possible channels in the generation of reactive oxygen species in biosystems.....	55
Figure 3.5: Pseudo-first order free radical kinetic behaviour in croton char particulates	57
Figure 3.6: FTIR spectrums for croton char particulate	58
Figure 3.7: SEM image of <i>C. megalocarpus</i> bio-oil char at an associated magnification of (a) $\times 20000$ at 200 nm and (b) of $\times 100000$ at 100 nm.	59
Figure 3.8: Estimated size distribution of particulate matter from croton bio-oil thermal emissions using Image J and Igor version 5.0.	60
Figure 4.1: SEM image of biodiesel – fossil diesel at an associated magnification of	73
Figure 4.2: Particulate size distribution for the co-pyrolysis of croton biodiesel and fossil diesel blend.....	74
Figure 4.3: Diesel blend thermal char electron paramagnetic resonance spectra - radical intensity as a function of magnetic field (EPR spectra showing intensity as a function of g-value are reported in supplementary material S3, a & b).....	75
Figure 4.4: FTIR absorption bands for the char formed from the co-pyrolysis of croton biodiesel and conventional diesel.	76
Figure 5.1: Regional respiratory (Head, trachea and bronchioles and pulmonary) tract co-pyrolysis PM deposition fraction from the Multipath Particle Deposition model version 3.04, for particles with count medium diameter of (a) 32 nm and (b) 22 nm having a geometric standard deviation of 1 nm inhaled by an infant.	90

Figure 5.2: Regional respiratory tract co-pyrolysis PM deposition fraction from the Multipath Particle Deposition model version 3.04, for particles with count medium diameter of (a) 32 nm and (b) 22 nm having a geometric standard deviation of 1 nm inhaled by an 8 years old.	91
Figure 5.3: Regional respiratory tract co-pyrolysis PM deposition fraction from the Multipath Particle Deposition model version 3.04, for particles with count medium diameter (a) 22 nm and (b) 32 nm with a geometric standard deviation of 1 nm inhaled by a 21 years old	92
Figure 6.1: Reactor assembly and gas-phase trapping apparatus	103
Figure 6.2: Gas chromatograms for diesel blends (biodiesel: Fossil diesel) at a pyrolysis temperature of 500 °C	106
Figure 6.3: Elemental % composition of biodiesel-fossil thermal char at 500 °C in the ratio 2:3.	112
Figure 6.4: Elemental % composition of pure fossil diesel thermal char at 500 °C.....	113
Figure 6.5: The <i>C. megalocarpus</i> biochar, croton-fossil diesel char, fossil diesel char EPR overlay spectra - radical intensity as a function of magnetic field	114
Figure 7.1: Optimized structure of 3,4-dimethyl-3-cyclohexene-1-carbaldehyde and a plot showing its optimization steps (the red circle is the optimization level).....	128
Figure 7.2: Optimized structure of 5-(3-phenylpropanoyl) dihydro-2-(3H)-furanone and a plot showing its optimization steps (the red circle is the optimization level).....	129
Figure 7.3: Optimized structure of isopropenyl-4-methyl-1,2-cyclohexanediol and a plot showing its optimization steps (the red circle is the optimization level).....	131
Figure 7.4: Optimized structure of 4-(2,4-dimethylcyclohexyl)-2-butanone and a plot showing its optimization steps (the red circle is the optimization level).....	131
Figure 7.5: The HOMO-LUMO band gap for 4-(2,4-dimethylcyclohexyl)-2-butanone determined using Chemissian	133
Figure 7.6: The HOMO-LUMO band gap for 5-(3-phenylpropanoyl)dihydro-2-(3H)-furanone determined using Chemissian	134
Figure 7.7: 2-D Electron density map for 5-(3-Phenylpropanoyl)dihydro-2(3H)-furanone.....	135
Figure 7.8: 3-D Electron density map for 5-(3-phenylpropanoyl)dihydro-2(3H)-furanone at an isovalue of 0.020	135

LIST OF ABBREVIATIONS ANDACRONYMS

ADF	Amsterdam functional
ANOVA	Analysis of variance
ASTM	American density society for testing and materials
ATR-FTIR	Attenuated total reflection-fourier transform infrared
CMD	Count median diameter
DCM	Dichloromethane
DFT	Density functional theory
DNA	Deoxyribonucleic acid
DTBP	Di-tertbutylperoxide
EDX	Energy dispersive X-ray spectroscopy
EHT	High tension voltage
EPFRs	Environmentally persistent free radicals
EPR	Electron paramagnetic resonance spectroscopy
ETFs	Emerging transport fuels
GC-MS	Gas chromatography-mass spectrometry
GSD	Geometric standard deviation
HF	Hartree-Fock
HOMO	Highest occupied molecular orbital
LED	Light emitting diode
LUMO	Lowest unoccupied molecular orbital
MPPD	Multipath particle deposition
MSD	Mass selective detector
NACOSTI	National Commission for Science, Technology and Innovation
NIST	National institute of standard technology
PES	Potential energy surface
PCDD/s	Polychlorinated dioxins and polychlorinated dibenzo furans
ROS	Reactive oxygen species
SEM	Scanning electron microscopy
UHP	Ultra-high purity
VOCs	Volatile organic compounds
WD	Working distance

CHAPTER ONE

INTRODUCTION

1.1 Background information

Energy security, environmental pollution, public health problems and clean energy combustion are one of the greatest challenges facing the 21st century (Holley and Lecavalier, 2017). Petro-diesel is a non-renewable energy resource broadly used on a global scale. It has been estimated that 98% of carbon emissions are due to petro-diesel combustion (Bergthorson and Thomson, 2015). Petro-diesel combustion conventionally emits copious amounts of greenhouse gasses (Madvar *et al.*, 2019). Energy research is therefore focused towards new energy technologies in order to maintain secure renewable energy resources for sustainable development. Biofuels are considered promising renewable energy resources because they are mainly derived from low-cost non-edible oils and waste oil sources (Prabu *et al.*, 2017). The increase in energy demand precipitated by the depletion of fossil fuel reserves with an exponential rise in population and economic development has resulted in the search for alternative energy resources (Bergthorson and Thomson, 2015; Fontes and Freires, 2018). Furthermore, the toxic nature of the exhaust emissions of petro-diesel-fueled vehicular systems has deepened the search for alternative fuels such as biodiesel and binary transport fuels. Several studies have examined the impact of mixing diesel and biodiesel fuel on engine performance and emission characteristics (Ali *et al.*, 2016; Mahmudul *et al.*, 2017; Qasim *et al.*, 2018). Renewable energy derived from biomass reduces reliance on fossil fuels and it does not add new carbon dioxide to the atmosphere (White *et al.*, 2011; Varuvel *et al.*, 2012).

The Kyoto Protocol, together with the desire to reduce society's dependence on imported crude oil, has motivated research on the use of biomass as an energy source and, more specifically, for the reduction of costs and harmful pollutants as efficient transport fuels (Corma *et al.*, 2007). Environmental concerns regarding the use of petrol-based diesel have increased the urgent pressure on clean energy combustion aimed at minimizing the emission of toxic particulates from vehicle exhaust, while at the same time embracing environmentally friendly biomass transport fuels such as biofuels and model biodiesel – fossil diesel binary mixtures (Ruhul *et al.*, 2016; Khan *et al.*, 2018). The motivation behind this study was to explore the nature of the molecular and particulate matter emitted and the surface bound free

radicals formed during thermal degradation of diesel mixtures in order to assess the health and environmental consequences of the use of binary transport fuels in combustion engines.

Commercial diesel engines emit massive amounts of particulate matter, nitrogen oxides and greenhouse gases compared to biodiesel (Mofijur *et al.*, 2016) while, on the other hand, biodiesel-based engines significantly reduce environmental pollutants such as particulate matter, carbon monoxide and unburned hydrocarbons (Chhetri and Islam, 2008). Biodiesel blends of 20% produce a 15 % reduction in particulate matter emissions, carbon monoxide, total hydrocarbons and a group of toxic compounds such as polycyclic aromatic hydrocarbons (PAHs), aldehydes and ketones (McCormick, 2007) depending on the design of the engine. Bio-diesel can be prepared locally from non-edible oils, including *C. megalocarpus* oil, castor oil or edible vegetable oil waste. This presents an economic renewable fuel resource that has lower emissions than diesel-based petroleum. Biodiesel can be used on its own or in binary forms with fossil fuels. In this study, *C. megalocarpus* seed oil has been used for the biodiesel production. The *C. megalocarpus* plant and its seeds are shown in Figure 1.1 which are the central source of the biofuel used in this study.



Figure 1.1: The *C. megalocarpus* plant (a) and *Croton* seeds (b) (photos taken by the author).

From a thermal degradation standpoint, pyrolysis is one of the major promising thermochemical conversion technologies for obtaining energy from biomass materials (SriBala *et al.*, 2019). The complex nature and uncertain processes occurring in the pyrolysis of biomass materials has generated interest in the study of the thermal degradation of biopolymeric mixtures as well as individual biopolymer components. An important by-product

of feed stock from non-edible oils pyrolyzed at elevated temperatures is thermal char (biochar) which has several applications ranging from agricultural practices, catalytic processes, water remediation processes among other uses (Milla *et al.*, 2013; Tan *et al.*, 2015). Retention of inhaled particulate matter in human lungs is an important indicator of respiratory health risks (De Grove *et al.*, 2018). The inhalation and clearance of particulate emissions cannot easily be estimated by conventional means (Protano *et al.*, 2017). For this reason, particulate deposition models have been designed to accurately predict the deposition of particulates in human lungs. Multiple-path particle deposition (MPPD) Model version 3.04 is one of the most robust models advanced in respiratory studies (Manojkumar *et al.*, 2019).

On the hand, computational chemistry is often used to estimate the thermodynamic properties such as enthalpy, entropy, heat capacity, free energy of various systems, and parameters of molecular and free radical species (Kirste, 2016). Therefore, by calculating the free energy differences between the minima of the potential energy surface (PES), the reaction equilibrium constants can be derived (Lewars, 2016). Analogously, the prediction of chemical reaction rate constants requires electronic quantum-mechanical calculations to obtain activation energy barriers (Piccini *et al.*, 2016). To determine these thermodynamic and kinetic properties from quantum results, the use of statistical mechanics is required to relate the microscopic properties of individual atoms and molecules to the macroscopic bulk properties of materials under study in the laboratory (Canneaux *et al.*, 2014). Predicting rate constants is one of the major goals of computational chemistry. Nonetheless, calculations of rate constants require a delicate balance between the accuracy of the dynamical theory and the efficiency in obtaining accurate potential energy information (Duncan *et al.*, 1998).

In general, the atmosphere has become a major transport corridor for environmentally persistent free radicals and particulate pollution from combustion activities (Freitas *et al.*, 2005). As a result, environmental concerns about the use of petrol-based diesel have increased the need for clean energy combustion, with a view of minimizing the emission of toxic particulates from vehicle exhaust, while at the same time embracing environmentally-friendly biomass transport fuels such as biofuels and model biodiesel – fossil diesel binary mixtures (Arshad, 2017). To this end, the aim of this study is to study the nature of organic volatiles, thermal char and persistent free radicals of environmental concern as by-products of binary fuel pyrolysis. Secondly, the deduction of the rate constants of environmentally

persistent free radicals (EPRs) from commercial diesel and bio-diesel pyrolysis is an important component of this study.

1.2 Statement of the problem

Fossil fuels are characterized by high emissions of environmental pollutants which may have long-term or short-term effects on humans and the natural environment (Covert *et al.*, 2016). The particulate matter such as thermal char, tar and volatile organic compounds associated with combustion of fossil fuels may cause eye irritations, respiratory tract infections and even cancer in humans. Moreover, greenhouse gases are known to cause acid rains which affect plants and animals as well. Therefore, there is need to enhance the search for alternative renewable clean energy resource with minimum environmental health impacts. This study focused on the co-pyrolysis of biodiesel and fossil fuel blends (biodiesel and commercial diesel) in order to explore the nature of radicals, molecular by-products and optimum fuel blend with reduced molecular products, free radicals and particulate emissions. This study, to the best of my knowledge, has not been carried out elsewhere. Decomposition by products of biofuels and their blends are complex, therefore computational simulation and kinetic modeling offers a better understanding of their characteristic behaviour during combustion. The biodiesel used in this study was obtained from *C. megalocarpus* oil which is a non edible oil, hence it is economically viable. The *C. megalocarpus* biodiesel is an emerging option for biofuel production due to its availability across the world particularly in Sub-Saharan Africa, Latin America and parts of Asia (von Maltitz *et al.*, 2013; Tan *et al.*, 2015).

1.3 Objectives

1.3.1 General objective

To investigate the molecular nature of by-products, particulate emissions, and kinetic parameters fundamental from the gas-phase formation of free radicals generated from the pyrolysis of *Croton megalocarpus* biodiesel and binary transport fuels.

1.3.2 Specific objectives

- i) To identify the selected gas phase molecular products and free radicals at various pyrolysis temperatures of *Croton megalocarpus* bio-diesel and petroleum diesel blends.
- ii) To determine the size of particulate matter from high temperature pyrolysis of diesel blends and *Croton megalocarpus* bio-diesel at 500 °C and 600 °C using scanning electron microscopy (SEM).

- iii) To develop a kinetic model for the formation of selected gas phase free radicals at different life times.
- iv) To compute molecular orbital geometries and band-gap energies for selected gas phase molecular products and free radicals using Chemissian and Quantum mechanics level of theory using the Density functional theory (DFT) formalism.

1.4 Hypotheses

- i) The gas phase molecular products and free radicals from the co-pyrolysis of biodiesel and petroleum diesel at various temperatures will not be significantly different.
- ii) The size of particulate matter from the pyrolysis of biodiesel and petroleum blends at 500°C and 600 °C will not be significantly different.
- iii) The kinetic model for the formation of selected gas phase free radicals at different life times will not be significantly different.
- iv) Molecular orbital geometries and band-gap energies of selected gas phase molecular products and free radicals generated using CHEMISSIAN are not different from those generated from DFT program software.

1.5 Justification

The world's energy needs tend to increase exponentially with population and economic growth (Hall, 2017). In order to satisfy this requirement, the development of clean energy resources with comparable caloric properties as fossil fuels but with minimum molecular environmental pollutants is necessary. Therefore, the diminishing reserves and negative environmental impacts caused by greenhouse gases (CH₄, H₂O, CO₂, NO_x etc.) and acid rain from combustion of fossil fuels has led the world energy community to look for alternative renewable and cleaner energy resources. The production of energy from renewable sources such as biomass involves chemical, biochemical and thermochemical processes (Zhang and Brown, 2019).

The advantages of using biomass-derived fuels include low amounts of SO_x, NO_x and fewer volatile organic pollutants associated with respiratory problems such as bronchitis and emphysema, cardio pulmonary diseases and various types of cancers such as throat and cancer of the lungs. The use of biofuels may lead to reduced carbon dioxide and particulate emissions and environmentally persistent free radicals. However, the caloric value of biofuels has been found to be low in comparison to fossil fuels. Therefore this study attempts to optimize the caloric value of binary transport fuels so as to model a sustainable energy

resource with minimum environmental impacts. Besides, this contribution distinguishes itself as a potential experimental design that would optimize the viability of binary mixtures of biodiesel and fossil diesel at selected ratios aimed at achieving clean energy combustion. The co-pyrolysis of biodiesel and fossil diesel at various temperatures and their kinetic parameters is yet to be investigated; hence this study is very important. Furthermore, the computational modelling of the combustion by-products of binary diesel gives the interaction characteristics between reaction by-products of transport fuels in general. This work therefore, is important in understanding clean energy combustion processes. Data on radical immobilization on the char surface is a new area of study and thus contributes immensely to the existing body of knowledge.

References

- Ali, O. M., Mamat, R., Abdullah, N. R. and Abdullah, A. A. (2016). Analysis of blended fuel properties and engine performance with palm biodiesel–diesel blended fuel. *Renewable Energy*, **86**: 59-67.
- Arshad, M. (2017). Clean and sustainable energy technologies. In *Clean Energy for Sustainable Development* (73-89). Elsevier: Amsterdam, The Netherlands.
- Bergthorson, J. M. and Thomson, M. J. (2015). A review of the combustion and emissions properties of advanced transportation biofuels and their impact on existing and future engines. *Renewable and Sustainable Energy Reviews*, **42**: 1393-1417.
- Canneaux, S., Bohr, F. and Henon, E. (2014). KiSThElP: a program to predict thermodynamic properties and rate constants from quantum chemistry results. *Journal of Computational Chemistry*, **35**: 82-93.
- Chhetri, A. and Islam, M. (2008). Towards producing a truly green biodiesel. *Energy Sources, Part A*, **30**: 754-764.
- Corma, A., Iborra, S. and Velty, A. (2007). Chemical routes for the transformation of biomass into chemicals. *Chemical Reviews*, **107**: 2411-2502.
- Covert, T., Greenstone, M. and Knittel, C. R. (2016). Will we ever stop using fossil fuels?. *Journal of Economic Perspectives*, **30**:117-38.
- De Grove, K. C., Provoost, S., Brusselle, G. G., Joos, G. F. and Maes, T. (2018). Insights in particulate matter-induced allergic airway inflammation: focus on the epithelium. *Clinical and Experimental Allergy*, **48**: 773-786.
- Duncan, W., Bell, R. and Truong, T. (1998). TheRate: Program for ab initio direct dynamics calculations of thermal and vibrational-state-selected rate constants. *Journal of Computational Chemistry*, **19**: 1039-1052.
- Fontes, C. H. D. O. and Freires, F. G. M. (2018). Sustainable and renewable energy supply chain: A system dynamics overview. *Renewable and Sustainable Energy Reviews*, **82**: 247-259.
- Freitas, S.R., Longo, K.M., Dias, M.A.S., Dias, P.L.S., Chatfield, R., Prins, E., Artaxo, P., Grell, G.A. and Recuero, F.S. (2005). Monitoring the transport of biomass burning emissions in South America. *Environmental Fluid Mechanics*, **5**: 135-167.
- Hall, C. A. (2017). Energy, economic growth and sustainability: an energy primer for the twenty-first century. *Handbook on Growth and Sustainability*. Edward Elgar Publishing.

- Holley, C. and Lecavalier, E. (2017). Energy governance, energy security and environmental sustainability: A case study from Hong Kong. *Energy Policy*, **108**: 379-389.
- Khan, K., Kumar, G., Sharma, A. K., Kumar, P. S., Mandal, C. and V. Chintala (2018). Performance and emission characteristics of a diesel engine using complementary blending of castor and karanja biodiesel. *Biofuels*, **9**: 53-60.
- Kirste, B. (2016). Applications of Density Functional Theory to theoretical organic chemistry. *Chemical Science Journal*, **7**:127.
- Lewars, E. G. (2016). The concept of the potential energy surface. *Computational Chemistry*: 9-49.
- Mahmudul, H., Hagos, F., Mamat, R. Adam, A. A., Ishak, W. and Alenezi, R. (2017). Production, characterization and performance of biodiesel as an alternative fuel in diesel engines—A review. *Renewable and Sustainable Energy Reviews*, **72**: 497-509.
- Mofijur, M. G. R. M., Rasul, M. G., Hyde, J., Azad, A. K., Mamat, R. and Bhuiya, M. M. K. (2016). Role of biofuel and their binary (diesel–biodiesel) and ternary (ethanol–biodiesel–diesel) blends on internal combustion engines emission reduction. *Renewable and Sustainable Energy Reviews*, **53**: 265-278.
- Manojkumar, N., Srimuruganandam, B. and Nagendra, S. S. (2019). Application of multiple-path particle dosimetry model for quantifying age specified deposition of particulate matter in human airway. *Ecotoxicology and Environmental Safety*, **168**: 241-248.
- McCormick, R. L. (2007). The impact of biodiesel on pollutant emissions and public health. *Inhalation Toxicology*, **19**(12): 1033-1039.
- Milla, O. V., Rivera, E. B., Huang, W. J., Chien, C. C. and Wang, Y. M. (2013). Agronomic properties and characterization of rice husk and wood biochars and their effect on the growth of water spinach in a field test. *Journal of Soil Science and Plant Nutrition*, **13**(2): 251-266.
- Piccini, G., Alessio, M. and Sauer, J. (2016). Ab initio calculation of rate constants for molecule–surface reactions with chemical accuracy. *Angewandte Chemie International Edition*, **55**: 5235-5237.
- Prabu, S. S., Asokan, M., Roy, M., Francis, F. and Sreelekh, M. (2017). Performance, combustion and emission characteristics of diesel engine fuelled with waste cooking oil bio-diesel/diesel blends with additives. *Energy*, **122**: 638-648.
- Rotano, C., Manigrasso, M., Avino, P. and Vitali, M. (2017). Second-hand smoke generated by combustion and electronic smoking devices used in real scenarios: Ultrafine

- particle pollution and age-related dose assessment. *Environment International*, **107**: 190-195.
- Qasim, M., Ansari, T. M. and Hussain, M. (2018). Experimental investigations on a diesel engine operated with fuel blends derived from a mixture of Pakistani waste tyre oil and waste soybean oil biodiesel. *Environmental Science and Pollution Research*, **25**(24): 23657-23666.
- Ruhul, A., Kalam, M., Masjuki, H., Alabdulkarem, A., Atabani, A., Fattah, I. R. and Abedin, M. (2016). Production, characterization, engine performance and emission characteristics of *C. megalocarpus* and *Ceiba pentandra* complementary blends in a single-cylinder diesel engine. *RSC Advances*, **6**(29): 24584-24595.
- Ruhul, A., Kalam, M., Masjuki, H., Shahir, S., Alabdulkarem, A. Teoh, Y., How, H. and Reham, S. (2017). Evaluating combustion, performance and emission characteristics of *Millettia pinnata* and *C. megalocarpus* biodiesel blends in a diesel engine. *Energy*, **141**: 2362-2376.
- Soo, Y. N. (2019). *Application of liquid biofuels to internal combustion engines*. Springer Verlag, Singapor.
- SriBala, G., Carstensen, H. H., Van Geem, K. M. and Marin, G. B. (2019). Measuring biomass fast pyrolysis kinetics: state of the art. *Wiley Interdisciplinary Reviews: Energy and Environment*, **8**(2). <https://doi.org/10.1002/wene.326>.
- Tan, X., Liu, Y., Zeng, G., Wang, X., Hu, X., Gu, Y. and Yang, Z. (2015). Application of biochar for the removal of pollutants from aqueous solutions. *Chemosphere*, **125**: 70-85.
- Varuvel, E. G., Mrad, N., Tazerout, M. and Aloui, F. (2012). Experimental analysis of biofuel as an alternative fuel for diesel engines. *Applied Energy*, **94**: 224-231.
- von Maltitz, G. P. and Setzkorn, K. A. (2013). A typology of Southern African biofuel feedstock production projects. *Biomass and Bioenergy*, **59**: 33-49.
- White, J. E., Catallo, W. J. and Legendre, B. L., (2011). Biomass pyrolysis kinetics: A comparative critical review with relevant agricultural residue case studies. *Journal of Analytical and Applied Pyrolysis*, **91**(1): 1-33.
- Zhang, X. and Brown, R. C. (2019). Introduction to Thermochemical Processing of Biomass into Fuels, Chemicals, and Power. *Thermochemical Processing of Biomass: Conversion into Fuels, Chemicals and Power*, 1-16.

CHAPTER TWO

LITERATURE REVIEW

2.1 The *Croton megalocarpus* seed oil

The *Croton megalocarpus* is a drought resistant non-edible plant native to the America, parts of Asia, and sub-Saharan Africa (de Oliveira *et al.*, 2009). The plant is found commonly in East African region in various areas ranging from hilly areas of Tanzania, Uganda na Kenya (Kipkore *et al.*, 2014). The *C. megalocarpus* trees grows in various climatic conditions in Kenya (Busuru, 2018) at an altitude of 1300 – 2200 m with an annual rainfall ranging from 800 – 1600 mm and mean temperature of 11 – 26 °C (Aliyu *et al.*, 2010). The seeds of *C. megalocarpus* are a source of oil which may be exploited for commercial production of biodiesel. *Croton megalocarpus* oil has high engine performance as that of fossil diesels (Ruhul *et al.*, 2016) but ageing, oxidation, and the ability to form gums for various biofuels has minimized its use in internal combustion engines (Fazal *et al.*, 2019). Nonetheless, the low sulphur content in biodiesel indicates less sulphur (IV) oxide emission when used as fuel compared to fossil diesel (Zaharin *et al.*, 2017). The fact that *C. megalocarpus* harbours biodiesel yield of 82 % to 100 % (w/w) in its kernel has made this plant a promising source of fuel besides being a feedstock for the production of soap, lubricant, chicken feed and wood coating (Fekadu *et al.*, 2019).

The *Croton megalocarpus* biodiesel usage in engines has previously been demonstrated and results indicated that internal combustion engine could run without any modifications using a 10% mixture of dewaxed and degummed *C. megalocarpus* oil in normal diesel while blends of up to 50% could be used by preheating the fuel up to 27 °C (Sharma *et al.*, 2008). Another study also proved that oil either preheated or in low blend concentrations, resulted in combustion performance and emission characteristics close to that of mineral diesel in a single-cylinder, direct injection diesel engine (Agarwal and Agarwal, 2007; Dhanamurugan and Subramanian, 2015). Presently, bio-oil produced from the pyrolysis of biomass can be used directly or after further modification of physicochemical processes to heat up boilers, or even drive diesel engines or turbines (Chhetri and Islam, 2008; Demirbas *et al.*, 2009). The engines that run in pure biodiesel have been known for short term performance due to build up of carbon particles on the injector (Soo, 2019). Therefore, blending biofuels with commercial diesel (reduces particulate build up in the injector. A study carried out on the blending of fossil fuels and bioethanol, B20 (20% biodiesel blend), B20E5 (20% biodiesel +

5% bioethanol blend), and B20E10 (20% biodiesel + 10% bioethanol blend) showed a reduction in smoke and CO emissions but causes an increase in NO_x (Teoh *et al.*, 2019) across all the blends. A comparative research on performance and emission parameters of poon blended biodiesel at different ratios, neat (P100), 40% biodiesel, P40 and 20% biodiesel, P20 of Poon biodiesel showed a general reduction in CO₂, CO and hydrocarbons but increase in NO_x (Devan and mahalahkshmi, 2009). Further, study during the combustion of bio-oil, there is a net zero CO₂ as well as lesser NO_x and/or SO_x emissions as compared to fossil fuels (Faizal and Ateeb, 2018; Saroya *et al.*, 2018). This makes it a potential liquid fuel replacement (Varuvel *et al.*, 2012). Biodiesel and fossil diesel blends, no research has extensively been performed so far on the nature of radicals immobilized on thermal char, particulate characterization, and molecular emissions of binary transport fuels reported in this work.

2.2. Transesterification of bio-oil

Biodiesel is a renewable energy resource obtained from conversion of animal fats, plant based oils, waste oils, microalga and other microbes through transesterification or pyrolysis of biomass materials (Rodionova *et al.*, 2017). Transesterification reaction involves reaction of plant oils or animal fats in presence of alcohol and a catalyst. Batch transesterification (Figure 2.1) reaction involves proper control of temperature in order to obtain total conversion of triglycerides (De *et al.*, 2016).

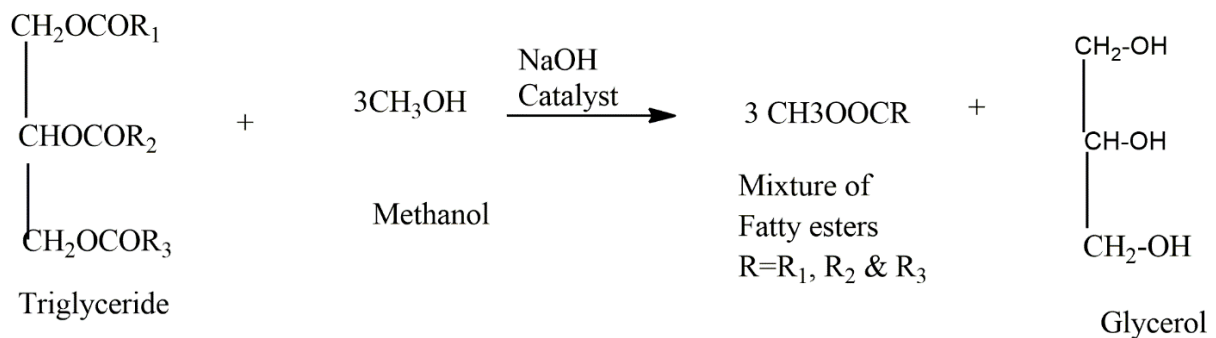


Figure 2.1: Batch transesterification chemical reaction (Opondo, 2010).

Transesterification is most preferred method for conversion of bio-oil to biodiesel (Venkatesan and Sivamani, 2019). These fats and oils constitute glycerides of various fatty acids which are normally referred to as Triglycerides. The biodiesel obtained is more or less the same with the fossil diesel in the performance (Mahmudul *et al.*, 2017). The challenge in deriving biodiesel is high viscosity, easily oxidized, low calorific, gum formation, free fatty acids and freezing at very low temperatures as opposed to fossil diesel (Yusuf *et al.*, 2011).

Transesterification of the bio-oil is aimed at solving the problem of viscosity hence improve performance when applied to internal combustion engines and other heat systems. Biodiesels which is normally referred to as alkyl esters are derived from reaction of triglycerides with methanol in presence of a catalyst (dos Santos *et al.*, 2017). Catalyst are used to speed up the transesterification process which could have otherwise be a slow process (Tran *et al.*, 2017). Catalysts used in transesterification can either be alkaline, enzymatic or acidic in nature (Tacias-Pascacio *et al.*, 2019). The use alkaline catalysts is most preferred than acid catalyst because of their high solubility in alcohol hence increasing the rate of reaction (Borges and Díaz, 2012). However, this method suffers some setbacks due to difficulty in recovery of biodiesel since the final products are homogeneous (Mumtaz *et al.*, 2017). The alkaline catalysts commonly used are NaOH and KOH with methanol, ethanol, and/or butanol (Verma and Sharma, 2016; Maitera *et al.*, 2017). The general transesterification process shown in Scheme 1.1 involve the use of methanol and NaOH as the case in most reactions and this study.

2.3 Biodiesel fuel

Biodiesel consists of mono-alkyl esters of fatty acids extracted from animal fats, vegetable oils such as sunflower oils, canola oils, palm oils etc. and from non-edible oils from *C. megalocarpus*, olive and castor seed oils (Singh and Dipti, 2010). Use of non-edible seed oil is economical in the sense that food oils will be preserved for human consumption and avoid rise in food prices due to competition. Biodiesels are produced through trans-esterification of triglycerides extracted from a variety of bio-lipids (Cooney and Young, 2013). Biodiesel can be used in its pure form or it can be blended with petroleum diesel, which is a common practice.

Biodiesel production that meets American Society for Testing and Materials D 6751 (ASTM D 6751) standards requires the oil or fats to be processed in order to reduce its viscosity. Methods that can be used to reduce viscosity include micro emulsification, pyrolysis and trans-esterification (Ramalingam *et al.*, 2018). Fuel obtained through Trans-esterification has been found to meet ASTM's definition of biodiesel (Ma and Hanna, 1999). It involves reacting the fat or oil with an alcohol, in the presence of a catalyst to produce glycerol and esters (Larson, 2006). Biodiesel properties depend on the chemical composition and content of fatty acid esters from plant oil or animal fats origin (Sajjadi *et al.*, 2016). Most fatty acids have carbon chain length in the range of 16-18 whose physical properties correspond to fossil

fuels' 10-20 carbon atoms (Shahir *et al.*, 2014). The oil extracted from *C. megalocarpus* seeds can be recovered up to 97 % by weight as biodiesel through trans-esterification and can be used in diesel engines or other applications (Kumar *et al.*, 2008). Despite availability of several studies on biodiesel modelled compounds and their reaction mechanisms, the experimental data on biodiesel blends as transport fuels is limited in literature. A number of studies have focused on smaller methyl esters such as methyl butanoate, methyl crotonate, methyl decenoate and methyl decanoate (Fisher *et al.*, 2000; Sarathy *et al.*, 2007; Sarathy, 2010; Westbrook *et al.*, 2011; Alfazazi *et al.*, 2015). This study invests on the co-pyrolysis of *C. megalocarpus* biodiesel and commercial diesel blends to explore their interaction behaviour and distribution of molecular by-products with pyrolysis temperature, radical intermediates, char and optimization of transport fuels. Because of the complex composition of fuels, kinetic modelling of its pyrolysis reaction products requires a high dimensional approach of differential equations. Therefore, modelling and simulation could be the best option towards understanding the thermochemical reaction mechanism and optimization of pyrolysis processes (Yue *et al.*, 2014). As a result, numerous modelling works on pyrolysis have been carried out dealing with a range of parameters including convectional heat transfer (Moghtaderi, 2006), particle size, residence time, vapour condensation (Papadikis *et al.*, 2010) and chemical kinetics (Thunman *et al.*, 2002).

2.4 Types of biofuels

There is increase search for alternative renewable energy resource. Biomass derived fuels is any solid, liquid, or gaseous fuel produced from organic matter (Demirbas, 2008). Biofuels can take different forms depending on feedstock used and method of processing (Ambat *et al.*, 2018) and can be produced either directly from plants or indirectly from industrial, commercial, domestic, or agricultural wastes (Aladin, 2017). Biofuels can be classed into different types according to the feedstock used, such as first, second and third generation (Aro, 2016). The first generation biofuels are obtained from edible feedstocks such as those from corn, sunflower, sugarbeets, barley and sugarcane (Alalwan *et al.*, 2019). This kind of biofuel may result into a challenge towards food competition, which is why it is a concern for food stability in society (Anuar and Abdullah, 2016). Second generation biofuels offers an alternative to first generation biofuels and municipal solid wastes. Thus, second generation biofuels are those obtained from non-edible biomass (EASAC, 2012). However, second generation biofuels still pose a challenge towards food production in terms of land use (Bai *et al.*, 2016). This can be managed by use of proper land management skills. Third generation

biofuels are biofuels generated from algal feedstocks. This is one of the recent research areas in biofuel production (Leong *et al.*, 2018).

There are three main methods for the development of biofuels: the burning of dry organic wastes such as household refuse, industrial and agricultural wastes, straw, wood, and peat (dos Santos *et al.*, 2016); the fermentation of wet wastes for instance animal waste in the absence of oxygen to produce biogas (Kougias and Angelidaki, 2018), or the fermentation of sugarcane or corn to produce alcohol and esters (Botton *et al.*, 2018); and energy forestry (Toklu, 2017). Biodiesel is one of the biofuels produced by conversion of plant based oils, animal fats and recycled cooking oils through transesterification process (Kayode and Hart, 2019). There are variety of plants that are used in generation of biodiesel which include *Jatropha carcus* (Thapa *et al.*, 2018), *Croton megalocarpus* (Aziz *et al.*, 2017), sunflower (Marinkovic *et al.*, 2016), soya (Can *et al.*, 2016), Rapeseed (Dieng *et al.*, 2019), castor (Keera *et al.*, 2018), palm and peanut (Moyib and Omotola, 2018). Use of non-edible oils and fats such as *Jatropha carcus*, *Croton megalocarpus* and castor is economical since they do not pose any competition with edible oils sunflower, soya and peanut.

The advantages of using biodiesel includes renewability and sustainability, minimum environmental pollutants such as sulphur-free, less carbon monoxide, hydrocarbons, particulate matter and aromatic compound emissions (Kesieme *et al.*, 2019), improves earning livelihoods of the population (Renzaho *et al.*, 2017), Can be used in unmodified diesel engines (Mahmudul *et al.*, 2017), they are not affected by external market prices and they are biodegradable and safe for use (Kharina *et al.*, 2018). On the other hand, biofuels have experienced great challenges, these includes high viscosity and ageing problems (Datta *et al.*, 2019), release of a lot of char and tar deposits in the engine due poor combustion thus causing the filter to clog and eventually engine knocks (Laksmono *et al.*, 2013).

2.5 Pyrolysis

Pyrolysis can be defined as the direct decomposition of an organic matrix or model biomass materials to obtain an array of reaction products in limited oxygen. Generally, biomass pyrolysis remains a critical chemical process in the utilization of renewable energy from feed stocks (Shin *et al.*, 2001; Jiang *et al.*, 2010). The main by-products from biomass pyrolysis include liquid oil, charcoal and gases depending on operating conditions such as temperature, particle size, heating rate and reactor configuration (Yaman, 2004). Based on the heating rate and temperature, pyrolysis can be of two forms; conventional pyrolysis and fast pyrolysis

(Jairul *et al.*, 2012). Fast pyrolysis is defined as the process in which the biomass is heated at a high heating rate within a short period of time in the absence of oxygen (Mohan *et al.*, 2006; Ciesielski *et al.*, 2018). Slow pyrolysis processes are performed at low heating rates and a long residence time (Sharma *et al.*, 2015). Long residence times can cause secondary cracking of the primary products thus reducing the yield, affects biofuel properties and may increase energy input (Amin and Prabandono, 2017). The preferred technology therefore is fast or flash pyrolysis at high temperatures with very short residence times (Demirbas, 2004).

2.5.1 Pyrolysis of binary mixture of *Croton megalocarpus* biodiesel and fossil diesel.

Diesel engines powered by fossil fuels are known to emit enormous particulate matter, nitrogen oxides and greenhouse gases (Shahsavari and Akbari, 2018). Therefore, there is need to develop a cleaner energy resource. Biodiesel has been shown to reduce environmental pollutants such particulate matter, carbon monoxide and unburned hydrocarbons (Chhetri and Islam, 2008; Damanik *et al.*, 2018; Zhang *et al.*, 2018). The hydrocarbon emissions has been shown in research to decrease when binary diesel is used instead of pure fossil diesel (Hasan and Rahman, 2017;) In general, volatile organic compounds (VOCs) from the thermal decomposition of organic matrices are considered toxic to biological systems and the natural environment (Vallero, 2019). Fuel biodiesel could be utilized in pure form or in blends (Suresh *et al.*, 2018) in compression-ignition engines without major modification (Hasan and Rahman, 2017). To comprehensively evaluate the importance of emission reduction measures on a fuel, various studies on fuel emissions characterization have been carried out (San José *et al.*, 2018). However, this study seeks to determine the nature of molecular organic emissions produced by the co-pyrolysis of *C. megalocarpus* biodiesel blends and compare them with the neat fuels in order to make an informed choice of a viable clean energy resource. *Croton megalocarpus* plant is a common plant that grows in the wild and diverse climate conditions in Kenyan and produce non-edible oil which offers a competitive energy resource since competition with edible oils is minimal.

2.5.2 Solid particulate matter

The side-effects of pyrolysis incorporate different particulate issue, for example, fluid beads, mist concentrates, sediment, smoke, exhaust, debris and solids blends (Donahue, 2018). Warm singe is a vaporized of fluid beads (the particulate stage) suspended inside a blend of gases and semi-unstable mixes accepted to contain surface headed radicals liable for genuine lung harm, and considered antecedents for an assortment of infirmities including malignancy and cardiopulmonary passings (Chen *et al.*, 2017). Particulate issue are grouped by size

primarily in view of the diverse wellbeing impacts related with them. Particulate issue that has a streamlined measurement of about 2.5 is named PM_{2.5} while those with 10 micrometers and less are named well as PM₁₀ (Tecer *et al.*, 2008). Particulate issue, PM_{2.5} is ultrafine and more poisonous than PM₁₀ in light of the fact that they have high infiltration power somewhere down in the lungs as well as alveolar covering (D'Amato *et al.*, 2016). Examination has demonstrated that PM₁₀ or PM_{2.5} can live in the lungs and result in gentle to extreme sickness and can cause genuine ailments and dangerous diseases (Terzano *et al.*, 2010, Chen *et al.*, 2018). A few epidemiological investigations have shown that nonstop presentation to high groupings of PM particularly ultrafine ones have a relationship with human respiratory and cardiovascular wellbeing dangers (Hosgood III *et al.*, 2011; Burnett *et al.*, 2014; Madaniyazi *et al.*, 2015; Maji *et al.*, 2018). Hence, the measurement of PM statement and their leeway in the human air-pathways are fundamental in assessing respiratory wellbeing dangers. Moreover, the pace of disposal of PM through procedures, for example, body digestion, synthetic activity and exhalation additionally influences the measure of PM clearing in the respiratory framework.

2.5.3 Biochars

Thermal decomposition of biomass in absence of oxygen or limited supply results in the formation of biochars among other by-products such as organic volatiles, and tar (Sfakiotakis and Vamvuka, 2018). Biochar is a porous carboneous solid containing embedded molecular funtional groups with high degree of aromatism and are resistant to decomposition (Richard *et al.*, 2016; Dey and Adhikary, 2020). Biochar has gained great interest in research due to its wide application in agriculture, environment and industry (Lehmann *et al.*, 2006). The major properties explored in the use of biochars in variuos sectors is the adsorption power, morphology of the chars (porosity and surface area) and the surface functional groups (Liu *et al.*, 2018). For instance, biochars adsorption capacity in the soil contributes to soil pH improvement, soil hydrological properties and soil nutrients enhancement (thus increasing crop yield) (Burrell *et al.*, 2016; Obia *et al.*, 2016; Suliman *et al.*, 2016). Furthermore, functional and charged groups present in the surface of the biochars is used in remediation of greenhouse gases by creating a permanent 'carbon sink' to mitigate against climate change, and pollutant adsorption, e.g. polycyclic aromatic hydrocarbons (PAHs) and soil heavy metals (SHMs) (Omondi *et al.*, 2016; Liu *et al.*, 2017; Wang *et al.*, 2019). Biochars can also be used as catalysts in industries (Lee *et al.*, 2017). Regardles of the many advantages it has, biochars may also contain organic compounds not limited to furans, aldehydes, polyaromatic

hydrocarbons (PAHS), ketones and persistent free radicals immobilised on the surfaces of biochars (Syed-Hassan *et al.*, 2017). The presence of this organic compounds and stable free radicals renders biochars unsafe for agricultural use and other applications (Hussain *et al.*, 2017). Therefore elemental analysis and characterisation is indispensable. Particulate size of the biochars are varied and they range from ultrafine particulates to coarse particulates (Maienza *et al.*, 2017). The ultrafine and fine particulates with aerodynamic diameter ranging from 1nm to 100 μm are a threat to human health and therefore, they are known to be among the precursors of respiratory ailments and cancer (Camatini *et al.*, 2017; Dubey *et al.*, 2018). The ultrafine ($<0.01\mu\text{m}$) and fine ($<2.5 \mu\text{m}$) particulates are known to travel deep into respiratory tissues and their clearance is difficult as compared to coarse ($< 10 \mu\text{m}$) (Li *et al.*, 2016).

2.5.4 Elemental composition of biochars

The thermal degradation of biomass at very high temperatures in absence or limited oxygen produces biochar as one of the by-products (Crombie *et al.*, 2013). Biochar is an acronym of biomass charcoal. Biochars are known to be highly carbonaceous, porous surface and high adsorption properties therefore, making it to be used in soil amendment and catalyst in industries (Khorram *et al.*, 2016; Najmi *et al.*, 2018; Weber and Quicker, 2018). Biochars are perfect in soil amendment not in adding carbon but its porous structure allows retention of water in the soil hence increasing the water holding capacity of the soil (Sun and Lu, 2014). Additionally, biochar morphology has active negative sites (functional groups) which binds nutrients such as magnesium, calcium and potassium (Archanjo *et al.*, 2017). This results in improvement of soil alkalinity which is favourable to most plants (Oliveira *et al.*, 2017). Further, biochar is used as bio-sorbent in remediation of inorganic and organic water contaminants (Awad *et al.*, 2017)

Biochars being by-products of biomass pyrolysed at very high temperatures is majorly carbonaceous with absence of polyaromatic compounds (PAHs) hence it is safe for use (Agarwal *et al.*, 2015). Biochars are known to have high carbon content that depend on the biomass used and low content of hydrogen and oxygen (Cha *et al.*, 2016). The levels of these elements in a particular biochar are majorly dependent on the pyrolysis temperatures, the type of pyrolysis whether slow or fast, and biomass feed used (Dhyani and Bhaskar, 2018).

Biochar mainly contains C, H, N, S, O and other trace elements depending the feedstock used and pyrolysis conditions (Lehmann *et al.*, 2011; Kim *et al.*, 2013; Kwak *et al.*, 2019). The

elemental quantification of carbon, hydrogen and nitrogen in biochars helps in understanding its quality (Yuan *et al.*, 2012). The elemental analysis is determined from their corresponding oxides, CO₂, H₂O and NO₂ respectively (Enders *et al.*, 2017). The carbon content for most biochars is quite (> 80 %) while hydrogen is found to be almost constant at 1.4 % and nitrogen and other organic materials are in trace amounts (Kim *et al.*, 2013). A study carried out of various biomass derived char (wood maize and meadow grass) showed that nitrogen content is below 2 % by wt, hydrogen content is more or less 2%, whereas oxygen content varies between 13% and 23% and carbon content varies between 44% and 64% (Břendová *et al.*, 2012).

Biochars are very stable in the soil environment and can remain unleached for very many years (Chen *et al.*, 2019). This property of biochars has been explored for use in soil sequestration. Additionally, the level of metals such as K, Na, Ca, Mg and Al in biochar vary with the biomass (Nanda *et al.*, 2013).

2.6 Kinetic modeling and computational chemistry

2.6.1 Radical kinetics

The kinetics of biomass decomposition is routinely predicted on a single reaction (Capart *et al.*, 2004; Várhegyi, 2007). A study carried out by Jiang demonstrated that most biomass fuels follow first order decomposition rate law (Jiang *et al.*, 2010). Moreover, the formation of char from various biomass materials is usually taken as or calculated to be first order by many studies (Jauhiainen *et al.*, 2004; Senneca, 2007; Naranjo *et al.*, 2012). Consequently, a global kinetic model was employed to obtain the kinetic parameters for the formation behaviour of pyrolysis products and environmentally persistent free radicals (Orfao *et al.*, 1999). Pseudo-unimolecular reactions were applied in which the empirical rate of decomposition of the initial product is first order as expressed by equation 2.1. In order to determine the kinetic characteristic behaviour of the free radicals, a pseudo-first order reaction kinetic model was employed in which the empirical equation 2.1 was used.

$$\ln C = \ln C_0 - kt \tag{2.1}$$

A plot of $\ln C$ as a function of time t (s), was generated as shown in Figure 3.5 (Chapter 3) from which the kinetic parameters: rate constant k and the original concentration (C_0) of free radicals in the thermal char in spins/g were determined. The conventional expression presented in equation 2.2 was used to compute the half-life decay of the free radicals.

$$t_{1/2} = \frac{\ln 2}{k}$$

2.2

2.6.2 Pyrolysis model

In order to examine the severity of secondary decomposition of char from diesel blend (co-pyrolysis of biodiesel and fossil diesel) pyrolysis, the characteristic time (t_{crack}), which is the reciprocal of rate constant (k_{TC}) in Arrhenius form, is usually estimated using the experimentally derived kinetic parameters ($A = 10^{14} s^{-1}$ and $E_a = 210 kJ/mol$) for vapour-phase cracking of eugenol, a typical biomass structural entity (Ledesma *et al.*, 2013; Xu *et al.*, 2017). The results showed that even at the highest temperature, i.e., 500 °C, the calculated characteristic time regarding tar cracking reactions was 2.2 s, which is fairly close to the gas-phase residence time (2 s) proposed in this study. Moreover, research on the secondary vapour phase reactions of biomass-derived oligomers demonstrated that it takes around 10 s for the molecular products to go above 90% decomposition at 500 °C (Zhou *et al.*, 2013). Therefore, the char cracking reactions were not considered in the pyrolysis model. The proposed pyrolysis model in this study consists of two lumped parallel reactions, with k_{PG} , and k_{PC} denoting the rate constants of gas and char formation respectively as presented in Figure 2.2

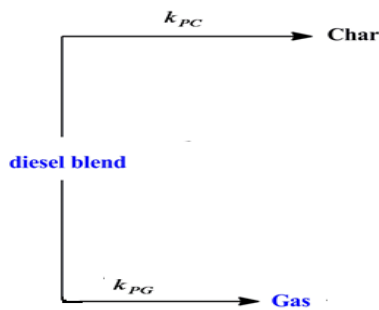


Figure 2.2: The kinetic model scheme for the co-pyrolysis of diesel blend (fossil diesel and bio-diesel)

2.7 Reactor design for the thermal degradation of biomass fuels

Many parameters influence the gas-phase thermal degradation of materials (Pielichowska and Pielichowski, 2014). Contact temperature, residence time, and the composition of gas-phase environment are three critical variables (Joseph *et al.*, 2016). A typical residence time is maintained for each run. The pyrolysis gas is usually varied in such a way that the residence time is held constant for every temperature change (Yaman, 2004). This is in accordance with the combined gas law (Dickerson *et al.*, 1979) (equation 2.3).

$$\frac{V_0 P_0}{T_0} = \frac{V_1 P_1}{T_1} \quad 2.3$$

where V is volume, P is pressure and T is temperature. The subscript 0 and 1 denote the ambient and reactor conditions respectively. By substituting V_1 with the volume of the reactor $\pi r^2 l$ and taking the flow through the reactor to be equal to $V_0 = F_0 t_0$, where F_0 and t_0 represent the flow rate and residence time respectively, the following relationship (equation 2.4) is established.

$$\frac{\pi r^2 l P_1}{T_1} = \frac{F_0 t_0}{T_0} \quad 2.4$$

The differential pressure, P_d , can be described as $P_1 - P_0$ if the resistance to the gas flow of the quartz tube reactor is much less than the sum of the downstream resistance to the gas flow (the transfer lines and the cryogenic trap). Consequently, the average residence time admitted to a high temperature tubular-flow reactor is described by equation 2.5

$$t_0 = \left(\frac{\pi r^2 L}{F_0} \right) \left(\frac{T_1}{T_0} \right) \left[1 + \frac{P_d}{P_0} \right] \quad 2.5$$

2.8 Computational chemistry

Computational science depends on electronic structure, quantum science (Lewars, 2015) and semi-observational models for ascertaining the required thermodynamics and motor boundaries. In these models, three dimensional structures of the burning species are indicated and its vitality structure is inferred (Batsanov and Batsanov, 2012; Canneaux *et al.*, 2014). Sub-atomic displaying contains every single hypothetical strategy and computational strategies used to show or copy the conduct of particles (Badrinarayan *et al.*, 2015). The techniques are applied in different computational fields which incorporate medication plan, computational science and material science for contemplating sub-atomic frameworks extending from little synthetic frameworks to huge organic particles (Rangel-Vázquez, 2015). The basic computations can be performed by hand, yet definitely PCs are required to perform atomic displaying of any framework (Mukesh and Rakesh, 2011).

2.8.1 The density functional theory (DFT)

Most of the equations presented in this section are obtained from references (McQuarrie and Simon, 1997); (Inostroza-Rivera *et al.*, 2012). Density functional theory is a highly accurate computational method which can be considered an improvement of the Hartree-Fock (HF)

theory where the many electron system of the electron correlation is modelled by a function of electron density (Ghosh *et al.*, 2018). Density functional theory is comparable to HF computationally but provides significantly better results and contains no approximations (Jensen, 2017). The electronic energy is written in the DFT application and expressed in terms of equation 2.6 (Ochterski 2000, Frisch *et al.*, 2004)

$$\varepsilon_{el}[p] = \varepsilon_l[p] + \varepsilon_J[P] + \varepsilon_X[P] + \varepsilon_C[P] \quad 2.6$$

where the square brackets represent a functional of the one-electron density $\rho(r)$. The first term on the right-hand side gives the one-electron energy, the second term is the Coulomb contribution, the third term the exchange and the fourth term gives the correlation energy (McQuarrie and Simon, 1997).

In discussing the nature of various functionals, it is convenient to adopt some of the notation commonly used in the field. For instance, the functional dependence of ε_{XC} on the electron density is expressed as an interaction between the electron density and an ‘energy density’ ε_{XC} that is dependent on the electron density (Kohn *et al.*, 1996), equation 2.7.

$$E_{XC[\rho(r)]} = \int \rho(r)\varepsilon_{XC}[\rho(r)]dr \quad 2.7$$

The energy density ε_{XC} is always treated as a sum of individual exchange and correlation contributions. Within this formalism, it is clear that the Slater energy density is given by equation 2.8.

$$\varepsilon_X[P(r)] = \frac{9\alpha}{\pi} \left(\frac{3}{\pi}\right)^{\frac{1}{3}} \rho^{\frac{1}{3}}(r) \quad 2.$$

Another convention expresses the electron density in terms of an effective radius such that exactly one electron would be contained within the sphere defined by that radius were it to have the same density throughout as its centre. This behaviour is given by equation 2.9.

$$rS = \left(\frac{3}{4\pi\rho(r)}\right)^{\frac{1}{3}} \quad 2.9$$

In defining spin density, the individual functionals of α and β (spin functionals) are used. The spin densities at any position are typically expressed in terms of ζ , the normalized spin polarization as presented in equation 2.10.

$$\zeta(r) = \frac{\rho^\alpha(r) - \rho^\beta(r)}{\rho(r)} \quad 2.10$$

so that the α spin density is simply one-half the product of the total ρ and $(\zeta + 1)$, and the β spin density is the difference between that value and the total ρ .

2.8.2 Chemissian software

Chemissian *ver.4.38* (Leonid (2012)) is a computational code for determining a molecule's electronic structure and vibrational spectra. It is used to develop molecular orbital energy-level diagrams (band-gap energies), simulated UV-Vis electronic spectra, natural transition orbitals and electronic and/or spin density maps. It has a user-friendly graphical interface and it can examine and visualize data from the output of quantum chemical program packages such as Gaussian. Chemissian computational program also helps to investigate the nature of transitions in UV-Vis spectra and the bonding nature of molecules (Wójcik *et al.*, 2013).

2.8.3 Multipath particle deposition model (MPPD)

The multiple Path Particle Deposition (MPPD) model was developed by Applied Research Associates, Inc. to mimic the respiration and clearance of particulates in human lungs. The MPPD model is a computational semi-empirical dosimetry model based on the physical and physiological parameters that govern the particulate matter transport within the respiratory tract (Zwozdziak *et al.*, 2017). Additionally, it predicts how the deposition fractions for variable particulate matter sizes get distributed and retained in the respiratory system. This model makes it possible for otherwise laboratory experiments that are tedious to be carried out. The main objective of this simulation is to predict the dosimetry of inhaled particles and establish regions in the respiratory tract where toxicity is likely to occur (Jebet *et al.*, 2018).

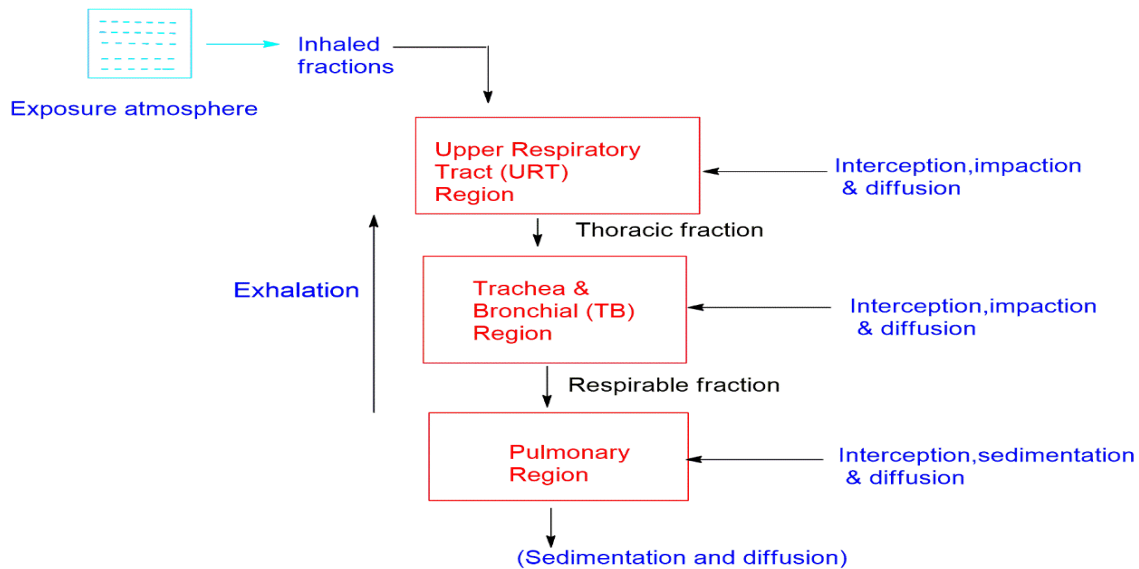


Figure 2.3: The fate of inhaled particles through different regions of the respiratory system based on mechanisms of transport and deposition (Asgharian *et al.*, 2018).

Dosimetry displaying may give an understanding structure to interspecies extrapolation, set presentation limits for normally happening prolonged mineral particles or new man-made extended mineral particles that might be made by ignition occasions, or in vivo to in vitro extrapolation of mechanical examines (Asgharian *et al.*, 2018). The circulation of breathed in particulate issue in the respiratory framework is summed up in Figure 2.3.

There are eight pathways accessible in the model. They incorporate, Yeh-Schum, stochastic, age-explicit, Weibel and Pacific Northwest National Laboratories models (Asgharian *et al.*, , 2018). Every one of these models fall under two classifications, single-way and multiple-path technique. Single way technique is utilized to assess particulate issue statement in a commonplace way though various ways are intended for all aviation routes of the lung. Lobar explicit affidavit is acquired distinctly in different way strategy. The estimation of PM testimony parts depends on statement efficiencies got hypothetically from different instruments, for example, dissemination, impaction, and sedimentation (Manojkumar *et al.*, 2019). The MPPD model offers hypothetical comprehension of medication conveyance i.e helps in tranquilize detailing and evaluation of viability and forecast of testimony of compound, natural, radiological and atomic operators in the respiratory tract (Asgharian, 2018).

2.9 The theory of electron paramagnetic resonance spectroscopy (EPR)

The term electron paramagnetic resonance refers to the resonant absorption of the electromagnetic radiation by electronic systems which possess permanent magnetic moments due to the orbital as well as spin angular momentum of electrons which are therefore paramagnetic (Lancaster, 1967, Kibet *et al.*, 2015). According to Lancaster (1967), for a free electron having a total angular momentum J situated in a magnetic field B , the energy levels are given by equation 2.11.

$$W_{MJ} = g\beta BM_J \quad 2.11$$

Accordingly, EPR is a spectroscopic method used to distinguish species having at least one unpaired electron (Kibet *et al.*, 2012). At the point when an outer attractive field is applied, the paramagnetic electrons can either arrange toward a path equal or against corresponding to the way of the attractive field (Assenheim, 2014). This wonder makes two distinctive vitality levels for the unpaired electrons, making it feasible for ingestion of electro-attractive radiation to happen when electrons are engaged between the two vitality levels as indicated expectedly in Figure 2.4, *vide infra*. The condition where the attractive field and the microwave recurrence produce retention is known as the reverberation condition (Slichter, 2013)

The g -factor is characteristic of EPR analysis. It is a dimensionless quantity proportional to the frequency and the magnetic field at resonance condition and is given by equation 2.12.

$$h\nu = g\mu_o B \quad 2.12$$

where h is Planck's constant (6.63×10^{-34} Js), ν is the frequency (Hz), μ_o is the Bohr magneton (9.27×10^{-24} J T⁻¹), and B is the magnetic field in Gauss.

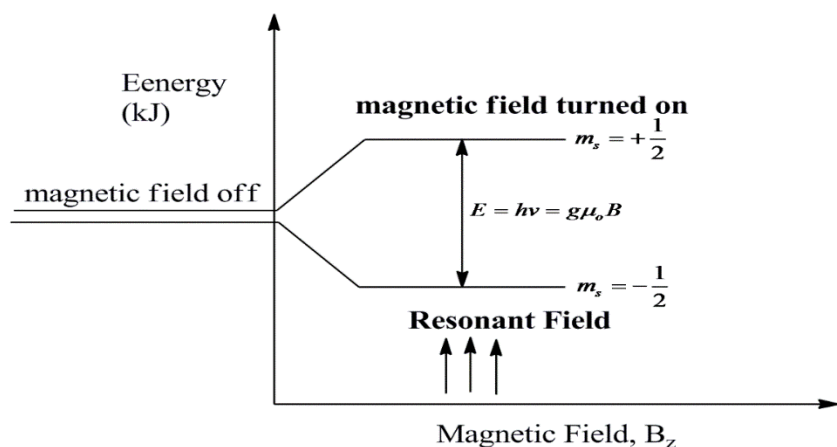


Figure 2.4: Energy levels for an electron spin ($m_s = \pm 1/2$) in an applied magnetic field, B_z . The g-factor (spectroscopic splitting factor) is given by the Lande's formula (equation 2.13):

$$g = 1 + \left[\frac{J(J+1) + S(S+1) - L(L+1)}{2J(J+1)} \right] \quad 2.13$$

where J and L are the orbital and the spin angular momenta respectively (Lancaster, 1967; Maskos *et al.*, 2008).

References

- Agarwal, A. K., Gupta, T., Shukla, P. C. and Dhar, A. (2015). Particulate emissions from biodiesel fuelled CI engines. *Energy Conversion and Management*, **94**: 311-330.
- Agarwal, D. and Agarwal, A. K. (2007). Performance and emissions characteristics of Jatropha oil (preheated and blends) in a direct injection compression ignition engine. *Applied Thermal Engineering*, **27**: 2314-2323.
- Aladin, A., Alwi, R. S. and Syarif, T. (2017). Design of pyrolysis reactor for production of bio-oil and bio-char simultaneously. In *American Institute of Physics Conference Series*, **1840**: 11. <https://doi.org/10.1063/1.4982340>.
- Alalwan, H. A., Alminshid, A. H. and Aljaafari, H. A. (2019). Promising evolution of biofuel generations. Subject review. *Renewable Energy Focus*, **28**: 127-139.
- Alfazazi, A., Sarathy, M. and Kuti, O. A. (2015). Modelling Ignition Processes of Palm Oil Biodiesel and Diesel Fuels Using a Two Stage Lagrangian Approach, SAE Technical Paper.
- Aliyu, B., Agnew, B. and Douglas, S. (2010). *Croton megalocarpus* (Musine) seeds as a potential source of bio-diesel. *Biomass and Bioenergy*, **34**: 1495-1499.
- Ambat, I., Srivastava, V. and Sillanpää, M. (2018). Recent advancement in biodiesel production methodologies using various feedstock: A review. *Renewable and Sustainable Energy Reviews*, **90**: 356-369.
- Amin, S. and Prabandono, K. (2017). Biodiesel Production from Microalgae. *Algal Biofuels* (66-102). Boca Raton, Florida, USA.
- Anuar, M. R. and Abdullah, A. Z. (2016). Challenges in biodiesel industry with regards to feedstock, environmental, social and sustainability issues: a critical review. *Renewable and Sustainable Energy Reviews*, **58**: 208-223.
- Archanjo, B.S., Mendoza, M.E., Albu, M., Mitchell, D.R., Hagemann, N., Mayrhofer, C., Mai, T.L.A., Weng, Z., Kappler, A., Behrens, S. and Munroe, P. (2017). Nanoscale analyses of the surface structure and composition of biochars extracted from field trials or after co-composting using advanced analytical electron microscopy. *Geoderma*, **294**: 70-79.
- Aro, E. M. (2016). From first generation biofuels to advanced solar biofuels. *Ambio*, **45**(1): 24-31.

- Asgharian, B., Owen, T. P. Kuempel, E. D. and Jarabek, A. M. (2018). Dosimetry of inhaled elongate mineral particles in the respiratory tract: The impact of shape factor. *Toxicology and Applied Pharmacology*, **361**: 27-35.
- Assenheim, H. M. (2014). *Introduction to electron spin resonance*. Springer. Science and Business Media.
- Awad, Y.M., Lee, S.E., Ahmed, M.B.M., Vu, N.T., Farooq, M., Kim, I.S., Kim, H.S., Vithanage, M., Usman, A.R.A., Al-Wabel, M. and Meers, E. (2017). Biochar, a potential hydroponic growth substrate, enhances the nutritional status and growth of leafy vegetables. *Journal of Cleaner Production*, **156**: 581-588.
- Aziz, M.A.A., Puad, K., Triwahyono, S., Jalil, A.A., Khayoon, M.S., Atabani, A.E., Ramli, Z., Majid, Z.A., Prasetyoko, D. and Hartanto, D. (2017). Transesterification of croton megalocarpus oil to biodiesel over WO₃ supported on silica mesoporous-macroparticles catalyst. *Chemical Engineering Journal*, **316**: 882-892.
- Badrinarayan, P., Choudhury, C. and Sastry, G. N. (2015). Molecular modeling. *Systems and Synthetic Biology*, Springer: 93-128.
- Bai, Y., Ouyang, Y. and Pang, J. S. (2016). Enhanced models and improved solution for competitive biofuel supply chain design under land use constraints. *European Journal of Operational Research*, **249**(1): 281-297.
- Batsanov, S. S. and Batsanov, A. S. (2012). *Introduction to Structural Chemistry*, Springer Science and Business Media.
- Borges, M. E. and Díaz, L. (2012). Recent developments on heterogeneous catalysts for biodiesel production by oil esterification and transesterification reactions: a review. *Renewable and Sustainable Energy Reviews*, **16**(5): 2839-2849.
- Botton, V., Piovan, L., Meier, H. F., Mitchell, D. A., Cordova, J. and Krieger, N. (2018). Optimization of biodiesel synthesis by esterification using a fermented solid produced by *Rhizopus microsporus* on sugarcane bagasse. *Bioprocess and Biosystems Engineering*, **41**: 573-583.
- Břendová, K., Tlustoš, P., Száková, J. and Habart, J. (2012). Biochar properties from different materials of plant origin. *European Chemical Bulletin*, **1**(12): 535-539.
- Burnett, R. T., Pope III, C. A., Ezzati, M., Olives, C., Lim, S. S., Mehta, S., Shin, H. H., Singh, G., Hubbell, B. and Brauer, M. (2014). An integrated risk function for estimating the global burden of disease attributable to ambient fine particulate matter exposure. *Environmental Health Perspectives*, **122**: 397-403.

- Burrell, L. D., Zehetner, F., Rampazzo, N., Wimmer, B. and Soja, G. (2016). Long-term effects of biochar on soil physical properties. *Geoderma*, **282**: 96-102.
- Busuru, C. (2018). *Propagation and regeneration of important indigenous tree species in Kakamega forest Kenya* (Doctoral dissertation, Egerton University).
- Camatini, M., Gualtieri, M. and Sancini, G. (2017). Impact of the Airborne Particulate Matter on the Human Health. *Atmospheric Aerosols*. (597-643). Wiley-VCH Verlag GmbH and KGaA, Zürich, Switzerland.
- Can, Ö., Öztürk, E., Solmaz, H., Aksoy, F., Çınar, C. and Yücesu, H. S. (2016). Combined effects of soybean biodiesel fuel addition and EGR application on the combustion and exhaust emissions in a diesel engine. *Applied Thermal Engineering*, **95**: 115-124.
- Canneaux, S., Bohr, F. and Henon, E. (2014). KiSThElP: A program to predict thermodynamic properties and rate constants from quantum chemistry results. *Journal of Computational Chemistry*, **35**(1): 82-93.
- Capart, R., Khezami, L. and Burnham, A. K. (2004). Assessment of various kinetic models for the pyrolysis of a microgranular cellulose. *Thermochimica Acta*, **417**: 79-89.
- Cha, J. S., Park, S. H., Jung, S. C., Ryu, C., Jeon, J. K., Shin, M. C. and Park, Y. K. (2016). Production and utilization of biochar: A review. *Journal of Industrial and Engineering Chemistry*, **40**: 1-15.
- Chen, C. W., Hsieh, Y. H., Su, H. C. and Wu, J. J. (2018). Causality test of ambient fine particles and human influenza in Taiwan: Age group-specific disparity and geographic heterogeneity. *Environment International*, **111**: 354-361.
- Chen, J., Li, C., Ristovski, E., Milic, A., Gu, Y., Islam, M. S., Wang, S., Hao, J., Zhang, H. and He, C. (2017). A review of biomass burning: Emissions and impacts on air quality, health and climate in China. *Science of The Total Environment*, **579**: 1000-1034.
- Chen, W., Meng, J., Han, X., Lan, Y. and Zhang, W. (2019). Past, present, and future of biochar. *Biochar*, **1**(1): 75-87.
- Chhetri, A. and Islam, M. (2008). Towards producing a truly green biodiesel. *Energy Sources, Part A* **30**: 754-764.
- Ciesielski, P. N., Pecha, M. B., Bharadwaj, V. S., Mukarakate, C., Leong, G. J., Kappes, B., Crowley, M. F., Kim, S., Foust, T. D. and Nimlos, M. R. (2018). Advancing catalytic fast pyrolysis through integrated multiscale modeling and experimentation:

- Challenges, progress, and perspectives. *Wiley Interdisciplinary Reviews: Energy and Environment*, **7**(4): e297. <https://doi.org/10.1002/wene.297>.
- Cooney, M. J. and Young, G. (2013). Methods and compositions for extraction and transesterification of biomass components. *U.S. Patent No. 8,598,378*. Washington, DC: U.S. Patent and Trademark Office.
- Crombie, K., Mašek, O., Sohi, S. P., Brownsort, P. and Cross, A. (2013). The effect of pyrolysis conditions on biochar stability as determined by three methods. *Gcb Bioenergy*, **5**(2): 122-131.
- D'Amato, G., Vitale, C., Lanza, M., Molino, A. and D'Amato, M. (2016). Climate change, air pollution, and allergic respiratory diseases: an update. *Current Opinion in Allergy and Clinical Immunology*, **16**(5): 434-440.
- Damanik, N., Ong, H. C., Tong, C. W., Mahlia, T. M. I. and Silitonga, A. S. (2018). A review on the engine performance and exhaust emission characteristics of diesel engines fueled with biodiesel blends. *Environmental Science and Pollution Research*: 1-19.
- Datta, A., Hossain, A. and Roy, S. (2019). An overview on biofuels and their advantages and disadvantages. *Asian Journal of Chemistry*, **31**: 1851-1858.
- de Oliveira, J. S., Leite, P. M., de Souza, L. B., Mello, V. M., Silva, E. C., Rubim, J. C., Meneghetti, S. M. and Suarez, P. A. (2009). Characteristics and composition of *Jatropha gossypifolia* and *C. megalocarpus* L. oils and application for biodiesel production. *Biomass and Bioenergy*, **33**: 449-453.
- Demirbas, A. (2004). Current technologies for the thermo-conversion of biomass into fuels and chemicals. *Energy Sources*, **26**: 715-730.
- Demirbas, A. (2008). Biofuels sources, biofuel policy, biofuel economy and global biofuel projections. *Energy Conversion and Management*, **49**: 2106-2116.
- Demirbas, M. F., Balat, M. and Balat, H. (2009). Potential contribution of biomass to the sustainable energy development. *Energy Conversion and Management* **50**: 1746-1760.
- De, R., Bhartiya, S. and Shastri, Y. (2016). Dynamic optimization of a batch transesterification process for biodiesel production. In *2016 Indian Control Conference (ICC)* (117-122). Institute of Electrical and Electronics Engineers.

- Devan, P. K. and Mahalakshmi, N. V. (2009). Performance, emission and combustion characteristics of poon oil and its diesel blends in a DI diesel engine. *Fuel*, **88**: 861-867.
- Dey, D. and Adhikary, T. (2020). A Preview on the Production Technologies of Biochar. *Biotica Research Today*, **2**: 210-213.
- Dhanamurugan, A. and Subramanian, R. (2015). Emission and Performance Characteristics of A Diesel Engine Operating on Diesel-Bael (*Aegle marmelos*) Biodiesel Blends. *Nature Environment and Pollution Technology*, **14**(2): 331- 336.
- Dickerson, R. E., Gray, H. B. and Haight, G. P. (1979). The Combined Gas Law. *Chemical Principles*, 105-122.
- Dieng, M. T., Iwanaga, T., Yurie, Y. C. and Torii, S. (2019). Production and Characterization of Biodiesel from Rapeseed Oil through Optimization of Transesterification Reaction Conditions. *Journal of Energy and Power Engineering*, **13**: 380-391.
- Dhyani, V. and Bhaskar, T. (2018). A comprehensive review on the pyrolysis of lignocellulosic biomass. *Renewable Energy*, **129**: 695-716.
- Donahue, N. M. (2018). Air Pollution and Air Quality. *Green Chemistry*, Elsevier: 151-176.
- dos Santos, R. G., Bordado, J. C. and Mateus, M. M. (2016). Potential biofuels from liquefied industrial wastes—Preliminary evaluation of heats of combustion and van Krevelen correlations. *Journal of Cleaner Production*, **137**: 195-199.
- dos Santos, R. J., Celante, D., Simoes, S. S., Bassaco, M. M., da Silva, C. and de Castilhos, F. (2017). Efficiency of heterogeneous catalysts in interesterification reaction from macaw oil (*Acrocomia aculeata*) and methyl acetate. *Fuel*, **200**: 499-505.
- Dubey, B., Pal, A. K. and Singh, G. (2018). Airborne particulate matter: source scenario and their impact on human health and environment. In *Climate Change and Environmental Concerns: Breakthroughs in Research and Practice* (447-468). IGI Global, United Kingdom.
- EASAC. (2012). The current status of biofuels in the European Union, their environmental impacts and future prospects. *EASAC Policy Report 19*. <http://www.easac.eu>.
- Enders, A., Sohi, S., Lehmann, J. and Singh, B. (2017). Total elemental analysis of metals and nutrients in biochar. *Biochar: a guide to analytical methods, 1st edn*. CSIRO Publishing, Clayton South, Melbourne Victoria, 95-108.

- Faizal, M. and Ateeb, S. (2018). Energy, Economic and Environmental Impact of Palm Oil Biodiesel in Malaysia. *Journal of Mechanical Engineering Research and Developments*, **41**(3): 93-95.
- Fazal, M. A., Rubaiee, S. and Al-Zahrani, A. (2019). Overview of the interactions between automotive materials and biodiesel obtained from different feedstocks. *Fuel Processing Technology*, **196**: 106178.
- Fekadu, M., Feleke, S. and Bekele, T. (2019). Selection of seed oil biodiesel producing tree species, emission reduction and land suitability. *Agricultural Engineering International: CIGR Journal*, **21**(4): 132-143.
- Fisher, E. M., Pitz, W. J., Curran, H. J. and Westbrook, C. K. (2000). Detailed chemical kinetic mechanisms for combustion of oxygenated fuels. *Proceedings of the Combustion Institute*, **28**: 1579-1586.
- Frisch, A., Frisch, M. J. and Trucks, G. W. (2003). *Gaussian 03 user's reference*, Gaussian, Incorporated.
- Frisch, M. J., Trucks, G. W., Schlegel, H. B., Scuseria, G. E., Robb, M. A., Cheeseman, J. R. and Millam, J. M. (2004). GAUSSIAN 03 (Revision D. 01) Wallingford. CT: *Gaussian Incorporated, Wallingford, Connecticut, U.S.A*, **26**.
- Ghosh, S., Verma, P., Cramer, C. J., Gagliardi, L. and Truhlar, D. G. (2018). Combining wave function methods with density functional theory for excited states. *Chemical Reviews*, **118**: 7249-7292.
- Hasan, M. and Rahman, M. (2017). Performance and emission characteristics of biodiesel–diesel blend and environmental and economic impacts of biodiesel production: A review. *Renewable and Sustainable Energy Reviews*, **74**: 938-948.
- Hosgood III, H. D., Wei, H., Sapkota, A., Choudhury, I., Bruce, N., Smith, K. R. and Lan, Q. (2011). Household coal use and lung cancer: systematic review and meta-analysis of case–control studies, with an emphasis on geographic variation. *International Journal of Epidemiology*, **40**: 719-728. <https://doi.org/10.1080/15567036.2019.1649759>.
- Inostroza-Rivera, R., Herrera, B. and Toro-Labbé, A. (2012). Applying Sanderson rules to the formation reaction of hydrogen-bonded dimers. *Computational and Theoretical Chemistry*, **990**: 222-226.
- Jahirul, M. I., Rasul, M. G., Chowdhury, A. A. and Ashwath, N. (2012). Biofuels production through biomass pyrolysis—a technological review. *Energies*, **5**(12): 4952-5001.

- Jauhiainen, J., Conesa, J. A., Font, A. and Martín-Gullón, I. (2004). Kinetics of the pyrolysis and combustion of olive oil solid waste. *Journal of Analytical and Applied Pyrolysis*, **72**: 9-15.
- Jebet, A., Kibet, J. K., Kinyanjui, T. and Nyamori, V. O. (2018). Environmental inhalants from tobacco burning: Tar and particulate emissions. *Scientific African*, **1**: e00004.
- Jensen, F. (2017). *Introduction to Computational Chemistry*. John Wiley & Sons.
- Jiang, G. Z., Nowakowski, D. J. and Bridgwater, A.V. (2010). A systematic study of the kinetics of lignin pyrolysis. *Thermochimica Acta*, **498**: 61-66.
- Jiang, G. Z., Nowakowski, D. J. and Bridgwater, A.V. (2010). Effect of the Temperature on the Composition of Lignin Pyrolysis Products. *Energy and Fuels*, **24**: 4470-4475.
- Joseph, P., Tretsiakova- McNally, S. and Zhang, R. (2016, April). Techniques for assessing the combustion behaviour of polymeric materials: some current perspectives and future directions. In *Macromolecular Symposia*, **362**:105-118.
- Kayode, B. and Hart, A. (2019). An overview of transesterification methods for producing biodiesel from waste vegetable oils. *Biofuels*, **10**(3): 419-437.
- Keera, S. T., El Sabagh, S. M. and Taman, A. R. (2018). Castor oil biodiesel production and optimization. *Egyptian Journal of Petroleum*, **27**: 979-984.
- Kesieme, U., Pazouki, K., Murphy, A. and Chrysanthou, A. (2019). Biofuel as an alternative shipping fuel: technological, environmental and economic assessment. *Sustainable Energy and Fuels*, **3**: 899-909.
- Kharina, A., Searle, S., Rachmadini, D., Kurniawan, A. A., & Prionggo, A. (2018). The potential economic, health and greenhouse gas benefits of incorporating used cooking oil into indonesia's biodiesel. *White Paper*, **26**.
- Kibet, J. K., Khachatryan, L. and Dellinger, B. (2012). Molecular products and radicals from pyrolysis of lignin. *Environmental Science Technology*, **46**:12994-13001.
- Kibet, J. K., Khachatryan, L. and Dellinger, B. (2015). Phenols from pyrolysis and co-pyrolysis of tobacco biomass components. *Chemosphere*, **138**: 259-265.
- Kim, K. H., Kim, T. S., Lee, S. M., Choi, D., Yeo, H., Choi, I. G. and Choi, J. W. (2013). Comparison of physicochemical features of biooils and biochars produced from various woody biomasses by fast pyrolysis. *Renewable Energy*, **50**: 188-195.
- Kipkore, W., Wanjohi, B., Rono, H. and Kigen, G. (2014). A study of the medicinal plants used by the Marakwet Community in Kenya. *Journal of Ethnobiology and Ethnomedicine*, **10**: 24. <https://doi.org/10.1186/1746-4269-10-24>.

- Kohn, W., Becke, A. D. and Parr, R. G. (1996). Density functional theory of electronic structure. *The Journal of Physical Chemistry*, **100**: 12974-12980.
- Khorram, M. S., Zhang, Q., Lin, D., Zheng, Y., Fang, H. and Yu, Y. (2016). Biochar: a review of its impact on pesticide behavior in soil environments and its potential applications. *Journal of Environmental Sciences*, **44**: 269-279.
- Kougias, P. G. and Angelidaki, I. (2018). Biogas and its opportunities—A review. *Frontiers of Environmental Science and Engineering*, **12**:14. <https://doi.org/10.1007/s11783-018-1037-8>.
- Kumar, R., Singh, S. and Singh, O. A. (2008). Bioconversion of lignocellulosic biomass: biochemical and molecular perspectives. *Journal of Industrial Microbiology and Biotechnology*, **35**(5): 377-391.
- Kwak, J. H., Islam, M. S., Wang, S., Messele, S. A., Naeth, M. A., El-Din, M. G. and Chang, S. X. (2019). Biochar properties and lead (II) adsorption capacity depend on feedstock type, pyrolysis temperature, and steam activation. *Chemosphere*, **231**:393-404.
- Laksmono, N., Paraschiv, M., Loubar, K. and Tazerout, M. (2013). Biodiesel production from biomass gasification tar via thermal/catalytic cracking. *Fuel Processing Technology*, **106**: 776-783.
- Lancaster, G. (1967). Electron Paramagnetic Resonance (A Review). *Journal of Materials Science*, **2**(5): 489-495.
- Larson, E. D. (2006). A review of life-cycle analysis studies on liquid biofuel systems for the transport sector. *Energy for Sustainable Development*, **10**: 109-126.
- Ledesma, E. B., Campos, C., Cranmer, D. J., Foytik, B. L., Ton, M. N., Dixon, E. A., Chirino, C., Batamo S. and Roy, P. (2013). Vapor-phase cracking of eugenol: distribution of tar products as functions of temperature and residence time. *Energy and Fuels*, **27**: 868-878.
- Lee, J., Kim, K. H. and Kwon, E. E. (2017). Biochar as a catalyst. *Renewable and Sustainable Energy Reviews*, **77**: 70-79.
- Lehmann, J., Gaunt, J. and Rondon, M. (2006). Bio-char sequestration in terrestrial ecosystems—a review. *Mitigation and Adaptation Strategies for Global Change*, **11**(2): 403-427.
- Lehmann, J., Rillig, M. C., Thies, J., Masiello, C. A., Hockaday, W. C. and Crowley, D. (2011). Biochar effects on soil biota—a review. *Soil Biology and Biochemistry*, **43**(9): 1812-1836.

- Leong, W. H., Lim, J. W., Lam, M. K., Uemura, Y. and Ho, Y. C. (2018). Third generation biofuels: A nutritional perspective in enhancing microbial lipid production. *Renewable and Sustainable Energy Reviews*, **91**: 950-961.
- Leonid, S. Chemissian v 4.38 2005–2010. <http://www.chemissian.com>.
- Lewars, E. G. (2011). Ab initio calculations. *Computational Chemistry*, Springer: 175-390.
- Li, N., Georas, S., Alexis, N., Fritz, P., Xia, T., Williams, M.A., Horner, E. and Nel, A., (2016). A work group report on ultrafine particles (American Academy of Allergy, Asthma & Immunology): Why ambient ultrafine and engineered nanoparticles should receive special attention for possible adverse health outcomes in human subjects. *Journal of Allergy and Clinical Immunology*, **138**(2): 386-396.
- Liu, Y., Lonappan, L., Brar, S. K. and Yang, S. (2018). Impact of biochar amendment in agricultural soils on the sorption, desorption, and degradation of pesticides: a review. *Science of the Total Environment*, **645**: 60-70.
- Liu, Z., Dugan, B., Masiello, C. A. and Gonnermann, H. M. (2017). Biochar particle size, shape, and porosity act together to influence soil water properties. *Plos one*, **12**(6). <https://doi.org/10.1371/journal.pone.0179079>
- Ma, F. and Hanna, M. A. (1999). Biodiesel production: a review. *Bioresource Technology*, **70**: 1-15.
- Madaniyazi, L., Nagashima, T., Guo, Y., Yu, W. and Tong, S. (2015). Projecting fine particulate matter-related mortality in East China. *Environmental Science and Technology*, **49**: 11141-11150.
- Madvar, M. D., Aslani, A., Ahmadi, M. H. and Ghomi, N. S. K. (2019). Current status and future forecasting of biofuels technology development. *International Journal of Energy Research*, **43**(3): 1142-1160.
- Mahmudul, H. M., Hagos, F. Y., Mamat, R., Adam, A. A., Ishak, W. F. W. and Alenezi, R. (2017). Production, characterization and performance of biodiesel as an alternative fuel in diesel engines. A Review. *Renewable and Sustainable Energy Reviews*, **72**: 497-509.
- Maienza, A., Genesio, L., Acciai, M., Miglietta, F., Pusceddu, E. and Vaccari, F. P. (2017). Impact of biochar formulation on the release of particulate matter and on short-term agronomic performance. *Sustainability*, **9**(7): 1131.

- Maitera, O. N., Louis, H., Dass, P. M., Akakuru, U. O. and Joshua, Y. (2017). Production and characterization of biodiesel from coconut extract (*Cocos nucifera*). *World News of Natural Sciences*, **9**: 62-70.
- Maji, K. J., Dikshit, A. K., Arora, M. and Deshpande, A. (2018). Estimating premature mortality attributable to PM_{2.5} exposure and benefit of air pollution control policies in China for 2020. *Science of The Total Environment*, **612**: 683-693.
- Manojkumar, N., Srimuruganandam, B. and Nagendra, S. S. (2019). Application of multiple-path particle dosimetry model for quantifying age specified deposition of particulate matter in human airway. *Ecotoxicology and Environmental Safety*, **168**: 241-248.
- Marinkovic, M. M., Stojkovic, N. I., Vasic, M. B., Ljupkovic, R. B., Rancic, S. M., Spalovic, B. R. and Zarubica, A. R. (2016). Synthesis of biodiesel from sunflower oil over potassium loaded alumina as heterogeneous catalyst: The effect of process parameters. *Hemijaska Industrija*, **70**: 639-648
- Maskos, Z., Khachatryan, L. and Dellinger, B. (2008). Formation of the persistent primary radicals from the pyrolysis of tobacco. *Energy and Fuels*, **22**: 1027-1033.
- McQuarrie, D. A. and Simon, D. J. (1997). *Physical Chemistry: a Molecular Approach*. Sausalito, CA, USA, Sterling Publishing Company.
- Moghtaderi, B. (2006). The state-of-the-art in pyrolysis modelling of lignocellulosic solid fuels. *Fire and Materials*, **30**: 1-34.
- Mohan, D., Pittman, C. U. and Steele, P. H. (2006). Pyrolysis of wood/biomass for bio-oil: a critical review. *Energy and Fuels*, **20**: 848-889.
- Moyib, O. K. and Omotola, O. E. (2018). Fatty acid methyl ester of Nigerian spent palm and peanut oils: Non-food option for biodiesel to safe food security and environment (Part I). *Journal of Applied Sciences and Environmental Management*, **22**: 797-802.
- Mukesh, B. and Rakesh, K. (2011). Molecular docking: a review. *International Journal of Research in Ayurveda and Pharmacy*, **2**(6): 1746-1751.
- Mumtaz, M. W., Adnan, A., Mukhtar, H., Rashid, U. and Danish, M. (2017). Biodiesel Production Through Chemical and Biochemical Transesterification: Trends, Technicalities, and Future Perspectives. In *Clean Energy for Sustainable Development* (465-485). Academic Press. USA.
- Najmi, N. H., Yunos, M., Diyana, N. F., Othman, N. K. and Asri Idris, M. (2018). Characterisation of reduction of iron ore with carbonaceous materials. In *Solid State Phenomena* (**280**: 433-439). Trans Tech Publications Ltd.

- Nanda, S., Mohanty, P., Pant, K. K., Naik, S., Kozinski, J. A. and Dalai, A. K. (2013). Characterization of North American lignocellulosic biomass and biochars in terms of their candidacy for alternate renewable fuels. *Bioenergy Research*, **6**(2), 663-677.
- Naranjo, R. A., Conesa, J. A., Pedretti, E. F. and Romero, O. R. (2012). Kinetic analysis: simultaneous modelling of pyrolysis and combustion processes of dichrostachys cinerea. *Biomass and Bioenergy*, **36**: 170-175.
- Obia, A., Mulder, J., Martinsen, V., Cornelissen, G. and Børresen, T. (2016). In situ effects of biochar on aggregation, water retention and porosity in light-textured tropical soils. *Soil and Tillage Research*, **155**: 35-44.
- Ochterski, J., W. (2000). Thermochemistry in gaussian. *Gaussian Inc, Pittsburgh, Pennsylvania, USA*: 1-17.
- Oliveira, F. R., Patel, A. K., Jaisi, D. P., Adhikari, S., Lu, H. and Khanal, S. K. (2017). Environmental application of biochar: Current status and perspectives. *Bioresource technology*, **246**: 110-122.
- Omondi, M. O., Xia, X., Nahayo, A., Liu, X., Korai, P. K. and Pan, G. (2016). Quantification of biochar effects on soil hydrological properties using meta-analysis of literature data. *Geoderma*, **274**: 28-34.
- Orfao, J., Antunes, F. and Figueiredo, J. L. (1999). Pyrolysis kinetics of lignocellulosic materials-three independent reactions model. *Fuel*, **78**: 349-358.
- Opondo, R. (2010). *Evaluation of transesterified waste vegetable oil for use as biodiesel fuel* (Doctoral dissertation, Egerton University).
- Papadikis, K., Gu, S. and Bridgwater, A. V. (2010). Computational modelling of the impact of particle size to the heat transfer coefficient between biomass particles and a fluidised bed. *Fuel Processing Technology*, **91**(1): 68-79.
- Pielichowska, K. and Pielichowski, K. (2014). Phase change materials for thermal energy storage. *Progress in Materials Science*, **65**: 67-123.
- Ramalingam, S., Ganesan, R., Rajendran, S. and Ganesan, P. (2018). A novel alternative fuel for diesel engine: a comparative experimental investigation. *International Journal of Global Warming*, **14**: 40-60.
- Rangel-Vázquez, N. A. (2015). Importance of molecular simulation for studying structural properties. *Material Science and Engineering with Advanced Research Journal*, **1**: 1-4.

- Renzaho, A. M., Kamara, J. K. and Toole, M. (2017). Biofuel production and its impact on food security in low and middle income countries: Implications for the post-2015 sustainable development goals. *Renewable and Sustainable Energy Reviews*, **78**: 503-516.
- Richard, S., Rajadurai, J. S. and Manikandan, V. (2016). Influence of particle size and particle loading on mechanical and dielectric properties of biochar particulate-reinforced polymer nanocomposites. *International Journal of Polymer Analysis and Characterization*, **21**(6): 462-477.
- Rodionova, M.V., Poudyal, R.S., Tiwari, I., Voloshin, R.A., Zharmukhamedov, S.K., Nam, H.G., Zayadan, B.K., Bruce, B.D., Hou, H.J.M. and Allakhverdiev, S.I. (2017). Biofuel production: challenges and opportunities. *International Journal of Hydrogen Energy*, **42**(12): 8450-8461.
- Ruhul, A. M., Kalam, M. A., Masjuki, H. H., Alabdulkarem, A., Atabani, A. E., Fattah, I. R. and Abedin, M. J. (2016). Production, characterization, engine performance and emission characteristics of *C. megalocarpus* and *Ceiba pentandra* complementary blends in a single-cylinder diesel engine. *RSC Advances*, **6**: 24584-24595.
- Sajjadi, B., Raman, A. A. A. and Arandiyani, H. (2016). A comprehensive review on properties of edible and non-edible vegetable oil-based biodiesel: composition, specifications and prediction models. *Renewable and Sustainable Energy Reviews*, **63**: 62-92.
- San José, J., Sanz-Tejedor, M. A. and Arroyo, A. (2018). Spray Characteristics, Combustion Performance, and Palm Oil Emissions in a Low-Pressure Auxiliary Air Fluid Pulverization Burner. *Energy and Fuels*, **32**: 11502-11510.
- Sánchez, N., Encinar, J. M., Nogales, S. and González, J. F. (2019). Biodiesel Production from Castor oil by Two-Step Catalytic Transesterification: Optimization of the Process and Economic Assessment. *Catalysts*, **9**(10): 864. <https://doi.org/10.3390/catal9100864>.
- Sarathy, S. M. (2010). *Chemical kinetic modeling of biofuel combustion* (Doctoral dissertation, University of Toronto).
- Sarathy, S., Gail, S. Syed, S. Thomson, M. and Dagaut, P. (2007). A comparison of saturated and unsaturated C 4 fatty acid methyl esters in an opposed flow diffusion flame and a jet stirred reactor. *Proceedings of the Combustion Institute*, **31**: 1015-1022.

- Saroya, S., Bansal, V., Gupta, R., Mathur, A. S. and Mehta, P. (2018, February). Comparison of Lipid Extraction from Algae (*Chlorella* Species) using Wet Lipid Extraction Procedure and Bligh and Dry Method. In *2018 IEEE International Students' Conference on Electrical, Electronics and Computer Science (SCEECS)*: 1-4.
- Senneca, O. (2007). Kinetics of pyrolysis, combustion and gasification of three biomass fuels. *Fuel Processing Technology*, **88**: 87-97.
- Sfakiotakis, S. and Vamvuka, D. (2018). Thermal decomposition behavior, characterization and evaluation of pyrolysis products of agricultural wastes. *Journal of the Energy Institute*, **91**(6): 951-961.
- Shahir, S. A., Masjuki, H. H., Kalam, M. A., Imran, A., Fattah, I. R. and Sanjid, A. (2014). Feasibility of diesel–biodiesel–ethanol/bioethanol blend as existing CI engine fuel: An assessment of properties, material compatibility, safety and combustion. *Renewable and Sustainable Energy Reviews*, **32**: 379-395.
- Shahsavari, A. and Akbari, M. (2018). Potential of solar energy in developing countries for reducing energy-related emissions. *Renewable and Sustainable Energy Reviews*, **90**:275-291.
- Sharma, A., Pareek, V. and Zhang, D. (2015). Biomass pyrolysis—A review of modelling, process parameters and catalytic studies. *Renewable and Sustainable Energy Reviews*, **50**: 1081-1096.
- Sharma, Y., Singh, B. and Upadhyay, S. (2008). Advancements in development and characterization of biodiesel: a review. *Fuel*, **87**: 2355-2373.
- Shin, E. J., Nimlos, M. R. and Evans, R. J. (2001). A study of the mechanisms of vanillin pyrolysis by mass spectrometry and multivariate analysis. *Fuel*, **80**: 1689-1696.
- Singh, S. and Dipti, S. (2010). Biodiesel production through the use of different sources and characterization of oils and their esters as the substitute of diesel: a review. *Renewable and Sustainable Energy Reviews*, **14**: 200-216.
- Slichter, C. P. (2013). *Principles of magnetic resonance*, Springer Science and Business Media.
- Suliman, W., Harsh, J. B., Abu-Lail, N. I., Fortuna, A. M., Dallmeyer, I. and Garcia-Perez, M. (2016). Influence of feedstock source and pyrolysis temperature on biochar bulk and surface properties. *Biomass and Bioenergy*, **84**: 37-48.

- Sun, F. and Lu, S. (2014). Biochars improve aggregate stability, water retention, and pore-space properties of clayey soil. *Journal of Plant Nutrition and Soil Science*, **177**(1): 26-33.
- Suresh, M., Jawahar, C. and Richard, A. (2018). A review on biodiesel production, combustion, performance, and emission characteristics of non-edible oils in variable compression ratio diesel engine using biodiesel and its blends. *Renewable and Sustainable Energy Reviews*, **92**: 38-49.
- Syed-Hassan, S. S. A., Wang, Y., Hu, S., Su, S. and Xiang, J. (2017). Thermochemical processing of sewage sludge to energy and fuel: Fundamentals, challenges and considerations. *Renewable and Sustainable Energy Reviews*, **80**: 888-913.
- Tacias-Pascacio, V. G., Torrestiana-Sánchez, B., Dal Magro, L., Virgen-Ortíz, J. J., Suárez-Ruíz, F. J., Rodrigues, R. C. and Fernandez-Lafuente, R. (2019). Comparison of acid, basic and enzymatic catalysis on the production of biodiesel after RSM optimization. *Renewable Energy*, **135**: 1-9.
- Tan, X., Liu, Y., Zeng, G., Wang, X., Hu, X., Gu, Y. and Yang, Z. (2015). Application of biochar for the removal of pollutants from aqueous solutions. *Chemosphere*, **125**: 70-85.
- Tecer, L. H., Süren, P. Alagha, O. Karaca, F. and Tuncel, G. (2008). Effect of meteorological parameters on fine and coarse particulate matter mass concentration in a coal-mining area in Zonguldak, Turkey. *Journal of the Air and Waste Management Association*, **58**: 543-552.
- Teoh, Y. H., How, H. G., Masjuki, H. H., Nguyen, H. T., Kalam, M. A. and Alabdulkarem, A. (2019). Investigation on particulate emissions and combustion characteristics of a common-rail diesel engine fueled with *Moringa oleifera* biodiesel-diesel blends. *Renewable Energy*, **136**: 521-534.
- Terzano, C., Di Stefano, F. Conti, V. Graziani, E. and Petroianni, A. (2010). Air pollution ultrafine particles: toxicity beyond the lung. *European Review for Medical and Pharmacological Sciences*, **14**: 809-821.
- Thapa, S., Indrawan, N. and Bhoi, P. R. (2018). An overview on fuel properties and prospects of *Jatropha* biodiesel as fuel for engines. *Environmental Technology and Innovation*, **9**: 210-219.

- Hussain, M., Farooq, M., Nawaz, A., Al-Sadi, A.M., Solaiman, Z.M., Alghamdi, S.S., Ammara, U., Ok, Y.S. and Siddique, K.H. (2017). Biochar for crop production: potential benefits and risks. *Journal of Soils and Sediments*, **17**(3): 685-716.
- Thunman, H., Leckner, B., Niklasson, F. and Johnsson, F. (2002). Combustion of wood particles—a particle model for Eulerian calculations. *Combustion and Flame*, **129**: 30-46.
- Toklu, E. (2017). Biomass energy potential and utilization in Turkey. *Renewable Energy*, **107**: 235-244.
- Tran, D. T., Chang, J. S. and Lee, D. J. (2017). Recent insights into continuous-flow biodiesel production via catalytic and non-catalytic transesterification processes. *Applied Energy*, **185**: 376-409.
- Vallero, D. A. (2019). Thermal pollution. *Waste (2nd Ed.)*: 381-404.
- Várhegyi, G. (2007). Aims and methods in non-isothermal reaction kinetics. *Journal of Analytical and Applied Pyrolysis*, **79**: 278-288.
- Varuvel, E. G., Mrad, N., Tazerout, M. and Aloui, F. (2012). Experimental analysis of biofuel as an alternative fuel for diesel engines. *Applied Energy*, **94**: 224-231.
- Venkatesan, H. and Sivamani, S. (2019). Evaluating the predicting capability of response surface methodology on biodiesel production from grapeseed bio-oil. *Energy Sources, Part A: Recovery, Utilization, and Environmental Effects*, 1-16.
- Verma, P. and Sharma, M. P. (2016). Review of process parameters for biodiesel production from different feedstocks. *Renewable and Sustainable Energy Reviews*, **62**: 1063-1071.
- Wang, B., Lee, X., Theng, B. K., Zhang, L., Cheng, H., Cheng, J. and Lyu, W. (2019). Biochar addition can reduce NO_x gas emissions from a calcareous soil. *Environmental Pollutants and Bioavailability*, **31**(1): 38-48.
- Weber, K. and Quicker, P. (2018). Properties of biochar. *Fuel*, **217**: 240-261.
- Westbrook, C. K., Naik, C. V., Herbinet, O., Pitz, W. J., Mehl, M., Sarathy, S. M. and Curran, H. J. (2011). Detailed chemical kinetic reaction mechanisms for soy and rapeseed biodiesel fuels. *Combustion and Flame*, **158**: 742-755.
- Wójcik, J., Peszke, J., Ratuszna, A., Kuś, P. and Wrzalik, R. (2013). Theoretical investigation of porphyrin-based photosensitizers with enhanced NIR absorption. *Physical Chemistry Chemical Physics*, **15**: 19651-19658.

- Xu, M. X., Khachatryan, L., Kibet, J. and Lomnicki, S. (2017). Lumped kinetic modeling of isothermal degradation of lignin under conventional pyrolytic and oxidative conditions. *Journal of Analytical and Applied Pyrolysis*, **127**: 377-384.
- Yaman, S. (2004). Pyrolysis of biomass to produce fuels and chemical feedstocks. *Energy Conversion and Management*, **45**: 651-671.
- Yuan, J. H., Xu, R. K. and Zhang, H. (2011). The forms of alkalis in the biochar produced from crop residues at different temperatures. *Bioresource technology*, 102(3): 3488-3497.
- Yue, D., You, F. and Snyder, S. W. (2014). Biomass-to-bioenergy and biofuel supply chain optimization: Overview, key issues and challenges. *Computers and Chemical Engineering*, **66**: 36-56.
- Yusuf, N. N. A. N., Kamarudin, S. K. and Yaakub, Z. (2011). Overview on the current trends in biodiesel production. *Energy Conversion and Management*, **52**(7): 2741-2751.
- Zaharin, M. S. M., Abdullah, N. R., Najafi, G., Sharudin, H. and Yusaf, T. (2017). Effects of physicochemical properties of biodiesel fuel blends with alcohol on diesel engine performance and exhaust emissions: A review. *Renewable and Sustainable Energy Reviews*, **79**: 475-493.
- Zhang, Y., Lou, D. Tan, P. and Hu, Z. (2018). Particulate emissions from urban bus fueled with biodiesel blend and their reducing characteristics using particulate after-treatment system. *Energy*, **155**: 77-86.
- Zhou, S., Garcia-Perez, M., Pecha, B., McDonald, A. G., Kersten, S. R. and Westerhof, R. J. (2013). Secondary vapor phase reactions of lignin-derived oligomers obtained by fast pyrolysis of pine wood. *Energy and Fuels*, **27**: 1428-1438.
- Zwozdziak, A., Gini, M. I., Samek, L., Rogula-Kozłowska, W., Sowka, I. and Eleftheriadis, K. (2017). Implications of the aerosol size distribution modal structure of trace and major elements on human exposure, inhaled dose and relevance to the PM_{2.5} and PM₁₀ metrics in a European pollution hotspot urban area. *Journal of Aerosol Science*, **103**: 38-52.

CHAPTER THREE

ENVIRONMENTALLY PERSISTENT FREE RADICALS AND PARTICULATE EMISSIONS FROM THE THERMAL DEGRADATION OF *Croton megalocarpus* BIODIESEL

Abstract

Pyrolysis of biodiesel at high temperatures may bring about the arrangement of transient and stable free radicals immobilized on particulate discharges. Thus, free radicals adsorbed on particulates are accepted to be precursors for wellbeing related sicknesses, for example, malignant growth, cardiac arrest, and oxidative pressure. This study investigates the nature of free radicals and particulate outflows created when *Croton megalocarpus* biodiesel is pyrolysed at 500 °C in an inert environment of streaming nitrogen at residence time of 0.5 s at 1 atm. The Molecular components of *C. megalocarpus* biodiesel was determined using GC hyphenated to a mass selective detector (MSD). The surface morphology of thermal outflows were imaged using a field emission gun scanning electron microscope (FEG SEM) while radical parameters were examined using an electron paramagnetic resonance spectrometer (EPR). The GC-MS output showed that the major components of *C. megalocarpus* biodiesel were majorly long chain hydrocarbon methyl esters, with methyl palmitate being predominant. The EPR results showed g-value of 2.0024 associated with a narrow ΔH_{p-p} of 3.65 G. The decay rate constant for the radicals was low ($1.86 \times 10^{-8} s^{-1}$) while the half-life was long ≈ 431 days. The observed EPR characterization of *C. megalocarpus* thermal particulates revealed the existence of free radicals typical of those found in coal. The low g-value and low decay rate constant suggests that the free radicals in particulates are possibly carbon-centred. The mechanistic channel for the formation of croton char from model biodiesel component (9-dodecenoic acid, methyl ester) has been proposed in this study. The SEM results indicated that the particulate size for *C. megalocarpus* was found to be ultrafine, approx. 22.90 ± 2.82 nm. These particulates are very minute and they can travel deep into the respiratory system thereby causing respiratory relate ailments.

Keywords: Biodiesel, Free radicals, Half-life, Thermal emissions, Pyrolysis.

3.1 Introduction

The *Croton megalocarpus* plant belongs to the Euphorbiaceae family (Maroyi, 2017). Other local names of the plant in Kenya include; Mukinduri (Kikuyu), Otwet (Kipsigis), Otonwe (Tugen), Mangkoit (Pokot), Muuti (Meru), muthulu (kamba). They make up to around 1,300

species, and are generally distributed in the tropical and sub-tropical regions of the world (Salatino *et al.*, 2007). The *C. megalocarpus* wood is hard and resistant to termites. These features are attractive for its use as timber and for poles used in fencing. *Croton megalocarpus* fruit contains three-ellipsoid or oblong-ellipsoid seeds which are rich sources of bio-oil, up to 30% by weight, and contain also proteins (Kivevele and Mbarawa, 2010). The high protein level in seed husks is potential for use in the manufacture of poultry feeds. Ground seeds have shown positive results in preliminary studies as chicken feed with no negative impacts on egg production and hatchability (Maroyi, 2017). The *C. megalocarpus* plant has therapeutic properties and it has been utilized to a great extent by indigenous people to treat a wide range of ailments (Maroyi, 2017; Gupta *et al.*, 2018). Furthermore, *C. megalocarpus* bio-oil is a rising star in the possibility for biofuel production, which has caught a lot of considerable attention in Africa (Wu *et al.*, 2013). Besides, the utilization of biodiesel as an option in contrast to petroleum-based diesel is accepted worldwide as an alternative renewable energy resource due to its prevention of health and environmental degradation (Kafuku *et al.*, 2010; Tan *et al.*, 2015). Besides, the utilization of biodiesel as an alternative to petroleum-based diesel is gaining worldwide interest because it promises to prevent both health and environmental degradation (Kafuku *et al.*, 2010; Tan *et al.*, 2015).

A useful by-product from non-edible oils pyrolysed at elevated temperatures is thermal char which has several applications ranging from agricultural practices- catalytic processes, water remediation among other uses (Varela *et al.*, 2013; Tan *et al.*, 2015). The nature of the functional groups adsorbed on thermal emissions is central in understanding the characteristic properties of *C. megalocarpus* char. Strangely, the native people of Kenya - the *Tugens* in particular, use *C. megalocarpus* char to treat wounds, lubricate cooking utensils, and soften hides and skins. The science behind these uses (by the *Tugens*) is not only yet to be understood, but also has not been well documented before in literature. This study, however; did not explore this type of chemistry but it investigated the characteristic properties and production of *C. megalocarpus* biodiesel particulates (thermal char).

Accordingly, this contribution explores the typical properties of environmentally persistent free radicals (EPFRs) and surface functionality of *C. megalocarpus* thermal emissions using electron paramagnetic resonance (EPR) spectroscopy and scanning electron microscopy (SEM) respectively. Both intermediate and surface bound free radicals are known to cause a variety of health conditions including cell oxidation and activation of numerous signalling

pathways involved in several human pathologies such as the aging process, promotion of cardiovascular diseases, and carcinogenesis (Bolton *et al.*, 2000; Valko *et al.*, 2016). Although prior examinations have thoroughly analysed the chemical composition of bio-oil, not very many investigations have been inspired to investigate the free radical characteristics and particulate emissions from the thermal decomposition of *C. megalocarpus* bio-oil (Kim *et al.*, 2015).

Past research has demonstrated that free radicals are even present in living plants and artificially extricated lignin (Hu *et al.*, 2012; Melkior *et al.*, 2012). Additionally, thermochemical transformation of biomass generates free radical intermediates in the gas-phase (Melkior *et al.*, 2012) though stable radicals are usually immobilized on the solid matter – thermal char and/or particulate emissions. This investigation aimed at establishing the type of free radicals, their concentration, and particulate size emitted during the production of *C. megalocarpus* char. Free radicals, if present in biodiesel particulate discharges may go about as antecedents for respiratory related maladies, for example, emphysema, interminable hacks, malignancies of the throat and larynx, and constant bronchitis (Kurgat *et al.*, 2016).

The presence of the most active free radicals and huge environmentally toxic by-products from the combustion of traditional fossil fuels has led to unprecedented atmospheric pollution and global warming and hence the increased interest in the search for alternative transport fuels from biomass materials (White *et al.*, 2011). Renewable fuels derived from biomass has desirable benefits which may eventually decrease the over reliance on fossil fuels without introducing new carbon dioxide to the atmosphere (White *et al.*, 2011; Varuvel *et al.*, 2012). The Kyoto Protocol and the need to reduce society 's reliance on crude oil have put urgent pressure on research aimed at developing efficient bio-oil resources for use as transport fuels in the current century and possibly in the centuries to come. (Corma *et al.*, 2007). This will be consistent with the 2015 Paris agreement on climate change. Commercial diesel engines are known to emit huge levels of particulate matter, NO_x, SO_x and hydrocarbons as opposed to biodiesel (Wood *et al.*, 2015). To this end, pyrolysis remains a critical chemical process in the utilization of renewable energy and pyrosynthesis of essential organic compounds (Jiang *et al.*, 2010; Shin *et al.*, 2001; Shen *et al.*, 2014; Wood *et al.*, 2015)

The generation of EPFRs on solid particulate matter has drawn significant research interests in recent times. EPFRs are well known combustion system reactive and toxic species

(Dellinger *et al.*, 2008; Khachatryan *et al.*, 2010). Persistent free radicals such as those detected in this study are highly aggressive and can cause severe oxidative stress, cell damage and obstructive pulmonary diseases (Khachatryan *et al.*, 2010; Gehling *et al.*, 2014). Free radicals are important precursors of reactive oxygen species (ROS) production in biological systems (Dellinger *et al.*, 2001). Reactive oxygen species, including lipids, proteins, and deoxyribonucleic acid (DNA), can contribute to severe oxidative stress within cells through the formation of oxidized cellular macromolecules (Moridani *et al.*, 2004).

This study presents one of the first comprehensive investigations of the thermal degradation of *C. megalocarpus* biodiesel. Therefore, the free radical chemistry presented in this study will inform further research into the potential use of *C. megalocarpus* char as a catalyst in various industrial processes, its use as an adsorbent and its use in agriculture (Qi *et al.*, 2017), given concerns that free radicals can trigger serious health and environmental impacts because it can precipitate NO_x emissions when it interacts with ammonia in the soil (Keiblinger *et al.*, 2018). In this investigation the concept and motivation to investigate, and establish the existence of particulates developed and free radicals produced during *C. megalocarpus* biodiesel thermal degradation is of primary importance. Deductions on the particulate size of emissions and the stability of free radicals produced during the thermal degradation of *C. megalocarpus* would be of interest to technological advancement.

3. 2 Materials and methods

3. 2.1 Sample collection and preparation

The *Croton megalocarpus* seeds were collected locally from the botanical garden at the Egerton University. Approximately 10.0 kg of *C. megalocarpus* seeds was weighed and oven dried at 110 °C for 8 hours. The seeds were allowed to cool then grounded and sieved to obtain uniform particle size of 50 microns. Commercial diesel was bought from a licensed petroleum dealer.

3.2.2 Bio-oil extraction

Bio-oil from *C. megalocarpus* seeds was extracted by solvent extraction method using *n*-hexane as the solvent (Kavunja, 2010). The ground dry seeds were refluxed with *n*-hexane in a soxhelt extractor for 4 hours (Keneni and Marchetti, 2017). After exhaustive extraction, the oil-hexane miscella was transferred to a rotary vacuum evaporator with the temperature of water bath set at 60 °C to remove *n*-hexane (Kedir, 2019). The oil yield was approximately 3.5 litres. The oil was then treated with 10 % (v/w) anhydrous sodium sulphate to remove

traces of water. The dry oil was weighed, bottled and stored in a freezer awaiting transesterification.

3.2.3 Extraction of biodiesel

The transesterification process was carried out as shown below and as described by Ma and Hanna (1999). For each sample of the oil, 100 mL was reacted with a solution of a predetermined amount of NaOH in 225 mL methanol (22.5 % by volume of oil) in a 2 liters quick-fit Erlenmeyer flask. A magnetic rod was placed inside the flask which was fitted with a double surfaced reflux condenser. The contents of the flask was heated in a hot plate magnetic stirrer (Stuart SB 162) with temperature set at 70 °C and magnetic revolutions at 700 rpm. The mixture was stirred and refluxed for 5 hours. The solution was then left to cool to room temperature and emptied into a 2 liters capacity separating funnel and left to stand for 12-20 hours. The mixture formed two layers, the bottom glycerol layer was drained and the crude ester layer was left in the separating funnel. The ester was purified by washing gently by sprinkling 20% (v/v) warm distilled water followed by draining the water from the bottom of the separating funnel. Rinsing was repeated until the discarded wash water reaches pH level of 6-7 and no soap bubbles appears. The ester was dried using 10 % (w/v) anhydrous Na₂SO₄ and stored in a freezer for fuel property analysis (Kanyua, 2016).

Ester conversion from the oil was tested in methanol; based on the fact that methyl esters are quite soluble in the methanol while triglycerides have a very low solubility. Exactly 27 mL of methanol was shaken with 3 mL of the ester sample at room temperature. Absence of oily material settling at the bottom of a test tube after 20 minutes indicated complete conversion of the oil into methyl esters.

3.2.4 Gas chromatography mass spectrometry (GC-MS) characterization of *Croton megalocarpus* biodiesel

The GC-MS characterization of biodiesel was done as shown below and was described in detailed by Kibet (2013). The *Croton megalocarpus* biodiesel (CMB) was characterized using an Agilent Technologies 7890A GC system connected to an Agilent Technologies 5975C inert XL Electron Ionization/Chemical Ionization (EI/CI) with a triple axis mass selective detector (MSD) on total ion current (TIC) mode, using a fused silica capillary column (cross-linked 5% phenyl methyl siloxane; 30 m x 250 µm, df 0.25 µm) (Hewlett-packard) was used. The temperature of the injector port was set at 250 °C to volatilize all the organic components so as to be amenable for GC analyses. Ultra high purity (UHP) helium

was used as the carrier gas at a flow rate of 3.3 mL/min. About 2 μ L of sample was injected in the split ratio 50:1 at 250 $^{\circ}$ C (Kibet *et al.*, 2019). The oven temperature was set at 50 $^{\circ}$ C for 3 minutes then raised to 10 $^{\circ}$ C /minute to 250 $^{\circ}$ C for 5 minutes, and held at 300 $^{\circ}$ C for 20 minutes. Electron Impact ionization energy of 70 eV was used. Of critical importance, the samples were run through the GC-MS in 3 replicates to ensure consistency in data collection. Standards of pure compounds were used to guarantee that the actual model compound of biodiesel was identified based on peak shapes, fragmentation pattern and retention times.

3.2.5 The combustion reactor system

The heater used in this investigation was a muffle furnace (Thermo-Scientific), USA, whose internal heating compartment has dimensions of 14 cm \times 12 cm \times 13 cm. The heater is fitted with a temperature regulating knob. The temperature of the heater ranges from 20 $^{\circ}$ C to 1000 $^{\circ}$ C. At the top of the heating compartment is a hole which allows the gas-phase trapping tube to pass through. The sample holder in the heating compartment was a quartz reactor of dimensions: 10 cm long with 1 cm internal diameter (volume \approx 7.85 cm³) which can withstand high temperatures of up to 1200 $^{\circ}$ C. The reactor assembly used in this study is presented in Figure 3.1. The transfer line was heated at about 200 $^{\circ}$ C to avoid condensation of particulates along the column.

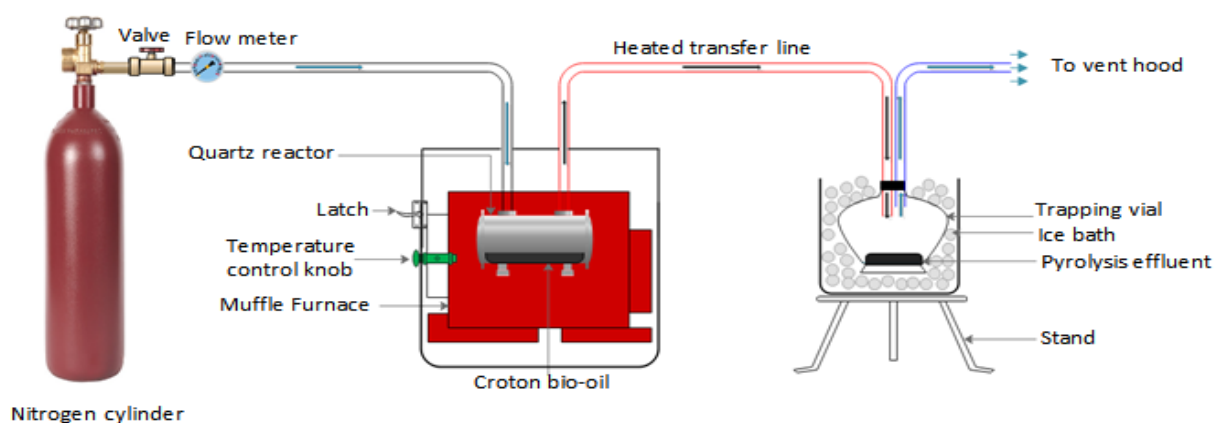


Figure 3.1: Reactor assembly and gas-phase trapping apparatus

In order to investigate the nature of particulate emissions and formation of free radicals, about 5 mL of *C. megalocarpus* bio-oil was placed in a quartz reactor housed in a muffle furnace (Thermo-Scientific Inc., USA). Pyrolysis was conducted at in a flow of nitrogen at a residence time of 0.5 sec at 1 atmosphere for a total pyrolysis time of 10 minutes. Ten replicates were conducted in this experiment. Particulate emissions were collected in a vial

immersed in an ice bath as shown in Figure 3.1 The thermal emissions condensed in the vial were weighed by the method of difference and carefully transferred into 2 mL crimp top amber vial for SEM and EPR spectroscopy. Each experiment yielded ~1.2 mg of particulates trapped in the vial immersed in the ice bath.

3.2.6 Electron paramagnetic resonance (EPR) spectroscopy

In order to determine the surface radical immobilization on *C. megalocarpus* char, approximately 5 mg sample of *C. megalocarpus* char particulates were analyzed using a Bruker EMX-20/2.7 X-band EPR spectrometer comprising of dual cavities, modulation and microwave frequencies of 100 kHz and 9.298 GHz respectively (Khachatryan *et al.*, 2010; Jebet, *et al.* 2017). The typical parameters were: sweep width of 200 G, EPR microwave power of 1–20 mW, and modulation amplitude of ≤ 6 G. The time constant was set at 16 sec while the sweep time was set at 30 sec. The g-factor was computed using Bruker's WINEPR program, which is a comprehensive line of software allowing control of the Bruker EPR spectrometer, data-acquisition, automation routines, tuning, and calibration programs on a Windows-based PC (Eaton *et al.*, 2010; Kibet *et al.*, 2012). The exact g-value for the key spectrum was determined by comparison with a 2,2-diphenyl-1-picrylhydrazyl (DPPH) standard (Adounkpe, *et al.*, 2008). The EPR runs were conducted in 3 replicates.

3.2.7 FTIR and scanning electron microscopy characterization of thermal emissions

Conventionally, absorption spectra were gathered utilizing an Agilent FTS 7000e FTIR bench top spectrometer outfitted with a fluid nitrogen-cooled mercury cadmium telluride finder and a warmed (65.1 °C) seven-reflection precious stone ATR gem (Concentrate IR, Harrick Scientific Products, Pleasantville, NY) (Gupta *et al.*, 2017). Attenuated total reflection Fourier-transform infrared (ATR-FTIR) spectroscopy was utilized in this examination. ATR-FTIR spectra (256 co-included outputs) were gathered at the 4 cm^{-1} goals over the wave number scope of 4,000–500 cm^{-1} at a normal of 4 sweeps (Kafuku *et al.*, 2010).

Then again, roughly 5 mg of test was set to aluminum SEM hits with carbon tape and in this manner gold covered in a Quorum Q150 RES falter coater. The examples were then imaged in a Zeiss Ultra Plus (Germany) field emission gun scanning electron microscope (FEG SEM). Energy dispersive X-ray (EDX) investigation was performed with Aztec (UK) programming software coupled to an Oxford detector (UK) (Corral, 2018).

3.3 Results and discussion

3.3.1 Molecular components of *Croton megalocarpus* biodiesel

The major components of *C. megalocarpus* biodiesel were found to be long chain hydrocarbon methyl esters. These components were characterized using GC hyphenated to a mass selected detector (MSD). To ensure the correct compounds were detected, standards were run through the GC-MS system under similar conditions as the sample and the retention times were compared. Replicate runs were conducted in order to enhance the integrity of the results. The GC-MS results are presented in Figure 3.2 and Table 3.1.

Table 3.1: Major molecular components of *C. megalocarpus* biodiesel characterized using GC-MS

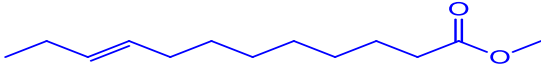
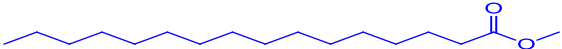
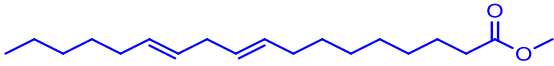
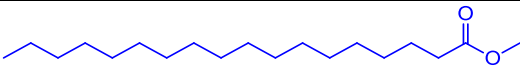
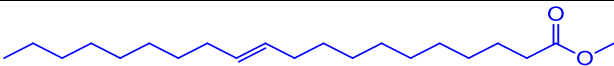
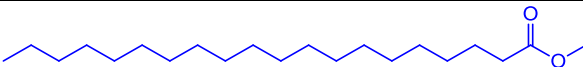
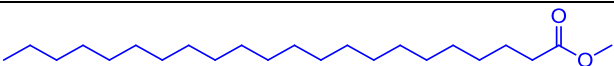
No.	RT (Mins.)	Molecular Structure	Compound name	Yield (μg)	MW (g/mol)
1.	12.46		(E)-methyl dodec-9-enoate	8.62 ± 1.42	212.18
2.	13.35		methyl palmitate	33.86 ± 3.04	270.26
3.	13.40		(9E,12E)-methyloctadeca-9,12-dienoate	7.23 ± 1.18	294.47
4.	14.06		methyl stearate	3.57 ± 0.84	298.50
5.	14.21		(E)-methyl icos-11-enoate	3.72 ± 0.82	324.54
6.	14.83		methyl icosanoate	4.94 ± 0.90	326.56
7.	15.56		methyl docosanoate	2.67 ± 0.46	354.35

Table 3.1 show that most of the model components in *C. megalocarpus* biodiesel are mainly terminal esters containing long chain hydrocarbons. This is consistent with literature reports (Kafuku *et al.*, 2010) whereby methyl palmitate was the major compound in the biodiesel, with a yield of $33.86 \pm 3.04 \mu\text{g}$ while methyl docosanoate was a minor component in the biodiesel matrix (yield, $2.67 \pm 0.46 \mu\text{g}$) as presented in Table 3.1. Compounds 1, 3 and 5 ((E)-methyl dodec-9-enoate, (9E,12E)-methyl octadeca-9,12-dienoate, and (E)-methyl icos-11-enoate) have C-C double bonds within the chain and may therefore be the most important precursors in the formation of char (thermal emissions from biodiesel).

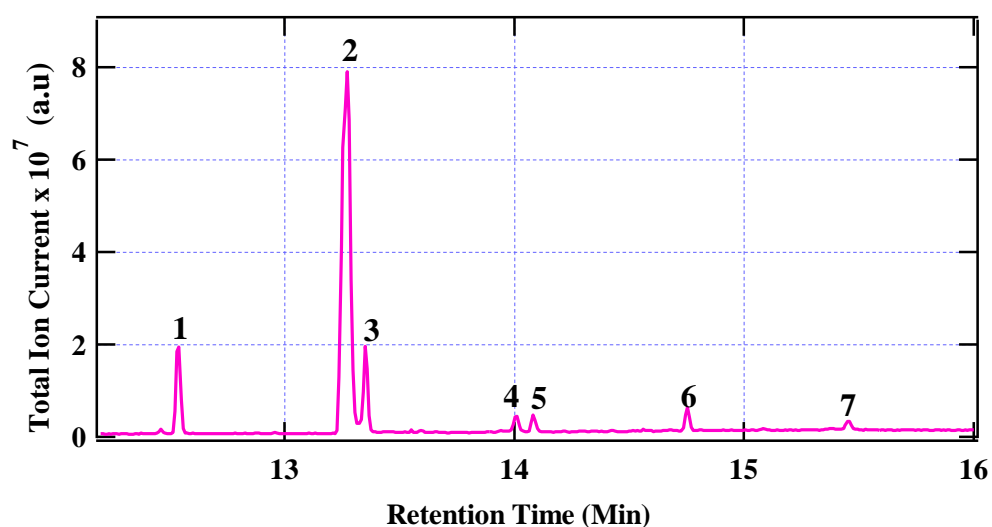
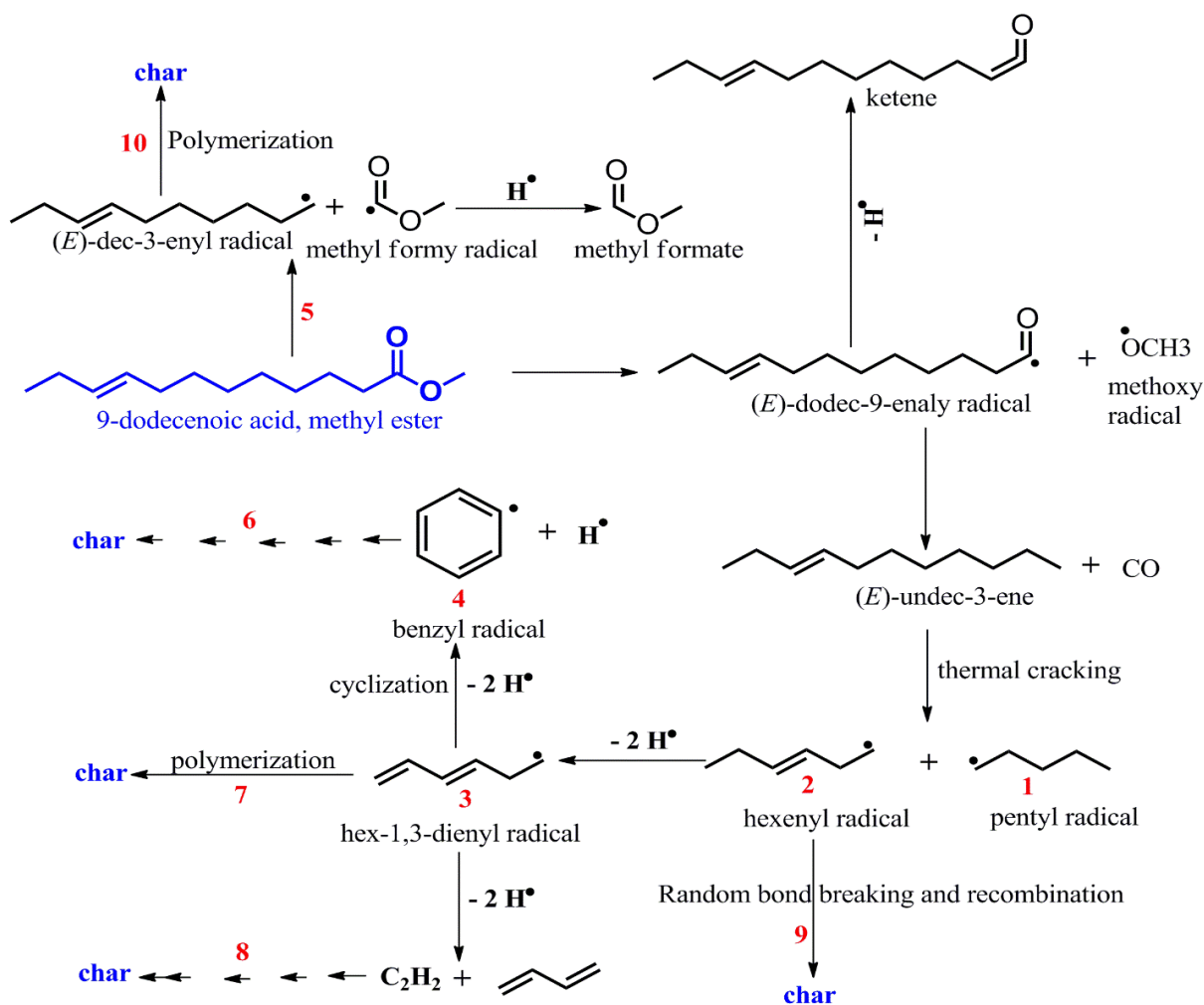


Figure 3.2: The Gas chromatogram showing the major components of *C. megalocarpus* biodiesel.

3.3.2 Mechanistic description for the formation of thermal char from model biodiesel compound

At elevated temperatures, the scission of the methoxy group occurs because it is the weakest bond in model ester compounds (Kim *et al.*, 2011). For simplicity, we will consider the formation of carbon-centred free radicals from model (Porterfield *et al.*, 2017) molecular component of croton biodiesel; (E)-methyl dodec-9-enoate.



Scheme 3.1: Proposed mechanistic pathways for the formation of carbon-centred free radicals from (E)-methyl dodec-9-enoate model compound.

The proposed channel for the formation of carbon centred free radicals; principal to this investigation is presented in Scheme 3.1. Evidently, at temperatures >500 °C, the carbon-centred radicals dominate while the oxygen-centred free radicals are significantly absent. This is consistent with literature reports that at about 500 °C, most oxygenated molecular by-products are completely evolved depending on the pyrolysis residence time (Sharma *et al.*, 2004; Porterfield *et al.*, 2017).

Longer residence times such as the one employed in this study will encourage the recombination of radical species through polymerization, rearrangement, and elimination of small molecules from the parent model compounds thus the probability of forming molecular species at high temperatures is small (Kibet *et al.*, 2012). Because of the high reactivity of OH and H radicals in the pyrolysis pool, oxygenated molecular products are rarely abundant

at temperatures $>500\text{ }^{\circ}\text{C}$ (Khachatryan *et al.*, 2003). Therefore, the thermal emissions formed at $600\text{ }^{\circ}\text{C}$ are primarily carbonaceous. From Scheme 3.1, it is clear that radicals 1-5 are carbon-centred and possibly among the most dominant free radicals in thermal emissions.

The formation of chars through polymerization is well captured in the scheme. Precursors such as methylene (C_2H_2) are also fundamental towards the formation of chars (Chhiti *et al.*, 2012). Reactions 6-7 (cf. Scheme 3.1) are predicted to lead to the formation of char from biodiesel. We are aware that many possible other reactions including oxidation and gasification are at play during the formation of char from biodiesel. Nonetheless, the example provided gives a hint of the various channels that initiate char formation from biodiesel.

3.3.3 Electron paramagnetic resonance (EPR) analysis

The EPR spectrum for *C. megalocarpus* particulates appears to be similar to what is observed in coals although they have significantly lower spin densities (Petrakis and Grandy, 1981). In this study, the radicals detected in *C. megalocarpus* particulates are believed to be radical centres on polyaromatic hydrocarbons which may also have varying spin densities on heteroatoms such as oxygen and nitrogen.

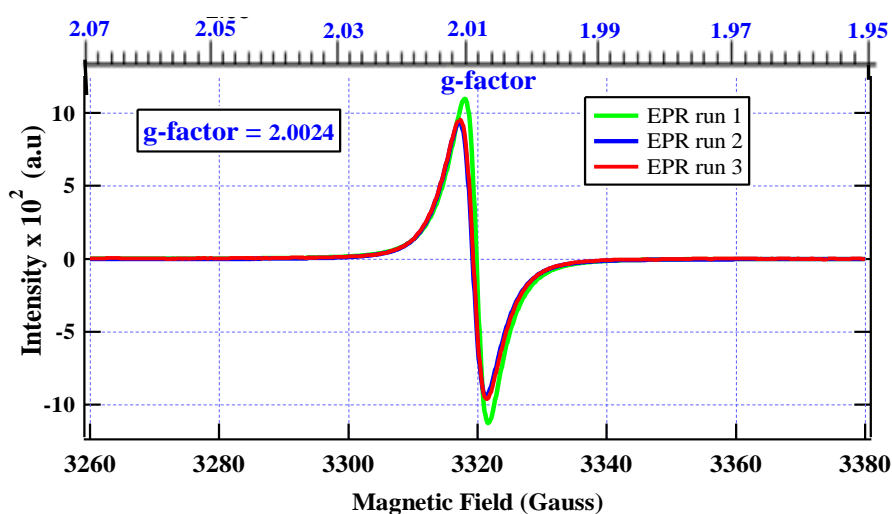


Figure 3.3: The *C. megalocarpus* char particulate EPR overlay spectra - radical intensity as a function of magnetic field.

The heteroatoms implied in this study are reported from elemental analysis carried out on croton char (Appendix I, S1). Additionally, there was a strong Heisenberg exchange interaction which narrowed and symmetrized the lines. The EPR spectrum of croton bio-oil

particulates had a strong anisotropic singlet peak at around 3320 Gauss and a low g-value of 2.0024, Figure 3.3.

Evidently from Figure 3.3, the free radicals in *C. megalocarpus* biodiesel thermal emissions have high intensities compared to those present in coal. The *C. megalocarpus* bio-oil particulates had spin densities of 9.12×10^{19} spins/g in the first run which is considerably high. Runs 2 and 3 conducted at different times; 50 and 60 days respectively show a minimal decrease in the intensities of the EPR signal of *C. megalocarpus* biodiesel thermal emissions (cf. Figure 3.3). The intensities for runs 2 and 3 were 8.51×10^{19} and 8.45×10^{19} spins/g respectively. The g-value for *C. megalocarpus* particulate emissions (2.0024) is very close to that of a free electron (2.0023) (Chalupsky, 2018).) whereas the peak-to-peak width - ΔH_{p-p} (3.65 G) was narrow.

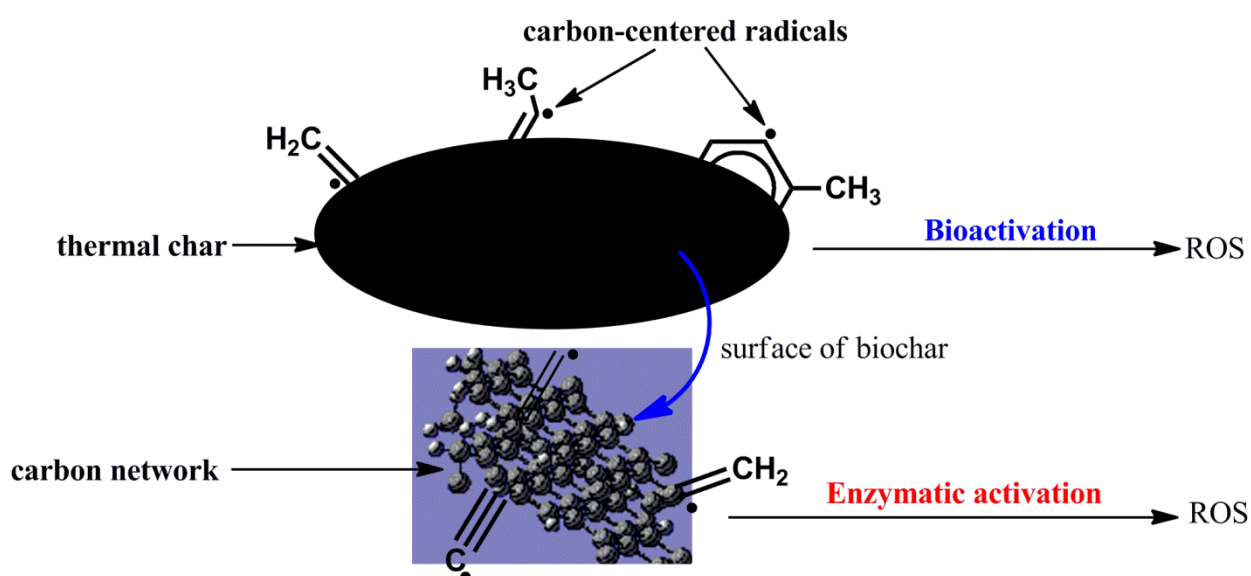


Figure 3.4: A model of free radicals immobilized on the surface of croton char particulate and possible channels in the generation of reactive oxygen species (ROS) in biosystems.

Clearly, the existence of high spin density in croton biodiesel particulate emissions demonstrates that the radicals are very stable (Meng *et al.*, 2014). This could be due to the presence of highly delocalized unpaired electrons that make the free radicals stable in the matrix either as a result of mesomeric effects or the π - π system in the particulate phase (Kurgat *et al.*, 2016; Sharma *et al.*, 2004). Figure 3.4 is a suggested model for particulate (thermal char) with the free radicals immobilized on its surface.

The model simulates how reactive free radical species in thermal chars can act as precursors in the generation of reactive oxygen species (ROS) to cause grave biological damage and ultimately carcinogenesis, cell mutation, and other illnesses including cardiac arrest (Tan *et al.*, 2018). Based on the model, thermal chars may act as principal toxicants in biological and environmental systems.

3.3.4 The kinetics of free radicals in *Croton megalocarpus* particulates

The kinetic behaviour of the free radicals in croton bio-oil particulates was observed over a time of 80 days. The first EPR pursue was directed 20 days while the second was led following 50 days. The third and fourth pursues were directed 60 and 80 days individually. Obviously, the turn thickness of the radicals didn't change fundamentally over the whole time frame and this affirms the single particulates free radicals are steady. So as to decide the motor trademark conduct of the free radicals, a pseudo-first request response active model was utilized in which the condition 3.1 was utilized.

$$\ln C = \ln C_0 - kt \quad 3.1$$

A plot of $\ln C$ as a function of time t (s), was generated as shown in Figure 3.5 from which the kinetic parameters: rate constant k and the original concentration (C_0) of free radicals in the thermal char in spins/g were determined. The conventional expression presented in equation 3.2 was used to compute the half-life decay of the radicals.

$$t_{1/2} = \frac{\ln 2}{k} \quad 3.2$$

The slope of the graph (Figure 3.5) gives the free radical rate constant as $1.86 \times 10^{-8} \text{ s}^{-1}$. This rate constant is small, implying that the free radicals immobilized on char are very stable.

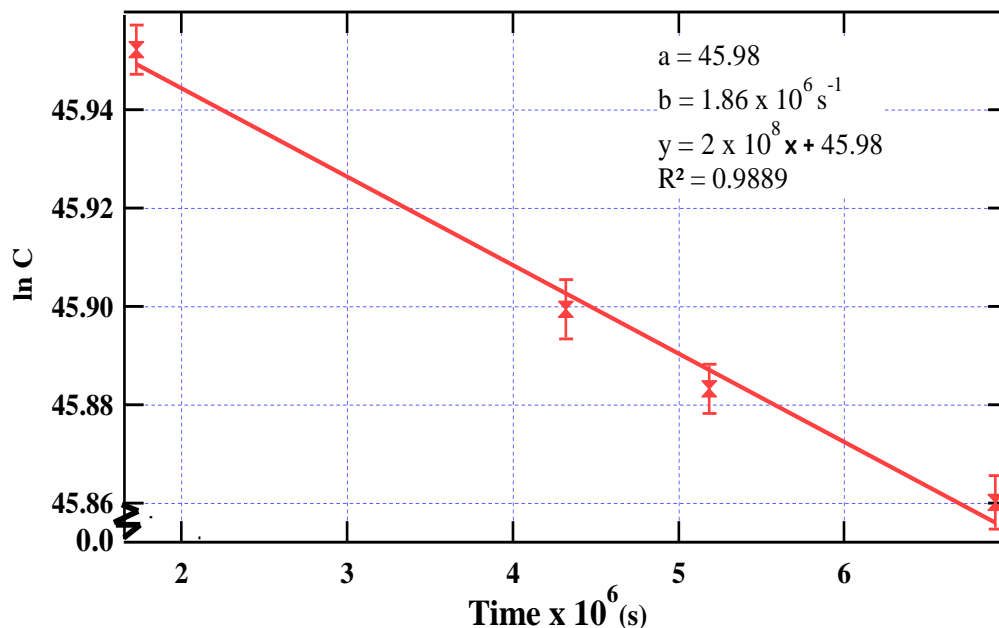


Figure 3.5: Pseudo-first order free radical kinetic behaviour in croton char particulates

Moreover, the half-life of the free radicals was determined using equation 3.2 and found to be $3.72 \times 10^7 \text{ s}$ (equivalent to ~ 431 days). Therefore, the free radicals take about 1.2 years to decay to a half their original concentration. The initial concentration (spins/g) in the thermal char was estimated from the y-intercept and found to be 9.35×10^{19} spins/g – that is if the thermal emissions were to be analyzed *in situ*.

3.3.5 Fourier transform infrared spectroscopy features of *Croton megalocarpus* bio-oil particulate

Absorption spectra were collected using an Agilent FTS 7000e FTIR bench top spectrometer equipped with a liquid nitrogen-cooled mercury cadmium telluride detector (Gupta *et al.*, 2017). The FTIR spectrum of *C. megalocarpus* bio-oil particulate char was characterized by several principle bands.

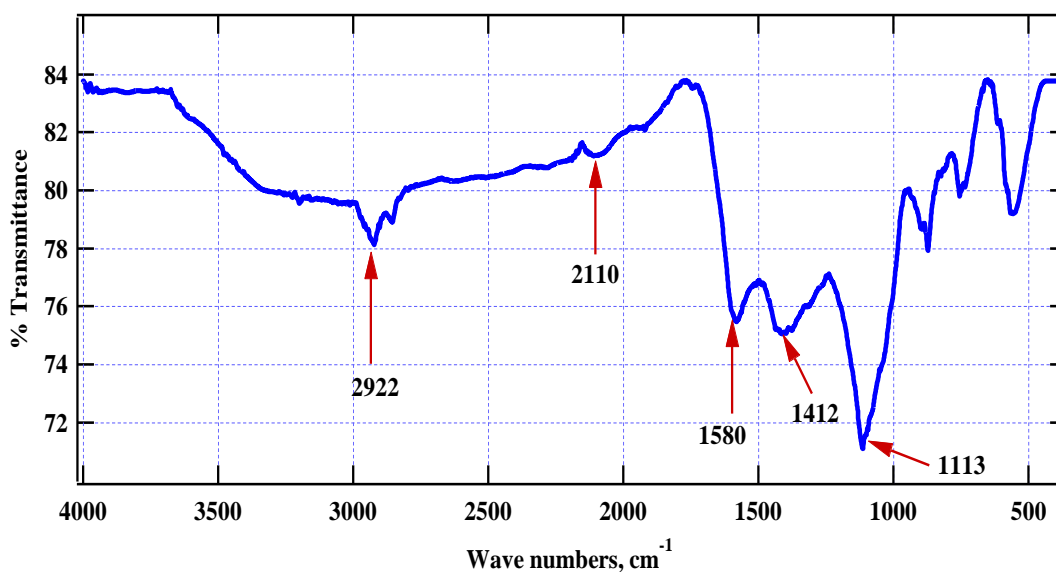


Figure 3.6: FTIR spectrums for croton char particulate

The intense broad absorption peak $\delta_s(1113\text{ cm}^{-1})$ is associated with biphenyl ethers or more precisely the in-plane bending of $-\text{CH}_3$ in the aromatic structure of croton char particulates. Nevertheless, at high temperatures, C-O bonds are usually absent because most organic by-products that are rich in oxygen are evolved at about $400\text{ }^\circ\text{C}$ (Shin *et al.*, 2001; Meng *et al.*, 2014). The absorption spectra presented in Figure 3.6 also indicates some absorption bands $\nu_{\text{sa}}(2922\text{ cm}^{-1})$ and $\nu_s(2857\text{ cm}^{-1})$ which are characteristic bands for asymmetrical and symmetrical stretching respectively, of methylene ($-\text{CH}_2-$) groups for long chain aliphatic hydrocarbons. Thus, the croton char particulates may contain long chain hydrocarbons adsorbed on its surface. The vibration $\nu_s(2110\text{ cm}^{-1})$ is assigned a $\text{C}\equiv\text{C}$ (alkyne) which could be present in the char polymeric network. Moderately weak absorption band at 1580 cm^{-1} is due to the presence of C-C double bond while $\delta_s(1412\text{ cm}^{-1})$ can reasonably be assigned to $-\text{CH}_2$ bending modes in aromatic structures. The vibrations modes at 872 and 754 cm^{-1} are respectively consistent with $\delta(-\text{CH})$ signature vibrations for in-plane and out of plane bending modes in aromatic compounds. A sharp band appearing around 559 cm^{-1} may correspond to in-plane bending of the $\text{O}=\text{C}-\text{N}$ group which could be present in the char. Generally, the results provided by FTIR are consistent with the results deduced from EPR which show that the *C. megalocarpus* char particulate is made up of dense structures of aromatic rings rich in stable free radical species.

3.3.6 Scanning electron microscopy (SEM) and Energy Dispersive X-ray Analysis (EDX)

The images presented in Figure 3.7 (a) and 3.7 (b) were obtained at various scanning parameters; an extra high tension voltage (EHT) of 20.0 kV and a working distance (WD) of 9.9 mm. At a significantly lower magnification ($\times 20\,000$), the croton char particulate is made up of conglomerates of porous particulate matter (cf. Figure 3.7 (a)). Given that the char is a highly porous and carbon-rich material, *C. megalocarpus* bio-oil thermal char may be a promising alternative to replace conventional carbon-based catalysts because generally, char is inexpensive, and is environmentally friendly if used in industrial catalytic processes (Lee *et al.*, 2017).

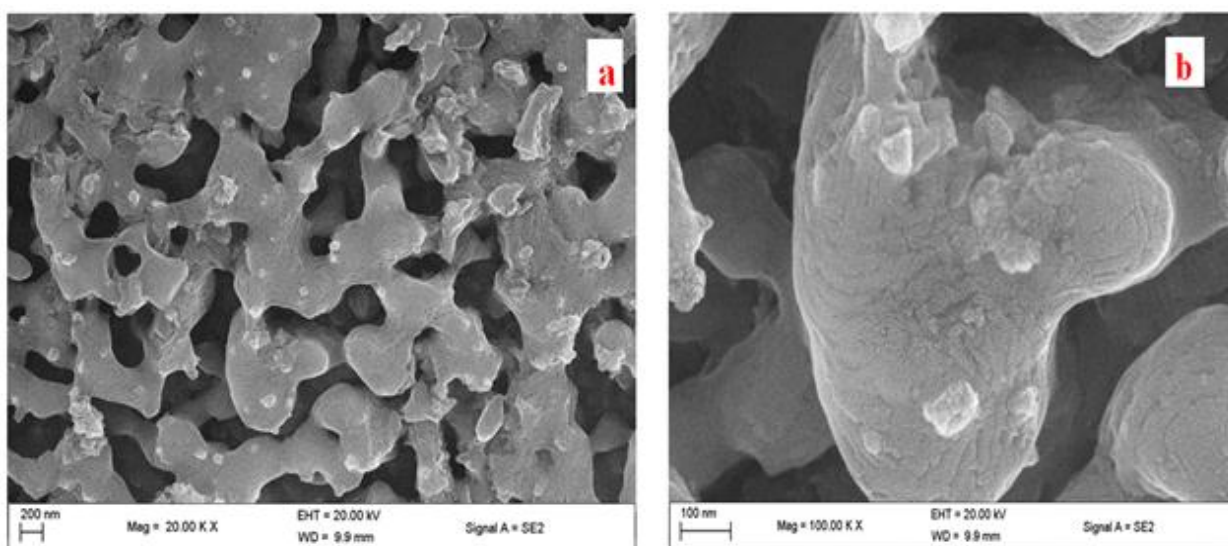


Figure 3.7: SEM image of *C. megalocarpus* bio-oil char at an associated magnification of (a) $\times 20\,000$ at 200 nm and (b) of $\times 100\,000$ at 100 nm.

At an associated magnification of $\times 100\,000$ at 100 nm, the carbon like polymeric structure of *C. megalocarpus* bio-oil particulate can be observed (cf. Figure 3.7(b) in a more detailed manner. Using energy dispersive X-ray analysis, approximately 52 % carbon, 27% oxygen, and 16% calcium were estimated from croton char (Appendix 1, S1). Minor elements determined included Mg, P, K, and Cl.

The particulate sizes from the thermal decomposition of *C. megalocarpus* bio-oil particulate were estimated from various SEM micrographs (4 micrographs in total) in order to obtain significant number of data to enable the generation of the distribution curve presented in Figure 3.8, *vide infra*. Image J computer software has robust capabilities of computing the

size distribution as well the average of particulates from SEM images as is the case in this study. The average size of particulates from the pyrolysis of croton bio-oil measured using image J was found to be ultrafine (22.90 ± 2.82 nm) - the equivalent of ~ 0.02 μm , Figure 3.8.

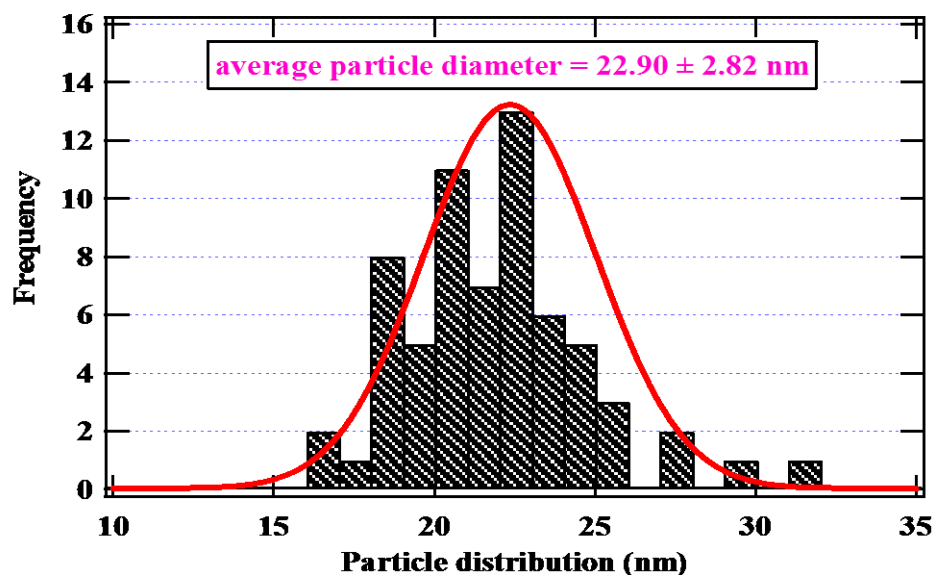


Figure 3.8: Estimated size distribution of particulate matter from croton bio-oil thermal emissions using Image J and Igor version 5.0.

Accordingly, the particulate emissions from the thermal degradation of *C. megalocarpus* bio-oil fall in the ultrafine category (< 0.1 microns) and if inhaled with free radicals immobilized on their surfaces, then serious biological damage such as cell aberration, cell injury, and ultimately cardiopulmonary death may occur. However, the health impacts of char particulates are beyond the scope of this investigation and will not be discussed further. Even so, the ultra-fine emissions identified in this study are remarkably micro molecular and may have large surface area so that in the event that they are inhaled, they can inflict maximum damage to the biological system. The extremely small particulate emissions carrying with them stable surface bound free radicals puts into question the health and environmental benefits of biofuels as emerging transport fuels (ETFs).

The stability of these free radicals in the pyrolysate of bio-oil have the ability to cause serious biological tissue damage not only to natural ecosystems but also to higher order animals such as man. Persistent free radicals can cause oxidative stress via oxidation of cells resulting in the production of reactive oxygen species (ROSs) which are well-known precursors for carcinogenesis and cell mutation (Barreto *et al.*, 2009; Khachatryan *et al.*, 2011). Although

most research is silent on the dangers of using thermal char to improve soil fertility and their uses in catalysis, it is definitely a serious concern which must be addressed accordingly. This concern has been necessitated by the fact that earlier studies have proven that free radicals are even present in living plants and chemically extracted lignin (Hu *et al.*, 2012; Chu *et al.*, 2013) and may therefore be potentially harmful.

Conclusions

This study has demonstrated that the concentrations of free radicals in *C. megalocarpus* particulate emissions is significantly high and are possibly stabilized by the π - π aromatic systems. The ultrafine nature of particulate emissions from the pyrolysis of croton biofuel (~22 nm) puts into doubt the predicted health and environmental benefits of using croton biofuel and possibly other bio-oils as transport fuels. The thermal char concentration of free radicals did not reduce significantly over the entire period of 80 days. The half-life of the free radicals was found to be approximately 431 days with an initial concentration of 9.35×10^{19} spins/g. The FTIR data revealed that most of the groups on the surface of the particulates are mainly aromatic with some aliphatic structures such as methyl and methylene groups. The scanning electron micrographs indicate that at high temperatures, the croton char is a porous network of carbon which may be a good adsorbent as well as a good catalyst. Furthermore, the ultrafine characteristics of emissions from the thermal degradation of *C. megalocarpus* bio-oil may pose serious health concerns such as aging, cancer, oxidative stress, and possible complex respiratory ailments.

References

- Adoukpe, J., Khachatryan, L. and Dellinger, B. (2008). Radicals from the gas-phase pyrolysis of hydroquinone: 1. Temperature dependence of the total radical yield. *Energy and Fuels*, **22**: 2986-2990.
- Barreto, G., Madureira, D., Capani, F., AonBertolino, L., Saraceno, E. and Alvarez-Giraldez, L. D. (2009). The role of catechols and free radicals in benzene toxicity: an oxidative DNA damage pathway. *Environmental Molecular Mutagen*, **50**: 771-780.
- Bolton, J. L., Trush, M. A., Penning, T. M., Dryhurst, G. and Monks, T. J. (2000). Role of quinones in toxicology. *Chemical Research Toxicology*, **13**: 135-160.
- Chalupsky, J. (2018). A classical approach to the electron g-factor. *arXiv preprint arXiv*, 1806-02274.
- Chhiti, Y., Salvador, S., Commandré, J. M. and Broust, F. (2012). Thermal decomposition of bio-oil: Focus on the products yields under different pyrolysis conditions. *Fuel* **102**: 274-281.
- Chu, S., Subrahmanyam, A. V. and Huber, G. W. (2013). The pyrolysis chemistry of a β -O-4 type oligomeric lignin model compound. *Green Chemistry*, **15**: 125-136.
- Corma, A., Iborra, S. and Velty, A. (2007). Chemical routes for the transformation of biomass into chemicals. *Chemical Reviews*, **107**: 2411-2502.
- Corral, C., Negrete, P., Estay, J., Osorio, S., Covarrubias, C., de Oliveira Junior, O. B., Barud, H., Negrete, P., Estay, J. and Osorio, S. (2018). Radiopacity and Chemical Assessment of New Commercial Calcium Silicate-Based Cements. *International Journal of Odontostomatol*, **12**(3): 262-268.
- Dellinger, B., D'Alessio, A., D'Anna, A., Ciajolo, A., Gullett, B., Henry, H. and Lucas, D. (2008). Report: Combustion byproducts and their health effects: Summary of the 10th International Congress. *Environmental Engineering Science*, **25**: 1107-1114.
- Dellinger, B., Pryor, W. A., Cueto, R., Squadrito, G. L., Hegde, V. and Deutsch, W. A. (2001). Role of free radicals in the toxicity of airborne fine particulate matter. *Chemical Research Toxicology*, **14**(10): 1371-1377.
- Eaton, G. R., Eaton, S. S., Barr, D. P. and Weber, R. T. (2010). *Quantitative EPR*: Springer Science and Business Media.
- Gehling, W., Khachatryan L. and Dellinger B. (2014). Hydroxyl Radical Generation from Environmentally Persistent Free Radicals (EPFRs) in PM(2.5). *Environmental Science Technology*, **48**: 4266-4272.

- Gupta, S., Jain, R., Kachhwaha, S. and Kothari, S. L. (2018). Nutritional and medicinal applications of *Moringa oleifera* Lam.—Review of current status and future possibilities. *Journal of Herbal Medicine*, **11**: 1-11.
- Hu, J., Shen, D., Xiao, R., Wu, S. and Zhang, H. (2012). Free-radical analysis on thermochemical transformation of lignin to phenolic compounds. *Energy and Fuels*, **27**(1): 285-293.
- Jebet, A., Kibet, J., Ombaka, L. and Kinyanjui, T. (2017). Surface bound radicals, char yield and particulate size from the burning of tobacco cigarette. *Chemical Central Journal*, **11**: 1-8.
- Jiang, G., Nowakowski, D. J. and Bridgwater, A. V. (2010). Effect of the temperature on the composition of lignin pyrolysis products. *Energy and Fuels*, **24**(8): 4470-4475.
- Kafuku, G. and Mbarawa, M. (2010). Biodiesel production from *C. megalocarpus* oil and its process optimization. *Fuel*, **89**(9): 2556-2560.
- Kafuku, G., Lam, M. K., Kandedo, J., Lee, K. T. and Mbarawa, M. (2010). *C. megalocarpus* oil: a feasible non-edible oil source for biodiesel production. *Bioresource Technology*, **101**(18): 7000-7004.
- Kanyua, N. P. (2016). *The potential of Telfairia pedata for liquid biofuel and soap production* (Doctoral dissertation, School of Pure and Applied Sciences, Kenyatta University).
- Kavunja, H. W. (2010). *Properties and performance testing of biodiesel from a mixture of jatropha curcas and croton megalocarpus blends* (Doctoral dissertation, University of Nairobi).
- Kedir, M. F. (2019). Selecting seed oil biodiesel producing tree species, land suitability and emission. *Agricultural Engineering International: CIGR Journal*, **21**(4):132-143.
- Keiblinger, K. M., Zehetner, F., Mentler, A. and Zechmeister-Boltenstern, S. (2018). Biochar application increases sorption of nitrification inhibitor 3,4-dimethylpyrazole phosphate in soil. *Environmental Science and Pollution Research*, **25**: 11173-11177
- Keneni, Y. G. and Marchetti, J. M. (2017). Oil extraction from plant seeds for biodiesel production. *AIMS Energy*, **5**: 316.
- Khachatryan, L., Asatryan R. and Dellinger B. (2003). Development of expanded and core kinetic models for the gas phase formation of dioxins from chlorinated phenols. *Chemosphere*, **52** (4): 695-708.

- Khachatryan, L., Asatryan, R., McFerrin, C., Adoukpe, J. and Dellinger, B. (2010). Radicals from the gas-phase pyrolysis of catechol. 2. Comparison of the pyrolysis of catechol and hydroquinone. *Journal of Physical Chemistry Letters A*, **114**: 10110-10116.
- Khachatryan, L., Vejerano, E., Lomnicki, S. and Dellinger, B. (2011). Environmentally persistent free radicals (EPFRs). 1. Generation of reactive oxygen species in aqueous solutions. *Environmental Science and Technology*, **45**: 8559-8566.
- Kibet, J., Khachatryan, L. and Dellinger, B. (2012). Molecular products and radicals from pyrolysis of lignin. *Environmental Science and Technology*, **46**: 12994-13001.
- Kibet, J.K. (2013). *Molecular Products from the Thermal Degradation of Selected Tobacco Components: Lignin, Tyrosine, Glutamic Acid, and Modeling of Lignin Pyrolysis using CHEMKIN Combustion Suite*. (Doctoral dissertation, Louisiana State University and Agricultural and Mechanical College).
- Kibet, J., Kurgat, C., Limo, S., Rono, N. and Bosire, J. (2016). Kinetic modeling of nicotine in mainstream cigarette smoking. *Chemical Central Journal*, **10**:1-9.
- Kibet, J. K., Jebet, A. and Kinyanjui, T. (2019). Molecular oxygenates from the thermal degradation of tobacco and material characterization of tobacco char. *Scientific African*, **5**: e00153.
- Kim, K. H., Bai, X., Cady, S., Gable, P. and Brown, R. C. (2015). Quantitative investigation of free radicals in bio-oil and their potential role in condensed-phase polymerization. *ChemSusChem*, **8**: 894-900.
- Kim, S., Chmely, S. C., Nimlos, M. R., Bomble, Y. J., Foust, T. D., Paton, R. S. and Beckham, G. T. (2011). Computational study of bond dissociation enthalpies for a large range of native and modified lignins. *Journal of Physical Chemistry Letters*, **2**: 2846-2852.
- Kivevele, T. T. and Mbarawa, M. M. (2010). Comprehensive analysis of fuel properties of biodiesel from Croton megalocarpus oil. *Energy and Fuels*, **24**(11): 6151-6155.
- Kurgat, C., Kibet, J. and Cheplogoi, P. (2016). Molecular modeling of major tobacco alkaloids in mainstream cigarette smoke. *Chemistry Central Journal*, **10**: 1-11.
- Lee, J., Kim, K. H. and Kwon, E. E. (2017). Biochar as a Catalyst. *Renewable and Sustainable Energy Reviews*, **77**: 70-79.
- Ma, F. and Hanna M.A.(1999). *Biodiesel production: A Review*. *Bioresource Technology*, **70**: 1-15.

- Maroyi, A. (2017). *Croton megalocarpus* Hutch. in tropical Africa: phytochemistry, pharmacology and medicinal potential. *Research Journal of Medicinal Plant*, **11**: 124-33.
- Melkior, T., Jacob, S., Gerbaud, G., Hediger, S., Le Pape, L., Bonnefois, L. and Bardet, M. (2012). NMR analysis of the transformation of wood constituents by torrefaction. *Fuel*, **92**: 271-280.
- Meng, J., Smirnova T. I., Song X., Moore, A. Ren X., Kelley S., Park S. and Tilotta D. 2014. Identification of free radicals in pyrolysis oil and their impact on bio-oil stability. *RSC Advances*, **4**: 29840-29846.
- Mili, M., Gupta, A. and Katiyar, V. (2017). Designing of poly (l-lactide)–nicotine conjugates: mechanistic and kinetic studies and thermal release behavior of nicotine. *ACS Omega*, **2**: 6131-6142.
- Moridani, M. Y., Siraki, A., Chevaldina, T., Scobie, H. and O'Brien, P. J. (2004). Quantitative structure toxicity relationships for catechols in isolated rat hepatocytes. *Chemical Biology Interactive*, **147**: 297-307.
- Petrakis, L. and Grandy, D. W. (1981). Free radicals in coals and coal conversion. 3. Investigation of the free radicals of selected macerals upon pyrolysis. *Fuel*, **60**(2): 115-119.
- Porterfield, J. P., Bross, D. H., Ruscic, B., Thorpe, J. H., Nguyen, T. L., Baraban, J. H., Stanton, J. F., Daily, J. W. and Ellison, G. B. (2017). Thermal decomposition of potential ester biofuels. part i: methyl acetate and methyl butanoate. *Journal of Physical Chemistry A*, **121**: 4658-4677.
- Qi, F., Kuppusamy, S., Naidu, R., Bolan, N.S., Ok, Y.S., Lamb, D., Li, Y., Yu, L., Semple, K.T. and Wang, H. (2017). Pyrogenic carbon and its role in contaminant immobilization in soils. *Critical Reviews in Environmental Science and Technology*, **47**(10): 795-876.
- Salatino, A., Salatino, M. L. F. and Negri, G. (2007). Traditional uses, chemistry and pharmacology of Croton species (Euphorbiaceae). *Brazil Chemical Society*, **18**: 11-33.
- Sharma, R. K., Wooten, J. B., Baliga, V. L., Lin, X., Chan, W. G. and Hajaligol, M. R. (2004). Characterization of chars from pyrolysis of lignin. *Fuel*, **83**: 1469-1482.
- Shen, Y., Zhao, P. and Shao, Q. (2014). Porous silica and carbon derived materials from rice husk pyrolysis char. *Microporous and Mesoporous Materials*, **188**: 46-76.
- Shin, E.-J., Nimlos, M. R. and Evans, R. J. (2001). A study of the mechanisms of vanillin pyrolysis by mass spectrometry and multivariate analysis. *Fuel*, **80**: 1689-1696.

- Tan, B. L., Norhaizan, M. E. and Liew, W. P. (2018). Nutrients and Oxidative Stress: Friend or Foe?. *Oxidative Medicine and Cellular Longevity*, 2018: 9719584-9719584.
- Tan, X., Liu, Y., Zeng, G., Wang, X., Hu, X., Gu, Y. and Yang, Z. (2015). Application of biochar for the removal of pollutants from aqueous solutions. *Chemosphere*, **125**: 70-85.
- Valko, M., Jomova, K., Rhodes, C. J., Kuča, K. and Musílek, K. (2016). Redox-and non-redox-metal-induced formation of free radicals and their role in human disease. *Archives of Toxicology*, **90**(1): 1-37.
- Varela, M., O., Rivera, E. B., Huang, W.-J., Chien, C. and Wang, Y. M. (2013). Agronomic properties and characterization of rice husk and wood biochars and their effect on the growth of water spinach in a field test. *Journal of Soil Science and Plant Nutrition*, **13**: 251-266.
- Varuvel, E. G., Mrad, N., Tazerout, M. and Aloui, F. (2012). Experimental analysis of biofuel as an alternative fuel for diesel engines. *Applied Energy*, **94**: 224-231.
- White, J. E., Catallo, W. J. and Legendre, B. L. (2011). Biomass pyrolysis kinetics: a comparative critical review with relevant agricultural residue case studies. *Journal of Analytical and Applied Pyrolysis*, **91**: 1-33.
- Wood, B. M., Kirwan, K., Maggs, S., Meredith, J. and Coles, S. R. (2015). Study of combustion performance of biodiesel for potential application in motorsport. *Journal Cleaner Production*, **93**: 167-173.
- Wu, D., Roskilly, A. P. and Yu, H. (2013). *Croton megalocarpus* oil-fired micro-trigeneration prototype for remote and self-contained applications: experimental assessment of its performance and gaseous and particulate emissions. *Interface Focus*, **3**: 20120041.

CHAPTER FOUR

FREE RADICALS AND ULTRAFINE PARTICULATE EMISSIONS FROM THE CO-PYROLYSIS OF *Croton megalocarpus* BIODIESEL AND FOSSIL DIESEL

Abstract

The atmosphere has become a major transport corridor for free radicals and particulate matter from combustion events. The motivation behind this study was to determine the nature of particulate emissions and surface bound radicals formed during the thermal degradation of diesel blends in order to assess the health and environmental hazards of binary transport fuels. Accordingly, this contribution explored the interactions that occur when *Croton megalocarpus* biodiesel and fossil diesel in the ratio of 1:1 by weight were co-pyrolyzed in a quartz reactor at a residence time of 0.5 sec under an inert flow of nitrogen at 600 °C. The surface morphology of the thermal char formed were imaged using a Feld emission gun scanning electron microscope (FEG SEM) while Electron paramagnetic resonance spectrometer (EPR) was used to explore the presence of free radicals on the surface of thermal char. Molecular functional groups adsorbed on the surface of thermal char were explored using Fourier transform infrared spectroscopy (FTIR). FTIR spectrum showed that the major functional groups on the surface of the char were basically aromatic and some methylene groups. The particulate emissions detected in this work were ultrafine (~32 nm). The particulates are consistent with the SEM images observed in this study. Electron paramagnetic resonance results gave a g-value of 2.0027 characteristic of carbon-based radicals of aromatic nature. Spectral peak-to-peak width (ΔH_{p-p}) obtained was narrow (4.42 Gauss). The free radicals identified as carbon-based are medically notorious and may be transported by various sizes of particulate matter (PM) on to the surface of the human lung which may trigger cancer and pulmonary diseases. The nanoparticles determined in this work can precipitate severe biological health problems among humans and other natural ecosystems.

Keywords: Biodiesel, Co-pyrolysis, Free radicals, Nanoparticulates

4.1 Introduction

In general, the atmosphere has become a major carrier for environmentally persistent free radicals and particulate pollution from combustion events (Jourabchi, 2015). As a result, environmental concerns about the use of petroleum-based diesel have increased the pressure on research into clean energy combustion with a view to minimizing the emission of toxic particulates from vehicle exhaust, while at the same time embracing environmentally friendly transport fuels from biomass materials such as biofuels and model biodiesel – fossil diesel binary mixtures. The motivation behind this study is the need to explore the nature of the particulates emitted and the surface bound radicals formed during thermal degradation of diesel blends in order to assess the health and environmental consequences of the use of binary transport fuels in combustion engines.

The major molecular components of biodiesel are mono-alkyl esters of fatty acids extracted from animal fats and plant-based oils such as *C. megalocarpus* oil, canola oil and castor oil (Singh and Singh, 2010). The use of non-edible seed oil for the production of biodiesel is significant because it is not only economic but also does not interfere with the human food chain.

The *Croton megalocarpus* is one of the major plant species in the Euphorbiaceae family and is well known for its diverse uses, ranging from medicinal to poultry feed to pesticide production for game meat hunting purposes (Capart *et al.*, 2004; Caruzo *et al.*, 2011; Wu *et al.*, 2013, Sanjid *et al.*, 2016). The plant is native and widely spread in the tropics, particularly in East and Sub-Saharan Africa (Kivevele and mbarawa *et al.*, 2010). Recently, there has been a strong interest in plant research as a viable biodiesel resource (Osawa *et al.*, 2015). Previous research surveys concluded that it has the highest raw oil production potential of 1.8 tonnes ha⁻¹yr⁻¹ compared with 1.0 tonne ha⁻¹yr⁻¹ of *C. megalocarpus* (Kafuku and Mbarawa, 2010). The plant species of the croton genus seeds contain approximately 32% oil yield by weight (Kafuku and Mbarawa, 2010). In addition, a study on *C. megalocarpus* seeds indicated that the annual yield of seed per tree was between 30 and 40 kg and the oil content was between 30 and 32% (Aliyu *et al.*, 2011).

On the other hand, fossil fuel-powered diesel engines are known to emit massive particulate matter, nitrogen oxides and greenhouse gases, which is why cleaner energy transport fuels need to be developed. Biodiesel has been shown to reduce environmental pollutants such as particulate matter, carbon monoxide and unburned hydrocarbons (Chhetri and Islam, 2008;

Kim *et al.*, 2018). Previous studies on biodiesel blends of ~20% indicated a reduction of about 15% in particulate matter emissions, carbon monoxide, total hydrocarbons, and other toxic molecular by-products of combustion such as aldehydes and polyaromatic hydrocarbons (McCormick, 2007). It is therefore understood that diesel blends of varying ratios (biodiesel and petroleum diesel) are capable of optimizing engine performance, but the toxicity of emission by-products is something that needs to be thoroughly investigated. In general, the particulate emissions from the combustion of transport fuels carry surface-bound radicals, which can have harmful effects on both human and environmental health. Pyrolysis experiments are indispensable for mimicking the actual reaction processes taking place within the internal combustion engine.

The basic phenomenon that occurs during the thermal degradation of the organic sample is the initiation of pyrolysis reaction events that result in the evolution of organic volatiles and the formation of thermal char (Babu, 2008). Pyrolysis therefore remains a central chemical process for the use of renewable energy and the aromatic feed-stocks generation stocks (Yaman, 2004; Jiang *et al.*, 2010). Organic volatiles, char and gases, are the main products of pyrolysis depending on operating conditions such as temperature, nature of the organic matrix, heating rate, residence time and engine design (Yaman, 2004).

Co-pyrolysis of organic mixtures explores the possibility of reducing the formation and emission of toxic free radicals and particulates to the environment, as well as the existence of interactions between biodiesel materials and fossil fuels in the formation of thermal chars (Ren *et al.*, 2011; Pou *et al.*, 2012). It is therefore essential to study the interaction of biomass components and fossil materials in combustion systems with a view to optimizing engine performance. Despite the availability of a lot of data from individual pyrolysis of model compounds of biodiesel components (croton oil, sunflower, olive oil, etc.) and fossil model materials such as coal and kerogen, the co-pyrolysis of biodiesel components and conventional diesel has received little attention hence co-pyrolysis studies of binary fuels (biofuel-fossil fuel) may provide crucial leads towards achieving clean energy combustion. The primary focus of these studies is on the determination of the formation of particulate emissions, the nature of the resulting thermal char and environmentally persistent free radicals for a thorough assessment of binary transport fuels.

Environmentally persistent free radicals, which are one of the pollutants produced during fuel combustion, may be responsible for oxidative stress resulting in cardiopulmonary diseases

and possibly exposure to airborne fine particles, which are major precursors to malignant growth that ultimately leads to cancer ((Thurston *et al.*, 2016). Vehicle exhaust from the combustion of gasoline , diesel and other petroleum fuels is a dominant contributor to fine (PM_{2.5}) and ultrafine (PM_{0.1}) particulate matter and may contain emissions of carbonaceous particles with fused and free polycyclic aromatic hydrocarbons (PAHs) (Pey *et al.*, 2009). In addition, ambient PM is believed to contain persistent free radicals and reactive oxygen species (ROS) usually involved in cellular damage and initiation of chronic pulmonary diseases(Dellinger *et al.*, 2001; Baulig *et al.*, 2003). Persistent free radicals contribute to decreased lung function, promotion of asthma , bronchitis and pneumonia, especially in children living in areas with high levels of particulate pollution (Brunekreef *et al.*, 1997). Although exposure to PM_{0.1} has been associated with decreased lung health, the underlying biological mechanisms responsible for increased exposure remain undefined (Ibald-Mulli *et al.*, 2002). Previous studies have also shown that women exposed to high levels of PM₁₀, especially those containing surface bound radicals, have given birth to children with small heads and small bodies, and this has been known to have a negative impact on their cognitive abilities as well as being vulnerable to carcinogens and mutagens (Wang *et al.*, 2013). It is against this evidence that the study of particulate emissions from model transport fuels has become important.

Although various researches on pyrolysis of pure biodiesel and pure petroleum diesel are available in the literature, very little information is available on co-pyrolysis of binary mixtures of biodiesel and petroleum diesel. However, some studies investigated binary blends in the range of 10 to 41% by weight and observed a reduction in NO_x and polycyclic aromatic hydrocarbon emissions (PAHs) (Osawa *et al.*, 2015). Binary diesel blends are predicted to achieve optimum engine efficiency. Accordingly, this investigation is limited to typical high-temperature combustion of a heat engine (600 ° C) and equimolar (by weight) mixtures of biodiesel and fossil diesel as model engine loads during combustion. This investigation will analyse extensively the particulate pollution, the nature of thermal char and surface bound radicals from the co-pyrolysis of *C. megalocarpus* biodiesel, and petroleum-based diesel believed to have significant consequences on both the physical and the biological environments.

4.2 Materials and Methods

4.2.1 Materials

All the chemicals and reagents used in this study were analytical grade and were purchased from Sigma Aldrich Inc. (St. Louis Missouri, USA) through its subsidiary, Kobian Kenya, Ltd. *Croton megalocarpus* oil was produced by solvent extraction using hexane before it was converted to biodiesel through a trans-esterification process (Reported in Chapter Three) and eventually submitted to the American Society for Testing and Materials (ASTM) D 6751 standards. Details on the laboratory preparation of Croton biodiesel are reported elsewhere in the literature (Ma and Hanna, 1999). Commercial diesel was purchased from a local outlet and used without further treatment. A temperature range muffle furnace of 20-1000 °C was purchased from Thermo-Scientific Inc., USA. The reactor was fabricated at the University of Nairobi – Department of Industrial and Applied Sciences, while ultra-high-purity nitrogen of 99.99% (grade 5.0) was purchased from BOC gasses in Kenya.

4.2.2 Co-pyrolysis of *Croton megalocarpus* biodiesel and petroleum diesel

In order to examine the nature of particulate matter emissions and the formation of environmentally persistent free radicals for the optimization of clean energy combustion, binary mixtures at a rate of 1:1 by weight have been introduced into the pyrolysis reactor. Consequently, 5 mg of *C. megalocarpus* biodiesel and 5 mg of petroleum diesel were mixed and placed in a 7.85 cm³ quartz reactor in a muffle furnace (Thermo-Scientific Inc. , USA). Pyrolysis was performed at 500 ° C under a nitrogen flow at a residence time of 0.5 sec at 1 atmosphere. In this experiment, five replicates were performed. Residence time was determined on the basis of the conventional ideal gas equation (equation 4.1).

$$t_0 = \left(\frac{\pi r^2 L}{F_0} \right) \left(\frac{T_1}{T_0} \right) x \left[1 + \frac{P_d}{P_0} \right]$$

4.1

where t_0 is the residence time, F_0 flow rate of the pyrolysis gas and P_d is the pressure difference between the inlet pressure and the pressure inside the reactor. Ideally the pressure difference is 0 because the ambient pressure and the reactor pressure are supposedly similar ~ 1 atm. while T , L and r represent the temperature, length of the reactor, and the radius of the tubular reactor respectively. The subscript ₀ denote original parameters (ambient) while the subscript ₁ denotes the parameters inside the reactor.

4.2.3 Electron paramagnetic resonance spectroscopy

About 5 mg thermal char sample from the co-pyrolysis of biodiesel and commercial diesel blend was analyzed using a Bruker EMX-20/2.7 EPR spectrometer (X-band) with dual cavities, modulation and microwave frequencies of 100 kHz and 9.516 GHz, respectively (Khachatryan *et al.* 2010, Goldstein *et al.*, 2017; Kurgat *et al.*, 2018). The typical parameters were: sweep width of 200 G, EPR microwave power of 1–20 mW, and modulation amplitude of ≤ 6 G. Time constant and sweep time were 16 seconds and 84 seconds, respectively. The value of the g factors was calculated using Bruker's WINEPR program, which is a comprehensive line of software that allows control of the Bruker EPR spectrometer, data-acquisition, automation routines, tuning, and calibration programs on a windows-based personal computer (Kibet *et al.*, 2012). The actual g-value for the spectrum was estimated by comparison with a 2,2-diphenyl-1-picrylhydrazyl (DPPH) standard.

4.2.4 Scanning electron microscopy (SEM) analysis

The determination of morphology of the thermal char was done as described by Bosire *et al.* (2016). In 1 ml of methanol, about 5 mg of thermal char was added and gold grids were dipped into the sample of prepared thermal char. A twister was used to collect the gold grids from the sample of the char. The sample was stuck in aluminum SEM stubs with carbon tape. These were subsequently gold coated in a Quorum Q150 RES sputter coater (Pongjanta *et al.*, 2008). The grids were allowed to dry in air before putting them into the analysis chamber of a Zeiss Ultra Plus (Germany) field emission gun scanning electron microscope (FEG SEM)(Konert and Vandenberghe, 1997). For enhanced image clarity, a second sample of char was coated with a 3 nm Au layer to allow for higher resolution images to be obtained. All images were taken at an angle of 45° to increase the definition of the surface morphology (Poynton *et al.*, 2014). The SEM machine was then switched on and imaging of the sample conducted at 20.0 kV using a light emitting diode (LED). The lens was varied at various resolutions to obtain a clear focus of the sample image. A detailed procedure for SEM analysis is reported elsewhere (Pongjanta *et al.*, 2008; Poynton *et al.*, 2014).

4.2.5 Fourier transform infrared (FTIR) spectroscopy

Conventionally, absorption spectra were collected using an Agilent FTS 7000e FTIR bench top spectrometer equipped with a liquid nitrogen-cooled mercury cadmium telluride detector and a heated (65.1 °C) seven-reflection diamond ATR crystal (Concentrate IR, Harrick Scientific Products, Pleasantville, NY) described elsewhere in literature (Mili *et al.*, 2017).

Attenuated total reflection Fourier-transform infrared (ATR-FTIR) spectroscopy was used in this investigation. ATR-FTIR spectra (256 co-added scans) were collected at the 4 cm^{-1} resolution over the wave number range of $4,000\text{--}500\text{ cm}^{-1}$ at an average of 4 scans (Reeves III, 1999; Almeida *et al.*, 2002). FTIR is one of the most important and versatile analytical techniques available to the current crop of scientist (Chen *et al.*, 2010). FTIR spectrum of the control (blank) sample was run, Appendix I, S3 (c).

4.3 Results and discussions

This work presents unique data on the co-pyrolysis of the equimassic mixture of croton biodiesel and fossil diesel. The thermal char analysis from a spectroscopic perspective is the central point of this investigation. Free radicals immobilized on the surface of particulate emissions suspected to be responsible for a number of health and environmental problems are of fundamental importance. It is well known in the combustion community that the shorter the residence time, the lower the particulate emissions, because shorter residence times discourage agglomeration in particle formation-the shorter the recombination time of the particle (Kibet *et al.*..., 2012).

4.3.1 Scanning electron microscopy

Scanning electron micrographs from which the particulate size presented in this work was derived from scanning electron microscope and are shown in Figure 4.1.

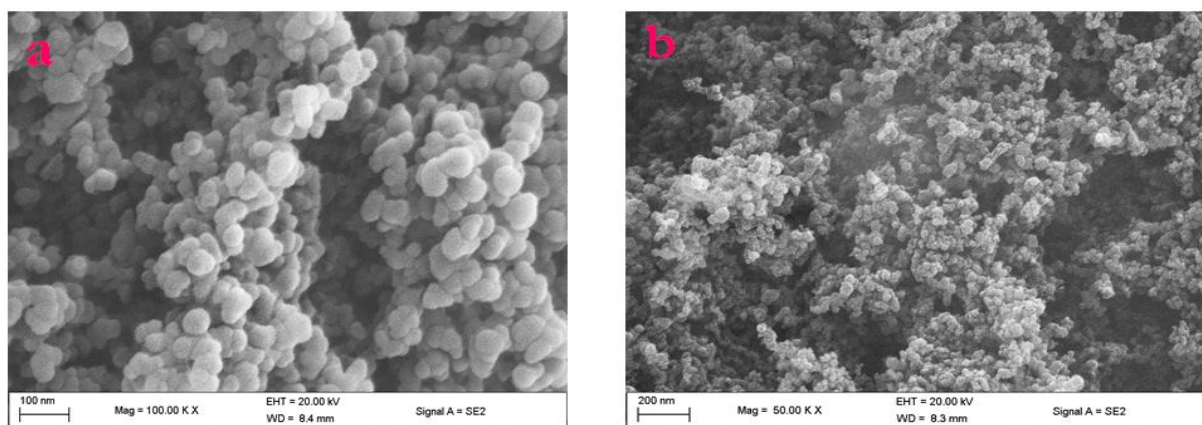


Figure 4.1: SEM image of biodiesel – fossil diesel at an associated magnification of $\times 50000$ at 200 nm (a) and a magnification of $\times 100000$ at 100 nm (b).

Figure 4.1 (a) was scanned at a magnification of $\times 100\ 000$ while Figure 4.1 (b) was imaged at a magnification of $\times 50\ 000$. Clearly, the particulate matter identified in this study is far much less than $\text{PM}_{0.1}$. *Image J* computer software has robust capabilities for computing the

distribution of sizes as well as the average of particles from SEM images (Goldstein *et al.*, 2017). The mean sizes of the char particulates at 500 °C was reported and presented as a Gaussian curve in which the peak of the curve gave the mean of the thermal particulates, Figure 4.2 below.

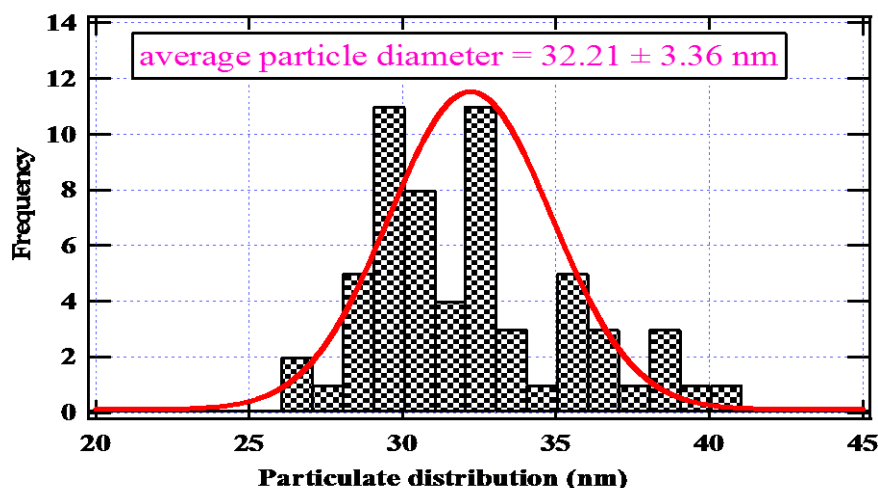


Figure 4.2: Particulate size distribution for the co-pyrolysis of croton biodiesel and fossil diesel blend (Ratio 1:1)

4.3.2 Electron paramagnetic resonance spectroscopy

The g-value of the free radicals in thermal char was found to be 2.0027 which can be considered as pure carbon-based radicals because they are significantly close to that of a free electron, 2.0023 (one of the most accurate conventional constants ever known in physics). The peak-to-peak width of the EPR signal was quite narrow, (4.42 G). The EPR spectrum of the thermal char had a strong anisotropic singlet peak at around 3320 Gauss (cf. Figure 4.3).

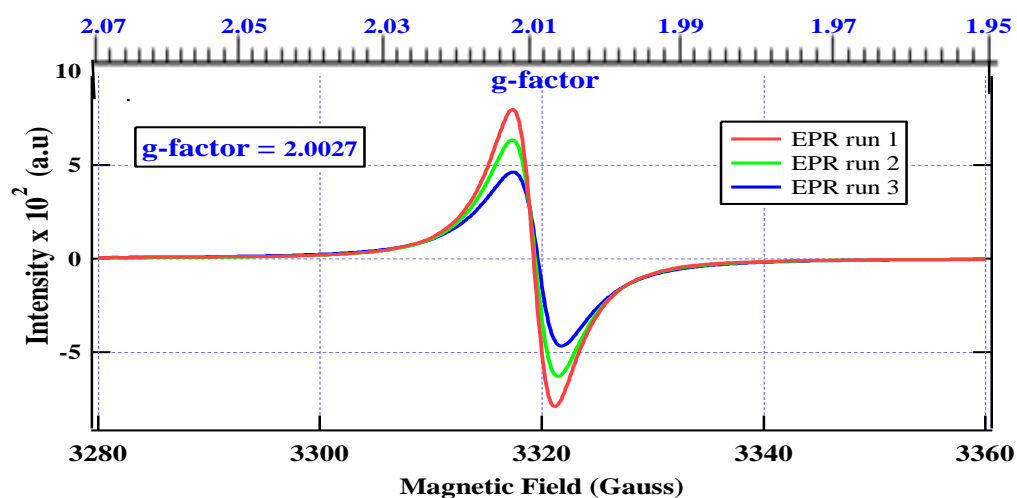


Figure 4.3: Diesel blend thermal char EPR spectra - radical intensity as a function of magnetic field (EPR spectra showing intensity as a function of g-value are reported in supplementary material S3, a & b)

The spin density for run 1 (conducted 20 days after the preparation of the thermal char) was found to be 9.18×10^{19} spins/g and 3.84×10^{17} spins/cm. The thermal char was monitored over a period of 80 days in order to investigate their stability. The EPR spectra for this study are presented in Figure 4.3. For clarity, the EPR signal for run 4 is not plotted in Figure 4.3. However, plots of g-values as a function of magnetic field for selected EPR runs (including run 4) are reported in the supplementary material S3 (b). EPR run 3 was significantly broad and had a lower intensity while runs 1 and 2 were symmetrical and quite intense. This broad feature in run 3 may be attributed to the break down in the Heisenberg exchange interaction. The EPR parameters for the thermal char explored in this work are presented in Table 4.1.

Table 4.1: The EPR parameters for the thermal char formed from the co-pyrolysis of the binary mixture of biodiesel and conventional diesel.

Char/Run	Time (days)	g/cm	spins/cm	spins/g
BCD (1)	20	0.0022	3.84×10^{17}	9.18×10^{19}
BCD (2)	50	0.0022	3.63×10^{17}	8.03×10^{19}
BCD (3)	60	0.0022	3.55×10^{17}	7.88×10^{19}
BCD (4)	80	0.0022	3.34×10^{17}	7.81×10^{19}

Legend: BCD- Binary mixture of biodiesel and conventional diesel

Evidently from Table 4.1, the thermal char had fairly high spin densities. Even after 80 days, the spin density (spins/g) in thermal char had decreased only by about 15% of the initial run conducted 20 days after the co-pyrolysis experiment. This decrease is also consistent with that realized for spins/cm over a similar period of time (~ 14%). These observations demonstrate that the free radicals bound on the surface of thermal char are, indeed, very stable and are can thus be accurately classified as environmentally persistent free radicals (EPRs).

4.3.3 FTIR spectrum of the thermal char

The investigation of the surface functional groups of the thermal char from the co-pyrolysis of the binary mixture - croton biodiesel and fossil diesel using FTIR gave several principal bands as shown in Figure 4.4. The intense broad absorption peak $\delta_s(1116 \text{ cm}^{-1})$ is associated

with in-plane bending of $-\text{CH}_3$ in the possible aromatic structure of thermal char. The absorption bands $\nu_{\text{sa}}(2929\text{ cm}^{-1})$ and $\nu_{\text{s}}(3008\text{ cm}^{-1})$ are characteristic of asymmetrical and symmetrical stretching of methylene ($-\text{CH}_2-$) groups for long chain aliphatic hydrocarbons. The sharp vibration $\nu_{\text{s}}(2115\text{ cm}^{-1})$ may be attributed to a $\text{C}\equiv\text{C}$ (alkyne) which could be present in the thermal char. The absorption peak $\nu_{\text{s}}(2325\text{ cm}^{-1})$ is probably a nitrile ($-\text{C}\equiv\text{N}$) that could be bonded to the char matrix. Moreover, the moderately weak absorption band $\nu_{\text{s}}(1590\text{ cm}^{-1})$ is an aromatic C-C double bond while $\delta_{\text{s}}(1415\text{ cm}^{-1})$ can judiciously be assigned to $-\text{CH}_2$ bending modes in arenes.

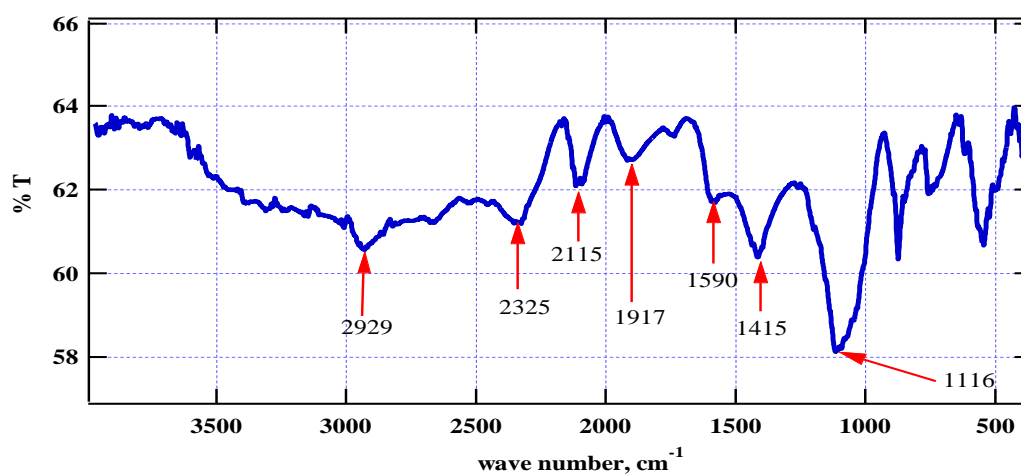


Figure 4.4: FTIR absorption bands for the char formed from the co-pyrolysis of croton biodiesel and conventional diesel.

The absorption bands at 874 and 756 cm^{-1} are consistent with $\delta(-\text{CH}_2)$ signature vibrations for in-plane and out of plane bending modes in aromatic compounds, respectively. A sharp band appearing around 544 cm^{-1} may correspond to in-plane bending of the $\text{O}=\text{C}-\text{N}$ group which could be present in the thermal char. All the surface functionalized groups identified in this investigation suggest that the thermal char is aromatic. Additionally, the stability of free radicals explored in this work as carbon-centered ones may be delocalized within a highly conjugated π - π system (Kato and Osuka, 2019).

4.3.4 The health and environmental concerns

The term particulate issue alludes to molecule contamination - a lattice of vaporized beads, residue, smoke and sediment of differing particulate sizes that present genuine wellbeing concerns (Geiser *et al.*, 2005). The results obtained in this study showed that particulate sizes

are ultrafine, approximately 32 nm (cf. Figure 4.3). These discoveries are upsetting from a natural and a wellbeing point of view.

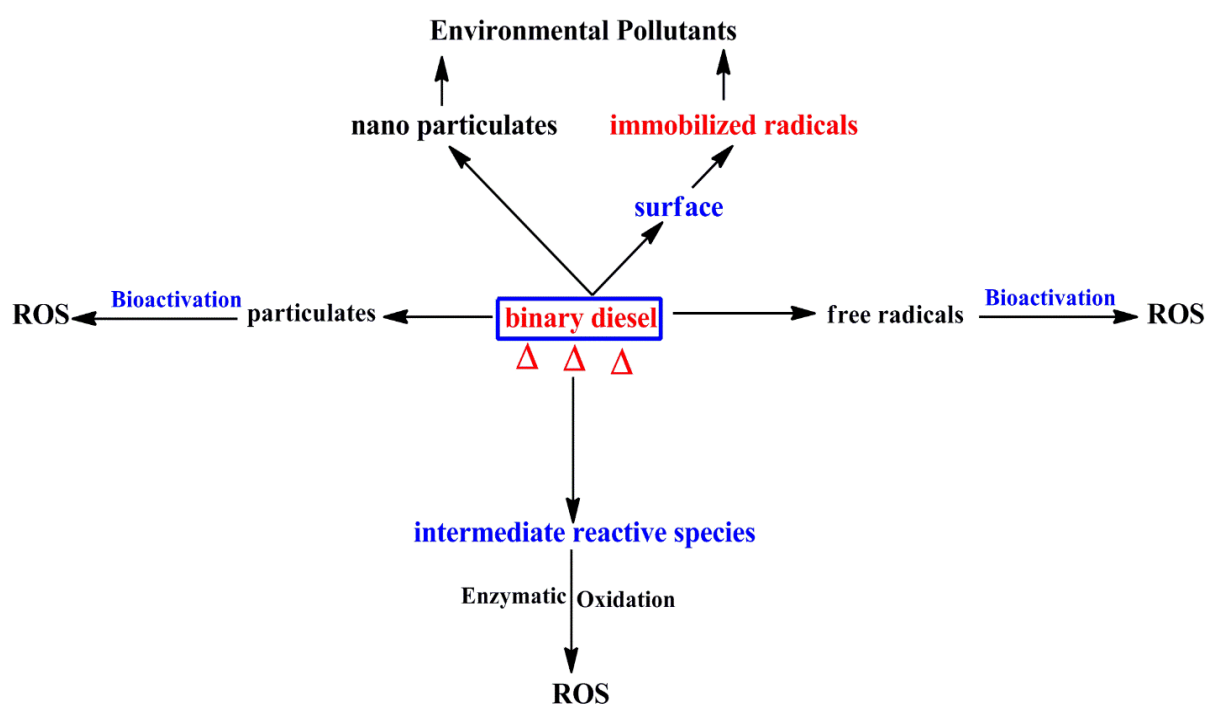
This examination has indicated that the warm debasement of a blend *C. megalocarpus* oil and fossil diesel offers ascend to particulate portions far substantially less than $PM_{0.1}$ and are along these lines considered the most harming of all PM particulates since they might be breathed in more profound into the lung tissues in this way making grave harm people and different living beings. Dawei and his colleagues (2013) proposed the strictest of emission policies to be followed when setting up combustion engine using biofuels inferable from ultrafine particulates related with its burning. Be that as it may, it isn't clear in their examination why ultrafine particulate outflows were not explored. When in doubt, the development of outflow particles in burning frameworks continues through homogeneous nucleation (particulates < 100 nm) and agglomeration (particulates > 900 nm) forms (Oberdörster *et al.*, 2005; Wu *et al.*, 2013). In this recommendation, emanation particles remain together to frame chain-like structures and may contain surface bound radicals (Oberdörster *et al.*, 2005) thought about damaging to the natural condition.

This examination has shown that the co-pyrolysis of croton biodiesel and oil based diesel offers ascend to ultrafine particles in the nano area (~ 32 nm) which may contain surface immobilized radicals, and whenever breathed in may encourage genuine wellbeing suggestions. For example, it has been built up through creature considers that particulate nanoparticles of ~ 22 nm distance across have discovered their way into the connective tissue of the heart, for example, the fibroblast of rodents (Chen *et al.*, 2010) and at last causing grave natural harm and cardiopulmonary illnesses. Additionally, there is convincing proof that inside 30 minutes of presentation, enormous amounts of intra-tracheal embedded nanoparticles of ~ 20 nm breadths have been found in platelets in the aspiratory vessels of rodents (Oberdörster *et al.*, 2005). Also, the discoveries on free radicals bound to nanoparticles from this examination are exceptionally upsetting in light of the fact that they are antecedents for serious ecological and medical issues.

Obviously, in the pursuit of elective vehicle fills, for example, paired diesel energizes investigated in this work, the topic of ultrafine discharges that convey with them surface bound radicals is of grave wellbeing concern. These particulates are very perilous particularly in light of the fact that they can be breathed in more profound and perhaps discover their way into the circulatory system and in this manner might be conveyed into the heart during the

blood course forms. Nanoparticles, consequently, are forebears for deadly injury in organic cells and may trigger the creation of responsive oxygen species (ROS) and at last reason oxidative pressure and heart maladies. Therefore nano particulate outflows distinguished in this work may to some degree recommend an obstacle in the quest for naturally inviting vehicle fills. In any case, motor plans fitted with productive reactant chambers and precipitators can hinder the emanation of ultrafine particulate, and most likely improve the effectiveness of parallel diesel mixes in engine frameworks.

The mechanistic processes culminating into the biological health and environmental health problems derived from this study are summarized in scheme 4.1.



Scheme 4.1: Mechanistic channels showing the generation of toxic species from the pyrolysis of binary diesel (Δ indicates pyrolysis) and their predictive effects on the biological and the environmental systems.

While intermediate reactive species (sub-atomic responsive species) have not been investigated in this work, we accept they are main sources of free radicals and are thusly similarly unsafe as particulate emanations and surface bound radicals. Bioactivation and enzymatic actuation are the essential procedures which happen when responsive species collaborate with natural frameworks to cause ailments, for example, malignant growth and aspiratory diseases (Dekant, 2009). These procedures encourage the arrangement of reactive oxygen species (ROS) liable for different clinical issues endured by man and different environments.

Surprisingly, toxicological and epidemiological examinations have demonstrated that presentation to ignition particulate outflows, particularly those conveying with them surface bound radicals just like the case in this investigation are notable forerunners for such infirmities as, wooziness, ceaseless respiratory issues, cardiopulmonary maladies, asthma and malignancy (Bogarra *et al.*, 2016). Different investigations have likewise settled that particulates can empower inheritable infections, for example, leukemia (Huang *et al.*, 2016). Other than wellbeing concerns, particulate emanations are known to consolidate with other air toxins to shape climatic earthy colored mists which are uncommon ancestors for various unfriendly ecological issues tormenting people and other living creatures (Thurston *et al.*, 2016). The way that past examinations proposed severe emanation guidelines to be applied when structuring biofuel based motors is a wellspring of worry in the quest for elective powers (Wu *et al.*, 2013). This is exceptionally steady with the discoveries progressed in this work.

Conclusions

This study has established that particulate emissions from the pyrolysis of a binary mixture of *C. megalocarpus* biodiesel and petroleum-based diesel (ratio 1:1) are ultrafine (~ 32 nm) and may be inhaled deeper into biological tissues, possibly finding their way into the red blood cells, alveoli, and the fibroblasts of the heart. The consequences of inhaling such particulates range from cell mutation, carcinogenesis, chronic coughs and cardiovascular diseases. Moreover, particulate emissions from the co-pyrolysis of croton biofuel and petroleum-based diesel carry with them surface bound radicals that may be of serious concern to both the biological and the physical environment. The free radicals identified in this study are carbon-based which may certainly be inhaled into the surface of the lungs being transported along by various sizes of particulate matter (PM) and are capable of causing pulmonary diseases, oxidation stress and cell aberrations. The spin intensity of the radicals decreased by 15% of the initial run performed 20 days after co-pyrolysis experiments, thus their moderate persistence in the environment. Based on the findings of this study it may be necessary to explore varying ratios of biofuels and conventional diesel in order to derive optimum working conditions of an internal combustion engine without compromising public and environmental safety.

References

- Aliyu, B., Shitanda, D., Walker, S., Agnew, B., Masheiti, S. and Atan, R. (2011). Performance and exhaust emissions of a diesel engine fuelled with C. megalocarpus(musine) methyl ester. *Applied Thermal Engineering*, **31**: 36–41.
- Almeida, E., Balmayore, M. and Santos, T. (2002). Some relevant aspects of the use of FTIR associated techniques in the study of surfaces and coatings. *Progress in Organic Coatings* **44**: 233-242.
- Babu, B. (2008). Biomass pyrolysis: a state-of-the-art review. *Biofuels, Bioproducts and Biorefining: Innovation for a Sustainable Economy* **2**: 393-414.
- Baulig, A., Garlatti, M., Bonvallot, V., Marchand, A., Barouki, R., Marano, F. and Baeza-Squiban, A. (2003). Involvement of reactive oxygen species in the metabolic pathways triggered by diesel exhaust particles in human airway epithelial cells. *American Journal of Physiology-Lung Cellular and Molecular Physiology*, **285**: L671-L679.
- Bogarra, M., Herreros, J. M., Tsolakis, A., York, A. P. E. and Millington, P. J. (2016). Study of particulate matter and gaseous emissions in gasoline direct injection engine using on-board exhaust gas fuel reforming. *Applied Energy*, **180**: 245-255.
- Bosire, J., Kibet, J., Kinyanjui, T. and Githaiga, B. (2016). Tire Combustion Emissions and Their Histochemical Implications on the Lung Tissues of Albino Mice. *Open Access Library Journal*, **3**(10): 1-14.
- Brunekreef, B., Janssen, N. A., de Hartog, J., Harssema, H., Knape, M. and van Vliet, P. (1997). Air pollution from truck traffic and lung function in children living near motorways. *Epidemiology*: 298-303.
- Capart, R., Khezami, L. and Burnham, A. K. (2004). Assessment of various kinetic models for the pyrolysis of a microgranular cellulose. *Thermochimica Acta* **417**: 79-89.
- Caruzo, M. B. R., Van Ee, B. W., Cordeiro, I., Berry, P. E. and Riina, R. (2011). Molecular phylogenetics and character evolution of the “sacaca” clade: novel relationships of Croton section Cleodora (Euphorbiaceae). *Molecular Phylogenetics and Evolution*, **60**: 193-206.
- Chen, Y., Bakrania, S., Wooldridge, M. and Sastry, A. (2010). Image Analysis and Computer Simulation of Nanoparticle Clustering in Combustion Systems. *Aerosol Science and Technology* **44**: 83-95.
- Chhetri, A. B. and Islam, M. R. (2008). Towards producing a truly green biodiesel. *Energy Sources, Part A*, **30**: 754-764.

- Dellinger, B., Pryor, W. A., Cueto, R., Squadrito, G. L., Hegde, V. and Deutsch, W. A. (2001). Role of free radicals in the toxicity of airborne fine particulate matter. *Chemical Research in Toxicology*, **14**: 1371-1377.
- Geiser, M., Rothen-Rutishauser, B., Kapp, N., Schürch, S., Kreyling, W., Schulz, H. and Gehr, P. (2005). Ultrafine particles cross cellular membranes by nonphagocytic mechanisms in lungs and in cultured cells. *Environmental Health Perspectives*, **113**: 1555-1560.
- Goldstein, J. I., Newbury, D. E., Michael, J. R., Ritchie, N. W., Scott, J. H. J. and Joy, D. C. (2017). *Scanning electron microscopy and X-ray microanalysis*. Springer. New York.
- Huang, H., Zhou, C., Liu, Q., Wang, Q. and Wang, X. (2016). An experimental study on the combustion and emission characteristics of a diesel engine under low temperature combustion of diesel/gasoline/n-butanol blends. *Applied Energy*, **170**: 219-231.
- Ibald-Mulli, A., Wichmann, H. E., Kreyling, W. and Peters, A. (2002). Epidemiological evidence on health effects of ultrafine particles. *Journal of Aerosol Medicine*, **15**: 189-201.
- Jiang, G., Nowakowski, D.J. and Bridgwater, A. V. (2010). Effect of the temperature on the composition of lignin pyrolysis products. *Energy and Fuels*, **24**: 4470-4475.
- Jourabchi, S. A. (2015). *Production and physicochemical characterisation of bio-oil from the pyrolysis of Jatropha curcus waste* (Doctoral dissertation, University of Nottingham).
- Kafuku, G. and Mbarawa, M. (2010). Biodiesel production from C. megalocarpos oil and its process optimization. *Fuel*, **89**: 2556-2560.
- Kato, K. and Osuka, A. (2019). Platforms for Stable Carbon-Centered Radicals. *Angewandte Chemie*, **131**(27): 9074-9082.
- Khachatryan, L., Asatryan, R., McFerrin, C., Adoukpe, J. and Dellinger, B. (2010). Radicals from the gas-phase pyrolysis of catechol. 2. Comparison of the pyrolysis of catechol and hydroquinone. *The Journal of Physical Chemistry A*, **114**: 10110-10116.
- Kibet, J., Khachatryan, L. and Dellinger, B. (2012). Molecular products and radicals from pyrolysis of lignin. *Environmental Science and Technology* **46**: 12994-13001.
- Kim, D. S., Hanifzadeh, M. and Kumar, A. (2018). Trend of biodiesel feedstock and its impact on biodiesel emission characteristics. *Environmental Progress and Sustainable Energy*, **37**(1): 7-19.

- Kivevele, T. T. and Mbarawa, M. M. (2010). Comprehensive analysis of fuel properties of biodiesel from *Croton megalocarpus* oil. *Energy and Fuels*, **24**(11): 6151-6155.
- Konert, M. and Vandenberghe, J. (1997). Comparison of laser grain size analysis with pipette and sieve analysis: a solution for the underestimation of the clay fraction. *Sedimentology*, **44**: 523-535.
- Kurgat, C., Jebet, A. and Kibet, J. (2018). The Chemistry of Tobacco Charcoal: A Potentially Harmful Residue from Tobacco Burning. *Africa Environmental Review Journal*, **3**(1): 118-124.
- Ma, N., Zhang, L., Zhang, Y., Yang, L., Yu, C., Yin, G. and Ma, X. (2016). Biochar improves soil aggregate stability and water availability in a mollisol after three years of field application. *PloS One*, **11**. <https://doi.org/10.1371/journal.pone.0154091>.
- McCormick, R. L. (2007). The impact of biodiesel on pollutant emissions and public health. *Inhalation Toxicology* **19**: 1033-1039.
- Mili, M., Gupta, A. and Katiyar, V. (2017). Designing of poly (l-lactide)–nicotine conjugates: mechanistic and kinetic studies and thermal release behavior of nicotine. *ACS Omega* **2**: 6131-6142.
- Oberdörster, G., Oberdörster, E. and Oberdörster, J. (2005). Nanotoxicology: an emerging discipline evolving from studies of ultrafine particles. *Environmental Health Perspectives* **113**(7): 823–839.
- Osawa, W., Sahoo, P., Onyari, J. and Mulaa, F. (2015). Experimental investigation on performance, emission and combustion characteristics of *C. megalocarpus* biodiesel blends in a direct injection diesel engine. *International Journal of Science and Technology* **4**(1): 26-33.
- Pey, J., Querol, X., Alastuey, A., Rodríguez, S., Putaud, J. P. and Van Dingenen, R. (2009). Source apportionment of urban fine and ultra-fine particle number concentration in a Western Mediterranean city. *Atmospheric Environment*, **43**:4407-4415.
- Pongjanta, J., Utaipatanacheep, A., Naivikul, O. and Piyachomkwan, K. (2008). Enzymes-resistant starch (RS III) from pullulanase-debranched high amylose rice starch. *Kasetsart Journal of Natural Science* **42**: 198-205.
- Pou, J. O., Alvarez, Y. E., Watson, J. K., Mathews, J. P. and Pisupati, S. (2012). Co-primary thermolysis molecular modeling simulation of lignin and subbituminous coal via a reactive coarse-grained simplification. *Journal of Analytical and Applied Pyrolysis*, **95**: 101-111.

- Poynton, S. D., Slade, R. C., Omasta, T. J., Mustain, W. E., Escudero-Cid, R., Ocón, P. and Varcoe, J. R. (2014). Preparation of radiation-grafted powders for use as anion exchange ionomers in alkaline polymer electrolyte fuel cells. *Journal of Materials Chemistry A*, **2**: 5124-5130.
- Reeves III, J. B. (1999). Mid-versus near infrared spectroscopic analysis of diversely treated feedstuffs. *Journal of Near Infrared Spectroscopy* **7**: 89-100.
- Ren, Q., Zhao, C., Chen, X., Duan, L., Li, Y. and Ma, C. (2011). NO_x and N₂O precursors (NH₃ and HCN) from biomass pyrolysis: Co-pyrolysis of amino acids and cellulose, hemicellulose and lignin. *Proceedings of the Combustion Institute*, **33**: 1715-1722.
- Sanjid, A., Kalam, M. A., Masjuki, H. H., Varman, M., Zulkifli, N. W. B. M. and Abedin, M. J. (2016). Performance and emission of multi-cylinder diesel engine using biodiesel blends obtained from mixed inedible feedstocks. *Journal of Cleaner Production*, **112**: 4114-4122.
- Singh, S. and Singh, D. (2010). Biodiesel production through the use of different sources and characterization of oils and their esters as the substitute of diesel: a review. *Renewable and Sustainable Energy Reviews* **14**: 200-216.
- Thurston, G. D., Ahn, J., Cromar, K. R., Shao, Y., Reynolds, H. R., Jerrett, M., Lim, C. C., Shanley, R., Park, Y. and Hayes, R. B. (2015). Ambient particulate matter air pollution exposure and mortality in the NIH-AARP diet and health cohort. *Environmental Health Perspectives*, **124**: 484-490.
- Wang, J. F., Hu, M. G., Xu, C. D., Christakos, G. and Zhao, Y. (2013). Estimation of citywide air pollution in Beijing. *PloS One*, **8**. <https://doi.org/10.1371/journal.pone.0053400>.
- Wu, D., Roskilly, A. P. and Yu, H. (2013). *Croton megalocarpus* oil-fired micro-trigeneration prototype for remote and self-contained applications: experimental assessment of its performance and gaseous and particulate emissions. *Interface Focus*, **3**: 20120041.
- Yaman, S. (2004). Pyrolysis of biomass to produce fuels and chemical feedstocks. *Energy Conversion and Management* **45**: 651-671.

CHAPTER FIVE

SIMULATING THE HEALTH IMPACT OF PARTICULATE EMISSIONS FROM TRANSPORT FUELS USING MULTIPATH PARTICLE DEPOSITION MODEL (MPPD)

Abstract

Combustion of fuels emit particulates of varying chemical nature and size. These particulates are known to cause respiratory problems of medical concern. The need to simulate the breathing characteristics of particulates generated from combustion events is very important in estimating the respiratory clearance of these particles. Consequently, this study examines the nature of particulate matter from the pyrolysis of a mixture *C. megalocarpus* biodiesel and fossil diesel, and pure biodiesel. The study was explored at an optimum temperature of 600 °C in an inert nitrogen environment at a contact time of 2 sec. Scanning electron microscope was used to examine the surface of the particulates. Multipath Particle Deposition (MPPD Ver. 3.04) model was used to determine the breathing phenomena of infants, teenagers and adults at different orientations. Co-pyrolytic Char particulates and pyrolytic croton thermal char were classified as ultrafine, PM_{0.03} and PM_{0.02} respectively. The MPPD model results indicated that ultrafine particles tend to be deposited in pulmonary regions more than head and trachea regions, due to high probability of diffusibility of ultrafine particles. It was noted that 8 year old exhibit a unique trend with high total deposition and poor respiratory clearance when compared to an adult of 21 years old.

Keywords: Combustion events, MPPD, Particulate emissions, Respiratory clearance

5.1 Introduction

The health implications occasioned by inhaling fuel particulate matter has been a medical area of concern for decades due to physico-chemical nature of the particulates and size. Exposure to particulate matter has been noted as the major cause of cardiovascular diseases, mostly those particulates that originate from combustion of fossil diesel (Saha *et al.*, 2018). Theoretical simulation of particulate matter distribution in the human respiratory system provides insight in solving problems related to exposure to pollutants present in air (Wang *et al.*, 2019; Warren and Bell, 2019; Bateson and Schwartz, 2007). Children tend to be more susceptible to health effects associated with particulate pollution than adults (e Oliveira *et al.*, 2019). The children body respiratory system is still developing and they have large surface area to volume ratio hence they inhale a lot of particles as compared to adults in the same

vicinity (Tabaku *et al.*, 2011). Furthermore, children immunity is known to be very low compared to that of adults hence they are vulnerable to the effects of fine and ultrafine solid particulates (Rissler *et al.*, 2017). In literature, particulate matter has been shown to be among the causative agents of asthma and other lung failure problems (Ab Manan *et al.*, 2017; Ding *et al.*, 2017; Rojas-Martinez *et al.*, 2007). Additionally, particulate matter has been shown to affect cognitive development and attention span in children (Shier *et al.*, 2019). There is rise in research aimed at finding out the effects of different particulate matter sizes in children, and specifically the ultrafine particulates (Heinzerling *et al.*, 2016; Ohlwein *et al.*, 2019). This is one major reason this study has been conducted. Generally, the mortality from air pollution drastically reduces human life span (Thakrar *et al.*, 2018). The long term exposure to PM concentrations above WHO guidelines ($10 \mu\text{g m}^{-3}$) is known in literature to initiate elevated dangers of mortality, particularly cardiovascular disease mortality (Apte *et al.*, 2018).

The by-products of pyrolysis include various particulate matter such as liquid droplets, aerosols, soot, smoke, fumes, ash and solids mixtures (Donahue, 2018).

Particulate issues are ordered by size for the most part due to the diverse wellbeing impacts related with them (Mueller *et al.*, 2020). Particulate issue that has a streamlined width of about 2.5 is named PM_{2.5} while those with 10 micrometers and less are named PM₁₀ (Tecer *et al.*, 2008). Particulate issue PM_{2.5} is ultrafine and more poisonous than PM₁₀ on the grounds that they have high infiltration power somewhere down in the lungs as well as alveolar (Herndon and Whiteside *et al.*, 2018). A worldwide report from 1990 to 2015 on death rates credited to surrounding air contamination detailed that encompassing PM_{2.5} was fifth-positioning mortality chance factor in 2015 (Cohen *et al.*, 2017). Besides, research has demonstrated that PM₁₀ or PM_{2.5} can live in the lungs and result in gentle to extreme sickness and could cause genuine diseases and dangerous illnesses (Terzano *et al.*, 2010; Chen *et al.*, 2018).

A few epidemiological investigations have demonstrated that constant introduction to high convergences of PM particularly ultrafine ones, have a connection with human respiratory and cardiovascular wellbeing dangers (Hosgood III *et al.*, 2011; Burnett *et al.*, 2014; Madaniyazi *et al.*, 2015; Maji *et al.*, 2018; Kyung and Jeong, 2020). In this way, the measurement of PM affidavit and their leeway in the human air-pathways are imperative for assessing wellbeing dangers. Furthermore, the pace of disposal of PM through procedures,

for example, body digestion, concoction activity and exhalation additionally influenced the measure of PM clearing in the respiratory framework. The particulate conveyance and statement in the respiratory framework differs as indicated by the boundaries, for example, particulate size, shape and the structure of respiratory framework (Kodros *et al.*, 2018).

Various computational models have been created so as to have an away from of vaporized statement in the lungs of people and creatures utilized in non-clinical investigations (Miller *et al.*, 2016). The maintenance of breathed in particulate issue in human lungs is a significant wellbeing hazard boundary. Notwithstanding, it isn't effectively evaluated by regular methods. Molecule testimony models have along these lines been intended to precisely foresee the affidavit of particulate issue in human lungs. Multipath Particle Deposition (MPPD) Model rendition 3.04 is such a significant model for anticipating PM testimony in human tracheobronchial aviation routes (Manojkumar *et al.*, 2019). In the MPPD study, the aviation route structures of newborn children, kids and grown-ups were thought of. When all is said in done, PM statement in body tissues is assessed by their dissemination rate from the lung surface to the epithelium cells and their maintenance in body tissues, with the point of evaluating the weight on the respiratory framework over most ages – newborn children (3 months old enough), youngsters (8 years old) and grown-ups (21 years old). The centrality of considering particulate statement in human respiratory framework is to comprehend the dangers related with the introduction to particulate issue, develop successful medication treatment strategies for constant aviation route ailments, and figuring dosimetry for word related cleanliness and restorative medicines (Rahimi-Gorji *et al.*, 2016).

5.2 Materials and Methods

5.2.1 The pyrolysis reactor system

A Thermo-Scientific heater, USA, with an internal heating compartment of dimensions 14 cm × 12 cm × 13 cm was used in this study to generate particulate emissions for selected transport fuels. The heater was fitted with a temperature regulating knob to regulate the temperature from ambient to 1000 °C. The set up for this study was reported in Chapter Three figure 3.

Fifty (50 mg) of bio-diesel and/or commercial diesel blend (ratio 1:1) was poured into the quartz reactor housed inside a furnace (Chapter Three Figure 3.1). The temperature was then set at 600 °C to simulate the pyrolytic conditions in an internal combustion engine. The flow rate of the pyrolysis gas (N₂) was set at 2.0 s. This translates to a gas delivery of 147 cm³ min⁻¹

¹ according to the expression reported in chapter three. Particulate emissions were collected using a clean glass at the end of the vent as shown in Figure 3.1 in Chapter three. The particulates which stuck on the glass were transferred into an amber vial using a clean glass rod and taken to the laboratory for microscopy analysis.

5.2.2 Scanning electron microscopy analysis and particulate distribution using image J

About 3 mg of particulate matter was introduced into 1 mL methanol and copper grids dipped into the prepared particulate matter. Twisters were used to pick the gold grids from the char sample. The sample was embedded to aluminium SEM stubs with carbon tape. Samples were subsequently gold coated in a Quorum Q150 RES sputter coater (Pongjanta *et al.*, 2008). The grids were allowed to dry in air before putting them into the analysis chamber of a Zeiss Ultra Plus (Germany) field emission gun scanning electron microscope (FEG SEM) (Konert and Vandenberghe, 1997).

Image *J* computational code was used to determine the particulate size of the particulate matter evolved from the burning of biodiesel, and biodiesel fossil mixture, and a distribution curve of particulate size was then prepared using *Igor* graphing software (Igor ver. 5.0). The mean sizes of the char particulates at 600 °C were then reported. Image *J* computational code is a highly intelligent software which apart from measuring the particulate size of particulates also generates the mean and the standard deviation of the particulates (Weerakkody *et al.*, 2018).

5.2.3 Respiratory tract deposition model

Deposition for biodiesel blend emission was predicted using MPPDV3.04 model. The model is used to simulate particle movement during respiration process. The human lung models comprise of Yeh-Schum, stochastic, age-specific, Weibel and Pacific Northwest National Laboratories provided models from computerized tomography models (Miller *et al.*, 2016). The age specific symmetric lung model (Asgharian *et al.*, 2001; Asgharian *et al.*, 2014) was used with input parameters such as airway morphometry, inhalant properties, exposure conditions and deposition. The data obtained in previous research, reported that the particulate matter from co-pyrolysis of *C. megalocarpus* biodiesel blend and neat commercial diesel were classified as ultrafine, PM_{0.03} and PM_{0.02}. These particulate sizes were used to model the deposition of particulate matter in MPPD model in human beings for ages 3 months, 8 years and 21 yrs. Other input parameters were not available experimentally and therefore, default values in the MPPD software were used. The default settings were

applied because experimental parameters were not available. Nonetheless, the simulated values used as defaults are considered to be very close to experimental values for the purpose of simulating breathing scenarios in humans.

5.3 Results and discussion

In this work, data on the particulate matter emissions of co-pyrolysis of *C. megalocarpus* biodiesel and petroleum diesel blend (binary diesel) reported in Chapter three (section 3.4.1) and Chapter four (section 4.3.1) respectively, were used to simulate the deposition of particulate matter in the human respiratory system using the MPPD ver.3.04 model. The central point of this investigation is the analysis of particulate matter emission from the co-pyrolysis of *C. megalocarpus* biodiesel and petroleum diesel blend. Of principle focus was to classify the particulate matter emitted by co-pyrolysis of *C. megalocarpus* biodiesel and petroleum diesel blend suspected to be the source of a number of health and environmental problems. It is known that the particulate matter of $PM_{2.5}$ is ultrafine and more fatal than PM_{10} because they have high penetration ability deep in the lungs and or alveolar (Schweitzer *et al.*, 2018). Previous findings reported in Chapters three and four of this study, the particulate matter was categorised as ultrafine with particulate sizes less than $PM_{0.1}$. Computational deposition model was used to understand more on particulate matter transportation into the respiratory system.

5.3.1 Respiratory tract deposition model for co-pyrolysis of *C. megalocarpus* biodiesel blend

The MPPD Ver.3.04 model by Applied Research Associates Inc., Albuquerque, New Mexico, USA was used to predict particle deposition fractions. The MPPD software calculates the deposition and clearance of particulate matter in the respiratory tracts of laboratory animals and human adults and children (deposition only) for particles ranging in size from ultrafine (0.001 μm) to coarse (100 μm) (Schroeter *et al.*, 2019). The MPPD model in this study was used to predict the particulate flow in human adults and children for the experimental particulates obtained from thermal decomposition of *C. megalocarpus* biodiesel and petroleum diesel blend. The age-specific model was used for infants, 8 year old and 21 year old.

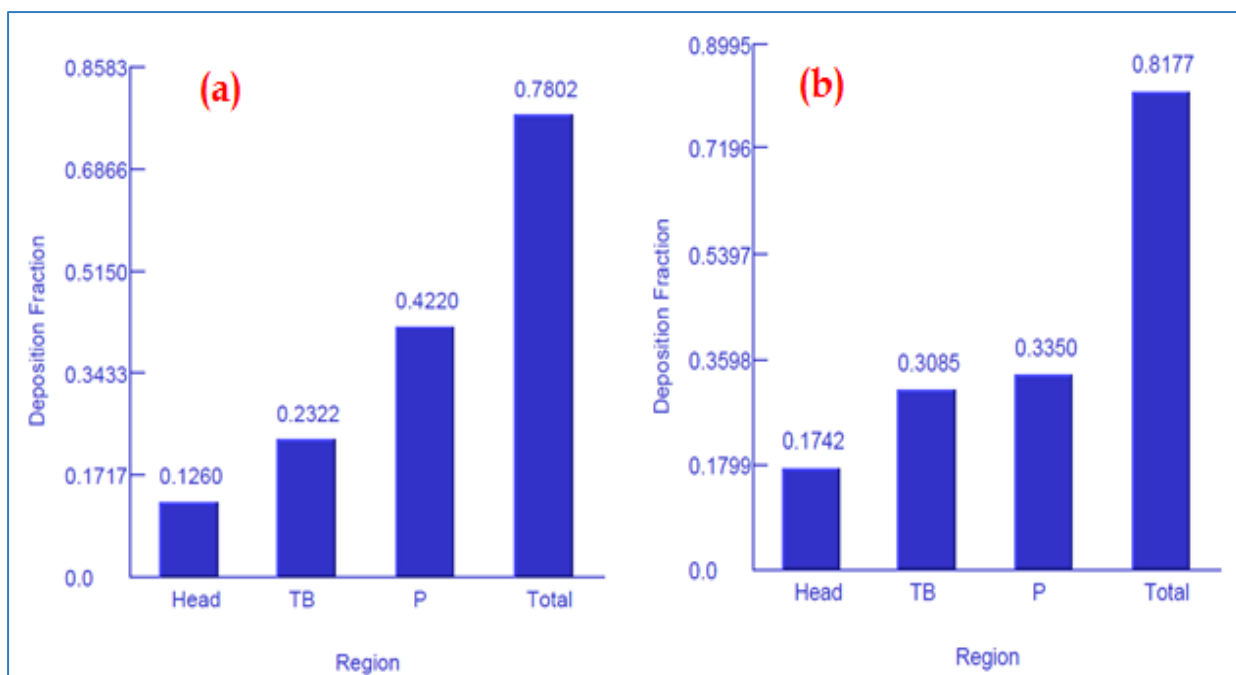


Figure 5.1: Regional respiratory (Head, trachea and bronchioles (TB) and pulmonary (P)) tract co-pyrolysis PM deposition fraction from the Multipath Particle Deposition (MPPD) model version 3.04, for particles with count medium diameter (CMD) of (a) 32 nm and (b) 22 nm having a geometric standard deviation (GSD) of 1 nm inhaled by an infant.

The MPPD model showed that the deposition fractions for biodiesel blend emissions, predicted for infants (Figure 5.1 (a)), 8 year old (Figure 5.2 (a)) and 21 year old (Figure 5.3 (b)) varied with particle size in various respiratory sections (head-H, trachea and bronchioles (TB) and pulmonary (P) as shown in Fig 5.1, 5.2 and 5.3. The MPPD infant (3 months) for particulate of geometrical diameter 32 nm (Figure 5.1 (a)) showed that the fractional deposition were 0.1260, 0.2322 and 0.4220 for head, TB and P respectively. The total lung deposition was 0.7802. On the other hand, the total deposition fraction for particulates of geometrical diameter 22 nm was 0.8177 (Figure 5.1(b)).

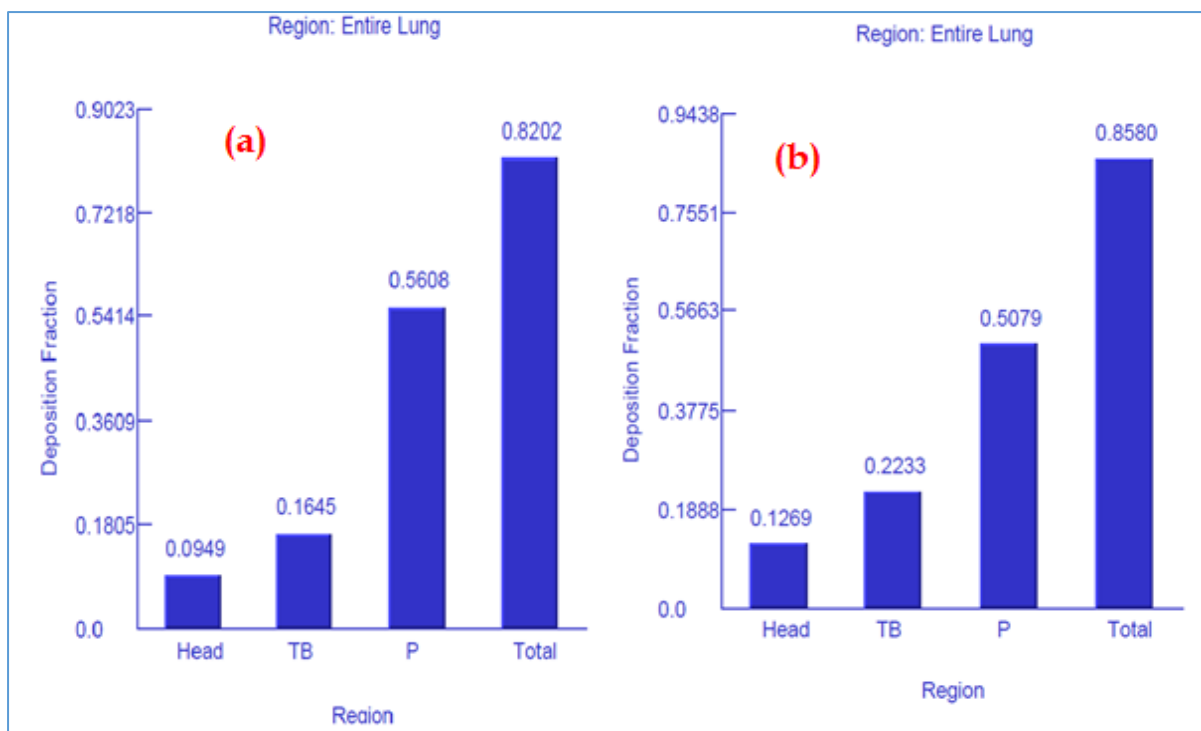


Figure 5.2: Regional respiratory tract co-pyrolysis PM deposition fraction from the Multipath Particle Deposition (MPPD) model version 3.04, for particles with count medium diameter (CMD) of (a) 32 nm and (b) 22 nm having a geometric standard deviation (GSD) of 1 nm inhaled by an 8 years old.

In the case of 8 years old, the depositions in head, trachea and bronchi and pulmonary were predicted to be 0.0949, 0.1645 and 0.5608 respectively, with the total deposition being 0.8202 (Figure 5.2(a)). The smaller particulates (22 nm) appeared to have been retained in excess of ~ 4% in comparison to the relatively larger particulates (32 nm). Evidently, the highest fractions of PM were deposited in the pulmonary region across all the ages considered. This could be attributed to higher flow rates and low size range (0.001-0.01 μ m) distributions having high residence time in the lower respiratory tract. Similar observations were made by (Sahu *et al.*, 2013).

The total deposition in the lungs appears not to be a function of age because there appears to be no linear correlation of deposition with the age bracket. The probable reason for this, could be that 8 years old population tend to be highly active (high respiration) and spend most of their time outdoors hence they breathe more kilograms of particulates per body weight than babies and adults.

In the case of 21 year old (herein referred to as adult), the deposition fractions were 0.0836, 0.1729, 0.4849 for the head TB, and pulmonary sections respectively while the total deposition fraction was observed as 0.7415 for particulates of 32 nm diameter (Figure 5.3 (b)).

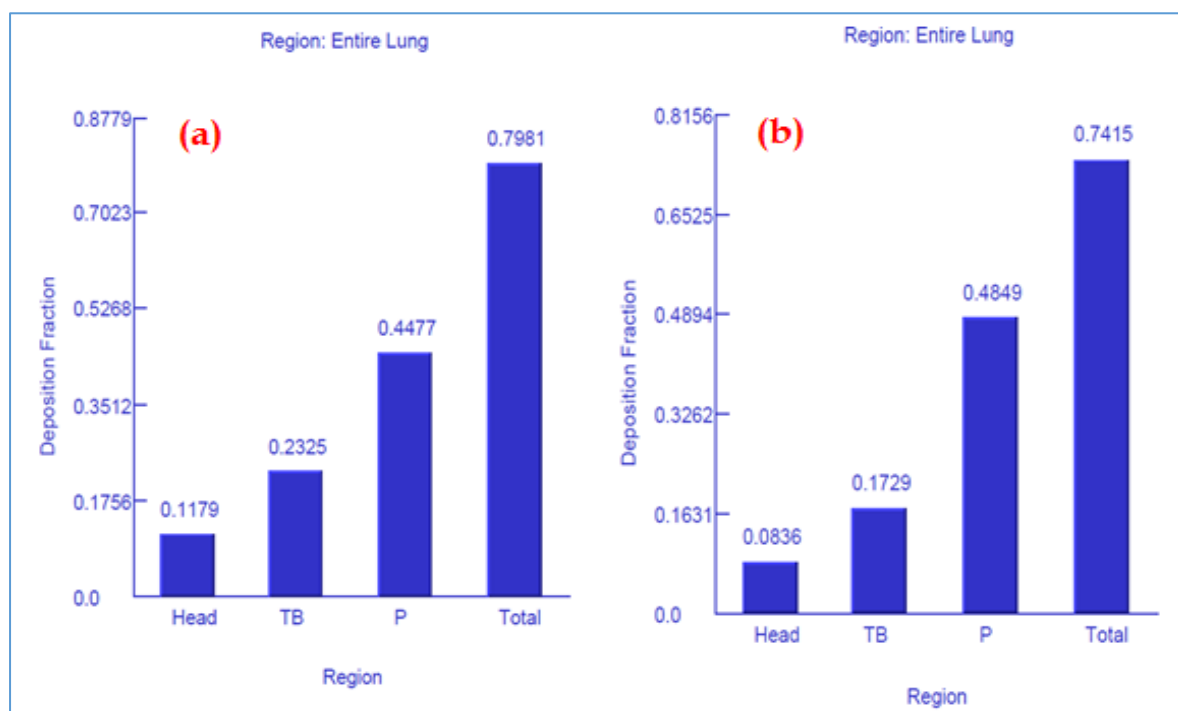


Figure 5.3: Regional respiratory tract co-pyrolysis PM deposition fraction from the Multipath Particle Deposition (MPPD) model version 3.04, for particles with count medium diameter (CMD) (a) 22 nm and (b) 32 nm with a geometric standard deviation (GSD) of 1 nm inhaled by a 21 years old

For comparison purposes, regional deposition predictions for pyrolysis of *C. megalocarpus* biodiesel (aerodynamic diameter of ~22 nm) particulate matter were done for similar age groups (Figures 5.1 (b) and 5.2 (b), and Figure 5.3 (a)). The Total lung deposition for 21 years (adult), 8 year and 3 months old were predicted to be 0.7981, 0.8580 and 0.7802 respectively. Evidently, the regional depositions shows high particulate depositions in the pulmonary region compared to the rest of the respiratory systems. This could be attributed to high diffusibility of the ultrafine particles compared to coarse particles. The size of the particles in *C. megalocarpus* char, PM \approx 22 nm are slightly smaller than in the biodiesel blend PM \approx 32 nm. This is clearly shown by high total depositions in respiratory regions in Figs. 5.1 (b) and 5.2 (b) and Figure 5.3 (a) for all age groups as compared to Figs. 5.1 (a), 5.2 (a) and 5.3 (b). The difference in total deposition in this study could be attributed to airway

geometry, particulate matter size and deposition patterns. The effects of particulate matter in inspiration process can be prevented by minimizing combustion events that have a serious impact on the environment and public health. Promotion of clean energy combustion is perhaps the most important measure against hazardous emissions from thermal events.

The major patterns affecting particulate deposition are sedimentation, diffusion and impaction hence this modelling work predicts the dose of inhaled PM and finds out the sections in the respiratory system where there is possible occurrence of toxicity. It is noticeable that blending biodiesel increase particulate sizes and remarkably lowers the risk of inhalation, even though in this study the increase in size is still within the ultrafine category. Thus, extremely ultrafine particulate matter reported in this work is toxic to humans and especially to residents living in polluted cities and industry.

Conclusions

This study has established that the particulate emissions from the thermal degradation of croton biodiesel and croton biodiesel/commercial diesel blend are ultrafine and can be transported deeply in the respiratory system, and circulated to other body tissues, hence may cause cardio-pulmonary deaths, oxidative stress, nervous system impairment as well as chronic coughs and cancers which are detrimental to human life. MPPD Version 3.04 runs indicated that pulmonary tissue retained the highest ratio of thermal emissions of croton bio-oil particulates for all ages (infants, 8 years and 21 years respectively) as compared to the particulates from the diesel pyrolysis mixtures. Clearly, infants retain a high fraction of particulates possibly because their lungs are not well developed and they have high volume ratio to weight, and this may be a major pre-cursor for child mortality. Additionally, blending biodiesel in the correct ratios may be one of the measures of mitigating against environmental pollution caused by transport fuels. Therefore, there is every reason to appreciate that clean energy combustion is important towards improving public health and reducing disease burden caused by thermal emissions of varying chemical nature and size.

References

- Ab Manan, N., Jaafar, M. H. and Hod, R. (2017). Air Pollution and Asthma in Children: A Literature Review. *International Journal of Public Health and Clinical Sciences*, **4**(3): 47-56.
- Apte, J. S., Brauer, M., Cohen, A. J., Ezzati, M. and Pope III, C. A. (2018). Ambient PM_{2.5} reduces global and regional life expectancy. *Environmental Science and Technology Letters*, **5**: 546-551.
- Asgharian, B., Hofmann, W. and Bergmann, R. (2001). Particle deposition in a multiple-path model of the human lung. *Aerosol Science and Technology*, **34**: 332-339.
- Asgharian, B., Price, O., Oldham, M., Chen, L.-C., Saunders, E., Gordon, T., Mikheev, V. Minard, K. and Teeguarden, J. (2014). Computational modeling of nanoscale and microscale particle deposition, retention and dosimetry in the mouse respiratory tract. *Inhalation Toxicology*, **26**: 829-842.
- Bateson, T. F. and Schwartz, J. (2007). Children's response to air pollutants. *Journal of Toxicology and Environmental Health, Part A*, **71**(3): 238-243.
- Burnett, R. T., Pope III, C. A. Ezzati, M. Olives, C. Lim, S. S. Mehta, S. Shin, H. H. Singh, G. Hubbell, B. and Brauer, M. (2014). An integrated risk function for estimating the global burden of disease attributable to ambient fine particulate matter exposure. *Environmental Health Perspectives*, **122**(4): 397-403.
- Chen, C. W., Hsieh, Y. H., Su, H. C. and Wu, J. J. (2018). Causality test of ambient fine particles and human influenza in Taiwan: Age group-specific disparity and geographic heterogeneity. *Environment International*, **111**: 354-361.
- Cohen, A. J., Brauer, M., Burnett, R., Anderson, H. R., Frostad, J., Estep, K., Balakrishnan, K., Brunekreef, B., Dandona, L. and Dandona, R. J. T. L. (2017). Estimates and 25-year trends of the global burden of disease attributable to ambient air pollution: an analysis of data from the Global Burden of Diseases Study 2015. *The Lancet*, **389**: 1907-1918.
- Ding, L., Zhu, D., Peng, D. and Zhao, Y. (2017). Air pollution and asthma attacks in children: A case–crossover analysis in the city of Chongqing, China. *Environmental Pollution*, **220**: 348-353.
- Donahue, N. M. (2018). Air Pollution and Air Quality. *Green Chemistry*, Elsevier: 151-176.
- e Oliveira, J. R. D. C., Base, L. H., de Abreu, L. C., Ferreira Filho, C., Ferreira, C. and Morawska, L. (2019). Ultrafine Particles and Children's Health: Literature Review. *Paediatric Respiratory Reviews*.

- Heinzerling, A., Hsu, J. and Yip, F. (2016). Respiratory health effects of ultrafine particles in children: A literature review. *Water, Air, and Soil Pollution*, **227**(1): 32.
<https://doi.org/10.1007/s11270-015-2726-6>.
- Herndon, J. M. and Whiteside, M. (2018). California wildfires: Role of undisclosed atmospheric manipulation and geoengineering. *Journal of Geography, Environment and Earth Science International*, **17**(3): 1-18.
- Hosgood III, H. D., Wei, H., Sapkota, A., Choudhury, I., Bruce, N., Smith, K. R. and Lan, Q. (2011). Household coal use and lung cancer: systematic review and meta-analysis of case-control studies, with an emphasis on geographic variation. *International Journal of Epidemiology*, **40**: 719-728.
- Kodros, J. K., Volckens, J., Jathar, S. H. and Pierce, J. R. (2018). Ambient particulate matter size distributions drive regional and global variability in particle deposition in the respiratory tract. *GeoHealth*, **2**(10): 298-312.
- Konert, M. and Vandenberghe, J. (1997). Comparison of laser grain size analysis with pipette and sieve analysis: a solution for the underestimation of the clay fraction. *Sedimentology*, **44**: 523-535.
- Kyung, S. Y. and Jeong, S. H. (2020). Particulate-Matter Related Respiratory Diseases. *Tuberculosis and Respiratory Diseases*, **83**(2): 116-121.
- Madaniyazi, L., Nagashima, T., Guo, Y., Yu, W. and Tong, S. (2015). Projecting fine particulate matter-related mortality in East China. *Environmental Science and Technology*, **49**: 11141-11150.
- Maji, K. J., Dikshit, A. K., Arora, M. and Deshpande, A. (2018). Estimating premature mortality attributable to PM_{2.5} exposure and benefit of air pollution control policies in China for 2020. *Science of the Total Environment*, **612**: 683-693.
- Manojkumar, N., Srimuruganandam, B. and Nagendra, S. S. (2019). Application of multiple-path particle dosimetry model for quantifying age specified deposition of particulate matter in human airway. *Ecotoxicology and Environmental Safety*, **168**: 241-248.
- Miller, F. J., Asgharian, B., Schroeter, J. D. and Price, O. (2016). Improvements and additions to the multiple path particle Dosimetry model. *Journal of Aerosol Science* **99**: 14-26.
- Mueller, W., Cowie, H., Horwell, C. J., Hurley, F. and Baxter, P. J. (2020). Health Impact Assessment of volcanic ash inhalation: A comparison with outdoor air pollution methods. *GeoHealth*, e2020GH000256. <https://doi.org/10.1029/2020GH000256>.

- Ohlwein, S., Kappeler, R., Joss, M. K., Künzli, N. and Hoffmann, B. (2019). Health effects of ultrafine particles: a systematic literature review update of epidemiological evidence. *International Journal of Public Health*, **64**(4): 547-559.
- Pongjanta, J., Utaipatanacheep, A., Naivikul, O. and Piyachomkwan, K. (2008). Enzymes-resistant starch (RS III) from pullulanase-debranched high amylose rice starch. *Kasetsart Journal of Natural Science*, **42**: 83-92.
- Rahimi-Gorji, M., Gorji, T. B. and Gorji-Bandpy, M. (2016). Details of regional particle deposition and airflow structures in a realistic model of human tracheobronchial airways: two-phase flow simulation. *Computers in Biology and Medicine*, **74**: 1-17.
- Rissler, J., Gudmundsson, A., Nicklasson, H., Swietlicki, E., Wollmer, P. and Löndahl, J. (2017). Deposition efficiency of inhaled particles (15-5000 nm) related to breathing pattern and lung function: an experimental study in healthy children and adults. *Particle and Fibre Toxicology*, **14**(1): 10.
- Rojas-Martinez, R., Perez-Padilla, R., Olaiz-Fernandez, G., Mendoza-Alvarado, L., Moreno-Macias, H., Fortoul, T., McDonnell, W., Loomis, D. and Romieu, I. (2007). Lung function growth in children with long-term exposure to air pollutants in Mexico City. *American Journal of Respiratory and Critical Care Medicine*, **176**(4): 377-384.
- Saha, P. K., Robinson, E. S., Shah, R. U., Zimmerman, N., Apte, J. S., Robinson, A. L. and Presto, A. A. (2018). Reduced ultrafine particle concentration in urban air: changes in nucleation and anthropogenic emissions. *Environmental Science and Technology*, **52**(12): 6798-6806.
- Sahu, S. K., Tiwari, M., Bhangare, R. C. and Pandit, G. G. (2013). Particle size distribution of mainstream and exhaled cigarette smoke and predictive deposition in human respiratory tract. *Aerosol Air Quality Research*, **13**: 324-32.
- Schroeter, J., Asgharian, B. and Kimbell, J. (2019). Mathematical modeling of inhaled therapeutic aerosol deposition in the respiratory tract. *Inhalation Aerosols: Physical and Biological Basis for Therapy*, **1**: 41-65.
- Schweitzer, M.D., Calzadilla, A.S., Salamo, O., Sharifi, A., Kumar, N., Holt, G., Campos, M. and Mirsaeidi, M. (2018). Lung health in era of climate change and dust storms. *Environmental Research*, **163**: 36-42.
- Shier, V., Nicosia, N., Shih, R. and Datar, A. (2019). Ambient air pollution and children's cognitive outcomes. *Population and Environment*, **40**(3): 347-367.
- Tabaku, A., Bejtja, G., Bala, S., Toci, E. and Resuli, J. (2011). Effects of air pollution on children's pulmonary health. *Atmospheric Environment*, **45**(40): 7540-7545.

- Tecer, L. H., Süren, P., Alagha, O., Karaca, F. and Tuncel, G. (2008). Effect of meteorological parameters on fine and coarse particulate matter mass concentration in a coal-mining area in Zonguldak, Turkey. *Journal of the Air and Waste Management Association*, **58**: 543-552.
- Terzano, C., Di Stefano, F., Conti, V., Graziani, E. and Petroianni, A. (2010). Air pollution ultrafine particles: toxicity beyond the lung. *European Review Medical Pharmacology Science*, **14**: 809-821.
- Thakrar, S. K., Goodkind, A. L., Tessum, C. W., Marshall, J. D. and Hill, J. D. (2018). Life cycle air quality impacts on human health from potential switchgrass production in the United States. *Biomass and Bioenergy*, **114**: 73-82.
- Wang, R., Chen, R., Wang, Y., Chen, L., Qiao, J., Bai, R., Ge, G., Qin, G. and Chen, C., (2019). Complex to simple: In vitro exposure of particulate matter simulated at the air-liquid interface discloses the health impacts of major air pollutants. *Chemosphere*, **223**: 263-274.
- Warren, J. L. and Bell, M. L. (2019). Alternative models for estimating air pollution exposures—Land Use Regression and Stochastic Human Exposure and Dose Simulation for particulate matter (SHEDS-PM). In *Handbook of Environmental and Ecological Statistics* (435-484). Chapman and Hall. New York.
- Weerakkody, U., Dover, J. W., Mitchell, P. and Reiling, K. (2018). Evaluating the impact of individual leaf traits on atmospheric particulate matter accumulation using natural and synthetic leaves. *Urban Forestry and Urban Greening*, **30**: 98-107

CHAPTER SIX

OPTIMIZATION OF BINARY MIXTURES OF BIODIESEL AND FOSSIL DIESEL FOR CLEAN ENERGY COMBUSTION

Abstract

There is an urgent interest initiated to develop clean energy resources with the aim of reducing exposure to environmental pollutants and explore model fuels that can hasten the achievement of clean energy combustion. This work investigates various ratios of biodiesel and commercial diesel in order to propose model binary fuels for clean energy combustion. Accordingly, diesel blends of ratios 1:1, 3:2 and 2:3 were each pyrolyzed at a contact time of 5 seconds in a quartz reactor at 1 atmosphere pressure. A model temperature of 500 °C was explored in these experiments. The charcoal content for pure fossil diesel was compared with the binary diesel residue. Gas-phase molecular components were determined using Gas chromatography (GC) coupled to a mass selective detector (MSD). Elemental composition of thermal char was determined using Smart Elemental Analyzer. Radical intensities for the three types of char (biochar, bio-fossil char, and fossil char) were measured using an X-band electron paramagnetic resonance spectrometer. It was noted that at a ratio of 2:3 (Biodiesel: Fossil diesel), harmful molecular products reduced significantly, 76 – 99%. Elemental analysis data indicated that the carbon content from commercial diesel was very high ($\approx 70.61\%$) as compared to approximately 53% for biodiesel-fossil diesel mixture in the same ratio 2:3. Interestingly, the free radical content was reduced by nearly 50% in favour of the biodiesel/fossil diesel mixture. These results are encouraging and suggest that a better optimized fuel mixture has been found for better clean energy combustion.

Keywords: Clean energy combustion, Diesel blends, Elemental composition, Thermal char.

6.1 Introduction

Some of the increasing challenges facing the 21st century is energy security, environmental pollution and human health complications including asthma, carcinogens, and acid rains. Renewable energies are considered to offer solutions to most of these challenges. Therefore, thorough research is of essence to gain insight on new energy technologies with the key focus on maintaining safe and renewable energy resources for sustainable development, better public health care and improved economies. The upsurge in fuel demand, possibility of depletion of fossil fuels reserves with exponential increase in population and economic growth is the precursor that has precipitated the search for alternative energy resources

(Fontes and Freires, 2018). Additionally, the toxic nature associated with exhaust emissions from vehicles fuelled by fossil diesel has emboldened the search for alternative fuels such as biodiesel and diesel blends (binary and ternary fuels from biodiesel and fossil diesel). A number of studies have reported the impact of blending fossil diesel and biodiesel fuel on engine performance and emission characteristics that may have serious environmental bearing on human health and other ecosystems (Ghazali *et al.*, 2015; Tutak *et al.*, 2015; Ali *et al.*, 2016; Ruhul *et al.*, 2016; Ruhul *et al.*, 2017; Mahmudul *et al.*, 2017; Damanik *et al.*, 2018; Khan *et al.*, 2018; Quasim *et al.*, 2018).

Conventionally, pyrolysis is the thermal degradation of biomass in absence or limited supply of oxygen (Guedes *et al.*, 2018) to form enormous pyrolysis reaction products (benzene and its derivatives, furans and dioxins) and particulate emissions considered harmful to human health and natural ecosystems (Czajczyńska *et al.*, 2018). Secondary oxidation products may include aldehydes, ketones, low molecular acids and volatile organic compounds, resulting in the increase of acidity as the degradation progresses (Chendynski *et al.*, 2019). The by-products of pyrolysis also include an array of particulate matter such as liquid droplets, aerosols, soot, and tar (Chhetri and Islam, 2008). Nonetheless, the thermal processing of biomass in general represents a promising method for recovery of renewable energy for industrial applications (Altarawneh and Dlugogorski, 2015).

Biodiesel is a potential renewable biodegradable fuel resource comprising of fatty acid methyl esters (Sundus *et al.*, 2017; Yahagi *et al.*, 2019). The major routes for the production of biodiesel are chemical esterification catalyzed by sodium methoxide (NaOCH_3) or sodium hydroxide (NaOH) and enzymatic trans-esterification using *Candida antarctica* lipase as reported in literature (Ma and Hanna, 1999; Mumtaz *et al.*, 2012). Transesterification generally is a process in which an ester is transformed into another ester through alkali or enzyme catalyzed reversible reactions in presence of an alcohol to produce an ester and a glycerol (Ma and Hanna, 1999). Remarkably, the complicated structural composition of biomass materials makes it difficult to link the formation of organic pollutants to specific chemical reactions although significant attempts have been conducted by Mohamednoor and his co-workers using surrogates representative of the structure of biomass materials crucial in the production of biofuel (Altarawneh and Dlugogorski, 2015).

Previous studies that advanced the use of ternary fuel blends indicated that about 5–10% of ethanol with 20–25% biodiesel can be added with petro-diesel effectively to reduce global

emission, promote public health and reduce environmental impacts (Mofijur *et al.*, 2016; Yahagi *et al.*, 2019). Both biodiesel–diesel and ethanol–biodiesel–diesel blending plays an important role in reducing exhaust gas emissions particularly carbon monoxide (CO), hydrocarbons (HC), and particulate matter (PM) (Mumtaz *et al.*, 2012; Mofijur *et al.*, 2016; Arroyo *et al.*, 2019). Whereas the current work does not discuss the particulate emissions arising from the co-pyrolysis of binary fuels (biodiesel and fossil diesel), it focuses primarily on binary fuel ratios aimed at decreasing harmful molecular emissions – it seeks to establish the best ratio for better combustion that would minimize environmental molecular pollutants for green energy strategies. Study carried out in Chapter three was mainly motivated by the pyrolysis of equimasic mixture of biodiesel and fossil diesel with the exclusive focus of determining particulate emissions and the formation of free radicals in binary transport fuels. This contribution, however, distinguishes itself as a potential experimental design that would optimize the viability of binary mixtures of biodiesel and fossil diesel at selected ratios aimed at achieving clean energy combustion. The selected ratios were developed from our laboratory while taking into account previous work reported in literature on the pyrolysis of, for example, palm oil biodiesel methyl ester blended with diesel fuel (B20) in presence of cetane number improver-di-tert-butyl peroxide (DTBP) and fossil diesel (Musthafa *et al.*, 2018). Besides, it borrows significantly from the efforts by several countries to introduce a compulsory addition of biodiesel to fossil diesel, such as the mandatory addition of 30% biodiesel to fossil diesel fuel regulation by Czech Republic and Slovakia, 20% by United States and Canada as well as 5% in the European Union, and Argentina (Yahagi *et al.*, 2019).

Although biodiesel is slowly replacing fossil fuels, its pyrolysis by-products are too difficult to understand due to complex cross reactions that occur during pyrolysis. Current research on transport fuels is advanced towards sustainable development of renewable energies with lower environmental impacts and greater economic output (Yahagi *et al.*, 2019). Moreover, biofuel has been considered a promising alternative to fossil fuel because of the proposed public health and environment quality occasioned by reduction in harmful emission from biofuel operated diesel engines (Mofijur *et al.*, 2016). Consequently, biodiesel has been touted as a potential renewable energy resource but certain inherent challenges including instability, metal contamination, ageing, moisture absorption and its corrosive nature impede its application as a transport fuel (Sundus *et al.*, 2017; Yahagi *et al.*, 2019). Metal contamination for instance can occur by direct contact with the container or presence of metal fragments in biodiesel during production (Chendynski *et al.*, 2019). Nonetheless, biodiesel

find its use as an alternative source of energy because of the diminishing petroleum reserves despite the shortcomings in biodiesel viability as it currently stands (Pusparizkita *et al.*, 2018).

Previously, studies revealed that the use of biodiesel as a transport fuel has seen reduction in environmental pollutants such particulate matter, carbon monoxide, unburned hydrocarbons and volatile organic compounds (VOCs) considered toxic to biological systems and natural ecosystems (Tsai *et al.*, 2016; Damanik *et al.*, 2018; Zhang *et al.*, 2019; Liu *et al.*, 2019). Biodiesel may be utilized in pure form or in blends but it has not been fully optimized to attain the necessary calorific value to power internal combustion engines (Suresh *et al.*, 2018). To do so, major modifications including optimizing viscosity and pH have to be done (Hasan *et al.*, 2017). Oxidation of biodiesel molecular products can lead to polymerization to form gums which may make biodiesel unsuitable for use thus resulting in engine damage and probably engine loss (Chendynski *et al.*, 2019). These are serious challenges that must be overcome in order to ensure viable use of biodiesel.

To comprehensively evaluate the importance of emission reduction measures of a fuel, various studies on fuel emissions characterization must be conducted (San José *et al.*, 2018). Accordingly, this study seeks to determine the nature of molecular organic emissions produced from the co-pyrolysis of *C. megalocarpus* biodiesel and fossil diesel at various ratios, and compare with combustion of neat fuels from which an informed decision can be proposed on which binary mixture can be adopted for clean energy combustion. The study explores potential binary mixtures between biodiesel and commercial diesel (fossil diesel) that may produce fewer molecular products, radicals and, carbonaceous material in form of particulate matter. *Croton megalocarpus* plant is a common plant in that grows in the wild and diverse climatic conditions in Kenya and produce non-edible oil, which may offer a competitive energy resource since there is no competition with edible oils (Kigen *et al.*, 2017). Therefore, this study explores molecular reaction products and thermal emissions at an optimum pyrolysis temperature of 500 °C at different ratios of *C. megalocarpus* and fossil diesel.

The cost of producing biodiesel is significantly high (Nejad and Zahedi, 2018) compared to the production of fossil fuel. Therefore, mixing biodiesel with fossil fuel to optimize the combustion capacity of the binary mixture would be a compromise towards clean energy combustion and better engine performance. The primary focus of this study is to investigate

the binary ratios of biodiesel and commercial diesel that are beneficial to the environment and public health during combustion. We believe this assessment will provide leads towards cheaper fuel with reduced thermal emissions. Therefore, the primary focus of the current study was identify which diesel blends would be suitable for clean energy combustion with minimum environmental impacts. It also aims at comparing the density of free radicals generated by pyrolysis of pure biodiesel and the binary mixture of biodiesel and fossil diesel with a view to assessing their environmental impacts.

6.2 Materials and methods

Chemicals used in this study were of analytical grade (purity > 99%) and were purchased from Sigma Aldrich Inc., (St. Louis Missouri, USA) through its subsidiary, Kobian Kenya, Ltd. The reagents were used without further treatment. Croton oil was prepared by solvent extraction method using hexane followed by conversion to biodiesel via trans-esterification using NaOH solution as a catalyst (Chapter Three). The resultant biodiesel ultimately subjected to American Society for Testing and Materials (ASTM) D 6751 standards (Ma *et al.*, 2016; Thirugnanasambandham *et al.*, 2016). Commercial diesel was purchased from a local out let and used without further treatment. The heater (Figure 6.1) with a temperature range $\approx 20 - 1000$ °C, a muffle furnace was purchased from Thermo-Scientific Inc., USA. The furnace has a temperature gradient of 10 °C. The reactor used in this work was fabricated at the University of Nairobi – Department of Industrial and Applied Sciences laboratory by a glass blower while nitrogen of ultrahigh purity $\geq 99.99\%$ (grade 5.0) was purchased from BOC gases, Kenya. The reactor has various parts including a transfer line constantly heated at 250 °C to prevent condensation of tar along the transfer line.

6.2.1 Co-pyrolysis of *C. megalocarpus* biodiesel and petroleum diesel

In order to investigate the nature of molecular products for optimization for clean energy combustion, different binary mixtures in the ratio of 1:1, 3:2 and 2:3 w/w for *C. megalocarpus* biodiesel to petroleum diesel, were separately introduced into a pyrolysis reactor. The *C. megalocarpus* biodiesel and fossil diesel were mixed and placed in a quartz reactor of volume 7.56 cm³ housed in a furnace (Thermo-Scientific Inc., USA), Figure 6.1. Pyrolysis was conducted at an optimum temperature of 500 °C under a flow of nitrogen at a residence time of 5 sec at 1 atmosphere, as model pyrolysis conditions in the reactor ideally representative of the conditions inside a combustion engine. The reactor used in this study is presented in Figure 6.1.

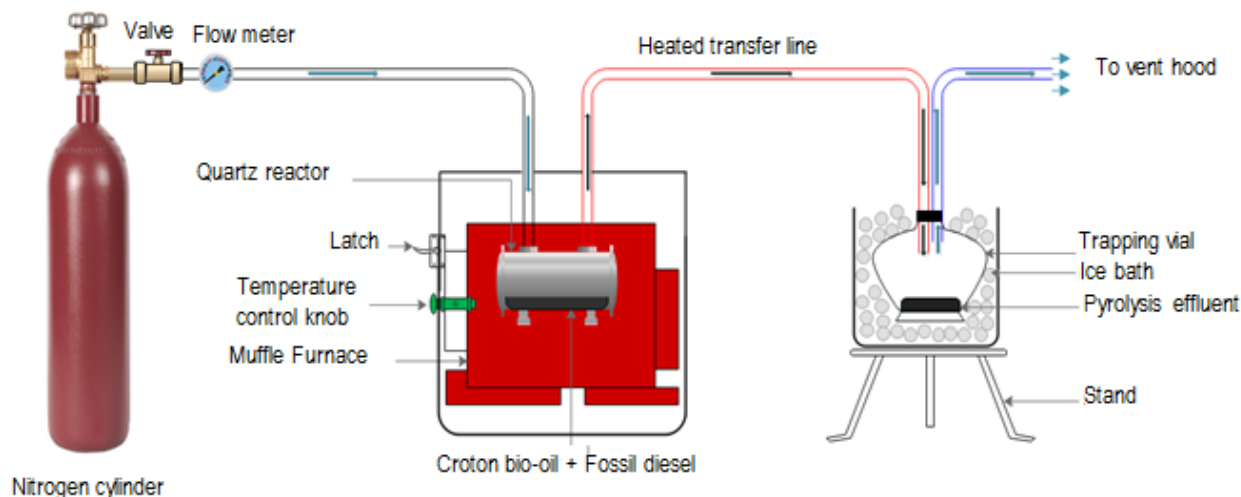


Figure 6.1: Reactor assembly and gas-phase trapping apparatus

6.2.2 GC-MS identification of molecular products

Condensable gas-phase molecular by-products from the co-pyrolysis of *C. megalocarpus* biodiesel and fossil diesel, was passed through 10 mL dichloromethane solution (DCM) solution in an ice bath, filtered using a Whatman no. 10 filter paper and analysed using an Agilent Technologies 7890A GC system connected to an Agilent Technologies 5975C inert XL EI/CI MSD with triple axis detector. The GC-MS column for this work was HP-5MS 5% phenyl methyl siloxane (30 m × 250µm × 0.25 µm). The port injector temperature was set at 250 °C to vaporize organic components to be amenable for GC-MS analysis (Chapter Four). The carrier gas was ultra-high pure (UHP) helium (99.999%) and the flow rate was 3.3 mL min⁻¹. The oven temperature was set at 100 °C. The initial temperature was 50 °C holding for 3 min and the rate was set at 10 °C /min to 150 °C, holding for 5 min, then changed to 15 °C/min up to 300 °C and held at 300 °C for 20 min. Exactly 2 µL of sample was injected in the split ratio 50:1 at 250 °C. Data was run through the NIST (National Institute of Standard Technology) library database as an additional tool to confirm identity of compounds. Additionally, pure compounds were run through the GC-MS system and the retention times compared with the compounds of interest. The data reported in this work are average of two replicates.

6.2.3 Electron paramagnetic resonance spectroscopy

A quantification of free radicals present in thermal char resulting from heat treatment of fossil diesel, biodiesel and diesel blends was conducted using Electronic Paramagnetic Resonance spectroscopy (EPR). The EPR measurements were performed using Bruker EMX-20/2.7 EPR

spectrometer operating at X-band (~ 9.5 GHz) with dual cavities. All EPR spectra were obtained with a magnetic field modulation of 100 KHz, 1 mW microwave power, 20 G modulation amplitude and scans of 4 min. The details of EPR experiments are reported elsewhere (Jebet *et al.*, 2017).

6.3 Results and discussion

A series of experiments to determine the optimum mixture for clean energy combustion was explored in this work. Consequently, various biodiesel-fossil diesel ratios of 1:1, 2:3 and 3:2 respectively were investigated. Eight representative compounds were selected in all the ratios in order to explore which ratio would be promising towards clean energy combustion. A model temperature of 500 °C was explored in this work. Evidently, a ratio of 2:3 was proposed to yield better combustion results based in Table 6.1 which decreased the yields of oxygenated molecular products. This is beneficial in the combustion efficiency of biodiesel which has been noted to suffer from low oxidation ability, increased acidity and corrosion problems (Yahagi *et al.*, 2019). It is expected that addition of hydrocarbons from fossil fuel to the methyl ester chain present in

biodiesel may suppress the formation of harmful reaction products. Generally, biofuel has been considered a promising alternative to fossil fuel because of the proposed public health and environmental benefits occasioned by reduction of harmful emission from biofuel operated

Table 6.1: Yield of molecular products from the pyrolysis of various diesel blends

Yields (diesel Blends – B:F) (μg)						
No.	Compounds	RT (mins)	MW (g/mol)	1:1	3:2	2:3
1	tetradecane	16.48	198.23	0.050 ± 0.001	1.914 ± 0.01	0.141 ± 0.01
2	pentadecane	19.03	226.27	0.054 ± 0.001	0.225 ± 0.01	0.158 ± 0.04
3	hexadecane	21.35	282.55	0.083 ± 0.02	2.225 ± 0.08	0.146 ± 0.01
4	5-(3-phenylpropanoyl)dihydro- 2(3H)-furanone	23.75	218.09	1.258 ± 0.04	1.835 ± 0.07	0.163 ± 0.05
5	2,6,10,14-tetramethylhexadecane	25.80	282.55	0.372 ± 0.03	1.600 ± 0.05	0.097 ± 0.01
6	methyl hexadecanoate	28.41	270.26	0.327 ± 0.02	0.662 ± 0.002	0.157 ± 0.03
7	methyl 8,11-Octadecadienoate	31.45	294.26	2.160 ± 0.06	7.455 ± 1.12	1.494 ± 0.05
8	methyl linoleate	31.80	294.26	12.251 ± 1.15	27.758 ± 2.56	0.990 ± 0.02
9	methylstearate	32.09	297.28	0.448 ± 0.02	5.724 ± 0.92	0.085 ± 0.02

diesel engines (Mofijur *et al.*, 2016). Accordingly, addition of fossil diesel to biofuel in the appropriate ratio may not only reduce volatile organic pollutants emitted to the environment but may also enhance engine efficiency. Oxygenated products during combustion usually yield the most reactive hydroxyl radical considered detrimental to both public and environmental health.

Curiously, a ratio of 1:1 decreased the levels of long chain hydrocarbons but a ratio of 3:2 realized an increase in the level of hydrocarbons. Model hydrocarbon compounds including tetradecane for instance decreased by approximately 92% in the ratio 2.3 as compared to a ratio of 3:2 whereas pentadecane decreased by 29%. On the other hand 2,6,10,14-tetramethylhexadecane decreased by \approx 93%. For the oxygenated model compounds, a reduction of about 76, 80, 96.4 and 85% for methyl hexadecanoate, methyl-8,11-octadecadienoate, methyl linoleate, and methyl methylstearate was observed respectively.

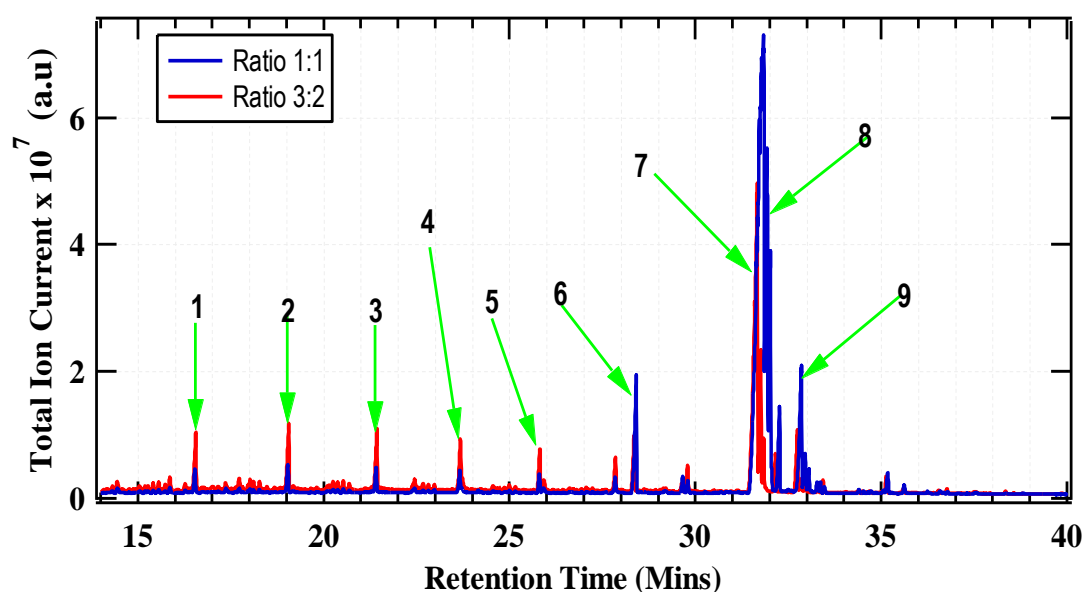

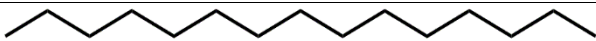
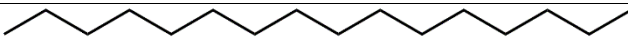
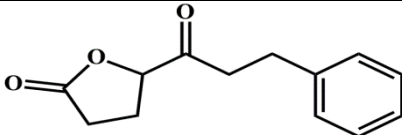
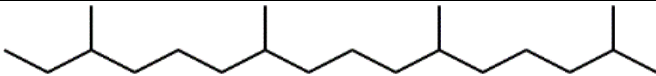
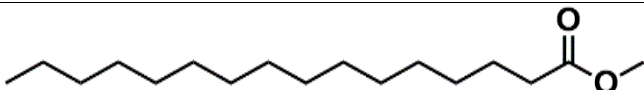
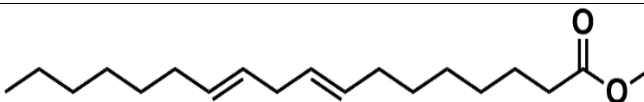
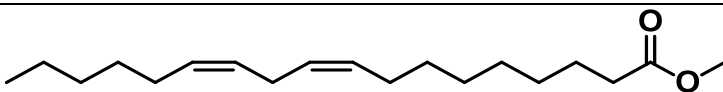
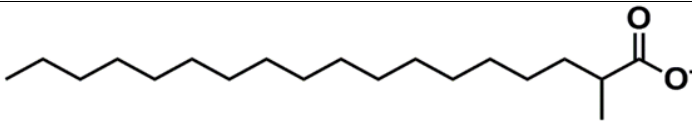


Figure 6.2: Gas chromatograms for diesel blends (biodiesel: Fossil diesel) at a pyrolysis temperature of 500 °C

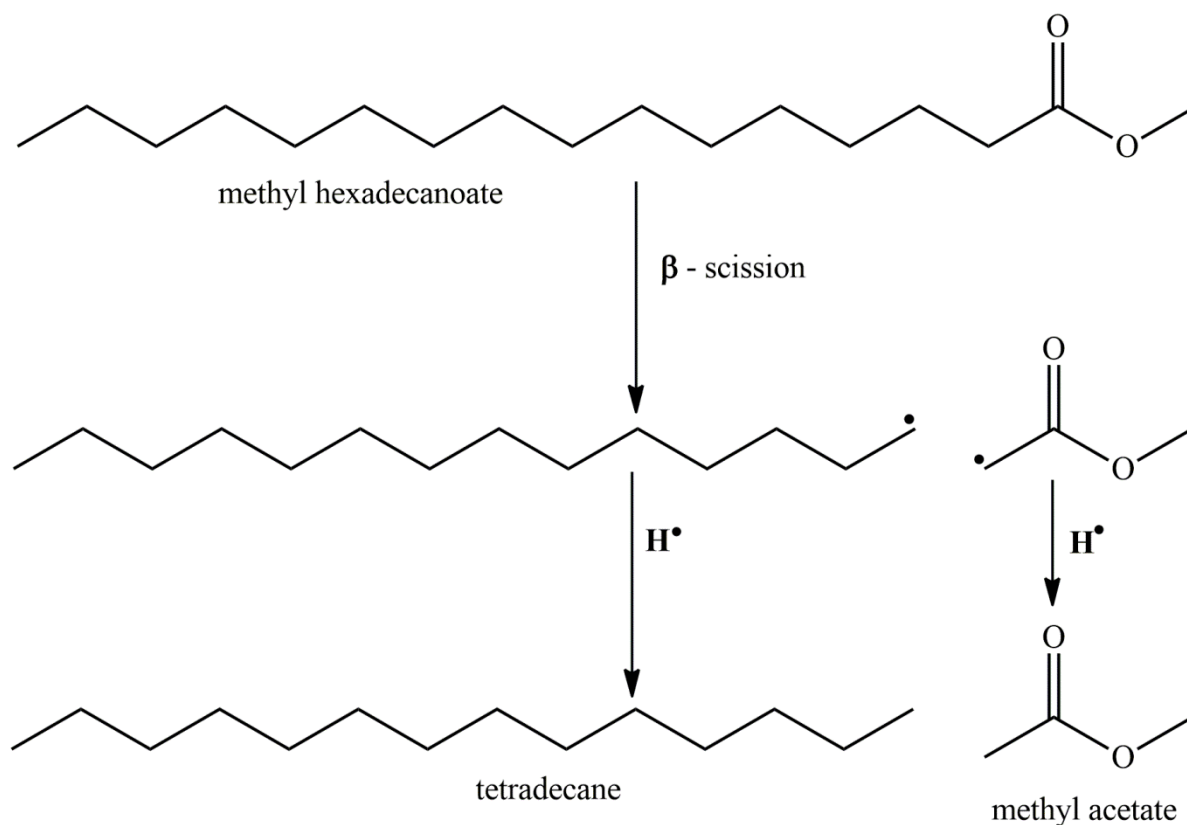
Naturally a synergetic inhibition may occur during the co-pyrolysis of biodiesel blends thus the decrease in molecular products at certain binary ratios. These results suggest that a biodiesel ratio of 40% to 60% fossil diesel may produce a better clean energy resource. The corresponding chromatographic peaks for the molecular compounds reported in Table 6.1, is presented in Figure 6.2. The molecular structures of the compounds of interest are presented in Table 6.2. Most of the reaction products were long chain hydrocarbons and methyl esters containing long chain hydrocarbon tail.

Table 6.2: Molecular structures of the compounds identified using GC-MS

#	Name of compound	Molecular structure
1.	tetradecane	
2.	pentadecane	
3.	hexadecane	
4.	5-(3-phenylpropanoyl)dihydro-2(3H)-furanone	
5.	2,6,10,14-tetramethylhexadecane	
6.	methyl hexadecanoate	
7.	methyl 8,11-Octadecadienoate	
8.	methyl linoleate	
9.	methylstearate	

6.3.1 Mechanistic description for the formation of reaction products

In order to provide a clear understanding of the mechanistic pathways for the formation of pyrolysis products of biodiesel and fossil fuel, the major components of these transport fuels must be known. A previous study done in Chapter Three, established that the primary components of *C. megalocarpus* biodiesel before pyrolysis include methyl dodec-9-enoate, methyl hexadecanoate, methyl octadeca-9,12-dienoate, methyl octadecanoate, methyl icos-11-enoate, methyl icosanoate, and methyl docosanoate. On the other hand, the major molecular components of fossil diesel are essentially long chain hydrocarbons.



Scheme 6.1: Proposed mechanistic pathway for the formation of tetradecane

Clearly, the cross reaction products during pyrolysis are quite different although similarities are noted in the terminal ester group for some compounds (Compounds 5-8, Table 6.2). The mechanistic description for the formation of compounds presented in Table 6.2 is proposed to form through various reactions pathways including $C - C$ scission, rearrangement, concerted reactions and polymerization reactions. It is, therefore, difficult to consider that one mechanistic channel could be responsible for the observed reaction products. Nonetheless, radical polymerization is believed to be the dominant reaction pathway. Notably, at elevated temperatures, the scission of the methoxy group occurs rapidly because it is the weakest bond ester bearing compounds (Battin-Leclerc *et al.* 2013; Kim *et al.*, 2015). The reaction channel for methyl hexadecanoate – and other reaction products containing the methyl ester groups proceeds via a $C - C$ β -scission (a relatively weak bond) accompanied by addition of a H radical as shown in schme 6.1, to give tetradecane and a small molecule (methyl acetate) which was detected in significant amounts in this study. The generation of long chain hydrocarbons such as pentadecane and hexadecane may proceed via simultaneous abstraction of a terminal H and addition of a methyl radical present in the pyrolysis pool. Alternatively, the scission of the terminal ester group in the corresponding methyl ester compound may lead

to the formation of long chain alkane (pentadecane and hexadecane). Nevertheless, some of the smaller fragments of decomposition of biodiesel blends include transient radicals and stable species which result in the evolution of CO₂ (decarboxylation reaction), olefins, water, aldehydes, ketones, and small alkanes such as methane, ethane and propane (Chendynski *et al.*, 2019).

6.3.2 The fate of elements during biomass pyrolysis

Herein the inorganic elements which are contained in biomass materials and which may be transported to the pyrolytic products, and ultimately find their way to the environment thus causing serious environmental pollution in form of particulate emissions are explored (Liu *et al.*, 2017). Getting to understand their thermochemical conversion, distribution and evolution of the major inorganic elements in biomass during pyrolysis is of enormous implication because thermal degradation has been proven as an important pathway in the conversion of biomass materials to valuable energy resource and essential chemicals of economic value (Wiinikka *et al.*, 2017) which has inspired a lot of scientific interest as evidenced by increasing number of research. Elemental composition of biomass particularly C, N, S, P, Cl affects biomass pyrolytic conversation selectivity (Liu *et al.*, 2017). Additionally, some of these elements when released to the environment cause environmental pollution and public health problems (Wiinikka *et al.*, 2017). Therefore, more knowledge on their fate during biomass degradation is envisaged to minimize the risks of secondary pollution and enable efficient recovery of these elements that have the ability to compromise renewable energy resources and essential molecular compound production (Liu *et al.*, 2017). Carbon, hydrogen and oxygen are the most abundant in lignocellulosic biomass and contains over 90% C, H, and O (dry basis) mainly act as the building blocks of cellulose, hemicellulose, and lignin components, as well as other necessary organic compounds of the nucleic acid, protein, and hormone types (Liu *et al.*, 2017).

Recent analyses have shown that pyrolysis bio-oils contain more than 400 molecular compounds and been noted that these chemical functionalities in the bio-oil correlate strongly with the feed composition and the pyrolysis production conditions (Lyu *et al.*, 2015). Physical and chemical characterization of biochar are performed using such techniques as Brunauer-Emmett-Teller (BET), X-ray photoelectron spectroscopy (XPS), Fourier transform infrared (FTIR), and inductively coupled plasma atomic emission spectroscopy (ICP-AES) reveals that bio-char contains many functional groups –OH, –NH₂, C = C, and –COOH as

well as minerals such as N, P, S, Ca, Mg, and K (Mosonik *et al.*, 2019). Surface functionality and porosity makes bio-char a useful resource in the synthesis of many carbon based functional materials (Smith *et al.*, 2016). The tar represents a complex mixture of more than 100 compounds, including benzene, phenols, N-heterocyclic compounds, and polycyclic aromatic hydrocarbons (PAHs) (Abdel-Shafy and Mansour, 2016; Zhao *et al.*, 2019b). On the other hand, single-aromatic-ring compounds such as styrene and benzene are considered the main precursors for the two ring PAHs (Zhao *et al.*, 2019a). The tar yield of biomass pyrolysis and gasification varies from approximately 0.5 to 100 g/m³ depending on the pyrolysis reactors, operating conditions, and the nature of feedstock (Tripathi *et al.*, 2016). Tars are generally formed from the decomposition of the cellulose, hemicelluloses, and lignin (Liu *et al.*, 2017).

It has previously been noted that Na⁺ catalyzes the thermal decomposition process in both the pyrolysis and oxidation of sodium alginate and possible other biomass materials such as cellulose and lignocellulose (Li *et al.*, 2011; Ross *et al.*, 2011), although no mechanistic explanation has been reported for this behaviour before, the use of atomistic molecular dynamics lead to different inter chain proposed mechanisms, such as lateral association, “zipper mechanism”, and entanglement, where the mannuronic residues are shown to exhibit elasticity moderator characteristics and therefore stimulate chain association (Hecht and Srebnik, 2016). Generally, algae are a family of marine biological resources comprising approximately 250 genera and 2500 species that can be used as alternative sources of energy (Dote *et al.*, 1994; Peng *et al.*, 2001; Urbanova *et al.*, 2019). They are a linear co-polymer composed of two monomeric units, D-mannuronic acid and L-guluronic acid (Hecht and Srebnik, 2016; Ross *et al.*, 2009), containing carboxylic groups in their structures that define their adsorption capacity for metals (Ross *et al.*, 2009; Ross *et al.*, 2011). The polymer chain can be orientated in different directions depending on the linkage of the two acids (Ikeda *et al.*, 2000; Ross *et al.*, 2009; Urbanova *et al.*, 2019). The mineral content includes mainly Ca, Na, Mg, and K with smaller amounts of other metal pieces including Si and Sr (Ross *et al.*, 2009). The term “alginate” is normally used to describe the salts of alginic acid (Ross *et al.*, 2009). It is a naturally occurring ring biopolymers extracted from algae and has high adsorption ability for metal ions, consequently metal alginates are prepared from fresh algae using solvent extraction procedures (Pathak *et al.*, 2010).

6.3.3 Inorganic salts present in biomass materials

Inorganic compounds – especially potassium, calcium, sodium, silicon, phosphorus, and chlorine are the main constituents of the ash in biomass feedstocks, and during the thermal degradation of biomass, these inorganic species, particularly potassium and calcium, catalyze biomass decomposition and reactions that lead to char formation (Agblevor and Besler, 1996). Previous studies also indicated that alkali and alkaline earth metal ions naturally present in biomass materials changes the cellulose pyrolysis product distribution by altering the activation energy of competing reactions that led to enhancement in the formation of furans and low molecular weight (LMW) compounds at the expense of levoglucosan yield even when these metal ions are present in low concentrations (Patwardhan *et al.*, 2010a). Alkali earth metals, Mg/Ca are more effective than Na/K in catalyzing cellulose dehydration during heating-up (Liu *et al.*, 2014). The presence of impurities is known to affect the decomposition pathways for cellulose pyrolysis. The loaded salts (NaCl, KCl, MgCl₂, and CaCl₂) have significantly different influence on the contribution of dehydration and depolymerization reactions to the decomposition of sugar structures during cellulose fast pyrolysis at 325 °C (Liu *et al.*, 2014). As a consequence of the presence of the chlorides of alkali and alkaline earth metals in cellulose during pyrolysis, dehydration has been found to play a pivotal role in sugar conversions in heating up period whereas depolymerisation plays a major role in sugar conversion for chlorides of alkaline earth metals and minor role for alkali metals during isothermal pyrolysis (Liu *et al.*, 2014; Patwardhan *et al.*, 2010a). Another study reported that very small quantities of inorganic impurities (<0.1% mass) significantly alter the pyrolysis and combustion characteristics of cellulose. They further observed that the presence of alkali salts has a greater influence on the reaction mechanism as compared to temperature. In a study conducted on the catalytic effects of diammonium phosphate on wood pyrolysis, Di Blasi *et al.* (Di Blasi *et al.*, 2007) found that the yields of char and water continuously increase at the expense bio-oil and tar components, and also noted significant increase in the yields of char and water. Julien *et al.* (Julien *et al.*, 1993) studied the effect of different anions (SO₄²⁻, Cl⁻ and NO₃⁻) and found that Cl⁻ and SO₄²⁻ have an important impact in accelerating the formation of hydroxy-acetaldehyde and reducing the formation of levoglucosan (Chen *et al.*, 2020). However, the effect was not as significant as that reported for cations such as Mg²⁺ and Ca²⁺ (Al-Wabel *et al.*, 2019). The effect of alkali salts on the mechanism of cellulose pyrolysis could have an impact on the structure of resulting char (Xu *et al.*, 2017) and consequently influence the formation of PAHs is rare in literature

(Patwardhan *et al.*, 2010b). Although these elements are important in catalytic decomposition of biomass pyrolysis, there is a grave concern that they are emitted as particulate matter into the atmosphere thus causing adverse health impacts on human health (Agblevor and Besler, 1996; Feng *et al.*, 2018). Therefore, benchmarking of trace element release on a unit energy basis for individual fuel materials and mixed biofuels against conventional fuels is not only essential but also of practical importance (Feng *et al.*, 2018).

6.3.4 Elemental composition of char and electron paramagnetic spectra

This is a very important component in the characterization of thermal chars from various biodiesel and fossil diesel binary mixtures. The elemental analysis for the thermal chars from biodiesel and fossil diesel in the ratio 2:3 at 500 °C is reported in Figure 6.3 whereas the elemental analysis of pure fossil diesel is presented in Figure 6.4.

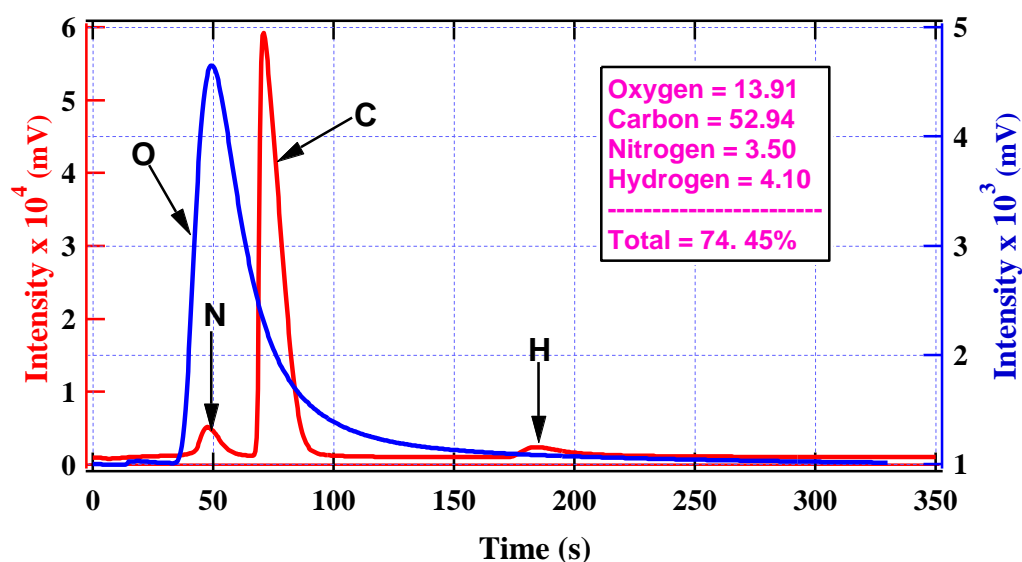


Figure 6.3: Elemental % composition of biodiesel-fossil thermal char at 500 °C in the ratio 2:3

It is evident from Fig 6.4 that the carbon content from commercial diesel is very high ($\approx 70.61\%$) as compared to approximately 53% (Figure 6.3) when the biodiesel and fossil diesel are co-pyrolyzed in the ratio 2:3 respectively. Thus, the carbon content was noted to decrease by $18\pm 3\%$ during the co-pyrolysis of diesel blends (Figs 6.3 and 6.4). This is predicted to reduce the amount of hazardous aromatic hydrocarbon emissions at high temperatures.

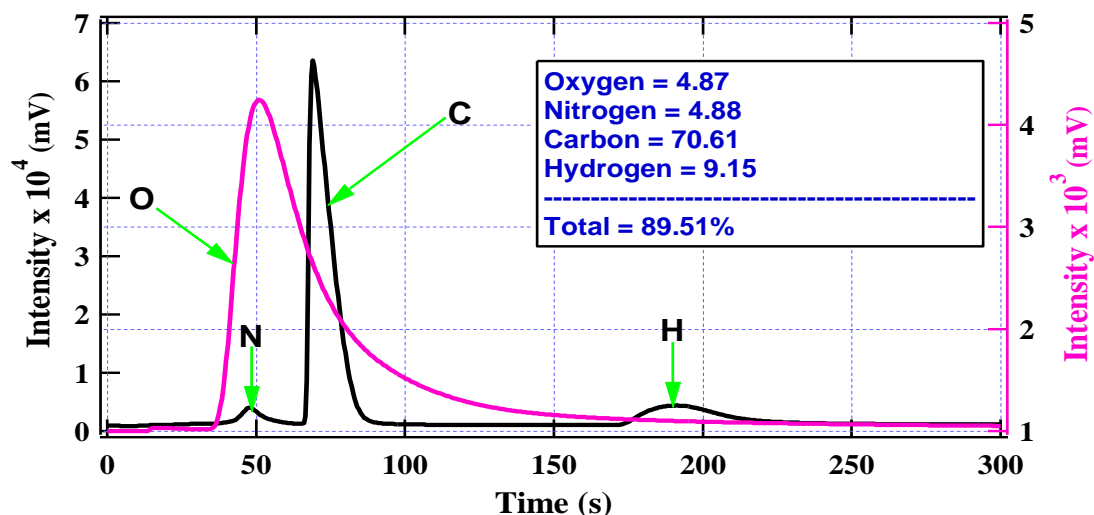


Figure 6.4: Elemental % composition of pure fossil diesel thermal char at 500 °C

Besides, hydrogen which is an important precursor in the formation hazardous hydrocarbons was decreased by about 50% during the mixture. The nitrogen content was equally reduced from 4.88% for the pyrolysis of pure fossil diesel to 3.50 % during the co-pyrolysis of biodiesel and fossil diesel in the ratio 2:3. The oxygen content, however, is significantly high in Figure 6.3 as (diesel binary mixture) as compared to that in Figure 6.4 (pure fossil diesel). This is expected because biodiesel components are methyl esters and carboxylic acids considered rich in oxygen (Saluja *et al.*, 2016; Sundus *et al.*, 2017). On the other hand, fossil diesel is conventionally rich in carbon.

In order to determine the radical content from thermal emissions, electron paramagnetic spectroscopy was conducted on the three types of chars; croton char, binar char (char from co-pyrolysis of croton diesel and fossil diesel in the ratio 2:3), and pure fossil diesel char. Evidently, the peak-to-peak width, $\Delta P-P$ of EPR signals were anisotropic and fairly narrow for all thermal chars; 3.65, 4.42 and 4.51 for croton, biodiesel blend and fossil diesel respectively. Notably, the radical peak intensity for biochar was found to be higher than that of conventional diesel. However, when co-pyrolyzed, the radical intensity significantly reduced by approximately 50%. In examining the EPR spectra presented in this work (Figure 6.5), it is necessary to note that the surface of thermal char may contain oxygenated centres or carbon centres adsorbed on the surface. Although, it is clear from the EPR spectra that carbon-based radicals dominate, there are possibilities that oxygen-based radicals may also be present at low concentrations. For this reason, this study has opted to discuss the oxygen-centred radicals from a literature perspective because of their critical significance in public

health and environmental health. This observation is supported by elemental analyses data that show oxygen as one of the major components of thermal char (Figs. 6.3 and 6.4).

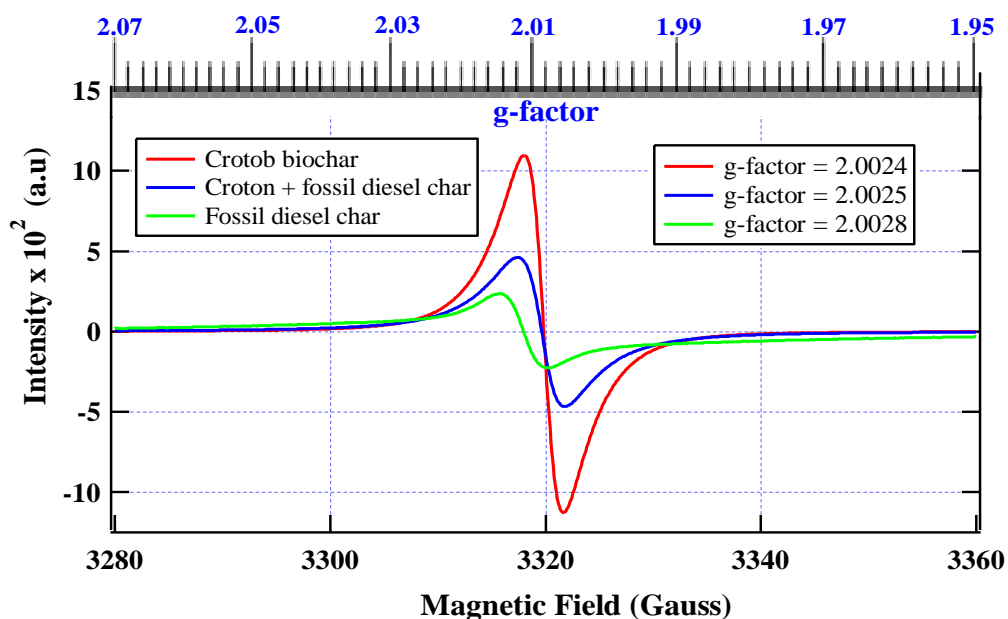


Figure 6.5: The *C. megalocarpus* biochar, croton-fossil diesel char, fossil diesel char EPR overlay spectra - radical intensity as a function of magnetic field

The spin densities for croton and diesel blends were reportedly high ranging from 1.82×10^{20} spins/g and 8.03×10^{19} spins/g, while fossil fuel showed a very low spin count of 2.22×10^{19} spins/g. High spin densities indicate that radicals are very stable (Power, 2003). Coal pyrolysis typically produces samples with radical concentrations ranging from $3 - 9 \times 10^{20}$ spins/g, depending on the origin of the coal (Petrakis and Grandy, 1981). The EPR spectrum for all the thermal char had a strong anisotropic singlet peak at approximately 3320 Gauss (cf. Figure 6.5). It is evident from Figure 6.5, that the radical intensity for thermal char from biodiesel was about 2 times higher than the radical intensity for the binary mixture of biodiesel and fossil diesel at a model ratio of 2:3. This is, therefore, another environmental benefit of using optimized diesel blends as opposed to pure biodiesel. The g-factors varied slightly between 2.0024 and 2.0028 suggesting a free electron in a $\pi - \pi$ C - C matrix. This is consistent with the elemental % carbon in the thermal chars reported in Figs. 6.3 and 6.4, *vide supra*. Previous work suggests that, at temperatures > 500 °C, the carbon based radicals dominate while the oxygen-centred free radicals are considerably absent (Trubetskaya *et al.*, 2016). More importantly, transport fuel research aims at obtaining mechanisms of formation and emission radical-bearing pollutants and harmful volatile organic pollutants (VOPs). It is evidently reported in literature that addition of the phenoxy O

atom in an o-semi quinone radical to ortho C(H) or C(OH) in a catechol molecule primarily results to the formation of hydroxylated diphenyl ethers which are important building blocks not only in biomass pyrolysis but also in biofuel pyrolysis (Altarawneh and Dlugogorski, 2015). Additionally, phenoxy radicals that are important intermediates in the thermal degradation of biomass and biofuel may be reported in an “en-ol” resonance structure (mesomer) in which the unpaired electron is located on an ortho-carbon denoted as o-C/; or para carbon denoted as $p - C/$; or a “keto” resonance structure in which the unpaired electron is associated with the oxygen, denoted as O/- as detailed in literature (Asatryan *et al.*, 2005; Altarawneh and Dlugogorski, 2015).

Radical species formed from thermal degradation events have generally been referred to as environmentally persistent free radicals (EPFRs) and represent a class of reactive species that have prolonged life time even under ambient environmental conditions (Assaf *et al.*, 2016). These radicals may be precursors for a group of environmentally persistent volatile organic pollutants such as phenols, dioxins and benzofurans which can easily be converted to the most toxic environmental pollutants ever known – polychlorinated dioxins and polychlorinated dibenzo furans (PCDD/Fs) in presence of small amounts of chlorine and a transition metals such as iron or copper and/or their corresponding oxides (Assaf *et al.*, 2016; Mosallanejad *et al.*, 2016).

Ultimately, traffic studies indicate that there are increased rates of respiratory and cardiovascular ailments and risks of premature deaths associated with busy urban highways because of lack of clean energy combustion strategies (Laumbach and Kipen, 2012). For instance, a 100% renewable energy would provide a long-term solution to the challenges caused by climate change, energy security, sustainability, and environmental pollution (Garcra-Olivares *et al.*, 2018). This would take into consideration major restructuring of infrastructure, improved engine designs and an internationally coordinated policy action towards green energy technologies (Garcra-Olivares and Ballabrera-Poy, 2015; Garcra-Olivares *et al.*, 2018).

Conclusions

From the GC-MS and elemental analysis data, it is clear that the optimum binary mixture of biodiesel and fossil diesel suggested for clean energy combustion is 2:3 (w/w) subject to further tests such as calorific heating value, viscosity, acidity, and ageing. Nonetheless, with the presence of nearly 60 % hydrocarbons in the mixture, there is every reason to believe that

a good combustion ability of the mixture has been proposed. Previous proposals to use pure croton biodiesel as a renewable energy resource may no longer be viable because of the evolution of toxic molecular compounds known to be carcinogenic as well as mutagenic. Moreover, it has been observed that pyrolysis of pure biodiesel generates a high amount of free radicals as opposed to when the biodiesel is mixed with fossil diesel in the ratio 2:3 (w/w). To this end, this study has noted that binary mixtures of renewable biofuels and non-renewable fossil fuels may be the solution in the search for fuels of good heating value without damaging combustion engines as well as the integrity of the natural environment.

References

- Ali, O. M., Mamat, R., Abdullah, N. R. and Abdullah, A. A. (2016). Analysis of blended fuel properties and engine performance with palm biodiesel–diesel blended fuel. *Renewable Energy*, **86**: 59-67.
- Altarawneh, M. and Dlugogorski, B. Z. (2015). Formation of dibenzofuran, dibenzo-p-dioxin and their hydroxylated derivatives from catechol. *Physical Chemistry Chemical Physics*, **17**: 1822-1830.
- Arroyo, Y., Sanz Tejedor, M., San José, J. and García Escudero, L. A. (2019). Statistical study of combustion characteristics and optimal operation factor determination in an emulsion burner fuelled with vegetable oils. *Energy and Fuels*, **33**(11): 10989-10998.
- Asatryan, R., Davtyan A, Khachatryan L. and Dellinger B.(2005) Molecular modeling studies of the reactions of phenoxy radical dimers: Pathways to dibenzofurans. *Journal of Physical Chemistry A*. **109**: 11198-205.
- Assaf, N. W., Altarawneh, M., Oluwoye, I., Radny, M., Lomnicki, S. M. and Dlugogorski, B. Z. (2016). Formation of Environmentally Persistent Free Radicals on α -Al₂O₃. *Environmental Science and Technology*, **50**: 11094-102.
- Battin-Leclerc, F., Curran, H., Faravelli, T. and Glaude, P. A. (2013). Specificities Related to Detailed Kinetic Models for the Combustion of Oxygenated Fuels Components. In *Cleaner Combustion* (93-109). Springer, London.
- Chendynski, L. T., Mantovani, A. C. G., Savada, F. Y., Messias, G. B., Santana, V. T., Salviato, A. and Borsato, D. (2019). Analysis of the formation of radicals in biodiesel in contact with copper and metallic alloys via electronic paramagnetic resonance (EPR). *Fuel*, **242**: 316-322.
- Chendynski, L. T., Mantovani, A. C. G., Savada, F. Y., Messias, G. B., Santana, V. T., Salviato, A. and Borsato, D. (2019). Analysis of the formation of radicals in biodiesel in contact with copper and metallic alloys via electronic paramagnetic resonance (EPR). *Fuel*, **242**: 316-322.
- Chhetri, A. B. and Islam, M. R. (2008). Towards producing a truly green biodiesel. *Energy Sources, Part A*, **30**: 754-764.
- Czajczyńska, D., Anguilano, L., Ghazal, H., Krzyżyńska, R., Reynolds, A. J., Spencer, N. and Jouhara, H. (2017). Potential of pyrolysis processes in the waste management sector. *Thermal Science and Engineering Progress*, **3**: 171-197.
- Damanik, N., Ong, H. C., Tong, C. W., Mahlia, T. M. I. and Silitonga, A. S. (2018). A review on the engine performance and exhaust emission characteristics of diesel

- engines fueled with biodiesel blends. *Environmental Science and Pollution Research*, **25**: 15307-15325.
- Fontes, C. H. D. O. and Freires, F. G. M. (2018). Sustainable and renewable energy supply chain: A system dynamics overview. *Renewable and Sustainable Energy Reviews*, **82**: 247-259.
- García-Olivares, A. and Ballabrera-Poy J. (2015). Energy and mineral peaks, and a future steady state economy. *Technological Forecasting and Social Change*, **90**: 587-98.
- García-Olivares, A., Solé, J. and Osychenko, O. (2018). Transportation in a 100% renewable energy system. *Energy Conversion and Management*, **158**: 266-285.
- Ghazali, W. N. M. W., Mamat, R., Masjuki, H. H. and Najafi, G. (2015). Effects of biodiesel from different feedstocks on engine performance and emissions: A Review. *Renewable and Sustainable Energy Reviews*, **51**: 585-602.
- Guedes, R. E., Luna, A. S. and Torres, A. R. (2018). Operating parameters for bio-oil production in biomass pyrolysis: a review. *Journal of Analytical and Applied Pyrolysis*, **129**: 134-149.
- Hasan, M. M. and Rahman, M. M. (2017). Performance and emission characteristics of biodiesel–diesel blend and environmental and economic impacts of biodiesel production: A review. *Renewable and Sustainable Energy Reviews*, **74**: 938-948.
- Jebet, A., Kibet, J., Ombaka, L. and Kinyanjui, T. (2017). Surface bound radicals, char yield and particulate size from the burning of tobacco cigarette. *Chemical Central Journal*, **11**: 1-8.
- Khan, K., Kumar, G., Sharma, A. K., Kumar, P. S., Mandal, C. and Chintala, V. (2018). Performance and emission characteristics of a diesel engine using complementary blending of castor and karanja biodiesel. *Biofuels*, **9**: 53-60.
- Kigen, G., Kipkore, W., Wanjohi, B., Haruki, B. and Kemboi, J. (2017). Medicinal plants used by traditional healers in Sangurur, Elgeyo Marakwet County, Kenya. *Pharmacognosy research*, **9**: 333-347.
- Kim, K. H., Bai, X., Cady, S., Gable, P. and Brown, R. C. (2015). Quantitative investigation of free radicals in bio- oil and their potential role in condensed- phase polymerization. *ChemSusChem*, **8**: 894-900.
- Laumbach, R. J. and Kipen, H. M. (2012). Respiratory health effects of air pollution: update on biomass smoke and traffic pollution. *Journal of Allergy and Clinical Immunology*, **129**: 3-11.

- Liu, H., Yoo, K. H., Boehman, A. L. and Zheng, Z. (2018). Experimental study of autoignition characteristics of the ethanol effect on biodiesel/n-heptane blend in a motored engine and a constant-volume combustion chamber. *Energy and Fuels*, **32**: 1884-1892.
- Ma, F. and Hanna, M. A. (1999). Biodiesel production: a review. *Bioresource Technology*, **70**: 1-15.
- Ma, N., Zhang, L., Zhang, Y., Yang, L., Yu, C., Yin, G. and Ma, X. (2016). Biochar improves soil aggregate stability and water availability in a mollisol after three years of field application. *PloS One*, **11**: e0154091. <https://doi.org/10.1371/journal.pone.0154091>.
- Mahmudul, H. M., Hagos, F. Y., Mamat, R., Adam, A. A., Ishak, W. F. W. and Alenezi, R. (2017). Production, characterization and performance of biodiesel as an alternative fuel in diesel engines—A review. *Renewable and Sustainable Energy Reviews*, **72**: 497-509.
- Mofijur, M., Rasul, M. G., Hyde, J., Azad, A. K., Mamat, R. and Bhuiya, M. M. K. (2016). Role of biofuel and their binary (diesel–biodiesel) and ternary (ethanol–biodiesel–diesel) blends on internal combustion engines emission reduction. *Renewable and Sustainable Energy Reviews*, **53**: 265-278.
- Mosallanejad, S., Dlugogorski, B. Z., Kennedy, E. M., Stockenhuber, M., Lomnicki, S. M. and Assaf, N. W. (2016). Formation of PCDD/Fs in Oxidation of 2-Chlorophenol on Neat Silica Surface. *Environmental Science and Technology*, **50**: 1412-8.
- Mumtaz, M. W., Adnan, A., Mahmood, Z., Mukhtar, H, Malik, M. F. and Ashraf, F. (2012) Biodiesel from Waste Cooking Oil: Optimization of Production and Monitoring of Exhaust Emission Levels From its Combustion in a Diesel Engine. *International Journal of Green Energy*, **9**: 685-701.
- Musthafa, M. M., Kumar, T. A., Mohanraj, T. and Chandramouli, R. A. (2018). Comparative study on performance, combustion and emission characteristics of diesel engine fuelled by biodiesel blends with and without an additive. *Fuel*, **225**: 343-348.
- Nejad, A. S. and Zahedi, A. R. (2018). Optimization of biodiesel production as a clean fuel for thermal power plants using renewable energy source. *Renewable Energy*, **119**: 365-374.
- Petrakis, L. and Grandy, D. W. (1981). Free radicals in coals and coal conversion. 3. Investigation of the free radicals of selected macerals upon pyrolysis. *Fuel*, **60**(2): 115-119.

- Power, P. P. (2003). Persistent and stable radicals of the heavier main group elements and related species. *Chemical Reviews*, **103**: 789-810.
- Pusparizkita, Y. M., Setiadi T. and Harimawan A. (2018). Effect of Biodiesel Concentration on Corrosion of Carbon Steel by *Serratia marcescens*. In *MATEC Web of Conferences*, **156**: 01008.
- Qasim, M., Ansari, T. M. and Hussain, M. (2018). Experimental investigations on a diesel engine operated with fuel blends derived from a mixture of Pakistani waste tyre oil and waste soybean oil biodiesel. *Environmental Science and Pollution Research*, **25**: 23657-23666.
- Ruhul, A. M., Kalam, M. A., Masjuki, H. H., Alabdulkarem, A., Atabani, A. E., Fattah, I. R. and Abedin, M. J. (2016). Production, characterization, engine performance and emission characteristics of *C. megalocarpus* and *Ceiba pentandra* complementary blends in a single-cylinder diesel engine. *RSC Advances*, **6**: 24584-24595.
- Ruhul, A. M., Kalam, M. A., Masjuki, H. H., Shahir, S. A., Alabdulkarem, A., Teoh, Y. H. and Reham, S. S. (2017). Evaluating combustion, performance and emission characteristics of *Millettia pinnata* and *C. megalocarpus* biodiesel blends in a diesel engine. *Energy*, **141**: 2362-2376.
- San José, J., Sanz-Tejedor, M. A. and Arroyo, Y. (2018). Spray Characteristics, Combustion Performance, and Palm Oil Emissions in a Low-Pressure Auxiliary Air Fluid Pulverization Burner. *Energy and Fuels*, **32**: 11502-11510.
- Saluja, R. K., Kumar, V. and Sham, R. (2016). Stability of biodiesel—A review. *Renewable and Sustainable Energy Reviews*, **62**: 866-881.
- Sundus, F., Fazal, M. A. and Masjuki, H. H. (2017). Tribology with biodiesel: A study on enhancing biodiesel stability and its fuel properties. *Renewable and Sustainable Energy Reviews*, **70**: 399-412.
- Suresh, M., Jawahar, C. P. and Richard, A. (2018). A review on biodiesel production, combustion, performance, and emission characteristics of non-edible oils in variable compression ratio diesel engine using biodiesel and its blends. *Renewable and Sustainable Energy Reviews*, **92**: 38-49.
- Thirugnanasambandham, K., Shine, K., Agatheeshwaren, A. and Sivakumar, V. (2016). Biodiesel production from castor oil using potassium hydroxide as a catalyst: Simulation and validation. *Energy Sources, Part A: Recovery, Utilization, and Environmental Effects*, **38**(19): 2898-2905.

- Trubetskaya, A., Jensen, P. A., Jensen, A. D., Glarborg, P., Larsen, F. H. and Andersen, M. L. (2016). Characterization of free radicals by electron spin resonance spectroscopy in biochars from pyrolysis at high heating rates and at high temperatures. *Biomass and bioenergy*, **94**: 117-129.
- Tsai, W. T. (2016). Toxic volatile organic compounds (VOCs) in the atmospheric environment: regulatory aspects and monitoring in Japan and Korea. *Environments*, **3**: 23.
- Tutak, W., Lukács, K., Szwaja, S. and Bereczky, Á. (2015). Alcohol–diesel fuel combustion in the compression ignition engine. *Fuel*, **154**: 196-206.
- Yahagi, S. S., Roveda A. C., Sobral A. T., Oliveira I. P., Caires A. R. L. and Gomes R. S. (2019). An Analytical Evaluation of the Synergistic Effect on Biodiesel Oxidation Stability Promoted by Binary and Ternary Blends Containing Multifunctional Additives. *International Journal of Analytical Chemistry*, **2019**: 1-10
- Zhang, Y., Lou, D., Tan, P. and Hu, Z. (2019). Experimental study on the emission characteristics of a non-road diesel engine equipped with different after-treatment devices. *Environmental Science and Pollution Research*, **26**(26): 26617-26627.
- Abdel-Shafy, H. I. and Mansour, M. S. M. (2016). A review on polycyclic aromatic hydrocarbons: Source, environmental impact, effect on human health and remediation. *Egyptian Journal of Petroleum*, **25**: 107-123.
- Agblevor, F. A. and Besler, S. (1996). Inorganic Compounds in Biomass Feedstocks. 1. Effect on the Quality of Fast Pyrolysis Oils. *Energy and Fuels*, **10**: 293-298.
- Al-Wabel, M. I., Rafique, M. I., Ahmad, M., Ahmad, M., Hussain, A. and Usman, A. R. A. (2019). Pyrolytic and hydrothermal carbonization of date palm leaflets: Characteristics and ecotoxicological effects on seed germination of lettuce. *Saudi Journal of Biological Sciences*, **26**: 665-672.
- Chen, L., Elias, W. C., Ben Yin, Y., Conrad Zhang, Z. and Wong, M. S. (2020). Acid-catalyzed pyrolytic synthesis of levoglucosan through salt-mediated ring locking. *Green Chemistry*, **22**: 1968-1977.
- Di Blasi, C., Branca, C. and Galgano, A. (2007). Effects of diammonium phosphate on the yields and composition of products from wood pyrolysis. *Industrial and Engineering Chemistry Research*, **46**: 430-438.
- Dote, Y., Sawayama, S., Inoue, S., Minowa, T. and Yokoyama, S. (1994). Recovery of liquid fuel from hydrocarbon-rich microalgae by thermochemical liquefaction. *Fuel*, **73**: 1855-1857.

- Feng, C., Zhang, M. and Wu, H. (2018). Trace Elements in Various Individual and Mixed Biofuels: Abundance and Release in Particulate Matter during Combustion. *Energy and Fuels*, **32**: 5978-5989.
- Hecht, H. and Srebnik, S. (2016). Structural Characterization of Sodium Alginate and Calcium Alginate. *Biomacromolecules*, **17**: 2160-2167.
- Ikeda, A., Takemura, A. and Ono, H. (2000). Preparation of low-molecular weight alginic acid by acid hydrolysis. *Carbohydrate Polymers*, **42**: 421-425.
- Julien, S., Chornet, E. and Overend, R. (1993). Influence of acid pretreatment (H₂SO₄, HCl, HNO₃) on reaction selectivity in the vacuum pyrolysis of cellulose. *Journal of Analytical and Applied Pyrolysis*, **27**: 25-43.
- Li, D. M., Chen, L. M., Zhang, X. W., Ye, N. H. and Xing, F. G. (2011). Pyrolytic characteristics and kinetic studies of three kinds of red algae. *Biomass and Bioenergy*, **35**: 1765-1772.
- Liu, D., Yu, Y., Hayashi, J. I., Moghtaderi, B. and Wu, H. (2014). Contribution of dehydration and depolymerization reactions during the fast pyrolysis of various salt-loaded celluloses at low temperatures. *Fuel*, **136**: 62-68.
- Liu, W. J., Li, W. W., Jiang, H. and Yu, H. Q. (2017). Fates of chemical elements in biomass during its pyrolysis. *Chemical Reviews*, **117**: 6367-6398.
- Lyu, G., Wu, S. and Zhang, H. (2015). Estimation and Comparison of Bio-Oil Components from Different Pyrolysis Conditions. *Frontiers in Energy Research*, **3**(28). <https://doi.org/10.3389/fenrg.2015.00028>.
- Mosonik, B. C., Kibet, J. K. and Ngari, S. M. (2019). Optimization of Binary Mixtures of Biodiesel and Fossil Diesel for Clean Energy Combustion. *Chemistry Africa*, **2**: 507-515.
- Pathak, T. S., Yun, J.-H., Lee, J. and Paeng, K. J. (2010). Effect of calcium ion (cross-linker) concentration on porosity, surface morphology and thermal behavior of calcium alginates prepared from algae (*Undaria pinnatifida*). *Carbohydrate Polymers*, **81**: 633-639.
- Patwardhan, P. R., Satrio, J. A., Brown, R. C. and Shanks, B. H. (2010a). Influence of inorganic salts on the primary pyrolysis products of cellulose. *Bioresource Technology*, **101**: 4646-4655.
- Patwardhan, P. R., Satrio, J. A., Brown, R. C. and Shanks, B. H. (2010b). Influence of inorganic salts on the primary pyrolysis products of cellulose. *Bioresource Technology*, **101**: 4646-4655.

- Peng, W. M., Wu, Q. Y., Tu, P. G. and Zhao, N. M. (2001). Pyrolytic characteristics of microalgae as renewable energy source determined by thermogravimetric analysis. *Bioresource Technology*, **80**: 1-7.
- Ross, A. B., Anastasakis, K., Kubacki, M. and Jones, J. M. (2009). Investigation of the pyrolysis behaviour of brown algae before and after pre-treatment using PY-GC/MS and TGA. *Journal of Analytical and Applied Pyrolysis*, **85**: 3-10.
- Ross, A. B., Hall, C., Anastasakis, K., Westwood, A., Jones, J. M. and Crewe, R. J. (2011). Influence of cation on the pyrolysis and oxidation of alginates. *Journal of Analytical and Applied Pyrolysis*, **91**: 344-351.
- Smith, A. M., Singh, S. and Ross, A. B. (2016). Fate of inorganic material during hydrothermal carbonisation of biomass: Influence of feedstock on combustion behaviour of hydrochar. *Fuel*, **169**: 135-145.
- Tripathi, M., Sahu, J. N. and Ganesan, P. (2016). Effect of process parameters on production of biochar from biomass waste through pyrolysis: A review. *Renewable and Sustainable Energy Reviews*, **55**: 467-481.
- Urbanova, M., Pavelkova, M., Czernek, J., Kubova, K., Vyslouzil, J., Pechova, A., Molinkova, D., Vyslouzil, J., Vetchy, D. and Brus, J. (2019). Interaction Pathways and Structure–Chemical Transformations of Alginate Gels in Physiological Environments. *Biomacromolecules*, **20**: 4158-4170.
- Wiinikka, H., Johansson, A.-C., Sandström, L. and Öhrman, O. G. (2017). Fate of inorganic elements during fast pyrolysis of biomass in a cyclone reactor. *Fuel*, **203**, 537-547.
- Xu, L., Liu, H., Fang, H., Gao, J. and Wu, S. (2017). Effects of various inorganic sodium salts present in Zhundong coal on the char characteristics. *Fuel*, **203**:120-127.
- Zhao, L., Kaiser, R. I., Lu, W., Xu, B., Ahmed, M., Morozov, A. N., Mebel, A. M., Howlader, A. H. and Wnuk, S. F. (2019a). Molecular mass growth through ring expansion in polycyclic aromatic hydrocarbons via radical-radical reactions. *Nature Communications*, **10**: 3689-3689.
- Zhao, S., Bi, X., Pan, X., Su, Y. and Wu, W. (2019b). The optimization of in-situ tar reduction and syngas production on a 60-kW three-staged biomass gasification system: theoretical and practical approach. *Biomass Conversion and Biorefinery*. <https://doi.org/10.1007/s13399-019-00536-9>.

CHAPTER SEVEN

MOLECULAR MODELLING OF SELECTED COMBUSTION BY-PRODUCTS FROM THE THERMAL DEGRADATION OF *Croton megalocarpus* BIODIESEL BLEND

Abstract

Computational models are very important in understanding the nature of interactions in chemical systems from which important geometry parameters for various organic compounds can be extracted. This study explores computationally the geometry parameters of selected volatile organic compounds from the co-pyrolysis of *C. megalocarpus* biodiesel blend using the Density functional theory (DFT) in conjunction with B3LYP correlation function at 6-31G basis set. Gaussian '16 computational and Chemissian version 4.43 computational codes were used to generate electron density maps, band gap energies and frontier molecular orbitals. Frontier orbitals are central in estimating the reactive nature of a given molecular compound. The results indicated that the thermal degradation of selected molecular products from the co-pyrolysis of *Croton megalocarpus* biodiesel blends proceeds via high energy barriers of between +400 and -1250 kJ/mol. Fundamentally the highest occupied and the lowest occupied molecular orbitals (MOs) are critical in determining the reactivity of a molecule. Moreover, the HOMO-LUMO band gap energies of 4-(2,4-dimethylcyclohexyl)-2-butanone, 3,4-dimethyl-3-cyclohexene-1-carbaldehyde, 5-(3-phenylpropanoyl)dihydro-2(3H)-furanone, and isopropenyl-4-methyl-1,2-cyclohexanediol were 0.674 eV, 3.918 eV, 3.393 eV, and 1.588 eV, respectively.

Keywords: Band gap, Density maps, Mechanisms and Optimization,

7.1 Introduction

Transport fuel emissions from fossil fuels have compromised air quality, affected human health for decades, and caused many health problems. As a result, biofuels have recently received a huge amount of attention because they are promising renewable energy resources. These fuels have been shown to reduce greenhouse gas emissions and other environmental pollutants. Previous studies by Cheruiyot *et al.* (2019) have shown that the ratio of biodiesel to fossil diesel produces better combustion results, which reduce the yield of toxic pollutant emissions. Biodiesel emissions have been known to be free of harmful aromatic compounds as opposed to commercial diesel emissions (Chen *et al.*, 2017). This is advantageous in the combustion efficiency of biodiesel, which has been shown to suffer from low oxidation,

increased acidity and corrosion problems (Agarwal *et al.*, 2017; Bateni *et al.*, 2019; Yahagi *et al.*, 2019). Environmentally persistent pollutants are considered stable and spend a long lifetime in the environment. Understanding the reactivity and stability of these pollutants is essential for public health practitioners and health authorities. One of the key factors controlling the physical properties of substances is the band gap energy, which forms the primary focus of this chapter. In addition, bond dissociation energies of these compounds is another determining factor in the interpretation of the reactivity and stability of molecular compounds. The expressively complex structural composition of biomass presents enormous difficulties in linking the formation of organic pollutants to specific chemical reactions (Altarawneh and Dlugogorski, 2015). In order to overcome this complexity, model molecular surrogates are often used to mimic the characteristics of bio-oil components (Murillo *et al.*, 2017; Zhen *et al.*, 2017; Gautam, 2018; Alviso *et al.*, 2020). The thermal decomposition of fuels results in the generation of smaller fragments of the decomposition of biodiesel blends, such as transient radicals and stable species, which result in the evolution of CO₂ (decarboxylation reaction), olefins, water, aldehydes, ketones and small alkanes, such as methane, ethane and propane (Chendynski *et al.*, 2019). Radicals formed from thermal degradation events have generally been referred to as environmentally persistent free radicals (EPFRs) and represent a class of reactive species that have a longer lifespan even under ambient environmental conditions (Assaf *et al.*, 2016). Radical stabilities and reactivity can be explored by the use of computational techniques as opposed to experimental methods due to their very short half-life. A study conducted in Chapter Four shows that some of the radicals produced by the thermal decomposition of biodiesel blends have a long half-life \approx 431 days. This research output sheds more light on the existence of environmentally persistent free radicals (EPRs) in the environment resulting from combustion events. The aim of this study is to examine the physical properties of certain selected volatile organic emissions from the co-pyrolysis of biodiesel blends with an inclination towards electronic properties. Computational chemistry provides an understanding of the molecular properties of a compound that would otherwise not be easy to determine experimentally. In addition, computational methods are cost-effective and time-efficient. This study examined in detail the electron density maps, molecular orbitals, band gap energies and geometry optimization of selected reaction by-products from thermal decomposition of *C. megalocarpus*; 4-(2,4-dimethylcyclohexyl)-2-butanone, 3,4-dimethyl-3-cyclohexene-1-carbaldehyde, 5-(3-phenylpropanoyl) dihydro-2-(3H)-furanone and isopropenyl-4-methyl-1,2-cyclohexanediol. The electron density contour maps generated was used to examine the nucleophilicity of

selected volatile organic compounds in order to gain more insight into how they interact with biological structures that cause toxicity and cellular impairment in respiratory systems. The process of optimization of the different pathways for 5-(3-phenylpropanoyl)dihydro-2(3H)-furanone and intermediate free radicals was investigated. In addition, thermochemistry and molecular models for the various mechanistic pathways of radical formation and their conversion to free molecules was proposed.

7.2 Materials and Methods

7.2.1 Density functional theory (DFT) Calculations

Density functional theory calculations were performed by use of Gaussian '16 computational software (Frisch *et al.* 2016). Geometry parameters such as compound energetics and bond energies were calculated at the ground state geometries employing B3LYP level of theory with 6-31G basis sets. To develop molecular orbital energy-level diagrams, electronic density contour maps and the determination of the band gap energy for selected molecules, Gaussian 16 software outputs were interfaced with Chemission version 4.43 (Skripnikov, 2016). All computational calculations were conducted at 298.15 K and 1 atmosphere. To compute the energy change for formation of a compound or a free radical from its constituents, the following thermodynamic equation (equation 7.1) was used (Ochterski, 2015).

$$\Delta_r H^0 = \sum(\varepsilon_0 - H_{corr})_{products} - \sum(\varepsilon_0 - H_{corr})_{Reactants} \quad 7.1$$

where, $\Delta_r H^0$ is change in enthalpy of the reaction, H_{corr} is correction to the thermal enthalpy and ε_0 is the sum of electronic and thermal enthalpies.

7.3 Results and discussion

7.3.1 Molecular geometries of major molecular emissions

Geometry parameters such as bond lengths and bond angles have a significant influence on the strength of the bonds of molecular structures. The structures of selected model components are presented in Scheme 1, *vide infra*. The optimization process presented below in Figures 7.1 - 7.4 show steps towards achieving an optimized Structure for 4-(2,4-Dimethylcyclohexyl)-2-butanone, 3,4-Dimethyl-3-cyclohexene-1-carbaldehyde, 5-(3-phenylpropanoyl)dihydro-2(3H)-furanone and isopropenyl-4-methyl-1,2-cyclohexanediol. This offers interesting quantum mechanics results that cannot easily be accomplished by experimental methods.

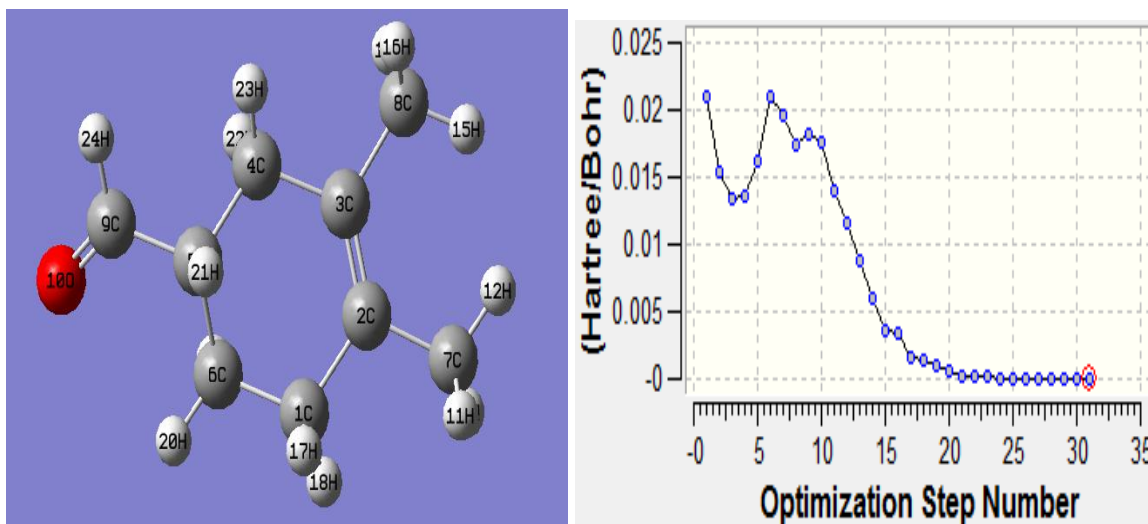


Figure 7.1: Optimized structure of 3,4-dimethyl-3-cyclohexene-1-carbaldehyde and a plot showing its optimization steps (the red circle is the optimization level)

The optimization of 3,4-dimethyl-3-cyclohexene-1-carbaldehyde proceeds 31 steps to attain a structure of zero energy (global minimum structure). Interestingly, 5-(3-phenylpropanoyl) dihydro-2(3H)-furanone (Figure 7.2) required 91 steps to attain a global minima structure. This is attributed to its large molecular weight of 218.09 g/mol. The scission of C5-C6 (cf. Figure 7.2) bond in 5-(3-Phenylpropanoyl) dihydro-2(3H)-furanone proceeds with a bond dissociation energy of 372.31 kJ/mol.

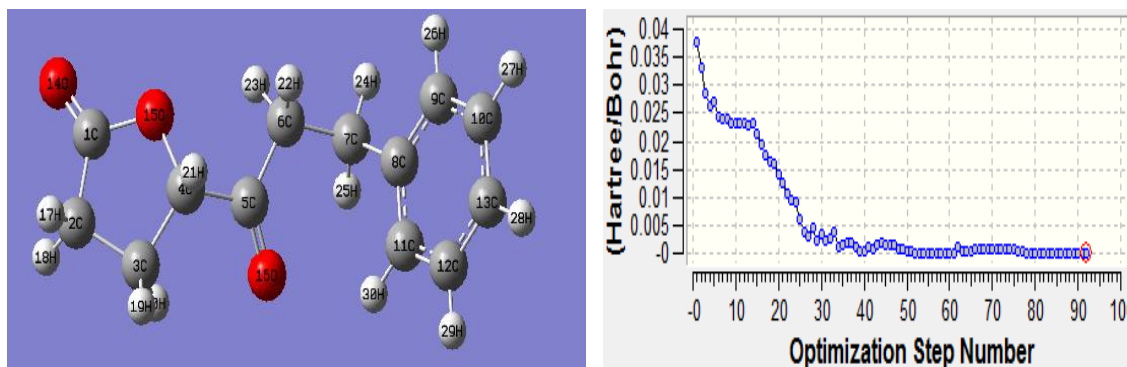


Figure 7.2: Optimized structure of 5-(3-phenylpropanoyl) dihydro-2(3H)-furanone and a plot showing its optimization steps (the red circle is the optimization level)

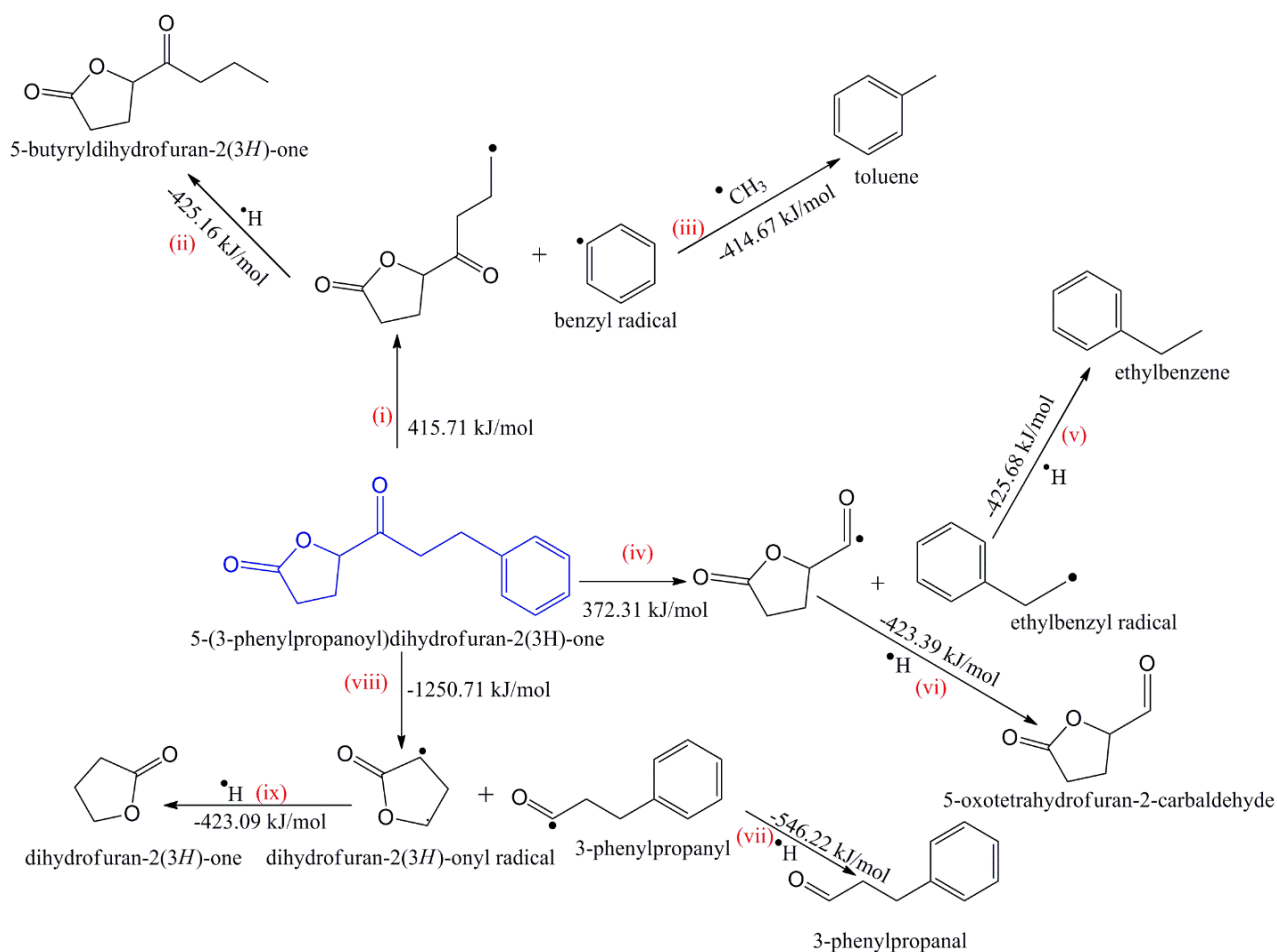
This was one of the thermodynamically feasible pathway (scheme 7.1, route (i) since it proceeds with lower energy compared to the rest of pathways. The scission of C4, C5 and C7, C8 proceed with energy barriers of -1250.75 and 415.71 kJ/mol respectively.

7.3.2 Mechanistic degradation of 5-(3-phenylpropanoyl) dihydro-2(3H)-furanone

Mechanistic channels attempt to show how starting materials are converted into products during chemical reactions. Thermal decomposition of fuels leads to emission of numerous particulate matter of various classifications that are of public health interest. These compounds include long chain hydrocarbons, oxygenated by-products, aromatic hydrocarbons among other eco-toxic organics (He, 2016). This study has also proposed the mechanistic formation of free radicals from selected oxygenated by-products, which are noted to be precursors of cancer, general respiratory human health problems and reactive oxidative stress (ROS). To investigate the energetics of the selected molecular emissions, Gaussian '16 software employing the B3LYP correlation function and 6-31G basis sets at DFT level of theory was conducted.

Clearly, the thermal degradation is predicted to occur via an endothermic energy barrier, Scheme 7.1 (routes 1, 2 and 3). Formation of radicals via route (i) proceeds with an energy of 415.71 kJ/mol considered less important to biological systems (Kibet, 2016). The scission of -C-C- bond in route (iv) for the formation of ethylbenzyl radical and 5-oxotetrahydrofuran-2-carbaldehydyl radical occurs with an enthalpy change of 372.31 kJ/mol which is thermodynamically feasible. Interestingly, route (viii) shows a highly exothermic reaction, with bond dissociation energy of -1,250.75 kJ/mol. The conversion of free radicals to their corresponding free molecules occurs through exothermic channels, routes (iii) and (v-ix), Scheme 7.1, *vide infra*.

Environmental pollutants blamed for a number of illnesses arise as unwanted by-products in various processes, especially in uncontrolled combustion events such as accidental fires, combustion of transport fuels, cigarette smoking and municipal waste incineration (Mosallanejad *et al.*, 2016). The major areas of concern focuses on the mechanistic formation of environmentally free radicals and their associated impact on human health (Nel, 2005), from chronic respiratory and cardiopulmonary dysfunction as a consequence of oxidative stress induced by reactive oxygen species (ROS) (Assaf *et al.*, 2016).



Scheme 7.1: Proposed mechanistic pathways for the thermal degradation of 5(3phenylpropanoyl)dihydro-2-(3H)-furanone

Density functional theory calculations have been found to be successful in giving theoretical insights into the reactivity of organic compounds. They provide possible reaction pathways which organic compounds can undergo without necessarily carrying out experimental work which may be both tedious and time consuming.

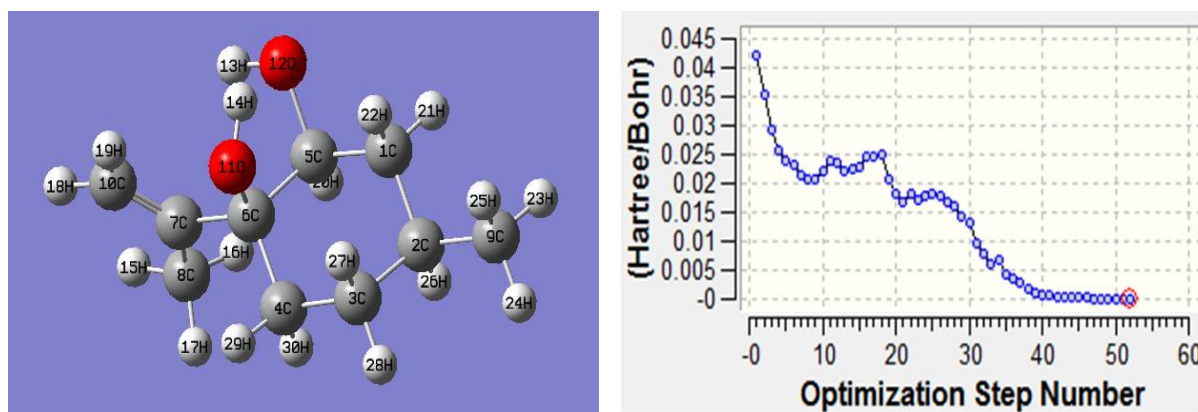


Figure 7.3: Optimized structure of isopropenyl-4-methyl-1,2-cyclohexanediol and a plot showing its optimization steps (the red circle is the optimization level)

On the other hand, isopropenyl-4-methyl-1,2-cyclohexanediol attained the global minima structure with 51 optimization steps (Figure 7.3)

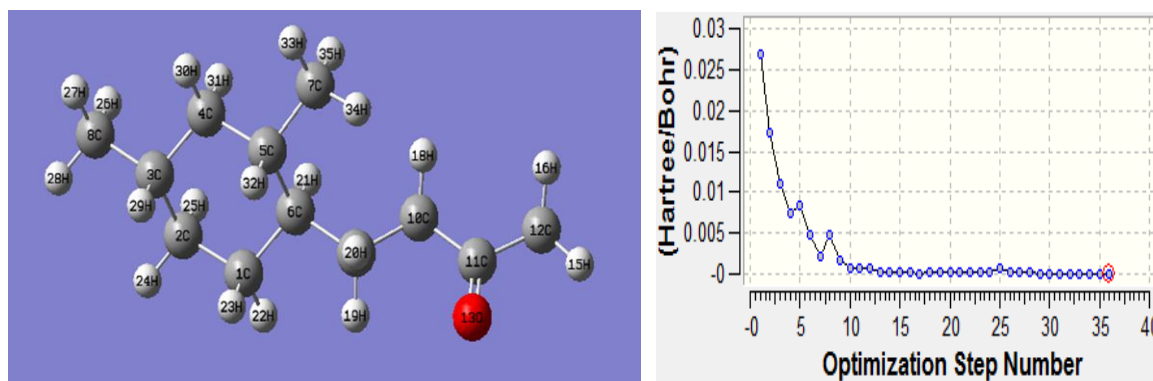


Figure 7.4: Optimized structure of 4-(2,4-dimethylcyclohexyl)-2-butanone and a plot showing its optimization steps (the red circle is the optimization level)

4-(2,4-Dimethylcyclohexyl)-2-butanone required fewer optimization steps (36) to attain a structure of minimum energy while the scission of C10, C11 bond occurs with a bond dissociation energy of 494.24 kJ/mol.

7.3.3 Frontier molecular orbitals and electron density maps

Conventionally, frontier orbitals are the highest occupied molecular orbitals (HOMO) and the lowest unoccupied molecular orbitals (LUMO). The molecular orbitals and electron density maps are of great significance in understanding the reactivity of molecular species. The HOMO and LUMO orbitals are orbitals that lie closer in energy of any pair of orbitals given any two molecules which tend to interact more strongly (Frisch *et al.*, 2009). The HOMO-LUMO band-gap energies for the selected volatile organic compounds considered in this study are shown in Table 7.1. The reactivity index (HOMO-LUMO gap) of the compounds

with small difference implies high reactivity and a large difference implies low reactivity in reactions (Ombaka et al., 2017). Therefore as the energy gap between the HOMO and LUMO becomes smaller, the rate of reaction is enhanced. The 4-(2,4-dimethylcyclohexyl)-2-butanone has the smallest HOMO-LUMO energy gap (0.674 eV) (Figure 7.5) and therefore considered more reactive compared to 3,4-Dimethyl-3-cyclohexene-1-carbaldehyde with a larger band gap of 3.918 eV. 5-(3-phenylpropanoyl) dihydro-2(3H)-furanone and isopropenyl-4-methyl-1,2-cyclohexanediol had band gap energies of 3.393 eV and 1.588 eV, respectively. However, 5-(3-phenylpropanoyl) dihydro-2-(3H)-furanone may have a relatively large HOMO-LUMO energy gap (Figure 7.6).

Table 7.1: HOMO-LUMO band gap energies for the selected volatile organic compounds

<i>Compound</i>	E_{HOMO} (eV)	E_{LUMO} (eV)	ΔH $= E_{LUMO} - E_{HOMO}$
3,4-dimethyl-3-cyclohexene-1-carbaldehyde	-4.027	-0.109	3.918
5-(3-phenylpropanoyl) dihydro-2-(3H)-furanone	-5.560	-2.167	3.393
4-(2,4-dimethylcyclohexyl)-2-butanone	-4.186	-3.512	0.674
isopropenyl-4-methyl-1,2-cyclohexanediol	-3.451	-1.863	1.588

Evidently, the HOMO-LUMO band-gap for 4-(2,4-dimethylcyclohexyl)-2-butanone is clearly low and therefore could be reactive especially towards biological structures contrary to the fact that ketones are known to be least reactive compared to alcohols and aldehydes. Generally, the band-gap between the HOMO and the LUMO is directly related to the electronic stability of the chemical species (Hanulikova *et al.*, 2016). This suggests that 5-(3-phenylpropanoyl) dihydro-2(3H)-furanone having a lower HOMO energy value of -5.560 eV is much more stable making it a good nucleophile compared to 4-(2,4-Dimethylcyclohexyl)-2-butanone which is energetically higher in the LUMO.

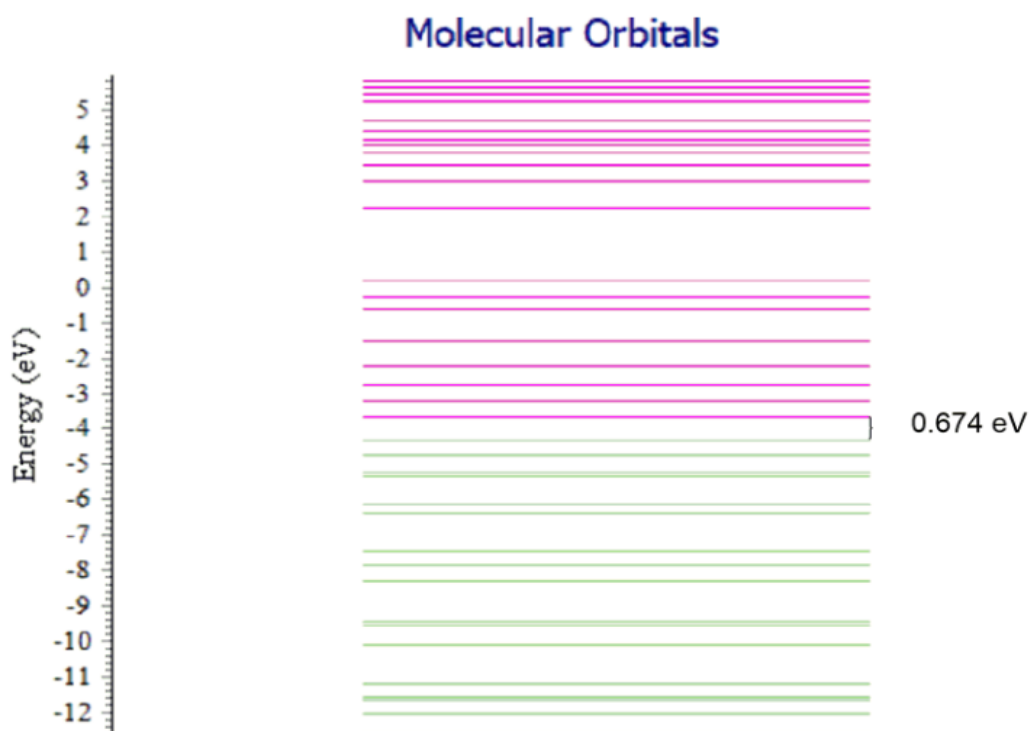


Figure 7.5: The HOMO-LUMO band gap for 4-(2,4-dimethylcyclohexyl)-2-butanone determined using Chemissian

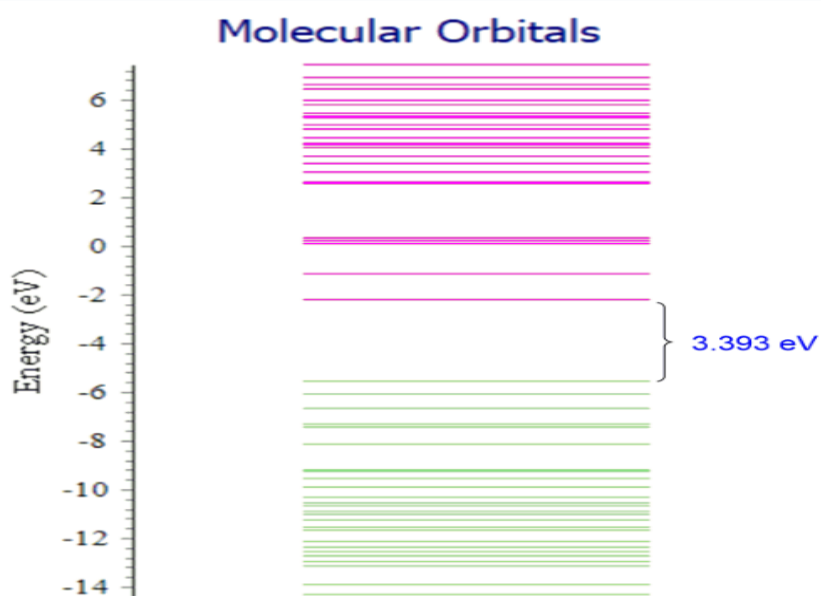


Figure 7.6: The HOMO-LUMO band gap for 5-(3-phenylpropanoyl)dihydro-2-(3H)-furanone determined using Chemissian

The key idea of the frontier molecular orbitals theory rests in the fact that most chemical reactions are dominated by the interaction between these frontier orbitals in an electron donor-acceptor regime. The energy gap between the HOMO-LUMO energy levels is a useful parameter of describing and understanding the reactivity of molecules or compounds.

7.3.4 Electron density contour maps

Electron density contour maps provide an understanding of the charge distributions on molecules. Electron density maps were done for 3, 4-dimethyl-3-cyclohexene-1-carbaldehyde, 5-(3-phenylpropanoyl) dihydro-2(3H)-furanone, and isopropenyl-4-methyl-1,2-cyclohexanediol as presented in appendix II. These Figures are critical in determining regions of high electron density within a molecule. Electron distribution gives insight on the behaviour of particular molecules in understanding the nucleophilic and electrophilic sites in molecular structures. Figures 7.7 and 7.8 gives the 2-D and 3-D electron density maps for 5-(3-phenylpropanoyl) dihydro-2(3H)-furanone as obtained from Chemissian and Gaussian computational platforms, respectively.

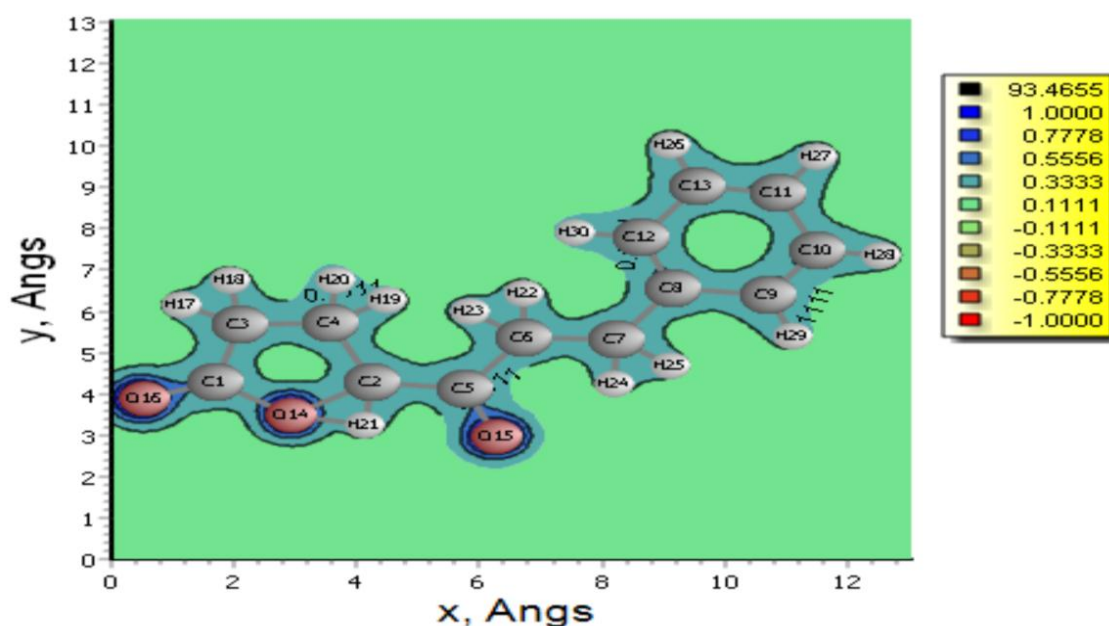


Figure 7.7: 2-D Electron density map for 5-(3-Phenylpropanoyl)dihydro-2(3H)-furanone

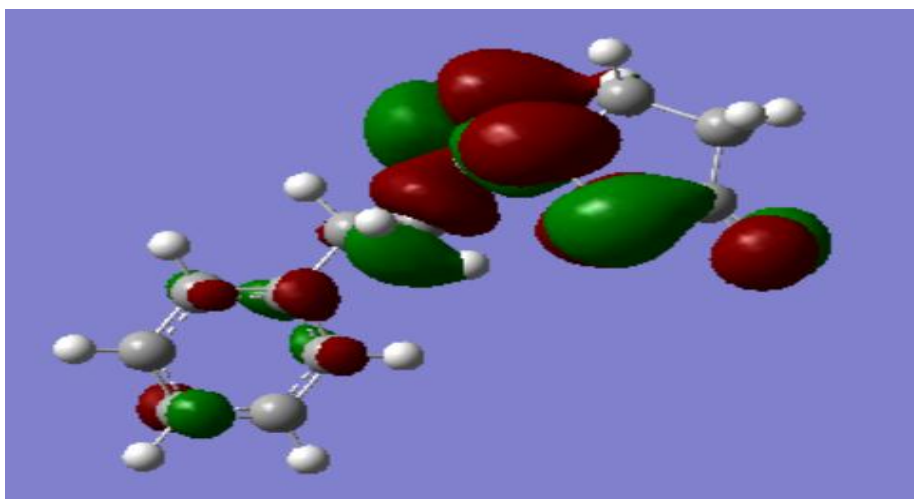


Figure 7.8: 3-D Electron density map for 5-(3-phenylpropanoyl)dihydro-2(3H)-furanone at an isovalue of 0.020

Predictably, the negative potential sites (red colour) represents regions of electrophilic reactivity and interactions through π - π bonding within the aromatic systems and positive potential sites (green colour) represents regions of nucleophilic reactivity figure 7.8, *vide supra*.

Conclusions

This study has demonstrated that the thermal decomposition of fuel components of *C. megalocarpus* biodiesel proceeds chiefly via endothermic energy barriers to form various radicals which may recombine to form free stable molecules proposed to be toxic to humans and the natural environment. The 5-(3-phenylpropanoyl)dihydro-2(3H)-furanone is more electronegative since it has three oxygen atoms compared to other molecules considered in this study which are more electron withdrawing atoms compared to C and H in the structure. Overall, it can be concluded that 5-(3-Phenylpropanoyl)dihydro-2-(3H)-furanone has more electrophilic reactive sites than 4-(2,4-Dimethylcyclohexyl)-2-butanone, 3,4-dimethyl-3-cyclohexene-1-carbaldehyde and isopropenyl-4-methyl-1,2-cyclohexanediol. This observation is supported by the electron density maps reported in this study.

References

- Agarwal, A. K., Gupta, J. G. and Dhar, A. (2017). Potential and challenges for large-scale application of biodiesel in automotive sector. *Progress in Energy and Combustion Science*, **61**: 113-149.
- Altarawneh, M. and Dlugogorski, B.Z. (2015) Formation of dibenzofuran, dibenzo-p-dioxin and their hydroxylated derivatives from catechol. *Physical Chemistry Chemical Physics*, **17**, 1822-1830.
- Alviso, D., Costa, M. W., Backer, L., Pepiot, P., Darabiha, N. and dos Santos, R. G. (2020). Chemical kinetic mechanism for diesel/biodiesel/ethanol surrogates using n-decane/methyl-decanoate/ethanol blends. *Journal of the Brazilian Society of Mechanical Sciences and Engineering*, **42**(2): 100. <https://doi.org/10.1007/s40430-020-2186-9>
- Assaf, N.W., Altarawneh, M., Oluwoye, I., Radny, M., Lomnicki, S.M. and Dlugogorski, B.Z. (2016) Formation of Environmentally Persistent Free Radicals on α -Al₂O₃. *Environmental Science and Technology*, **50**, 11094-11102.
- Batani, H., Saraeian, A., Able, C. and Karimi, K. (2018). Biodiesel Purification and Upgrading Technologies. *Biodiesel: From Production to Combustion*, **8**: 57-100.
- Chen, S. J., Tsai, J. H., Chang-Chien, G. P., Huang, K. L., Wang, L. C., Lin, W. Y. and Yeh, C. K. J. (2017). Emission factors and congener-specific characterization of PCDD/Fs, PCBs, PBDD/Fs and PBDEs from an off-road diesel engine using waste cooking oil-based biodiesel blends. *Journal of Hazardous Materials*, **339**: 274-280.
- Chendynski, L. T., Mantovani, A. C. G., Savada, F. Y., Messias, G. B., Santana, V. T., Salviato, A. and Borsato, D. (2019). Analysis of the formation of radicals in biodiesel in contact with copper and metallic alloys via electronic paramagnetic resonance (EPR). *Fuel*, **242**: 316-322.
- Cheng, X. (2016). *Development of reduced reaction kinetics and fuel physical properties models for in-cylinder simulation of biodiesel combustion* (Doctoral dissertation, University of Nottingham).
- Cheruiyot, N. K., Hou, W. C., Wang, L. C., and Chen, C. Y. (2019). The impact of low to high waste cooking oil-based biodiesel blends on toxic organic pollutant emissions from heavy-duty diesel engines. *Chemosphere*, **235**: 726-733.
- Frisch, M. J., Trucks, G.W., Schlegel, H.B., Scuseria, G.E., Robb, M.A., Cheeseman, J.R., Scalmani, G., Barone, V., Petersson, G.A., Nakatsuji, H. and Li, X. (2016). Gaussian 16 revision 03. *Gaussian Inc., Wallingford Connecticut, U.S.A.*

- Frisch, M., Trucks, H., Schlegel, G., Scuseria, M., Robb, A. and J. Cheeseman (2009). Gaussian 09, Revision B01. *Gaussian Inc., Wallingford Connecticut, U.S.A.*
- Gautam, S. (2018). *Molecular modelling to investigate biomass pyrolysis chemistry* (Master's thesis, Nanyang Technological University, Singapore).
- He, B. Q. (2016). Advances in emission characteristics of diesel engines using different biodiesel fuels. *Renewable and Sustainable Energy Reviews*, **60**: 570-586.
- Kibet, J. K. (2016). Computational Modeling of 2-Monochlorophenol and 2-Monochlorothiophenol. *Kabarak Journal of Research and Innovation*, **4**: 49-61.
- Mosallanejad, S., Dlugogorski, B.Z., Kennedy, E.M., Stockenhuber, M., Lomnicki, S.M., Assaf, N.W. and Altarawneh, M. (2016) Formation of PCDD/Fs in Oxidation of 2-Chlorophenol on Neat Silica Surface. *Environmental Science and Technology*, **50**, 1412-1418.
- Nel, A. (2005). Air Pollution-Related Illness: Effects of Particles. *Science*, **308**, 804.
- Ochterski, J. W. (2015). Thermochemistry in gaussian. *Gaussian Inc, Pittsburgh, Pennsylvania, USA*: 1-17.
- Ombaka, L. M., Ndungu, P. G., Kibet, J. and Nyamori, V. O. (2017). The effect of pyridinic- and pyrrolic-nitrogen in nitrogen-doped carbon nanotubes used as support for Pd-catalyzed nitroarene reduction: an experimental and theoretical study. *Journal of Materials Science*, **52**(18), 10751-10765.
- Skripnikov, L. (2016). Chemission Version 4.43, Visualization Computer Program.
- Soo, Y. N. (2019). *Application of liquid biofuels to internal combustion engines*. Springer Verlag, Singapor.
- Stewart, J. J. (2019). An examination of the nature of localized molecular orbitals and their value in understanding various phenomena that occur in organic chemistry. *Journal of Molecular Modeling*, **25**(1): 1-7.
- Yahagi, S. S., Roveda, A. C., Sobral, A. T., Oliveira, I. P., Caires, A. R., Gomes, R. S. and Trindade, M. A. (2019). An Analytical Evaluation of the Synergistic Effect on Biodiesel Oxidation Stability Promoted by Binary and Ternary Blends Containing Multifunctional Additives. *International Journal of Analytical Chemistry*, **2019**: 1-5.
- Zhen, X., Wang, Y. and Liu, D. (2017). An overview of the chemical reaction mechanisms for gasoline surrogate fuels. *Applied Thermal Engineering*, **124**: 1257-1268.
- Murillo, J. D., Biernacki, J. J., Northrup, S. and Mohammad, A. S. (2017). Biomass pyrolysis kinetics: a review of molecular-scale modeling contributions. *Brazilian Journal of Chemical Engineering*, **34**(1): 1-18.

CHAPTER EIGHT

GENERAL DISCUSSION, CONCLUSIONS AND RECOMMENDATIONS

8.1 General discussion

8.1.1 Rationale of the study

This study primarily explored the hazardous thermal emissions from the thermal degradation of *Croton megarlocarpus* biodiesel, increase in demand for alternative transport fuels, volatile markets and diminishing reserves associated with fossil diesels. This has motivated the search for alternative renewable clean energy resource for clean energy combustion. Therefore the motivation of this study was to probe the nature of molecular by-products and particulate matter emitted, and surface bound free radicals formed during the thermal degradation of *C. megalocarpus* biodiesel and its binary mixture with fossil diesel in order to evaluate the health and environmental consequences of using binary transport fuels in combustion engines at various proposed ratios. This study also simulated the transportation of different particulate sizes emitted from the co-pyrolysis of biodiesel and its blend in the human respiratory model using Multipath particle deposition (MPPD) program, version 3.04. Additionally, the study also assessed the optimum biodiesel and fossil diesel mixture with minimum environmental emission loads. The study also explored molecular modelling of selected molecular pyrolysis by-products from thermal degradation of *C. megalocarpus* biodiesel using the Density functional theory (DFT) formalism at B3LYP quantum level. The tested hypotheses arrived at the following observations;

- i) The gas phase molecular products and free radicals from the co-pyrolysis of biodiesel and petroleum diesel blends at various temperatures were similar.
- ii) The size of particulate matter from the pyrolysis of biodiesel and petroleum blends at 500°C and 600 °C had similar particulate sizes.
- iii) The kinetic model for the formation of selected gas phase free radicals immobilised on thermal char at different life times was consistent with pseudo-first order rate law..
- iv) Molecular orbital geometries and band-gap energies for selected gas phase molecular products and free radicals generated using CHEMISIAN and DFT were similar. The bandgap energies from both computational softwares were the same.

The *Croton megalocarpus* seeds used in this study were locally obtained from the Egerton University botanical garden and oven dried at 110 °C for 8 hours. The seeds were allowed to cool then ground and sieved to obtain uniform particle size of approximately 50 microns.

Commercial diesel was purchased from a licensed petroleum distributor. The bio-oil extraction from *C. megalocarpus* seeds was extracted by solvent extraction method using *n*-hexane as the solvent. The conversion of bio-oil to biodiesel was done through the process of trans-esterification. The analysis of biodiesel were done following the ASTM D 6751 standards. The first part of the study involved the pyrolysis of *C. megalocarpus* biodiesel at 600 °C in a quartz reactor in an inert atmosphere of flowing nitrogen at a residence time of 5 seconds. For subsequent studies the same procedure was applied for different proportions of biodiesel and fossil diesel at 500 °C. Characterisation of *C. megalocarpus* biodiesel, molecular and particulate emissions were carried out using gas chromatograph coupled to a mass selective detector (MSD), electron paramagnetic resonance (EPR) spectroscopy, elemental analyzer, Fourier-transform infrared spectroscopy (FTIR) and a scanning electron microscope (SEM). Computational studies were performed using Gaussian 09 computational code, Chemission computational program and Multipath particle deposition (MPPD) model, version 3.04 model.

8.1.2 Findings of the study

8.1.2.1 Environmentally persistent free radicals and particulate emissions from the thermal degradation of *Croton megalocarpus* biodiesel

The results obtained from GC-MS indicated that the major components of *C. megalocarpus* biodiesel comprised of long chain hydrocarbon methyl esters. The major hydrocarbon compound was methyl palmitate with a retention time of 13.35 minutes while methyl docosanoate was a minor compound with a retention time of 15.56 minutes. Methyl palmitate was the major compound in the biodiesel, with a yield of $33.86 \pm 3.04 \mu\text{g}$ while methyl docosanoate was a minor component in the biodiesel matrix (yield, $2.67 \pm 0.46 \mu\text{g}$). The other major compounds included; (E)-methyl dodec-9-enoate, (9E,12E)-methyl octadeca-9,12-dienoate, and (E)-methyl icos-11-enoate, which have C-C double bonds within the chain and may therefore be the most important precursors in the formation of char.

The observed EPR characterization of *C. megalocarpus* thermal particulates revealed that radicals immobilised on *C. megalocarpus* thermal char are carbon-centred similar to a free radical typical of those found in coal. They have low *g*-value of 2.0024 with a corresponding peak width of 3.65 G. The kinetic behaviour of *C. megalocarpus* thermal char was monitored over a period of 80 days and the data obtained was fitted to pseudo-first order kinetic model where, the rate constant, half-life and initial concentration was obtained from the

equation of the best fit ($y = mx+c$). The results showed that the free radicals take about 1.2 years to decay to a half their original concentration. The initial concentration (spins/g) in the thermal char was estimated from the y-intercept and found to be 9.35×10^{19} spins/g – that is if the thermal emissions were to be analyzed *in situ*.

The FTIR spectrum of *C. megalocarpus* biodiesel particulate char was characterized by several principal bands. The intense broad absorption peak $\delta_s(1113 \text{ cm}^{-1})$ at finger print region of the spectrum is associated with the in-plane bending of $-\text{CH}_3$ in the aromatic structure of croton char particulates while the absorption bands $\nu_{sa}(2922 \text{ cm}^{-1})$ and $\nu_s(2857 \text{ cm}^{-1})$ are characteristic bands for asymmetrical and symmetrical stretching, respectively, of methylene ($-\text{CH}_2-$) groups for long chain aliphatic hydrocarbons which might be present in the char. Thus, the croton char particulates may contain long chain hydrocarbons adsorbed on its surface.

8.1.2.2 Free radicals and ultrafine particulate emissions from the co-pyrolysis of *Croton megalocarpus* biodiesel and fossil diesel

The particulate emissions presented in this study from co-pyrolysis at 600°C of biodiesel blend (ratio 1:1 of biodiesel to fossil diesel by weight) were determined using scanning electron microscope and it was found to be ultrafine particulates (approx. 32 nm). This is less than $\text{PM}_{0.1}$ and are therefore considered to have the highest penetrating power in the respiratory tract tissues, hence highly toxic to humans. The EPR results showed that the nature of radicals of biodiesel blend thermal char are carbon-centered with a g-value of 2.0027 characteristic of carbon-based radicals of aromatic nature. The Spectral peak-to-peak width (ΔH_{p-p}) obtained was narrow (4.42 Gauss). The free radicals identified as carbon-based are hazardous and may be transported by various sizes of particulate matter (PM) on to the surface of the human lung which may trigger cancer and pulmonary diseases. The radical decay were monitored over a period of 80 days and it was observed that the spin density (spins/g) intensity could not decrease appreciably (15 %). This decrease is also consistent with that realized for spins/cm over a similar period of time (~ 14%). From this findings the radicals immobilized in the *C. megalocarpus* thermal char are very stable and can persist in the environment for quite sometime.

8.1.2.3 Simulating the health impact of particulate emissions from transport fuels using multipath particle deposition model (MPPD)

The particulates emitted during combustion of transport fuels are varied in terms of chemical nature and size. They are known to cause respiratory ailments and environmental degradation. The transportation of these particulates in the respiratory system and their clearance in the system pose a great challenge in determining the effects of these particulates in humans. Therefore there is a need to simulate the particulate transport in the system. In this study the multipath particle deposition model (MPPD) version 3.04 was used in understanding the transport of the particulates of pure biodiesel, for particles with count medium diameter (CMD) of 32 nm for pure biodiesel and 22 nm for blend having a geometric standard deviation (GSD) of 1 nm. The particulate transport was simulated by considering three age groups (3 months, 8 years and 21 years olds) in head, pulmonary, bronchials and trachea. The results showed that pulmonary tissue retained the highest ratio of thermal emissions of croton bio-oil particulates for all ages (infants, 8 years and 21 years respectively) as compared to the particulates from the diesel pyrolysis mixtures. Clearly, infants retain a high fraction of particulates possibly because their lungs are not well developed and this may be a major precursor for child mortality.

8.1.2.4 Optimization of binary mixtures of biodiesel and fossil diesel for clean energy combustion

This work investigates various ratios of biodiesel and commercial diesel in order to propose model binary fuels for clean energy combustion. Accordingly, diesel blends of ratios 1:1, 3:2 and 2:3 were each pyrolyzed at a contact time of 5 seconds in a quartz reactor at 1 atmosphere pressure. A model temperature of 500 °C was explored in these experiments. The charcoal content for pure fossil diesel was compared with the binary diesel residue. Gas-phase molecular components were determined using Gas chromatography (GC) coupled to a mass selective detector (MSD). Elemental composition of thermal char was determined using Smart Elemental Analyzer. Radical intensities for the three types of char (biochar, bio-fossil char, and fossil char) were measured using an X-band electron paramagnetic resonance (EPR) spectrometer. The results showed that during the combustion of the binary ratio of 2:3 (Biodiesel: Fossil diesel) by weight, harmful molecular products reduced significantly, 76 – 99%. Elemental analysis data indicated that the carbon content from commercial diesel was very high ($\approx 70.61\%$) as compared to approximately 53% for biodiesel-fossil diesel mixture in the same ratio 2:3. The free radical content was reduced by nearly 50% in favour of the

biodiesel/fossil diesel mixture. The ratio of 1:1 decreased the levels of long chain hydrocarbons but a ratio of 3:2 (w/w) realized an increase in the level of hydrocarbons. Model hydrocarbon compounds including tetradecane for instance decreased by approximately 92% in the ratio 2:3 as compared to a ratio of 3:2 whereas pentadecane decreased by 29%. On the other hand 2,6,10,14-tetramethylhexadecane decreased by $\approx 93\%$. For the oxygenated model compounds, a reduction of about 76, 80, 96.4 and 85% for methyl hexadecanoate, methyl-8,11-octadecadienoate, methyl linoleate, and methyl methylstearate was observed respectively. Additionally, it was observed that pyrolysis of pure biodiesel generates a high amount of free radicals as opposed to when the biodiesel is mixed with fossil diesel in the ratio 2:3 (w/w). To this end, this study has noted that binary mixtures of renewable biofuels and non-renewable fossil fuels may offer a solution in the search for fuels of good heating value without damaging combustion engines as well as the integrity of the natural environment.

8.1.2.5 Molecular modelling of selected combustion by-products from the thermal degradation of *Croton megalocarpus* biodiesel blend

Computational science gives a comprehension into the atomic properties of an aggravate that would not in any case be anything but difficult to decide tentatively. Moreover, computational techniques are affordable as far as cost and time. This examination explored in detail the electron thickness maps, atomic orbitals, band hole energies and geometry improvement of chose response results from the warm decay of *C. megalocarpus*; 4-(2,4-dimethylcyclohexyl)- 2-butanone, 3,4-dimethyl-3-cyclohexene-1-carbaldehyde, 5-(3-phenylpropanoyl) dihydro-2-(3H)- furanone and isopropenyl-4-methyl-1,2-cyclohexanediol. The electron thickness form maps produced was utilized to inspect the nucleophilicity of the chose unpredictable natural mixes so as to acquire knowledge on how they associate with organic structures to cause harmfulness and cell impedance in respiratory frameworks. The enhancement procedure for different pathways for the 5-(3-phenylpropanoyl) dihydro-2-(3H)- furanone and middle of the road free radicals was tested. The investigation showed that the warm deterioration of fuel parts of *C. megalocarpus* biodiesel continues mostly by means of endothermic vitality obstructions to frame different radicals. The 5-(3-phenylpropanoyl) dihydro-2-(3H)- furanone is increasingly electronegative since it has three oxygen iotas contrasted with other sub-atomic species considered in this investigation which are more electron pulling back molecules contrasted with C and H in the structure. Generally, it tends to be presumed that 5-(3-Phenylpropanoyl) dihydro-2-(3H)- furanone has more

electrophilic responsive locales than 4-(2,4-Dimethylcyclohexyl)- 2-butanone, 3,4-dimethyl-3-cyclohexene-1-carbaldehyde and isopropenyl-4-methyl-1,2-cyclohexanediol.

8.2 Conclusions

This work has revealed that various molecular products such as long chain hydrocarbons (tetradecane, pentadecane and hexadecane) of environmental concern are formed from the co-pyrolysis of *C. megalocarpus* biodiesel and fossil fuels (binary transport fuel). Methyl esters including methyl hexadecanoate, methyl linoleate, methylstearate were also formed in high amounts during the pyrolysis of diesel blends. *Croton megalocarpus* thermal char showed slightly higher concentrations of free radicals compared with the concentration of free radicals from the pyrolysis of binary transport fuel explored in this study. In particular, it has been noted that the thermal char by-product has high concentration of free radicals (9.12×10^{19} spins/g) with low g-value of 2.0024 and a narrow ΔH_p -p of 3.65 G. Moreover, the ratio of 2:3 (Biodiesel: Fossil diesel) binary fuel, indicated a reduction of harmful molecular products, 76 – 99%. It was also observed from elemental analysis data that the carbon content from commercial diesel was very high ($\approx 70.61\%$) as compared to approximately 53% for biodiesel-fossil diesel binary mixture, in the ratio 2:3. Therefore, an optimum ratio of 2:3 for biodiesel – fossil diesel binary fuel can result in clean energy combustion based on the data reported in this work.

The particulate matter of thermal char from thermal degradation of *C. megalocarpus* biodiesel and its blend at 500 °C were approximately 22 nm and 32 nm respectively. These particulates are categorized as ultrafine (PM_{<0.1}) and therefore they can be inhaled deep in the respiratory system and may pose serious health concerns such as aging, cancer, oxidative stress, and possible complex respiratory ailments as predicted using the Multipath Particle Deposition (MPPD) model discussed in this study.

The half-life of free radicals in *C. megalocarpus* thermal char were found to be a 431 days corresponding to a low decay rate constant ($1.86 \times 10^{-8} \text{ s}^{-1}$), hence they can reside in the environment for a longer periods. Additionally, the concentration of surface bound radicals on the binary fuel thermal char was relatively lower than that in *C. megalocarpus* char. Even after 80 days storage, the spin density (spins/g) had decreased only by about 15% the initial concentration of 9.18×10^{19} spins/g.

The thermal degradation of biofuels proceeds via an endothermic reaction channel with high activation energies (+372 and +400 kJ/mol) as predicted by the Density functional theory (DFT) formalism coupled with 3-21G basis at B3LYP Quantum level. This implies that the molecular pyrolysis products investigated were stable. Notably, the 5-(3-Phenylpropanoyl) dihydro-2-(3H)-furanone has more electrophilic reactive sites than 4-(2,4-Dimethylcyclohexyl)-2-butanone, 3,4-dimethyl-3-cyclohexene-1-carbaldehyde and isopropenyl-4-methyl-1,2-cyclohexanediol, respectively.

8.3 Recommendations

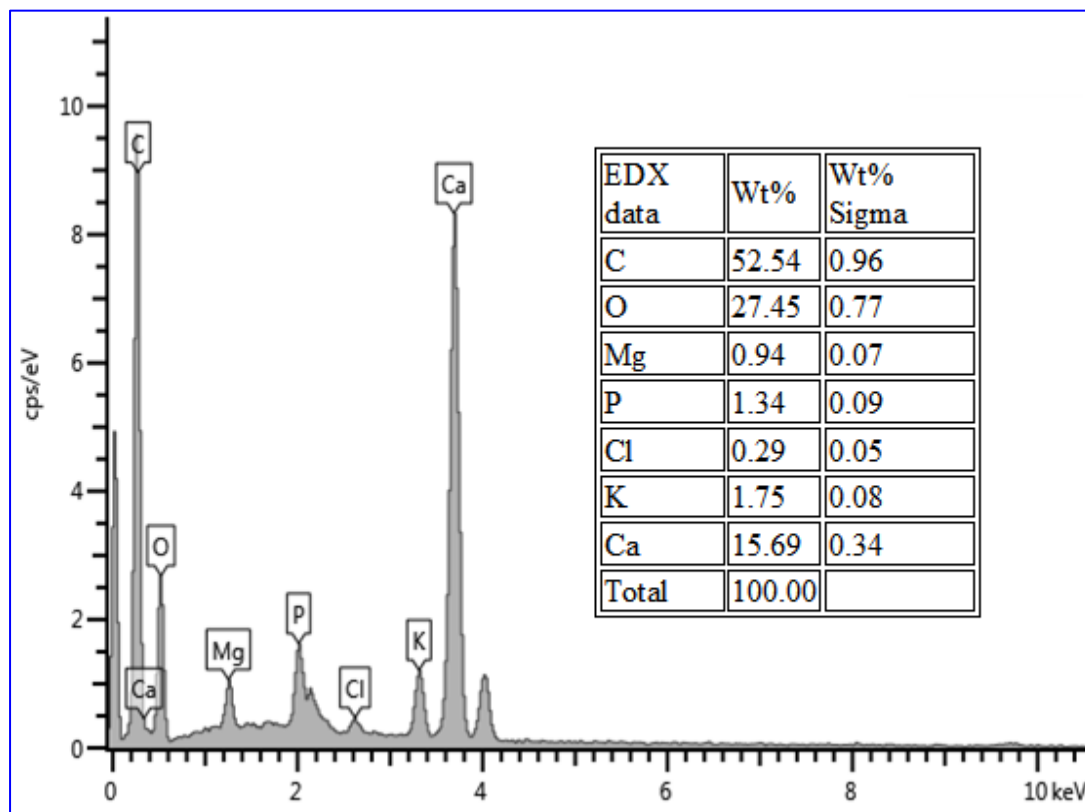
This work has thoroughly examined the particulate and molecular by-products from the co-pyrolysis of *C. megalocarpus* biodiesel blends. The kinetic behaviour of radicals was investigated in detail. The biological distribution of PM was also considered critically from a theoretical standpoint using the Multipath Particle Deposition (MPPD) model. However, a lot of work needs to be done in order to exhaustively draw serious conclusions on the use of biodiesel blends in the transport industry. The following are recommendations that can be drawn from this study.

- i) The pyrolysis ratio of 2:3 was found to be a promising blend for biodiesel and commercial diesel. This study recommends further tests such as calorific heating value, viscosity, acidity, and ageing to be conducted on this binary mixture.
- ii) The particulate sizes of various biodiesel blend ratios should be investigated.
- iii) The formation kinetics of major co-pyrolysis by-products of biodiesel blend at different residence times should be explored in future studies.
- iv) There is need to extend this investigation to other biofuels from non-edible oil producing plants such as *Jatropha* oil.

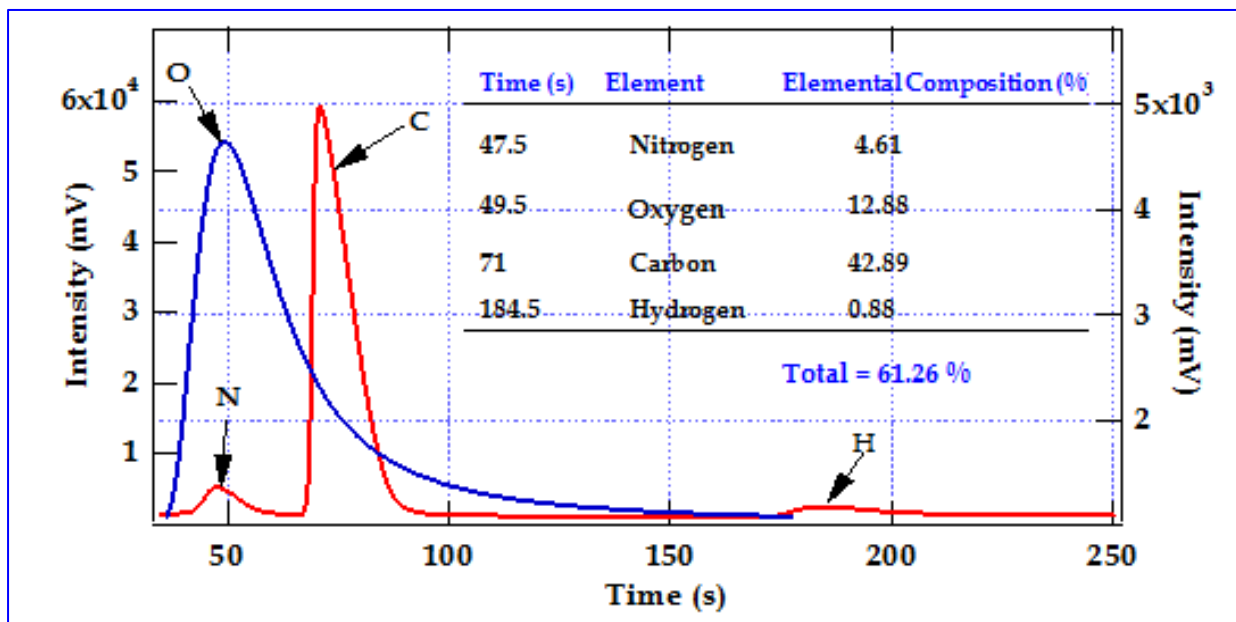
APPENDICES

Appendix I: Characterization of croton char

Appendix S1: The Energy Dispersive X-ray data for croton char performed with Aztec (UK) software coupled to an Oxford detector (UK)

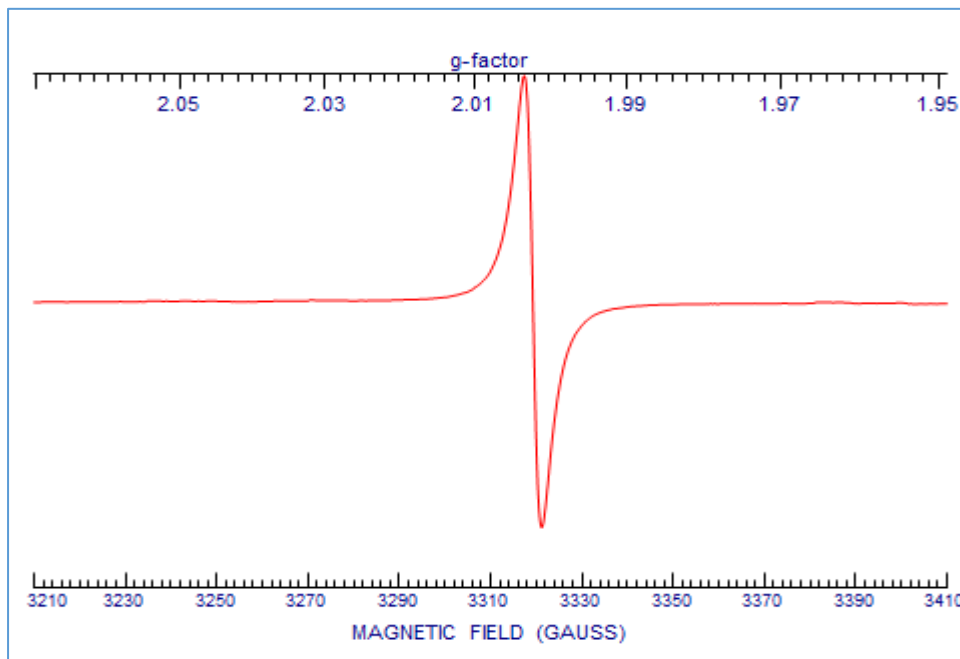


Appendix S2: The elemental analysis data (CHNO) for croton char performed with Elementary Analyzer (Germany). The letters C, H, N, and O represent Carbon, Hydrogen, Nitrogen, and oxygen respectively. The oxygen spectrum (Right axis) is appended to the CHN spectrum (Left axis).

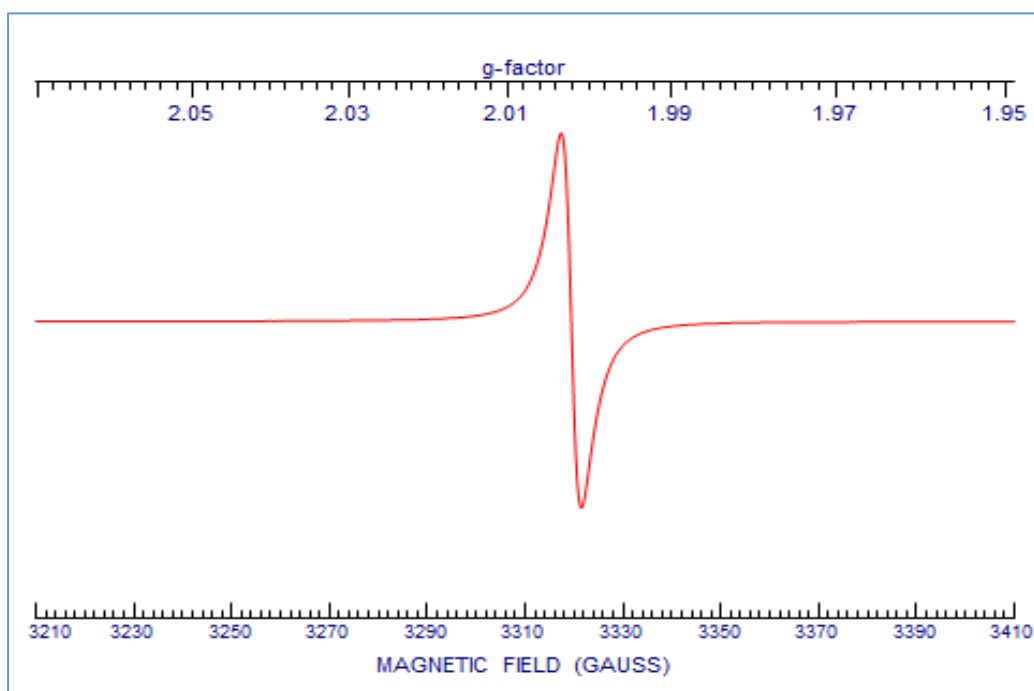


Appendix S3: The material presented here are important in enhancing the understanding of the concepts reported in the article. The Figures presented in the article were done using Igor graphing software (ver. 5.0).

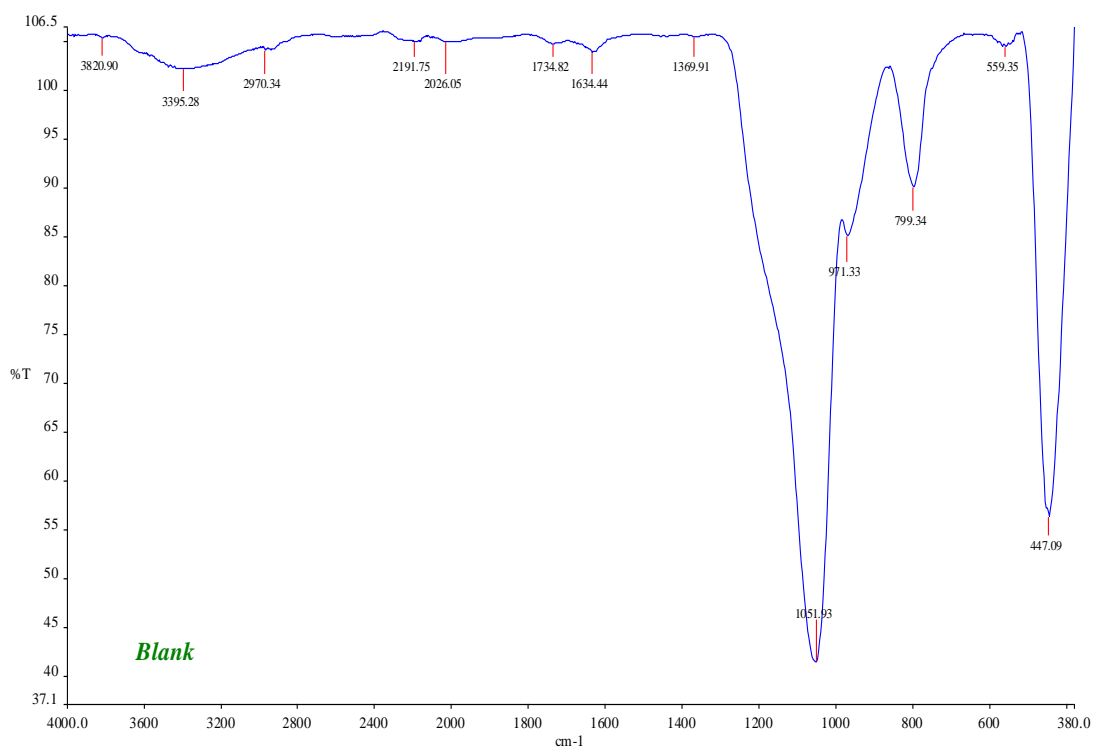
The diesel blend thermal char EPR spectra for runs 1 and 4; g-factor as a function of magnetic field



(a) EPR spectrum for run 1

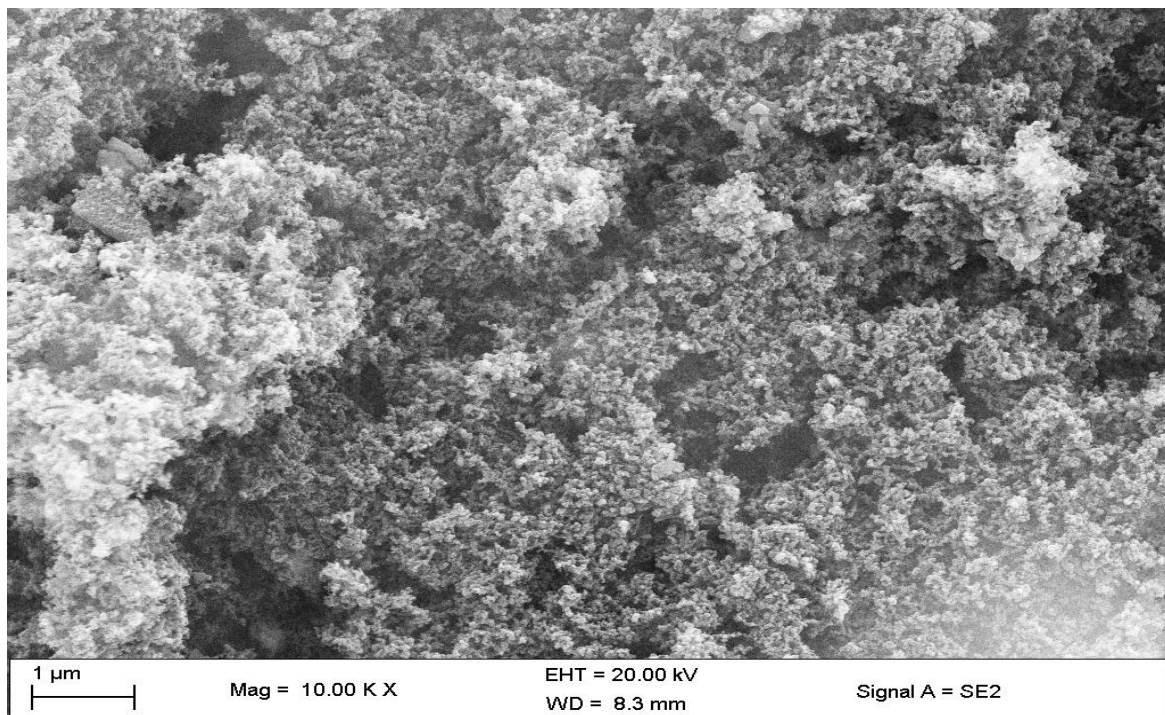


(b) EPR spectrum for run 4

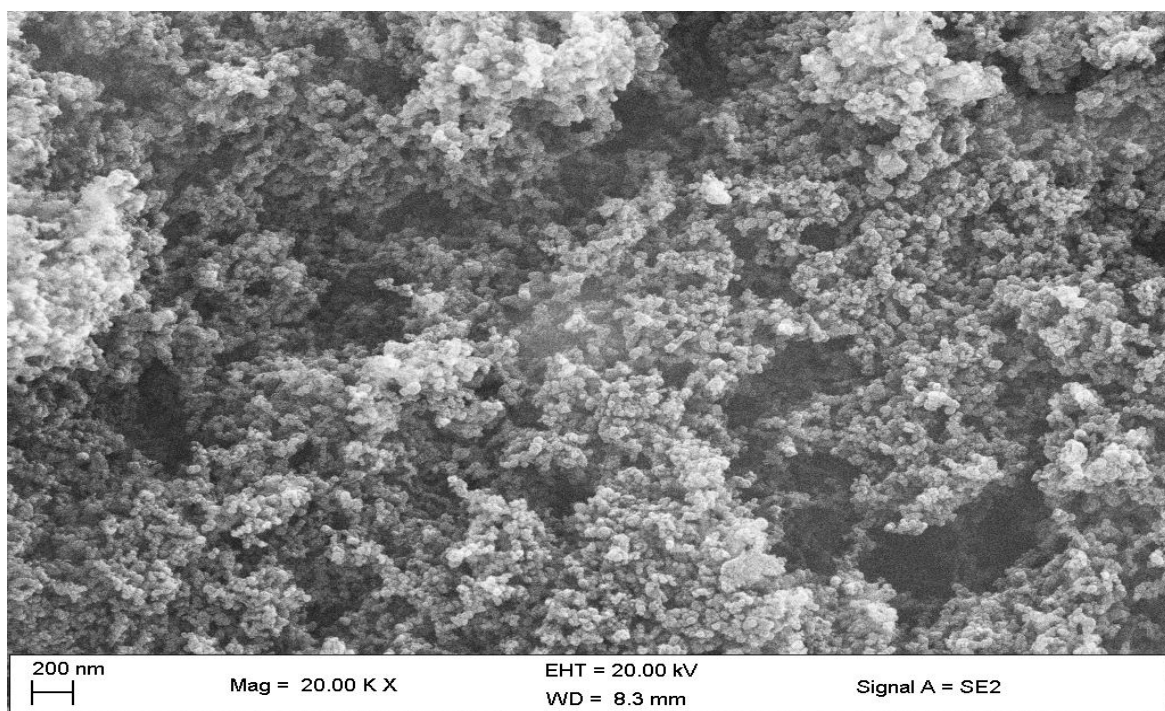


(c): FTIR spectrum for the blank

Appendix S4: SEM images of thermal char at various magnifications



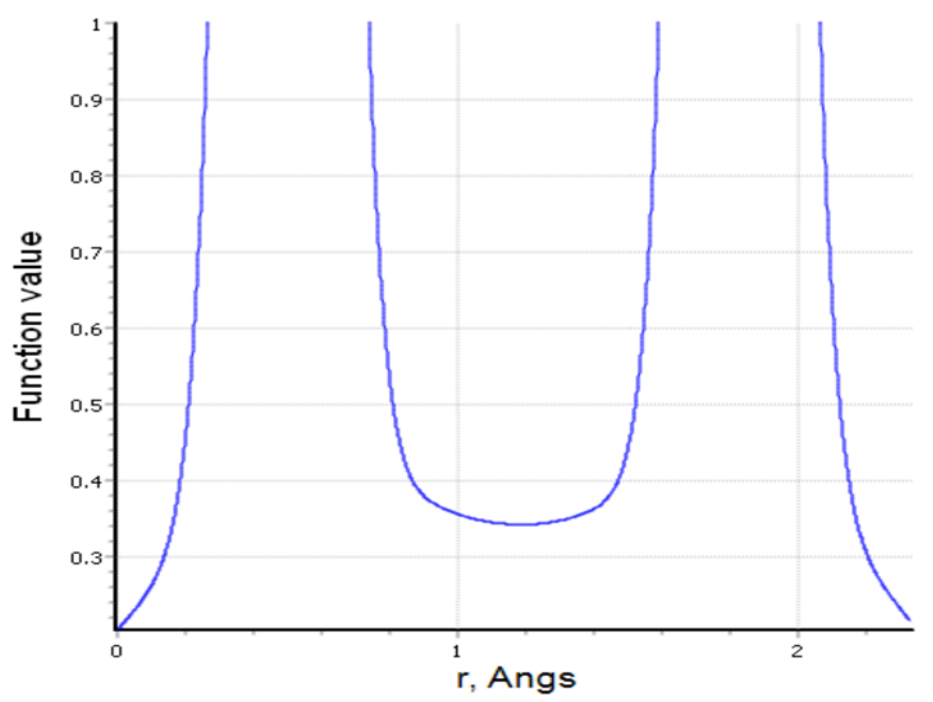
(a) SEM image at an associated magnification of X10,000 for the thermal char



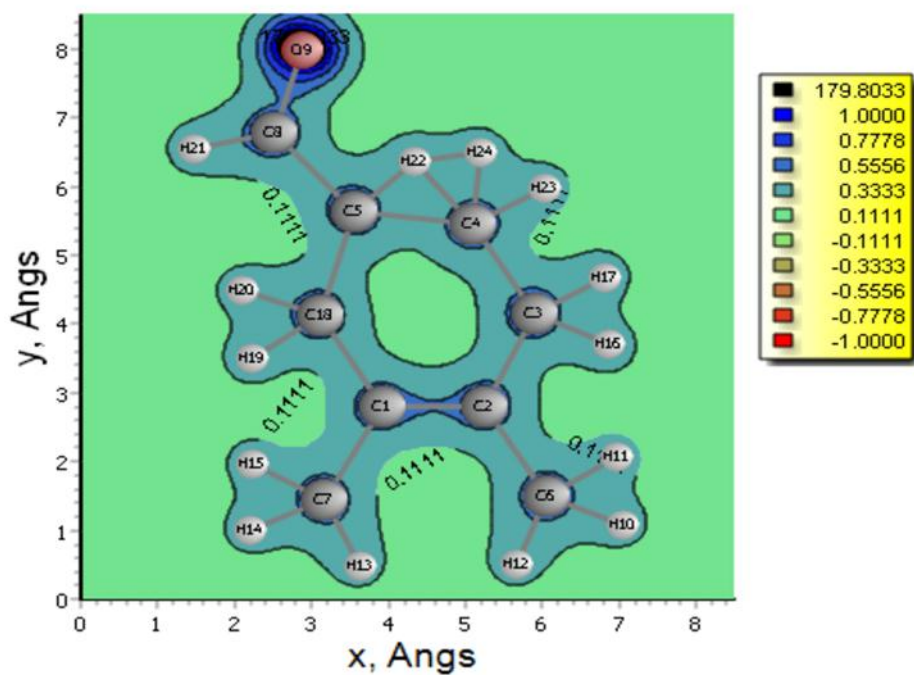
(b) SEM image at an associated magnification of X20,000 for the thermal char

Appendix II: Electron density maps and molecular orbitals

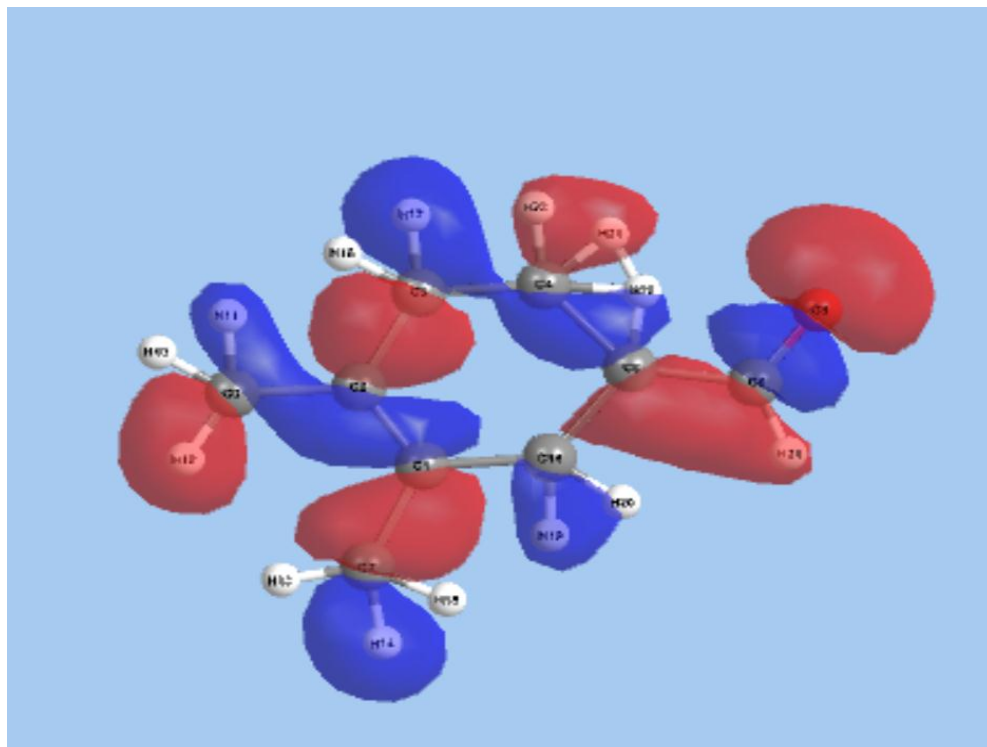
Appendix A1: 1-D electron density contour map for 3,4-Dimethyl-3-cyclohexene-1-carbaldehyde



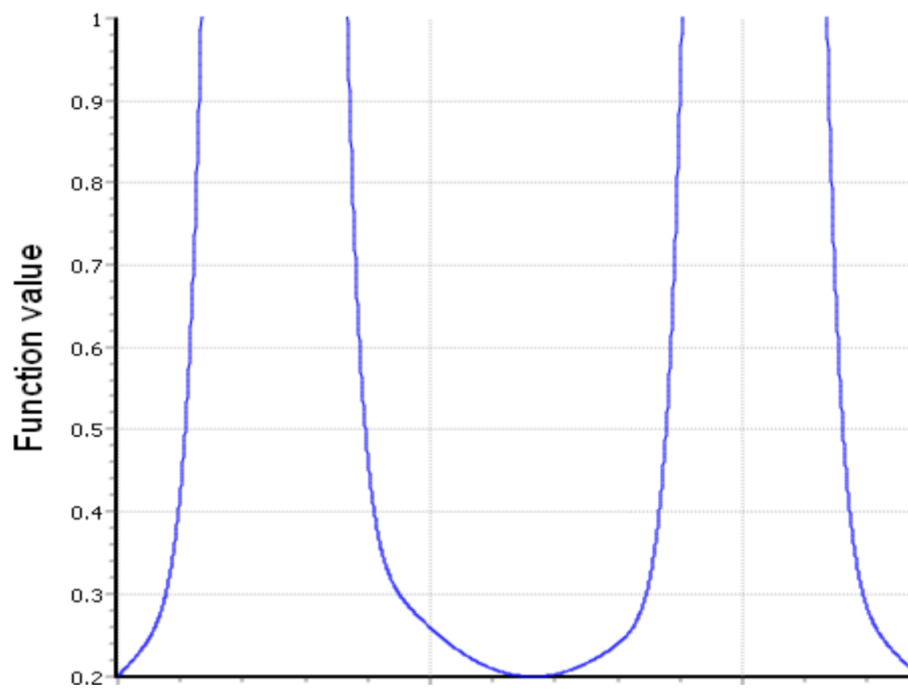
Appendix A2: 2-D electron density contour map for 3,4-Dimethyl-3-cyclohexene-1-carbaldehyde



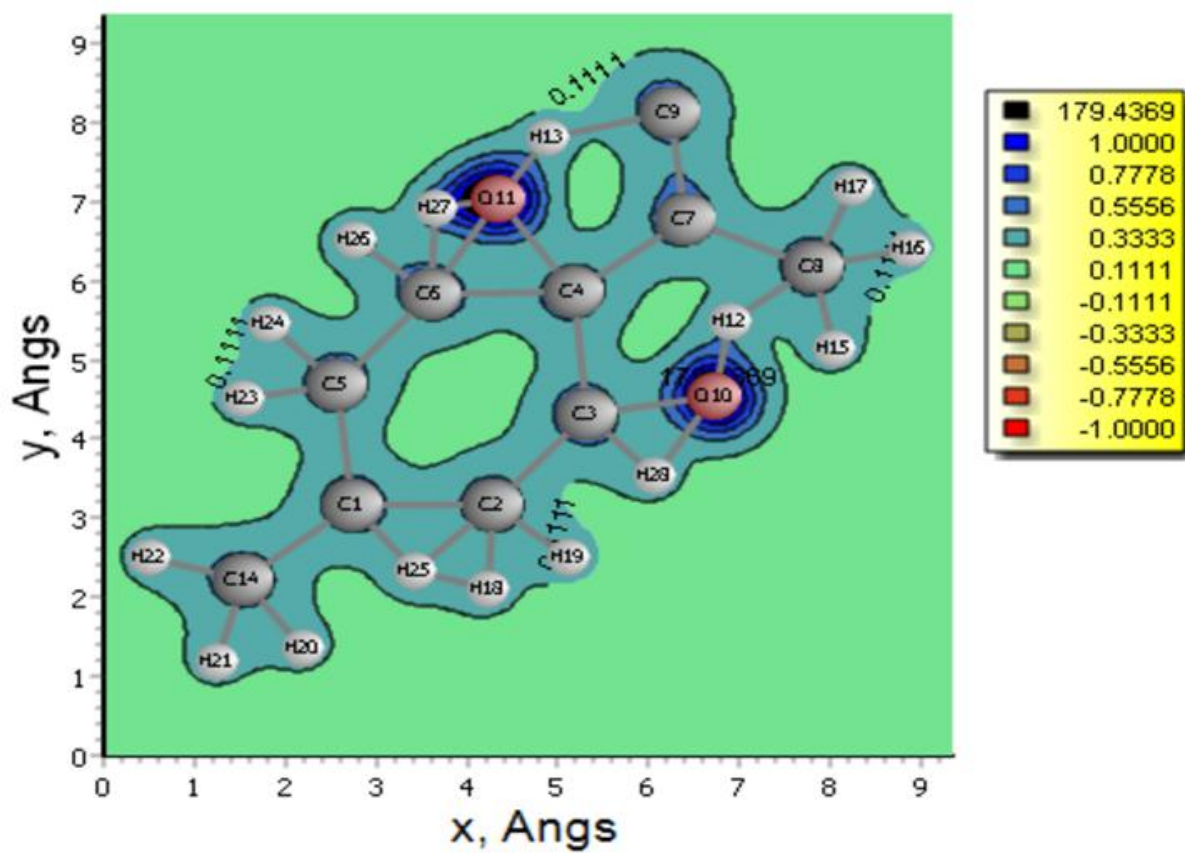
Appendix A3: 3-D electron density contour map for 3,4-Dimethyl-3-cyclohexene-1-carbaldehyde



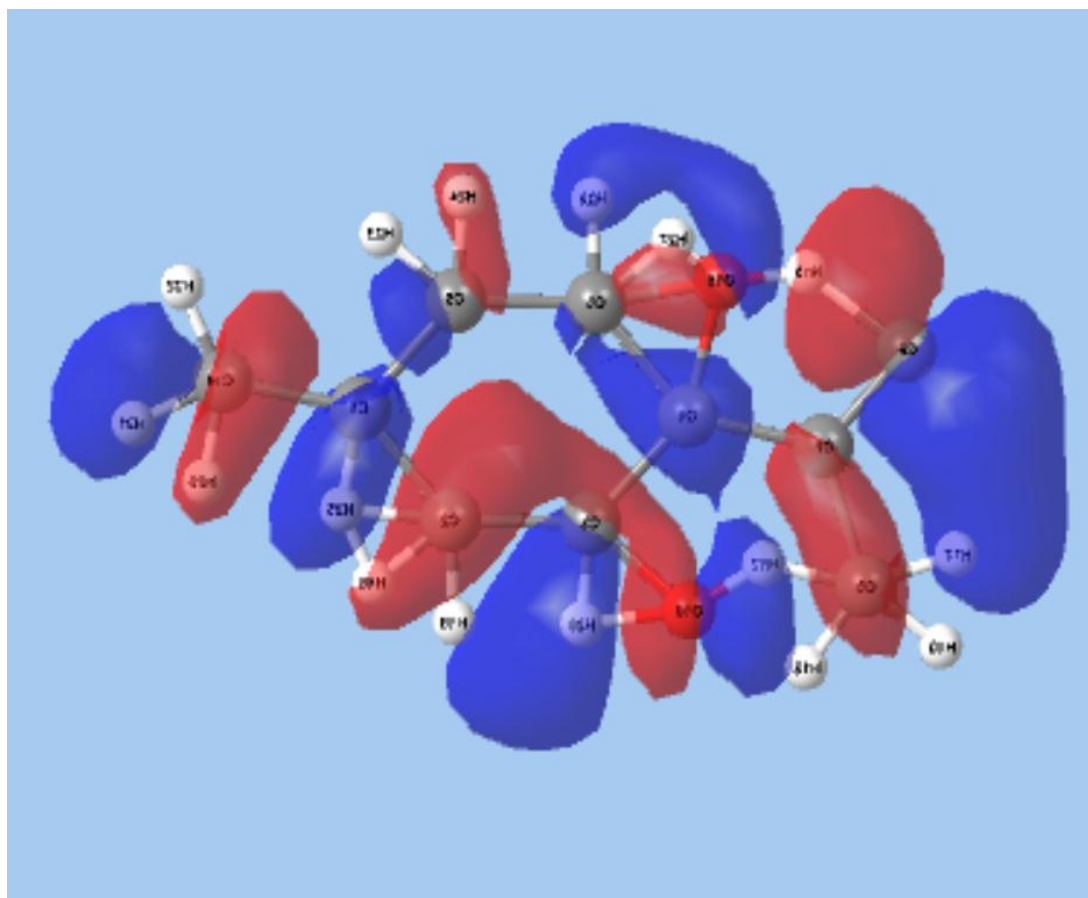
Appendix B1: 1-D electron density contour map for -Isopropenyl-4-methyl-1,2-cyclohexanediol



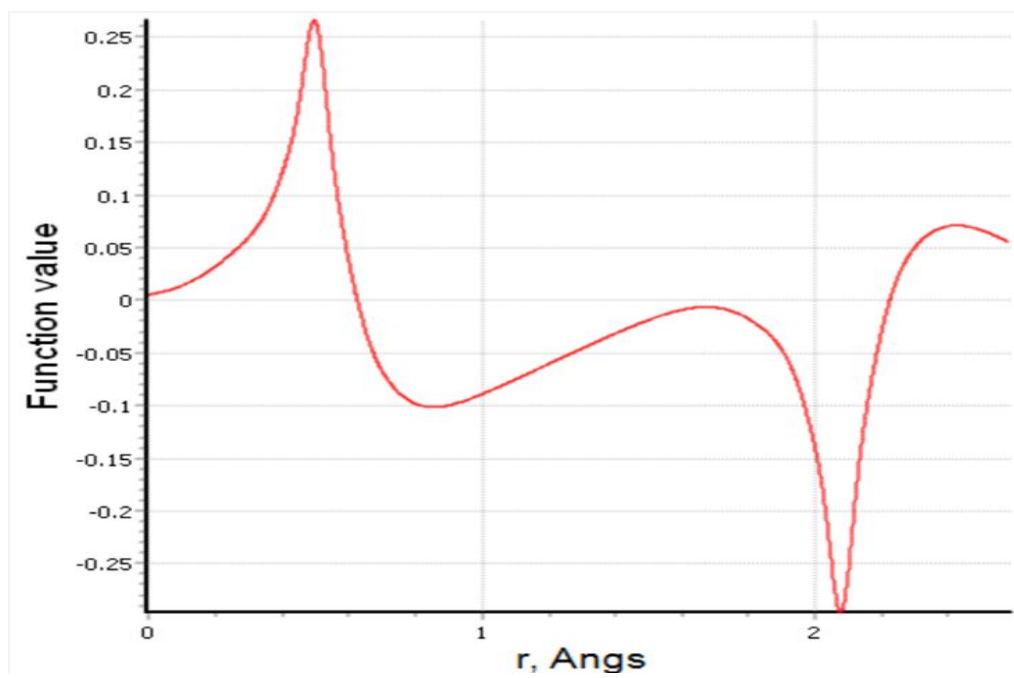
Appendix B2: 2-D electron density contour map for -Isopropenyl-4-methyl-1,2-cyclohexanediol



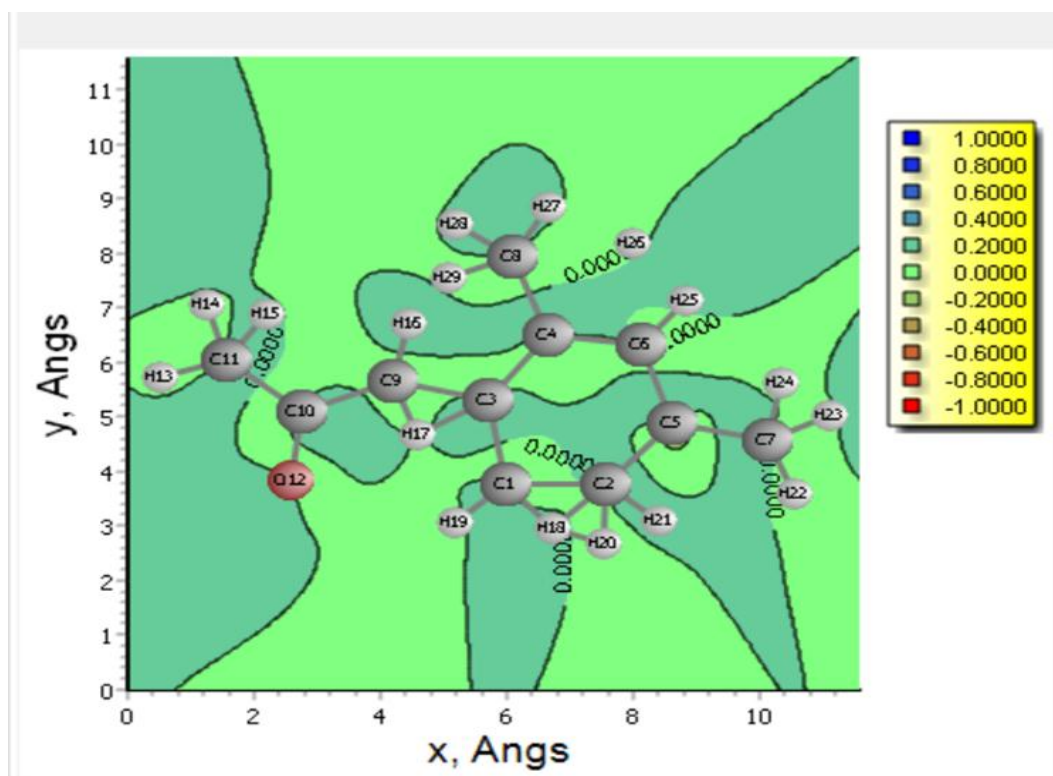
Appendix B3: 3-D electron density contour map for -Isopropenyl-4-methyl-1,2-cyclohexanediol at isovalue 0.020



Appendix C1: 1-D electron density contour map for 4-(2,4-dimethylcyclohexyl)-2-butanone



Appendix C2: 2-D electron density contour map for 4-(2,4-dimethylcyclohexyl)-2-butanone



Appendix III: Copyrights

1. Open Journal of Modelling and Simulation COPYRIGHT FORM

Scientific Research Publishing, Inc.

SCIRP, <http://www.scirp.org>

This form is intended for original material submitted to the Journal Open Journal of Modelling and Simulation (OJMSi) sponsored by Scientific Research Publishing Inc. (SCIRP). The following agreement must be signed and returned to the OJMSi Editorial Office before the manuscript can be published. Please read it carefully and keep a copy for your files

Journal: Open Journal of Modelling and Simulation (OJMSi). Paper ID: 2860153

Paper Title: Simulating the Health Impact of Particulate Emissions from Transport Fuels using Multipath Particle Deposition Model (MPPD)(2860153)

Author(s): Bornes Mosonik, Joshua Kibet, Silas Ngari

COPYRIGHT CONCESSION AGREEMENT

The undersigned hereby grants SCIRP a nonexclusive copyright that may exist in and to the above Work, and any revised or expanded derivative works submitted to the Journal OJMSi by the undersigned based on the Work on the understanding that on completion of the layout SCIRP will make the final paper available online without delay, SCIRP guarantees that no university library or individual reader will ever have to buy a subscription or buy access through pay-per-view fees to access the papers published in the Journal OJMSi. The undersigned hereby warrants that the Work is original and that he/she is the author of the Work; to the extent the Work incorporates text passages, figures, data or other material from the works of others, the undersigned has obtained any necessary permission including permission from any and all co-authors.

RETAINED RIGHTS, TERMS, AND CONDITIONS

Since the undersigned grants SCIRP a nonexclusive copyright, the undersigned retains the original copyright while SCIRP is granted the same set of rights including the right to sublicense the work. SCIRP will publish the Work under a Creative Commons license. By default this is the Creative Commons Attribution 4.0 International License, CC BY:

<http://creativecommons.org/licenses/by/4.0/>.

Alternatively upon request it is also possible for SCIRP to publish under: Creative Commons Attribution-Non Commercial 4.0 International Licenses, CC BYNC:

<http://creativecommons.org/licenses/by-nc/4.0/>

Author's choice (specify CC BY-NC only if you do not want the default CC BY)

Authors and their employers retain all proprietary rights in any process, procedure, or article of manufacture described in the work. Authors who are US Government employees may reproduce or authorize others to reproduce the work, material extracted verbatim from the work, or derivative works to the extent permissible under US's law for works authored by US Government employees, and for the author's personal use or for company or organizational use, provided that the source and any SCIRP copyright notice are indicated. The copies are not used in any way that implies SCIRP endorsement of a product or service of any employer, and the copies themselves are not offered for sale.

In the case of a Work performed under a China Government contract or grant, the SCIRP recognizes that the China Government has royalty-free permission to reproduce all or portions of the Work, and to authorize others to do so, for official China Government purposes only, if the contract/grant so requires.

SCIRP Copyright

It is the formal policy of SCIRP to be granted the nonexclusive copyrights to all copyrightable material in its technical publications and to the individual contributions contained therein, in order to protect the interests of SCIRP, its authors and their employers, and, at the same time, to facilitate the appropriate re-use of this material by others. SCIRP distributes its technical publications throughout the world and does so by various means such as hard copy, microfiche, microfilm, and electronic media. It also abstracts and may translate its publications, and articles contained therein, for inclusion in various compendiums, collective works, databases and similar publications. No royalties are paid to authors if SCIRP produces revenues by these activities.

Author/Employer Rights

If you are employed and prepared the work on a subject within the scope of your employment, the copyright in the Work belongs to your employer as a work-for-hire. In that case, SCIRP assumes that when you sign this Form, you are authorized to do so by your employer and that your employer has consented to granting the nonexclusive copyright, to the representation and warranty of publication rights, and to all other terms and conditions of this

Form. If such authorization and consent has not been given to you, an authorized representative of your employer should sign this Form as the Author. In the event the above work is not accepted and published by SCIRP or is withdrawn by the author(s) before acceptance by SCIRP, the foregoing granting the nonexclusive copyright shall become null and void and all materials embodying the work submitted to OJMSi was destroyed. The author signs for and accepts responsibility for releasing this material on behalf of any and all co-authors.

Creative Commons License Type:

Attention: Please choose either one of these two above.

*Signature: B.C.

Date (2019-03-30 01:48:47)

CC BY-NC

RE: {SrvReqNo:[8001674245]} Request for copyright permission



Journalpermissions <journalpermissions@springernature.com>

7/3/2019 1:48 PM



To: Bornes Rotich

Dear Bornes,

Thank you for your quick reply. See below for the case for each article –

Environmental Science and Pollution Research -

As an author, you retain certain non-exclusive rights over the 'Published Version' for which no permissions are necessary as long as you acknowledge and reference the first publication. These include:

- The right to reuse graphic elements contained in the Article and created by you in presentations or other works you author
- The right of you and your academic institution to reproduce the Article for course teaching. Note, this does not include the right to include in course packs for resale by libraries or by the institution
- **To reproduce, or allow a third party to reproduce the Article in whole or in part in any printed volume (book or thesis) authored by you.**

You may also wish to refer to our 'Reprints and Permissions' FAQs on [Springer.com](https://www.springernature.com):

<https://www.springernature.com/gp/partners/rights-permissions-third-party-distribution>

Best wishes,
Oda

Oda Siqveland
Rights Executive

SpringerNature
The Campus, 4 Crinan Street, London N1 9XW,
United Kingdom
T +44 (0) 207 014 6851

<http://www.nature.com>
<http://www.springer.com>
<http://www.palgrave.com>

Activate Windows
Go to Settings to activate Windows.

Chemistry Africa Journal

This work is licensed under the Creative Commons Attribution 4.0 International License, which permits unrestricted use, distribution, modification, and reproduction in any medium, provided you:

- a) Give appropriate acknowledgment to the original author(s) including the publication source,
- b) Provide a link to the Creative Commons license, and indicate if changes were made.

You are not required to obtain permission to reuse this article, but you must follow the above two requirements.

Images or other third party material included in the article are encompassed under the Creative Commons license, unless indicated otherwise in the credit line. If the material is not included under the Creative Commons license, users will need to obtain permission from the license holder to reproduce the material. To view a copy of the Creative Commons license, please visit <http://creativecommons.org/licenses/by/4.0/>

Appendix IV: Abstracts of published papers

Environmental Science and Pollution Research
<https://doi.org/10.1007/s11356-018-2546-5>

RESEARCH ARTICLE



Environmentally persistent free radicals and particulate emissions from the thermal degradation of *Croton megalocarpus* biodiesel

Bornes C. Mosonik¹ · Joshua K. Kibet¹  · Silas M. Ngari¹ · Vincent O. Nyamori²

Received: 11 March 2018 / Accepted: 13 June 2018
© Springer-Verlag GmbH Germany, part of Springer Nature 2018

Abstract

Pyrolysis of biodiesel at high temperatures may result in the formation of transient and stable free radicals immobilized on particulate emissions. Consequently, free radicals adsorbed on particulates are believed to be precursors for health-related illnesses such as cancer, cardiac arrest, and oxidative stress. This study explores the nature of free radicals and particulate emissions generated when *Croton megalocarpus* biodiesel is pyrolyzed at 600 °C in an inert environment of flowing nitrogen at a residence time of 0.5 s at 1 atm. The surface morphology of thermal emissions were imaged using a field emission gun scanning electron microscope (FEG SEM) while the radical characteristics were investigated using an electron paramagnetic resonance spectrometer (EPR). A g-value of 2.0024 associated with a narrow ΔH_{pp} of 3.65 G was determined. The decay rate constant for the radicals was low ($1.86 \times 10^{-8} s^{-1}$) while the half-life was long ≈ 431 days. The observed EPR characterization of *Croton megalocarpus* thermal particulates revealed the existence of free radicals typical of those found in coal. The low g-value and low decay rate constant suggests that the free radicals in particulates are possibly carbon-centered. The mechanistic channel for the formation of croton char from model biodiesel component (9-dodecenoic acid, methyl ester) has been proposed in this study.

Keywords Biodiesel · Free radicals · Half-life · Thermal emissions · Pyrolysis

Simulating the Health Impact of Particulate Emissions from Transport Fuels Using Multipath Particle Deposition Model (MPPD)

Bornes C. Mosonik, Joshua K. Kibet*, Silas M. Ngari

Department of Chemistry, Egerton University, Egerton, Kenya

Email: *jkibet@egerton.ac.ke

How to cite this paper: Mosonik, B.C., Kibet, J.K. and Ngari, S.M. (2019) Simulating the Health Impact of Particulate Emissions from Transport Fuels Using Multipath Particle Deposition Model (MPPD). *Open Journal of Modelling and Simulation*, 7, 115-124.
<https://doi.org/10.4236/ojmsi.2019.72006>

Received: March 11, 2019

Accepted: April 22, 2019

Published: April 25, 2019

Copyright © 2019 by author(s) and Scientific Research Publishing Inc. This work is licensed under the Creative Commons Attribution International License (CC BY 4.0).

<http://creativecommons.org/licenses/by/4.0/>



Open Access

Abstract

Transport fuels emit particulates of varying chemical nature and size. These particulates are known to cause respiratory problems of medical concern. The need to simulate the breathing characteristics of particulates generated from combustion events is very important in estimating the respiratory clearance of these particles. Consequently, this study examines the nature of particulate matter from the pyrolysis of a mixture *Croton megalocarpus* biodiesel and fossil diesel, and pure biodiesel. The study was explored at an optimum temperature of 600°C in an inert nitrogen environment at a contact time of 2 sec. Scanning electron microscope was used to examine the surface of the particulates. Multiple-Path Particulate Dosage (MPPD Ver. 3.04) model was used to determine the breathing phenomena of infants, teenagers and adults at different orientations. Co-pyrolytic Char particulates and pyrolytic croton thermal char were classified as ultrafine, PM_{0.03} and PM_{0.02} respectively. The MPPD model results indicated that ultrafine particles tend to be deposited in pulmonary regions more than head and trachea regions, due to high probability of diffusibility of ultrafine particles. It was noted that 8 years old exhibits a unique trend with high total deposition and poor respiratory clearance when compared to an adult of 21 years old.

Keywords

Particulate Emissions, Respiratory Clearance, MMPD, Combustion Events



Optimization of Binary Mixtures of Biodiesel and Fossil Diesel for Clean Energy Combustion

Bornes C. Mosonik¹ · Joshua K. Kibet¹ · Silas M. Ngari¹


Received: 7 February 2019 / Accepted: 24 May 2019
© The Tunisian Chemical Society and Springer Nature Switzerland AG 2019

Abstract

There is an urgent interest initiated to develop clean energy resources with the aim of reducing exposure to environmental pollutants and explore model fuels that can hasten the achievement of clean energy combustion. This work investigates various ratios of biodiesel and commercial diesel in order to propose model binary fuels for clean energy combustion. Accordingly, diesel blends of ratios 1:1, 3:2 and 2:3 were each pyrolyzed at a contact time of 5 s in a quartz reactor at 1 atmosphere pressure. A model temperature of 500 °C was explored in these experiments. The charcoal content for pure fossil diesel was compared with the binary diesel residue. Gas-phase molecular components were determined using Gas chromatography (GC) coupled to a mass selective detector (MSD). Elemental composition of thermal char was determined using Smart Elemental Analyzer. Radical intensities for the three types of char (biochar, bio-fossil char, and fossil char) were measured using an X-band electron paramagnetic resonance spectrometer. It was noted that at a ratio of 2:3 (Biodiesel: Fossil diesel), harmful molecular products reduced significantly, 76–99%. Elemental analysis data indicated that the carbon content from commercial diesel was very high ($\approx 70.61\%$) as compared to approximately 53% for biodiesel-fossil diesel mixture in the same ratio 2:3. Interestingly, the free radical content was reduced by nearly 50% in favour of the biodiesel/fossil diesel mixture. These results are encouraging and suggest that a better optimized fuel mixture has been found for better clean energy combustion.

Keywords Clean energy combustion · Elemental composition · Diesel blends · Thermal char

Appendix V: NACOSTI Permit



**NATIONAL COMMISSION FOR SCIENCE,
TECHNOLOGY AND INNOVATION**

Telephone: +254-20-2213471,
2241349, 3310571, 2219420
Fax: +254-20-318245, 318249
Email: dg@nacosti.go.ke
Website: www.nacosti.go.ke
When replying please quote

NACOSTI, Upper Kabete
Off Waiyaki Way
P.O. Box 30623-00100
NAIROBI-KENYA

Ref. No: **NACOSTI/P/19/92892/28236** Date: **14th February, 2019**

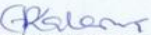
Bornes Chelangat Mosonik
Egerton University
P.O. Box 536-20115
NJORO

RE: RESEARCH AUTHORIZATION

Following your application for authority to carry out research on “*Computational and kinetic modeling of molecular products and radicals from the co-pyrolysis of bio-diesel blends*” I am pleased to inform you that you have been authorized to undertake research in **Nakuru County** for the period ending **14th February, 2020**.

You are advised to report to **the County Commissioner and the County Director of Education, Nakuru County** before embarking on the research project.

Kindly note that, as an applicant who has been licensed under the Science, Technology and Innovation Act, 2013 to conduct research in Kenya, you shall deposit a **copy** of the final research report to the Commission within **one year** of completion. The soft copy of the same should be submitted through the Online Research Information System.


GODFREY P. KALERWA MSc., MBA, MKIM
FOR: DIRECTOR-GENERAL/CEO

Copy to:

The County Commissioner
Nakuru County.

The County Director of Education
Nakuru County.

National Commission for Science, Technology and Innovation is ISO9001:2008 Certified

**THIS IS TO CERTIFY THAT:
MS. BORNES CHELANGAT MOSONIK
of EGERTON UNIVERSITY, 0-20115
NAKURU, has been permitted to conduct
research in Nakuru County**

**Permit No : NACOSTI/P/19/92892/28236
Date Of Issue : 14th February, 2019
Fee Received :Ksh 2000**

**on the topic: COMPUTATIONAL AND
KINETIC MODELING OF MOLECULAR
PRODUCTS AND RADICALS FROM THE
CO-PYROLYSIS OF BIO-DIESEL BLENDS**

**for the period ending:
14th February, 2020**



**Applicant's
Signature**

**Director General
National Commission for Science,
Technology & Innovation**